Pharmacological and Functional Characterisation of Two Novel *ShK-like* Peptides from The Nematode *Heligmosomoides polygyrus* on The Voltage-Gated Potassium Channel Kv1.3

Alessia Golluscio

A thesis submitted in partial fulfilment of the requirements of the University of Kent and the University of Greenwich for the Degree of Doctor of Philosophy

September 2021

DECLARATION

I certify that this work has not been accepted in substance for any degree, and is not concurrently being submitted for any degree other than that of Doctor of Philosophy being studied at the Universities of Greenwich and Kent. I also declare that this work is the result of my own investigation except where otherwise identified by references and that I have not plagiarised the work of others.

Candidate

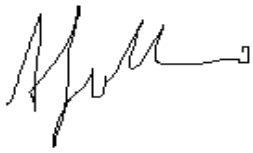

Signed: Alessia Golluscio

Date: September 2021

"E quindi uscimmo a riveder le stelle"

Dante Alighieri, Divina Commedia (Inferno XXXIV)

ACKNOWLEDGEMENTS

Firstly, I would like to express my deepest gratitude to my supervisors, Emma and Alistair. Without your help and guidance this project would not have been the same, especially with all the changes and adjustments we experienced in the past year.

To Emma, thank you for every time you offered me reassurance when I needed it the most, for all your suggestions and all the attention you gave to me and this project. I will always be grateful and will miss our coffees and chats by the rig.

I would like to express my gratitude to Vadim, for the help you offered me throughout these years and especially with the work on Jurkat cells. It was a pleasure to work with you.

Another big thank you is for Yvonne, for all the support offered with the cells, especially in the past year of restrictions. I appreciate everything.

I would also like to thank all my PhD colleagues for all the support shown during this journey. I will always keep the memories of all the lunches shared together in the tearoom, of all the chats and gossips and most importantly, of all the time we offered each other support when things were not easy.

To my family, thank you for all the support you gave me, in every single aspect. It is not easy to live apart and it never will be, I am forever grateful to count on you for everything even at a distance.

To Kevin, I do not have enough words to express how fundamental you are. Thank you for every time you stood by me, lifted me and made me see things under a different light. Times were hard but you made every single day brighter. *Ad infinitum*.

ABSTRACT

Animal venom have always represented a highly valuable source of peptides and compounds widely used since ancient times to serve several purposes and as a natural remedy to treat human conditions in the medical practice of some cultures. In modern ages, several venom-derived peptides have been included in the list of drugs currently used in medical practice whereas others are under evaluation. The extraordinary power of those peptides is mainly linked to their ability to target ion channels, that are often at the basis of several pathologies. Those peptides have been extensively studied thorough the years and now the number of those able to target ion channels have significantly expanded, including peptides derived from the venom of unrelated species, as well as peptides derived from the venom of plants.

The voltage-activated K^+ channel, Kv1.3, member 3 of the *Shaker*-related superfamily, is regarded as a therapeutical target for the treatment of several autoimmune disorders that involve T cells. The importance of K^+ channels in T cells is related to the regulation of Ca^{2+} signalling, essential to ensure T cells functions, and to the regulation of the membrane potential. Kv1.3 is upregulated in the subset of T cells, the effector memory T cells (T_{EM}), that mediate several autoimmune conditions including multiple sclerosis (MS), diabetes mellitus type-1 (DMT1), rheumatoid arthritis (RA) and many more. As such, inhibition of the channel with specific inhibitors is regarded as a promising approach to treat those and other diseases. A significant number of researches pointed out the attention on ShK toxin, derived from the sun sea anemone *Stichodactyla heliantus,* as a potent blocker of Kv1.3 channel and currently, an analogue of the toxin, is on clinical trials for the treatment of autoimmune conditions. ShK is not the only example of toxin that can target the channel but certainly represent the progenitor of the *ShK-like* toxins. *ShK-like* toxins include several toxins derived from different and unrelated species that share a characteristic functional domain, comprising a six cysteines motif and functional residues within the amino acidic sequence. More recently, toxins able to inhibit Kv1.3 channel, have been found in worms belonging to the phylum of nematodes, cestodes and trematodes. This research project is focused on the characterisation of two novel peptides from the parasitic nematode *Heligmosomoides polygyrus*. The two novel peptides, SXCL-1 and SXCL-6, sharing a characteristic *ShK-like* domain, are a promising novel class of potent Kv1.3 inhibitors. Using an electrophysiological approach including whole-cell patch clamp and perforated patch-clamp we present the pharmacological and functional implications of SXCL-1 and SXCL-6 on the voltage-gated K^+ channel Kv1.3 and we open up the possibility to include those novel peptides to the increasing list of Kv1.3 blockers derived from worms.

TABLE OF CONTENTS

LIST OF FIGURES

Chapter 1: Introduction

Chapter 2: Material and Methods

Chapter 3: Electrophysiological and functional characterisation of the two novel *ShK-like* peptides, SXCL-1 and SXCL-6, on Kv1.3 channel

Chapter 4: Electrophysiological characterisation of SXCL-1 and SXCL-6 on other members of the voltage-activated K^+ channel family

Chapter 5- Functional characterisation of a *de novo* variant in KCNB1 gene using Guangxitoxin-1E

Chapter 6- Investigation of the properties of SXCL-1 and SXCL-6 on Kv1.3 expressed in Jurkat cells

LIST OF TABLES

Chapter 1- Introduction

Chapter 3: Electrophysiological and functional characterisation of the two novel *ShK-like* peptides, SXCL-1 and SXCL-6, on Kv1.3 channel

Chapter 8- Appendix

ABBREVIATIONS

(2TM)	Two-transmembrane domain
(4TM)	Four-transmembrane domain
(6TM)	Six-transmembrane domain
$[Ca^{2+}]_i$	Internal calcium
4AP	4-aminpyridine
5-HT_3	5-hydroxitryptamine 3
95% CI	95% Confidence Intervals of the mean
A	Alanine
ACE	Angiotensin Converting Enzyme
AChEs	Acethylcolinesterases
AD	Autoimmune Diseases
AF	Atrial Fibrillation
Ag	Silver
AIS	Axonal initial segments
AMPS	Antimicrobial Peptides
AP	Action Potential
APC	Antigen Presenting Cells
APD	Action Potential Duration
APY-3	Apyrase
ASICs	Acid Sensing Ion Channels
Ba^{2+}	Barium
BB	Brain-Blood barrier
BgK	Bundosoma granulifera toxin
BK	Big conductance- Ca^{2+} -activated K^+ channels
BSA	Bovine Serum Albumin
C	Cysteine
Ca^{2+}	Calcium
CaM	Calmodulin
cAMP	Adenosine 3', 5'-Cyclic monophosphate
Cav	Voltage-activated calcium channels
CD	Chron's Disease

cGMP	Guanosine 3', 5'-Cyclic monophosphate
ChTX	Charybdotoxin
Cl_{swell}	Swelling-activate Cl^- channels
Cl^-	Chloride
Cm	Membrane Capacitance
CNG	Cyclic Nucleotide-Gated channels
CNS	Central Nervous System
CO_2	Carbon dioxide
CRAC	Calcium-Release Calcium-Activated Channel
Cs^+	Caesium
CS α–β	Cysteine stabilized α–helical and β-sheet
CTRL	Control
CYS	Cysteine
D	Aspartic Acid
DAP	2,3-Diaminophenazine
Dap22	1,3-diaminopropionic acid
DCT	Distal Convoluted Tubule
ΔG	Free energy of the binding
DMEM	Dulbecco's modified eagles media
DMSO	Dimethyl Sulfoxide
DTX-α	Dendrotoxin-a
DTX-k	Dendrotoxin-k
DTXs	Dendrotoxins
EA1	Episodic Ataxia type 1
EAE	Experimental Autoimmune Encephalomyelitis
EAG	Ether-a-go-go-related gene K^+ channels
EAs	Episodic Ataxias
EAST	Epilepsy, Ataxia, Sensorineural deafness and Tubulopathy syndrome
ECACC	European Collection of Cell Culture
EE	Epileptic encephalopathies
EGTA	Ethylene Glycol-bis (b-aminoethyl ether)- N, N, N', N'-Tetraacetic Acid
ELISA	Enzyme-Linked Immunosorbent Assay
ER	Endoplasmatic Reticulum

ErgTX	Ergtoxin
ES	Excretory-secretory products
FDA	Food and Drugs Administration
GABA A	γ-aminobutyric acid A
GFP	Green Fluorescent Protein
GluRS	Ionotropic Glutamate receptors
GMTs	Gating Modifiers Toxins
GOF	Gain-of-function
GPCRs	G-protein Coupled Receptors
GxTx-1E	Guangxitoxin-1E
H	Histidine
HaTX1	Hanatoxin-1
HaTX2	Hanatoxin-2
HEK-293	Embryonic kidney cell line
HEPA	High Efficiency Particulate Air
HEPES	4-(2-hydroxyethyl)- 1-piperazineethanesulfonic acid
HES	Adult excretory-secretory products
HIFBS	Heat-Inactivated Fetal Bovine Serum
HRP	Horseradish Peroxidase
HSA	Human Serum Albumin
I-V	Current-Voltage relationship
IBD	Inflammatory Bowel Diseases
IbTX	Iberiotoxin
IC50	Half maximal inhibitory concentration
ICK	Inhibitory Cystein Knot motif
IFN-γ	Interferon- γ
IgE	Immunoglobulin E
IK	Intermediate conductance- Ca^{2+}- activated K^+ channels
IK_{DR}	Delayed-rectifier K^+ current
IL-13	Interleukin-13
IL-2	Interleukin-2
IL-4	Interleukin-4
IL-5	Interleukin-5

IL-9	Interleukin-9
Ip	Current flowing into the pipette
IP3	1,4,5-inhositol-triphosphate
IP3R	1,4,5-inhositol-triphosphate Receptor
IS	Immunological Synapses
JNK	N-terminal kinase
JPX	Juxtaparanodal region
K	Lysine
K^+	Potassium
K2P	Two pore domain K^+ channels
Kca	Calcium- activated K^+ channel
KChiP	K^+ channel-interacting proteins
KCNE	Potassium voltage-gated channel subfamily E
KcsA	Bacterial K^+ channel isolated from Streptomyces levidans
Kir	Inward rectifier K^+ channels
KQT	Voltage-gated K^+ channels subfamily QT
KTX	Kaliotoxin
Kv	Voltage-gated K^+ channel
L-pTyr	L-phosphor-tyrosine
LA	Lupus Anticoagulant
LB	Lennox broth
LEU	Leucine
LFA-1	Leukocyte Function-Associated molecule-1
Li^+	Lithium
LOS	Loss-of-function
LQTS	Long-QT Syndrome
LVA	Low Voltage-Activated
LYS	Lysine
LYS-1	Lysozyme-1
LYS-2	Lysozyme-2
M1-M4	Transmembrane segments of K2P channels
Maxi K	High voltage Ca^{2+} sensitive K^+ channels
MD	Molecular Dynamic

Mg^{2+}	Magnesium
MgTX	Margatoxin
MHC	Major Histocompatibility Complex
MHC-II	Major Histocompatibility Complex-II
MS	Multiple Sclerosis
MSICs	Mechanosensitive Ion Channels
mV	Millivolt
Na^{+}	Sodium
nAch	Acetylcholine receptor
Nav	Voltage-gated sodium channels
NEAA	Non-Essential Amino Acid solution
NFAT	Nuclear factors of activated T cells
NK	Natural Killer
nM	Nanomolar
NMR	Nuclear Magnetic Resonance
NORs	Nodes of Ranvier
NTX	Noxiutoxin
OPD	*o*-phenylenediamine
OT	Occupational therapy
P	Proline
P2X	Purinergic 2X
pA	Picoampere
PBS	Phosphate Buffered Saline
PCR	Polymerase chain reaction
PD	Pore Domain
PDL	Poly-D-Lysine
PEG	Polyethylene glycol
pg	Picograms
PHA	Phytohemagglutinin
PHE	Phenylalanine
PKC	Protein Kinase C
PLC	Phospholipase C
PLCγ	Phospholipase Cγ

PLL	Poly-L-Lysine
PMA	Phorbol 12-myristate 13-activate
PNS	Peripheral Nervous System
P_o	Open probability
PT	Physical therapy
PUFAs	Polyunsaturated fatty acids
R	Arginine
RA	Rheumatoid Arthritis
Rb^+	Rubidium
RPMI	Roswell Park Memorial Institute Medium
Rs	Feedback resistor
Rs	Series Resistance
RT-PCR	Real Time- Polymerase chain reaction
sACE	Angiotensin Converting Enzymes
SEM	Standard error of the mean
SeSAM	Seizures, Sensorineural deafness, Ataxia, Mental retardation and electrolyte imbalance syndrome
ShK	Stichodactyla heliantus toxin
ShKT	Stichodactyla heliantus domains
SID	Self-Interacting Domain
SK	Small conductance- Ca^{2+}-activated K^+ channels
SMART	Simple Modular Architecture Research Tool
SMMCs	Small Molecular Mass Compounds
SQTS	Short-QT Syndrome
STM1	Stromal interaction molecule 1
STM2	Stromal interaction molecule 2
T	Tyrosine
T1DM	Type 1 Diabetes Mellitus
TALK	TWIK-Related Alkaline pH-Activated Potassium Channel
TASK	TWIK-Related Acid-Sensitive Potassium Channel
TBST	Tween 20 Phosphate Buffered Saline
T_{CM}	Central memory T cells
TCR	T Cells Receptor

TdP	Torsades de pointes
TEA	Tetraethylammonium
Teff	Effector T-cells
T_{EM}	Effector memory T cells
THIK	TWIK-Related Halothane-Inhibited Potassium Channel
TRAAK	TWIK-Related Arachidonic Acid Activated K+ Channel
Treg	Regulatory T- cells
TREK	TWIK-Related Potassium Channel
TRESK	TWIK-Related Spinal Cord Potassium Channel
T_{RM}	Resident-memory T cells
TRP	Transient Receptor Potential Channels
TRP	Tryptophan
TRPM6	Transient Receptor Potential cation channel, subfamily M, member 6
TRPM7	Transient Receptor Potential cation channel, subfamily M, member 7
TRPV1	Transient Receptor Potential Channels of the vanilloid subtype, isoform 1
TWIK	Tandem Pore Weak Inward Rectifier Potassium Channel
TYR	Tyrosine
UC	Ulcerative Colitis
V	Valine
V_0	Amplifier output
VAL	Venom allergen/ Ancylostoma secreted protein-like
VCMD	Command voltage
VHOLD	Holding voltage
Vm	Membrane Potential
VSD	Voltage Sensor Domain
VSDs	Voltage Sensor Domains
WT	Wild Type
Y	Tyrosine
Zn^{2+}	Zinc
ZO	Zona Occludens

Chapter 1: Introduction

1.1 Background

The first observations regarding the electrical phenomena in tissues and nerve started with the elaboration of the "*animal electricity hypothesis"* by the physicist Luca Galvani, based on the first observations on the frog's leg contraction. Galvani explained the electrical basis of nerve impulse (Piccolino M., 2008), that will be investigated later on, by the physicist and neurophysiologist Carlo Matteucci, who was the first to describe an outward current (defined as *injury current* or *demarcation current)* in resting nerve and muscle (Seyfarth E.A., 2005).
In 1868, Julius Bernstein constructed a differential rheotome or current slicer (Hoff and Geddes, 1957) in order to obtain a precise measure of the time course of electrical activity and the conduction velocity in nerve muscle preparation (Carmeliet E., 2019). The observations about the measurement of the electrical activity represent one of his major achievements together with the formulation of the *membrane hypothesis* (Bernstein J. 1902; Bernstein J. 1912). Indeed, Bernstein proposed that the membrane of excitable cells is selectively permeable to K^+ ions at rest conditions but, during excitation, becomes permeable to other ions. Although the investigations conducted by Bernstein led to the description of the function of the cell membrane, the composition, as we all know today, was still unclear. The first description was elaborated around the end of 19th century from Meyer (1899) and Overton (1901). In this proposed model, the lipids represented the main component of the membrane (Meyer 1899; Overton 1901). Eventually, in 1972 a complete picture of the composition of the membrane was described by Singer and Nicolson and defined as the "*fluid mosaic model*" (Singer S.J. and Nicolson G.L., 1972). The role of ions in the excitability of nerve and muscle, was defined in the early 1880s when, in a series of published papers, Sydney Ringer demonstrated that the solutions that perfuse the heart of a frog contains salts such as potassium (K^+), sodium (Na^+) and calcium (Ca^{2+}) in proportion (Ringer S., 1882 (a), 1882 (b), 1883 (a), 1883 (b), 1884, 1885; Ringer S. and Buxton D.W., 1887). Later on, in 1902, Overton demonstrated the importance of Na^+ to generate muscle contraction, describing the events during a nerve or skeletal muscle action potential (AP), an important postulate for the Hodgkin, Huxley and Katz "*Ionic theory"* (1947). According to Overton description, during an AP, the external Na^+ is exchanged with internal K^+ in the period between the stimulation and the start of contraction (Overton, 1902).

In 1939, Alan Hodgkin and Andrew Huxley in United Kingdom, and Cole and Curtis in the United States of America, obtained the first measurement of the resting and action potential

(AP) on the axon of giant squid (Hodgkin A.L. and Huxley A.F, 1939; Cole K.S. and Curtis H.J., 1939). In this delicate historical period, research was challenged and soon after the end of the world war II, the *Na^+ hypothesis* was confirmed (Hodgkin and Katz, 1949). The work carried by Hodgkin and Huxley on the role of Na^+ during the action potential and the involvement of ion channels, was worth the Nobel prize for Medicine in 1963 and represented a fundamental moment for the studies on ion channels. Late in 1970s, the introduction of the patch electrode by Erwin Neher and Bert Sakmann (Neher E. and Sakmann B., 1976 a) signed a new era in the electrophysiology field, with the recording of current from single channel (Neher E. and Sakmann B., 1976 b). This accomplishment gave to Neher and Sakmann the Nobel prize award in 1991.

The exceptional progresses in genetics and molecular biology, conveyed to the description of the first structure of the subunits forming the nicotinic acetylcholine receptor (nAch) (Noda *et al.,* 1983 a, b), followed by the description of the structure of the two voltage-gated channels, Na^+ (Noda *et al.,* 1984) and K^+ (Kamb *et al.,* 1988; Pongs *et al.,* 1988; Tempel *et al.,* 1987). These remarkable discoveries represent milestones in the field of ion channels and contributed significantly to increase the understating of the structure and the functions of these proteins in the cells.

1.2 Ion Channels

Ion channel are considered fundamental elements in excitable cells, responsible for excitation, generation and propagation of electrical signals in the nervous system (Hille B., 2001) and important contributors to cell signalling and homeostasis (Sigg D., 2014).

These integral membrane proteins possess a characteristic aqueous pore, which undergo conformational change in the structure, allowing the transit of ions. The conformational change can occur in response to specific environmental stimuli such as voltage, ligand concentration, temperature, membrane tension and many more (Hille B., 2001). When channels are open, they enable ions to cross the cell membrane (Hille B., 1978) in both directions, inside and outside the cell (Hille B., 1978). This movement is driven by thermal agitation and electrical field in the membrane (Armstrong, 1975) (Figure 1).

Ion channels are found in the membrane of both eukaryotic and prokaryotic cells and share two common properties, defined as *selectivity* and *gating* (Hille B., 2001). Selectivity represent a crucial parameter for electrical excitability in biological membrane and is essential for the generation and propagation of action potential (AP) (Benoît R., 2017). This property enables the channel to select the ionic species that can flow within the pore. For this reason, for example, potassium channels present a specific selectivity sequence of $K^+ \approx Rb^+ > Cs^+$, low permeability for the smallest alkali metal ions Na^+ and Li^+, and very high permeability for K^+ (Doyle D.A. *et al.,* 1998). Another important feature of ion channel is the *gating*. Gating refers to the mechanism that governs the conformational transitions of the channel between the closed state and the open state. These transitions occur in response to some specific stimuli, either in the form of chemical transmitter and other agents, or in response to changes in the voltage of the membrane (Hille B., 1978).

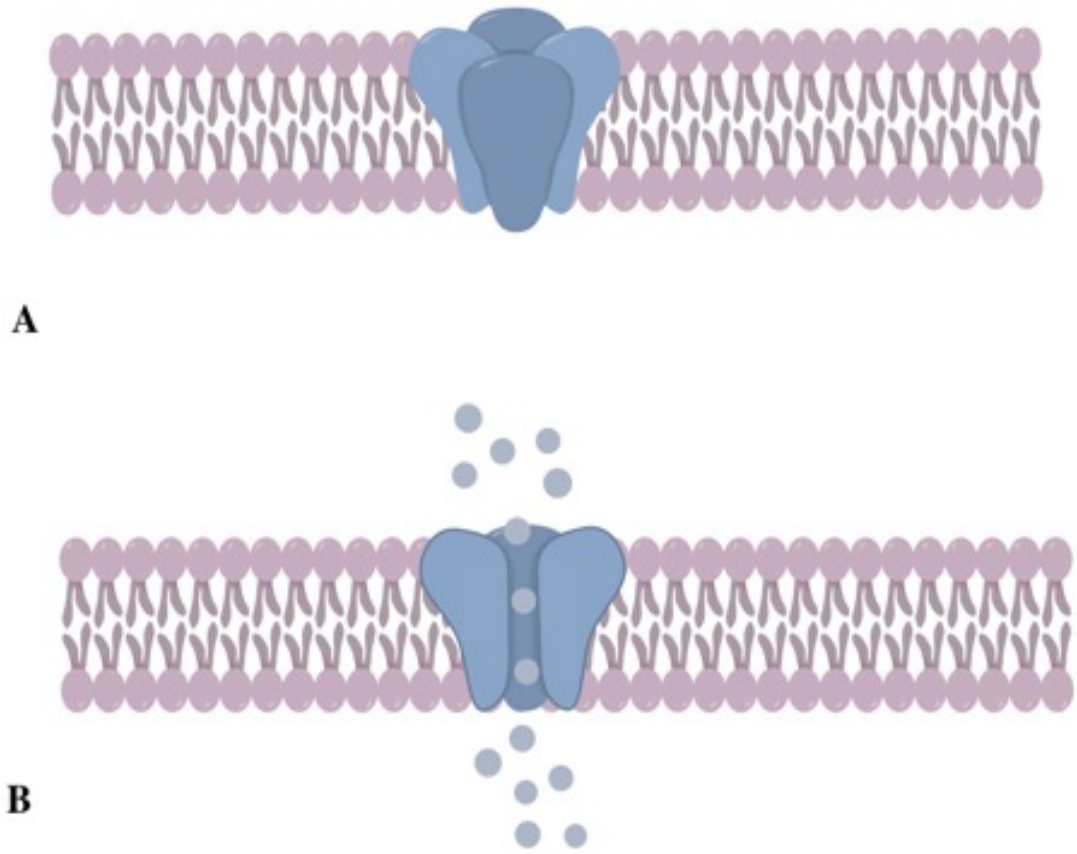

Figure 1. Cartoon representing ion channel in the main *status* closed (A) and open (B). When the channel is open a flux of ions can be observed due to conformational changing occurring in the pore region. Changes can occur in response to different stimuli.

Based on their gating properties, ion channels can be classified into *voltage-gated* (or voltage-activated) and *ligand-activated* channels. The voltage-activated ion channels require a change in the membrane potential to be activated (Hille B., 1978). Sodium (Na^+) channels, that support the initiation and propagation of electrical signals in excitable tissues such as muscle, heart and nerve (George A.L. Jr., 2005); potassium (K^+) channels, that contribute to the repolarization of the cell membrane (Kim D.M. *et al.,* 2016) and calcium (Ca^{2+}) channels that, by finely contributing to the Ca^{2+} signalling cascade, sustain a variety of Ca^{2+} dependent cellular events (Wu J. *et al.,* 2016), are paramount examples of voltage-gated channels.

The ligand-activated channels, also known as ionotropic receptors, regulates the gating properties in response to the binding of specific ligands to the extracellular domain of the protein (Collingridge G.L. *et al.,* 2009; Lev B. *et al.,* 2017). The binding causes a total

conformational change in the protein structure that determine, subsequently, the opening of the pore (Lev B. *et al.,* 2017). Examples of ionotropic receptors include the nicotinic acetylcholine receptors, 5-hydroxitryptamine 3 (5-HT_3), γ-aminobutyric acid A (GABA A), glycine, ionotropic glutamate and P2X receptor families. These ionotropic receptors are involved in fast synaptic transmission (Collingridge G.L. *et al.,* 2009). Furthermore, activation and inactivation of the ligand-activated channels, can be regulated by second messengers. This is the case of the cyclic nucleotide-gated channels (CNG), which activation is related to the cyclic nucleotides, guanosine 3', 5'-cyclic monophosphate (cGMP) and adenosine 3', 5'-cyclic monophosphate (cAMP). The CNG channels play a pivotal role in visual (Yau K.W. and Baylor D.A., 1998) and olfactory (Zufall F. *et al.,* 1994) transduction signals. They present a different selectivity to the cyclic nucleotide depending on their physiological role (Zagotta W.N. and Siegelbaum S.A., 1996).

The advancement of technology significantly contributed to reach a better understanding of the structure and function of ion channels. The advances made in molecular genetics conveyed to the cloning of individual channels and the sequencing of entire genomics (Hille B., 2001). Resolving the primary structure of the channels, represented a fundamental step to achieve a fully understanding of the channel properties, enabling not only to unravel the amino acidic sequence, but also to elucidate the transmembrane topology of the channels (Benzanilla F., 2008 a). The first sequence of the subunits forming the nicotinic acetylcholine receptor (nAchR) from *Torpedo californica* (Noda M. *et al.,* 1983 a, b) was obtained in 1983 followed, one year later, by the sequence of the voltage-gated Na^+ channel from the electric organ of the eel *Electrophorus electricus* (Noda M. *et al.,* 1984). Few years later, the primary sequence of the Shaker K^+ channel from a mutant of *Drosophila,* was also described (Kamb A. *et al.,* 1988; Pongs O. *et al.,* 1988; Tempel B.L. *et al.,* 1987). In the 1990s, Mackinnon and colleagues described the first potassium channel from the bacterium *Streptomyces lividans* (KcsA) (Doyle D.A. *et al.*, 1998). The bacterial potassium channel (KcsA) is composed by four subunits assembled around a central pore; each subunit presents two transmembrane segments and a P region which form the selectivity filter (del Camino D. and Yellen G., 2001). At present, numerous families and subfamilies of ion channels have been described and their physiological role within the cells have been elucidated.

1.3 Potassium channels

The family of the potassium channels is the most numerous, with genes encoding the channels found in both eukaryotic and prokaryotic (free living bacteria and archaea), except some parasites (Kuo M.M. *et al.,* 2005). Potassium channels conduct K^+ ions across the cell membrane according to the electrochemical gradient for K^+ (Mackinnon R., 2003). The movement of potassium ions across the membrane is essential for numerous biological processes, such as cell volume regulation, hormone secretion and electrical impulse generation in excitable cells (Hille B., 2001). In particular, in excitable cells, K^+ channels are involved in the regulation of skeletal and cardiac muscle contraction (Abbott G.W., 2020). It is reasonable to differentiate the potassium channels according to the way they gate. Based on their gating differences, the channels present also different structural domains. The voltage-gated potassium channels, which require changes in the voltage of the membrane to be activated, are equipped with a specific integral membrane domain, called the voltage-sensor domain (VSD), that senses the voltage differences across the cell membrane (Benanzilla F., 2008; Sigworth F.J., 1994). The ligand-gated channels require the binding of a ligand to modulate their gating and therefore, they have cytoplasmatic or extracellular domains where ligands can bind (Mackinnon R., 2003). One characteristic shared by potassium channels, regardless of how they regulate their gating, is a high conservative sequence of eight amino acids, known as the "*K^+ channel signature sequence*" (TXXTXGYG) (Heginbotham L. *et al.,* 1994). This sequence, found within the pore region of the channel, forms the selectivity filter and is responsible for K^+ channel highly efficient conduction (Kuang Q. *et al.,* 2015). In fact, mutations occurring in this sequence cause a disruption in the selectivity filter that dramatically reduces the selectivity of the channel (Heginbotham L. *et al.,* 1994).

In general, potassium channels can be divided in three broad classes according to their structure and function: two transmembrane domains (2TM), four transmembrane domains (4TM) and six transmembrane domains (6TM). Furthermore, potassium channels are also classified into four superfamily based on their permeation and gating properties: the *voltage-gated potassium channel* (Kvs), *the calcium-activated potassium channel* (Kca), the *inward rectifier* (Kir) and *the background* (K2P).

1.3.1 The two transmembrane domain channels (2TM)

The inwardly rectifier potassium channels represent a large family of potassium channels divided into at least six subfamilies (Kir1.x to 7.x) (Nicholson C.G. and Lopatin A.N., 1997). The term "*inwardly rectifier*" is associated with the characteristic way of the channels to conduct current, originally defined "*anomalous rectifier*" (Katz B., 1949), because opposite to the outward rectification seen in other channels (Nicholson C.G. and Lopatin A.N.,1997). In fact, at hyperpolarizing membrane potential, the channels conduct a greater flow of K^+ ions into the cell more than outside, thus generating an inward rectification (Hibino H. *et al.,* 2010). The rectifier nature of the conductance is caused by the voltage-dependent block of the channel by polyamines and Mg^{2+} ions (Ficker E. *et al.,* 1994; Taglialatela M. *et al.,* 1995; Yang J. *et al.,* 1995 a; Oliver D. *et al.,* 1998; Ruppersberg J.P., 2000). The inward rectifier channels are usually grouped into *strong* and *weak* rectifier. The first group of channels, the strong rectifiers, is found mainly in excitable cells such neuronal and muscle cells ($K_{ir}2$ and $K_{ir}3$), where they contribute to the regulation of the membrane potential and modulation of AP (Hille B., 1992). The weak rectifier channels, instead, are mostly involved in K^+ homeostasis (Ki_r1, Ki_r4 and $K_{ir}5$) (Zangerl-Plessl E.M. *et al.,* 2019).

K_{ir} channels are also involved in the regulation of the vascular tone, heart rate, renal salt flow and insulin release (Minor D.L. *et al.,* 1999). The expression of the inwardly rectifier potassium channels is wide. Channels are expressed in cardiac myocytes (Beeler G.W. *et al.,* 1970; Kurachi Y., 1985; McAllister RE and Noble D., 1996;Noble D., 1965; Rougier O. *et al.,* 1968), neurons (Brown D.A. *et al.,* 1990; Gähwiler B.H. and Brown D.A., 1985; Lacey M.G. *et al.,* 1988; North R.A. *et al.,* 1987; Takahashi T., 1990; William J.T. *et al.,* 1998), blood cells (Lewis D.L. *et al.,* 1991; McKinney, L.C. and Gallin, E.K.,1988), osteoclasts (Sims S.M. and Dixon S.J.,1989), endothelial cells (Silver M.R. and DeCoursey T.E., 1990), glial cells (Kuffler S.W. and Nicholls J.G.,1966; Newman E.A., 1984; Kofuji P. *et al.,* 2002) and epithelial cells (Greger R. *et al.,* 1990; Hebert S.C. *et al.,* 2005; Lorenz J.N. *et al.,* 2002; Lu M. *et al.,* 2002).

From a structural point of view, K_{ir} channels share a typical two transmembrane (2TM) arrangement (Figure 2). They are formed by four α-subunits arranged in a tetrameric complex (Glowatzki E. *et al.,* 1995; Yang J. *et al.,* 1995 b). Each α-subunit comprises two transmembrane segments (M1 and M2) connected by an extracellular forming region (H5), with both N- and C- termini at the cytoplasmatic side (Hibino H. *et al.,* 2010). The selectivity filter of the channels lays in the H5 region (Heginbotham L. *et al.,* 1994) and present the

signature sequence T-X-G-Y(F)-G, a common feature among all the potassium channels (Bichet D. *et al.,* 2003). The channels do not show the very well conserved S4 segments, classically detectible in the structure of voltage-gated channels such as Na^+, Ca^{2+} and K^+ (Hibino H. *et al.,* 2010). K_{ir} channels are able to form heteromeric and homomeric channels by assembling with other subunits thus enhancing the diversity among the channels (Hibino H. *et al.,* 2010).

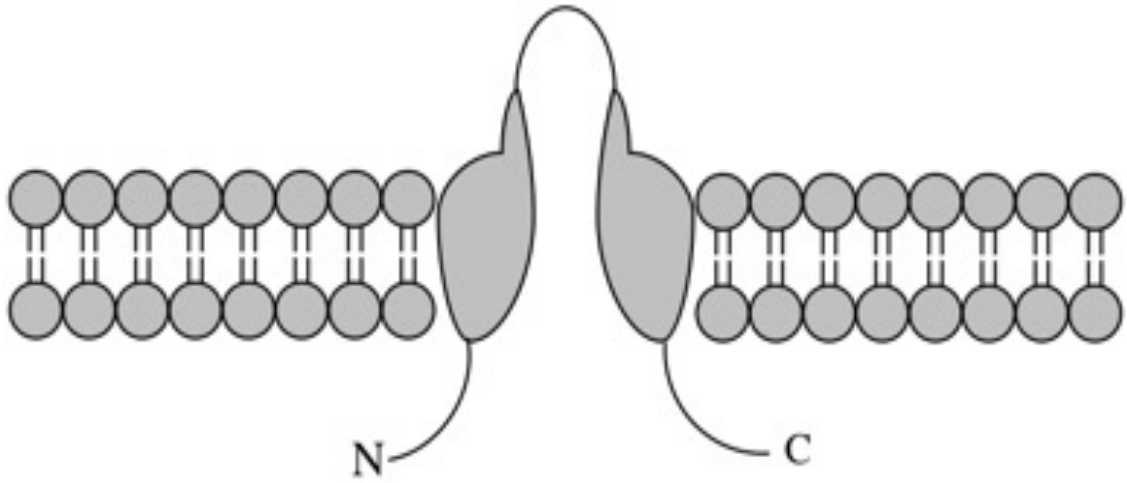

Figure 2. Characteristic topology presented by Kir channels (2 TM). α-subunits are formed by two transmembrane domains (M1-M2) connected by an extracellular loop. Both N-terminal and C-terminal are found within the intracellular side.

Considering the widespread expression of K_{ir} channels, it is not surprising that alterations in the homo- or heterotetrametric channels, result in disorders that involve several organs and tissues. Examples are *Bartter Syndrome* (Koulouridis E. and Koulouridis I., 2015), associated with a loss-of-function mutation of Kir1.1 (Zangerl-Plessl E.M. *et al.,* 2019); *Andersen-Tawil syndrome* (Nguyen H.L. *et al.,* 2013), resulting from a loss-of-function mutation of Kir2.1 that induces periodic skeletal paralysis, development of skeletal abnormalities and biventricular tachycardia (Zangerl-Plessl E.M. *et al.,* 2019); *SeSAME syndrome* (Seizures, Sensorineural deafness, Ataxia, Mental retardation and Electrolyte imbalance) also known as *EAST syndrome* (Epilepsy, Ataxia, Sensorineural deafness and Tubulopathy), associated with a loss-of-function mutation of Kir4.1 (Reichold M. *et al.,* 2010; Scholl U. *et al.,* 2009; Sala-Rabanal M. *et al.,*

2010), and many more. There are also several evidences that link alterations in K_{ir} channels to several CNS diseases such as white matter diseases, epilepsy and Parkinson (Neusch C. *et al.,* 2003).

1.3.2 The four transmembrane domain (4TM)

The two-pore domain channels or, simply, *K2P* channels, include fifteen members encoded by fifteen genes (KCNKx), divided into six subfamilies: *TWIK, TREK, TASK, THIK, TALK* and *TRESK* (Goldstein S.A. *et al.,* 2001; Goldstein S.A. *et al.,* 2005).
TWIK1, the prototypical of K2P channels family, has been identified in 1996 by *Lesage* and colleagues (Lesage F. *et al.,* 1996 b) and since then, all other members have been identified.
The two-pore domain channels are found in yeast, plants, zebrafish, nematode and fruit fly (Goldstein *et al.,* 2001). They play an important role in excitable and non-excitable cells, generating the so-called *leak* or *background* current (Enyedi P. and Czirják G., 2010), which is fundamental for the regulation of the resting membrane potential (Lesage F. and Lazdunski M., 2000; Goldstain S.A. *et al.,* 2001; Lotshaw D.P., 2007; Enyedi P. and Czirják G. 2010).
Ideal *background* currents are not voltage dependent (Enyedi P. and Czirják G., 2010) and, differently from the voltage-gated channel where P_o strictly depends by the variation in the membrane potential, the P_o in those channels is the same at all membrane potential (Enyedi P. and Czirják G., 2010). The gating of the K2P channels is independent from the membrane potential variations (Fink M. *et al.,* 1996; Lesage F. *et al.,* 1996 b; Duprat F. *et al.,* 1997). However, recently, Schewe and colleagues demonstrated that some K2P channels show a strong voltage-dependent activation, but the mechanism underlying this feature still remain unsolved (Schewe M. *et al.,* 2016). The two-pore domain channels are regulated by a broad *spectrum* of stimuli: mechanical force, polyunsaturated fatty acids (PUFAs), volatile anaesthetics, acidity/pH, pharmacological agents, heat and signalling events such as phosphorylation and protein-protein interaction (Braun A.P., 2012). Recently, the mechanosensitive TRAAK channel, was found to be activated by ultrasound with a mechanism that directly involve the lipid membrane (Sorum B. *et al.,* 2021). K2P channels show a different structural arrangement compared to other tetrameric channels, with two pore domains associate to function as a dimer (Niemeyer M.I. *et al.,* 2016). Each K2P subunit, consists of four

transmembrane segments (M1-M4), two pore forming domains and both N- and C- termini within the cytoplasmatic side (Zúñiga L. and Zúñiga R., 2016) (Figure 3).

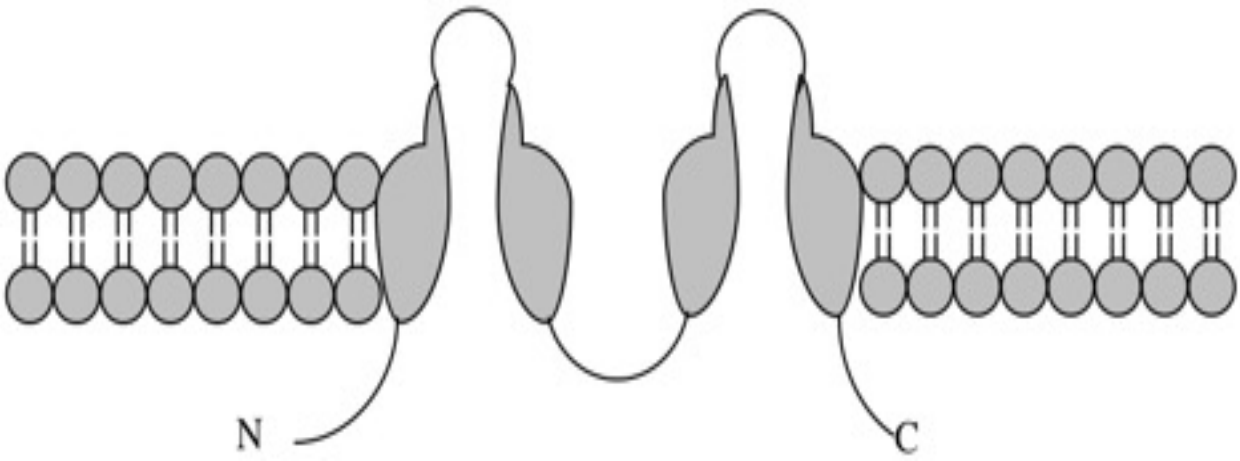

Figure 3. Representation of the four transmembrane topology shared among the K2P channels family. M1-M2 form the first pore domain and are linked by an extracellular loop; the second pore domain (M3-M4) is linked to M1-M2 by an intracellular loop. Both N-terminal and C-terminal are found within the cytoplasmatic portion.

A peculiarity in the structure of the K2P channels is the extracellular loop extended between the segment M1 and P1, that forms the so-called "self-interacting domain" (SID) (Lesage F. *et al.,* 1996 a). This domain is vital for the channel dimerization (Lesage F. *et al.,* 1996 a) and might play a role also in the channel regulation (Morton M.J. *et al.,* 2003; Morton M.J. *et al.,* 2005; Döring F. *et al.,* 2006). This extracellular loop is arranged into a helical cap that form the ion conduction pathway, mediating the passage of ions (Brohawn S.G et *al.,* 2012; Miller A.N. and Long S.B., 2012) and is stabilized by disulphide bridges established between cysteine residues at the top of the cap (Feliciangeli S. *et al.,* 2015). Indeed, the loop M1-P1 contains a cysteine residue in position 69 (Cys69), involved in the formation of covalent bridge between two subunits, and possibly significant for the stability of the dimer (Lesage F. *et al.,*1996 a). However significant, this Cys69 residue is not conserved among all the K2P channel members, such as TASK and THIK (Zuniga L. and Zuniga R., 2016). In 2016, work conducted by *Goldstein* and colleagues, elucidated the presence of the cap structure also in the K2P channels

that does not have the cysteine residue (Cys 69) within the M1-P1 link (Goldstein M. *et al.,* 2016). Overall, K2P channels preserve a similar structure, although is possible to point out some differences in the structural organization. In TASK1 and TASK3 is noticeable the absence of disulphide bonds in the cap structure (Feliciangeli S. *et al.,* 2015) whilst TRESK present a long intracellular M2-M3 loop, which act as a regulation site (Eneydi P. *et al.,* 2012; Feliciangeli S. *et al.,* 2015).

The two-pore domain channels are regarded as pharmaceutical targets for the treatments of several conditions (Mathie A. *et al.,* 2020) including pain and migraine (Mathie A. and Veale E.L., 2015; Mathie A., 2010), CNS disorders such as stroke, depression and epilepsy (Mathie A. and Veale E.L., 2007), pulmonary hypertension (Ma L. *et al.,* 2013; Cunningham K.P. *et al.,* 2018), atrial fibrillation (AF) (Schmidt C. *et al.,* 2017) as well as cancer (Mu D. *et al.,* 2003; Alvarez-Baron C.P. *et al.,* 2011).

1.3.3 The six transmembrane domain (6TM)

The voltage-gated potassium channel family, otherwise simply indicated as Kv (*Shaker*-related), includes twelve families (Kv1.x to Kv12.x) and counts the higher number of members among the potassium channel families (Tian C. *et al.,* 2014). Kv channels present the characteristically six transmembrane domains (6TM) topology, comprising of four α-subunits arranged around a central pore. Each of the four α-subunit contains six α-helical segments (S1-S6) and P-loop, comprising the extracellular S5-P linker, a pore helix containing the signature sequence TVGYG and the extracellular linker P-S6 (Doyle D.A. *et al.,* 1998). The voltage sensor domain (VSD), composed by the S1-S4 segments, is linked to the pore domain (Jiang L. *et al.,* 2003) (Figure 4). The α-subunits of the channels, can further assemble with other subunits to form functional hetero-tetramers. This is the case of the Kv1, Kv7 and Kv10 family, where the α-subunits can form hetero-tetramers with different subunits within the same family (Gutman G.A. *et al.,* 2005). Furthermore, α-subunits can assemble with accessories β-subunits (Pong O. and Schwarz J.R., 2010) that can modulate the properties of the channel (Tian C. *et al.,* 2014).

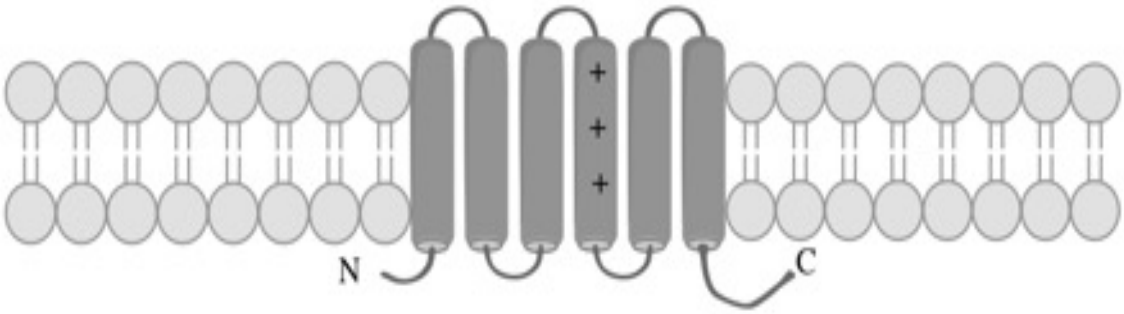

Figure 4. Six transmembrane (6TM) topology characteristic of voltage-gated K^+ channels. Segments S1-S4 constitute the voltage-sensor domain (VSD) and are linked to the pore domain (S5-S6) via internal loop. S4 is responsible for sensing the majority of the voltage changes. Both N-terminal and C-terminal are intracellular.

Three main domains are identifiable for the voltage-gated potassium channels: the *voltage sensor domain* (*VSD)*, composed by the segments S1-S4; the *conduction pathway*, represented by the segments S5-S6; and one or more *gates* (Barros F. *et al.,* 2012).

The segment S4 within the voltage-sensor domain, is a highly conserved structure (Lee *et al.,* 2005; Long S.B. *et al.,* 2005 a, b) that carries basic residues every third position (Arg and Lys) (Catteral W.A., 2010) and is regarded as the major contributor to the movement of the charges during the opening and/or closing of the channel (Seoh S.A. *et al.,* 1996). At resting potential these residues are located within the cytoplasmatic side of the membrane but, following depolarization, the residues move in direction of the electrical field, reaching the extracellular side of the membrane (Mannuzzu *et al.,* 1996) thus initiating the activation process (Catteral W.A., 1986 a,b; Guy H.R. and Seetharamulu P., 1986).

The pore domain (PD) is constitute by two α-helical segments, S5-S6, connected by a re-entrant P-loop. The pore region forms the selectivity filter of the channel and contains, in the narrowest portion, the highly conserved sequence, T-M-T-T-V-G-Y-G (Heginbotham L. *et al.,* 1994). The segment S6, lays at the intracellular side and form the intracellular gate (Yellen G. *et al.,* 1991; Liu Y. *et al.,* 1997; Doyle D.A. *et al.,* 1998; Yellen G., 2002).

In general, Kvs channels present three gates: a) *activation gate*, located at the cytoplasmatic side, at the end of the segment S6; b) the *pore* or *selectivity gate,* represented by the selectivity filter itself; c) the *inactivation gate* (Yellen G., 1998; Yellen G., 2002; Barros F. *et al.,* 2012).

K^+ channels are expressed in both excitable and non-excitable cells. They play a pivotal role in several physiological processes such as synaptic transmission, muscle contraction and hormone release (Sandhiya S. and Dkhar S.A., 2009). In the early *80s*, work carried by *De Coursey* and colleagues on T lymphocytes, elucidated the involvement of K^+ channels in cell proliferation (De Coursey T. E. *et al.,* 1984; Matteson D.R. and Deutsch C., 1984) and now their role is recognised in both normal and cancerous cells (Wonderlin W. and Strobl J., 1996; Kunzelmann K., 2005). K^+ channels are also important contributor in the regulation of the cell cycle progression (Ouadid-Ahidouch H. and Ahidouch A., 2013) by setting the resting membrane potential (V_m) and giving the driving force for Ca^{2+} influx (Ouadid-Ahidouch H. and Ahidouch A., 2013). They participate in the volume regulation process of growing cells (Lang F. *et al.,* 2007; Rouzaire-Dubois, B. *et al.,* 2000) and are also involved in in the regulation of different cell cycle checkpoints in cancer cells (Kunzelmann K.,2005; Lastraioli E. *et al.,* 2015; Ouadid-Ahidouch H. and Ahidouch A., 2013; Pardo L.A., 2004).
K^+ channels cover also an important role in apoptosis of tumour cells (Bortner C.D. and Cidlowski J.A., 2014; Wang Z., 2004). In non-excitable tissues such as kidney, lung, pancreatic islet, immune system, adipose tissue and epithelial cells, K^+ channels contribute in controlling the membrane resting potential via feedback mechanism and are involved in a wide range of biological processes (Szabò I. *et al.,* 2010).

It is remarkable to consider that this transmembrane topology is conserved among other voltage-gated K^+ channels, such as the *ether-a-go-go-related gene* (EAG) and KQT channels (Tian C. *et al.,* 2014), as well as non-voltage-gated channels. For the latter, examples are the hyperpolarization activated cation channels and TRP channels, whose gating properties are regulated by different stimuli (Barros F. *et al.,* 2012) and the cyclic nucleotide activated channels (CNG) (Jan LY, Jan YN., 1990), that regulate their gating through the binding of a ligand, c-AMP or c-GMP (Zagotta W.N. and Siegelbaum S.A., 1996). Moreover, SK/IK Ca^{2+}-activated K^+ channels, also share a similar transmembrane topology. In particular, the family of the Ca^{2+}-activated K^+ channels are classically divided into three subfamilies according to their single channel conductance: SK (small conductance) (Kca2.1, SK1; Kca2.2, SK2; Kca2.3, SK3); IK (intermediate conductance) (Kca3.1) and BK (big conductance) (Kca1.1) (Tian C. *et al.,* 2014). Among this subfamilies, SK and IK share a similar 6TM topology, whereas the BK channels, also called Maxi K-high voltage Ca^{2+} sensitive K^+ channel, present a 7 TM topology, related to the presence of a unique transmembrane segment (S0) within the N termini. This

segment is essential for accessory subunits modulation (Wallner M. *et al.,* 1996) and may act as voltage sensitivity modulator (Koval O.M. *et al.,* 2007).

1.4 The Role of T cells in Autoimmune diseases

The Immune System provides protection from external infectious pathogens, through the activation of a very high and specific immune response. To be effective, the immune response requires a small number of both B and T cells clones that binds to the antigen and undergo activation, proliferation and differentiation (Actor K.J., 2014). Lymphocytes are mainly two types, both derived from common haematopoietic precursors (Davis M.M. and Bjorkman P., 1988): T lymphocytes, so-called because of their development in the thymus, and B lymphocytes, derived from the bone marrow. T cells help to eliminate pathogens and contribute to mediate secondary responses, whereas B cells are mainly involved in humoral immunity as they are accountable for the production of antibodies (Actor K.J., 2014).

One of the most important requirements to ensure the harmonious functionality of the immune system, is a tight *equilibrium* between immunoreaction and immunoregulation. Autoimmune diseases (AD), caused by a continuous stimulation by antigens, can occur when this equilibrium is unbalanced (Zhao Y. *et al.,* 2015). AD are found in approximately 5-10% of the global population, although this percentage is continuously raising all over the world. The causes of this rise are still unclear, although a significant role is attributable to climate changes and industrialization (Devarajan P. and Chen Z., 2013). T cells play a pivotal role in balancing all the events taking place during an immune response. After exposure to antigen, Naïve T-cells, differentiate into activated effector T-cells (T_{EFF}), which migrate to the site of infection to counteract and ultimately clear the infection. After the infection is cleared, most of the T_{EFF} die, whilst some differentiate in memory T cells (Devarajan P. and Chen Z., 2013). How memory cells develop is still under debate and several developmental models have been proposed (Ahmed R. *et al.,* 2009). Memory T-cells exist in two main subtypes: T_{CM} (long-lived T cells) and $T_{EM,}$ (short-lived memory cells). Recent studies highlighted the presence of a third type of memory cells, T_{RM} (resident-memory) (Hu W. and Pasare C., 2013), that are found mainly in peripheral tissues (Ariotti S. *et al.,* 2012). Their function seems to be related to the tissue they are found in, although their specific involvement in tissue-specific diseases remain unclear (Bhargava P. and Calabresi P.A., 2015). Memory T cells are important contributors to

secondary immune responses, occurring from the exposure to previously encountered pathogens (Raphael I. *et al.,* 2020). However, when memory cells are autoreactive, such as in autoimmune diseases or chronic infections scenarios, they rise immune responses towards self-organs and tissues (Devarajan P. and Chen Z., 2013). During their development, particularly during the thymus selection, the autoreactive cells are eliminated via negative selection (Robey E. and Fowlkes B.J., 1994). However, some autoreactive cells can escape the selection and remain in circle. In normal conditions, auto reactive cells are regulated by the T_{reg} (regulatory T cell) but in autoimmune diseases, these fine regulatory mechanisms are lost, resulting in a persistent attack of self-organs and tissues by auto reactive T cells (Zhao Y. *et al.,* 2015). The number of autoreactive $CD4^+$ T memory cells (T_{CM}, T_{EM} and T_{RM}) is considerably higher in patients with autoimmune diseases compared to healthy patients, suggesting a critical role of these cells in the development of the disorders (Burns J. *et al.,* 1999; Allegretta M. *et al.,* 1990; Nielsen B.R. *et al.,* 2017). A typical setting in diseases such as Multiple Sclerosis (MS), type 1 diabetes mellitus (T1DM), psoriasis and many more, is represented by a very high number of T_{EM} cells and persistence of autoantigens (Devarajan P. and Chen Z., 2013). Considering the relevance of autoreactive T cells in the development of a wide *spectrum* of autoimmune diseases, it is highly desirable to design specific strategies aimed at targeting autoreactive T cells, still ensuring a normal functionality of naïve T cells (Wulff H. *et al.,* 2003 a,b).

T lymphocytes possess several ion channels within their membrane, involved in several processes, including the regulation of the membrane potential (V_m) and Ca^{2+} signalling, gene expression, apoptosis, proliferation, development, motility and regulation of the cell volume (Cahalan M.D. and and Chandy K.G., 2009). Investigations have conveyed to the identification of the major ion channel currents in T cells (Hamill OP *et al.,* 1981) (Figure 5), with a particular interest on the voltage-gated K^+ channel, Kv1.3, for the role played in the development of several diseases, including autoimmune and neuroinflammatory diseases, as well as some types of cancer. Kv1.3 together with the calcium-activated potassium channel, Kca3.1, are critical for T cells activation and are found to be differentially upregulated in the two subsets of T cells, T_{CM} and T_{EM} (Cahalan M.D. and Chandy K.G., 2009).

Kv1.3 has gained attention throughout the years as a potential therapeutical target for the treatment of human diseases, therefore a large number of studies is now focused on identify small molecules and/or peptide that can selectively target the channel.

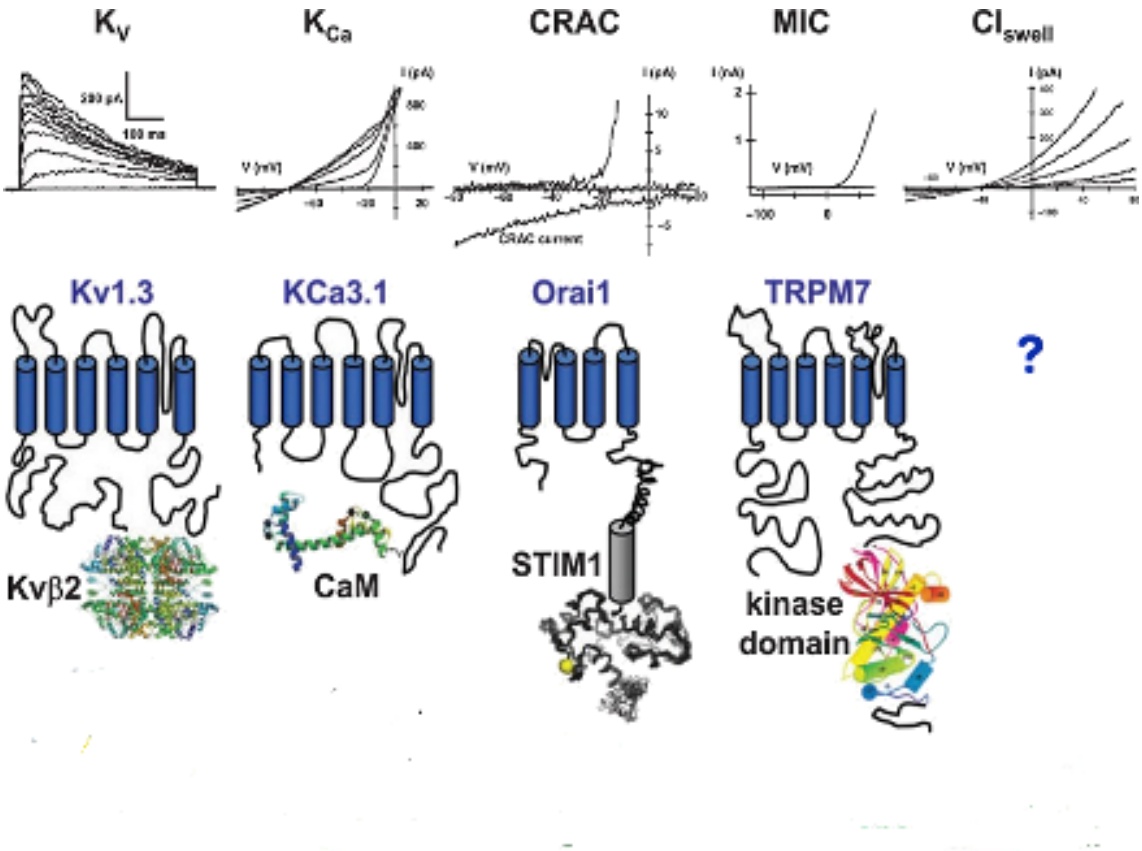

Figure 5. The main five types of ion channels expressed in T cells (Image adapted from Cahalan and Chandy, 2009). From left to right are showed the characteristic whole-cell patch clamp recordings and transmembrane structures for Kv1.3, Kca3.1, Orai1, TRPM7 and Cl_{swell}. For the latter the transmembrane structure was not reported.

1.4.1 The voltage-gated potassium channel Kv1.3

Kv1.3, encoded by KCNA3 gene, is a voltage-gated K^+ channel belonging to the *Shaker* related (Kv1, KCNA) subfamily. The structure of Kv1.3 is the typical showed by the voltage-gated channels. The channel is a tetramer, made up of four α-subunits assembled around a central pore and with a characteristic six transmembrane helices (6TM) architecture (Figure 6).
The segments (S1-S6) are connected by intra and extracellular loops; the pore domain is found between the segments S5-S6; the voltage sensor domain (VSD) is represented by the segment S1-S4, with the segment S4 charged positively and responsible for sensing the majority of the voltage differences across the membrane. Indeed, in response to the membrane depolarization, the charges move in direction of the electric field, thus determining the pore opening (Bezanilla F., 2000; Bezanilla F., 2008 b). The selectivity filter contributes to the high selectivity of the

channels towards K^+ ions and presents the typical "*signature sequence*" (TVGYG) conserved among the potassium channels. Kv1.3 can also associate with other subunits to generate the so-called *channelosome.* Association is seen with subunits such as Kvβ and KCNEs peptides, via the cytosolic domain (T1) within the -NH_2 end, as well as with a variety of membrane proteins such as integrins, as reported in T cells (Levite M. *et al.,* 2000); cortactin (Pérez-García M.T. *et al.,* 2018), PDZ proteins (Dlg1 and Dlg4) (Marks D.R. and Fadool, D.A., 2007; Szilágyi O. *et al.,* 2013) and caveolins (Pérez-García M.T. *et al.,* 2018).

Activation and inactivation properties of the channel are voltage dependent (Panyi G., 2005). In particular, inactivation of Kv1.3 is known as *C-type* or cumulative inactivation and is due to conformational changes at the external side of the pore of the channel (Grissmer S. and Cahalan M., 1989; Panyi G. *et al.,* 1995; Nguyen A. *et al.,* 1996). This type of inactivation differs from the classical "*ball and chain*" model observed in other K^+ or Na^+ channels (Cahalan and Chandy, 2009). Regarding the pharmacological properties, the channel is sensitive to common K^+ channels blockers such as tetraethylammonium (TEA) and 4-aminopyridine (4AP) and the current is also affected by micromolar concentration of quinine, verapamil and diltiazem (Cahalan M.D. *et al.,* 1985). The channel is also the target of peptides and toxins whose binding site is found at the outer vestibule of the pore region (Rodríguez de la Vega R.C. and Possani L.D., 2004; Giangiacomo K.M. *et al.,* 2004).

Kv1.3 is expressed mainly in the *Immune System* in T lymphocytes (Cahalan M.D. *et al,* 1985) and B lymphocytes (Wulff H. *et al,* 2004), but also in Natural killer (NK) cells (Koshy S. *et al,* 2013) and macrophages, where is found in association with Kv1.5 to form the hetero-tetrameric channel Kv1.3 / Kv1.5 (Villalonga N. *et al,* 2010). Kv1.3 is also expressed in the inner membrane of the mitochondria, where is the target of the apoptotic protein BAX (Szabo I. *et al.,* 2008; Szabo I. *et al.,* 2005). Although the major expression of Kv1.3 remains in the Immune System, the channel is also found in the *Nervous System*, in several subsets of neurons and glial cells: astrocytes (Grimaldi A. *et al.,* 2018), oligodendrocytes and microglia (Pérez-García M.T. *et al,* 2018).

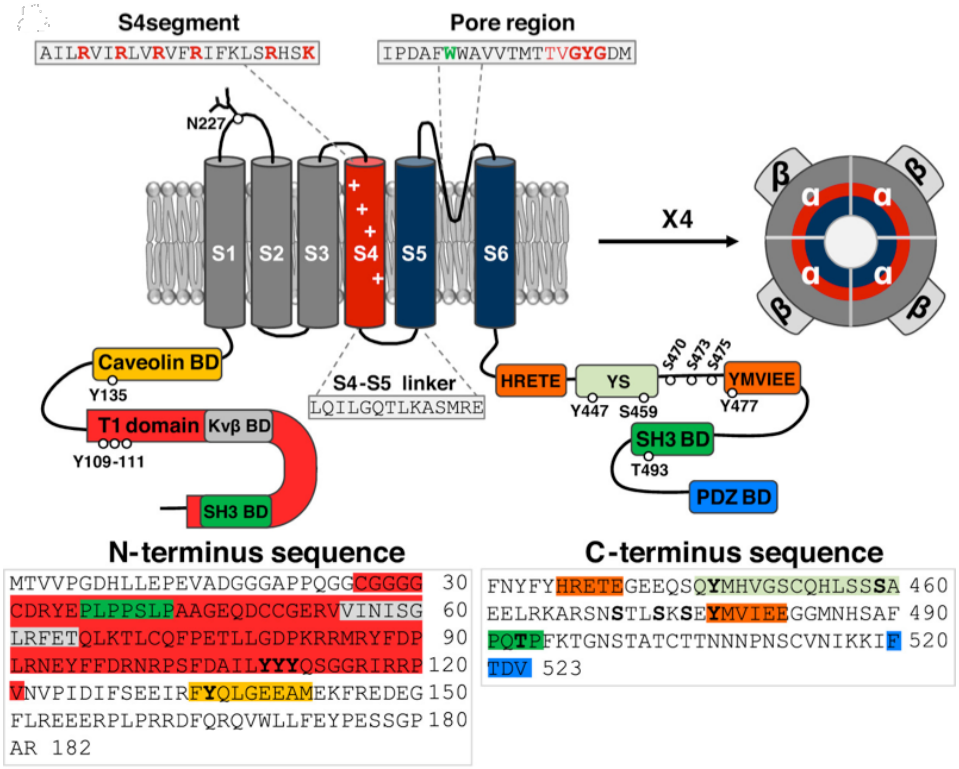

Figure 6. Characteristic Kv1.3 α-subunits arrangement (Image modified from Pérez-García M.T. *et al,* 2018). The segment S4 is highlighted in red and presents charged residues (+). Segments S5-S6 are highlighted in blue and form the pore region. The N-terminus sequence, C-terminus sequence and S4-S5 linker sequences are also showed.

1.4.2 Other ion channels found in T cells

Other channels found in T cells are: I) the calcium activated-K^+ channel Kca3.1; II) the calcium-release calcium-activated channel (CRAC); III) the swelling-activated Cl^- (Cl_{swell}) channel; IV) TRPM7 channel. Those represent the other major ion channel currents in T cells (Cahalan M.D. and Changy K.G., 2009). Additional K^+ channels, including Kv1.1, Kv1.2 and Kv1.6 have been found in mouse T cells (Freedman B.D. *et al.,*1995; Liu Q.H. *et al.,* 2002). The two pore domain channels, TASK-1 and TASK-3, have been discovered in human T cells (Meuth S.G. *et al.,* 2008) and TRESK in Jurkat T cells (Pottosin I.I. *et al.,* 2008). The latter, also express the Ca^{2+}-activated K^+ channel, Kca2.2 (Jäger H. et al., 2000). Furthermore, a small percentage of human T cells express also voltage-gated Na^+ channels (Cahalan M.D. *et al.,* 1985).

1.4.3 The role of Kv1.3 and Kca3.1 during the immune response

Both Kv1.3 and KCa3.1 play a critical role in T cells activation, a pivotal event to generate an immune response. T cells activation is triggered by the activation of T cell receptor (TCR) after antigen is presented by the antigen-presenting T cells (APC). This initial recognition determines an increase of the intracellular Ca^{2+} concentration (Ca^{2+}_i), essential for cytokines release (Nicolaou S.A. *et al.,* 2009). During an immune response (Figure 7), the first event derived from the engagement of the T cell receptor (TCR) with the antigen, bound to the major histocompatibility complex (MHC) on the antigen presenting cells (APC), induces the activation of the phospholipase Cγ (PLCγ) and the production of 1,4,5-inhositol-triphosphate (IP_3). IP_3 binds to the inositol-triphosphate- receptor (IP_3R) on the endoplasmic reticulum (ER), provoking the release of Ca^{2+} from the intracellular store. Stromal interaction molecule 1 (STM1) or stromal interaction molecule 2 (STM2), activates the opening of the calcium-release calcium-activated channel (CRAC), determining an influx of Ca^{2+} into the cells, which results in gene expression through calcineurin NFAT pathway (Zhao Y. *et al.,* 2015). The overall increase of Ca^{2+}, essential for T cell activation and cytokines production, is counterbalanced by the opening of the potassium channels Kv1.3 and Kca3.1 that mediate efflux of K^+ ions to balance the rise of Ca^{2+} in the cytoplasm (Wulff and Zhorov 2008; Feske S. *et al.,* 2012). In such way, the channels contribute to maintain the membrane potential hyperpolarized (Feske *et al.,* 2012).

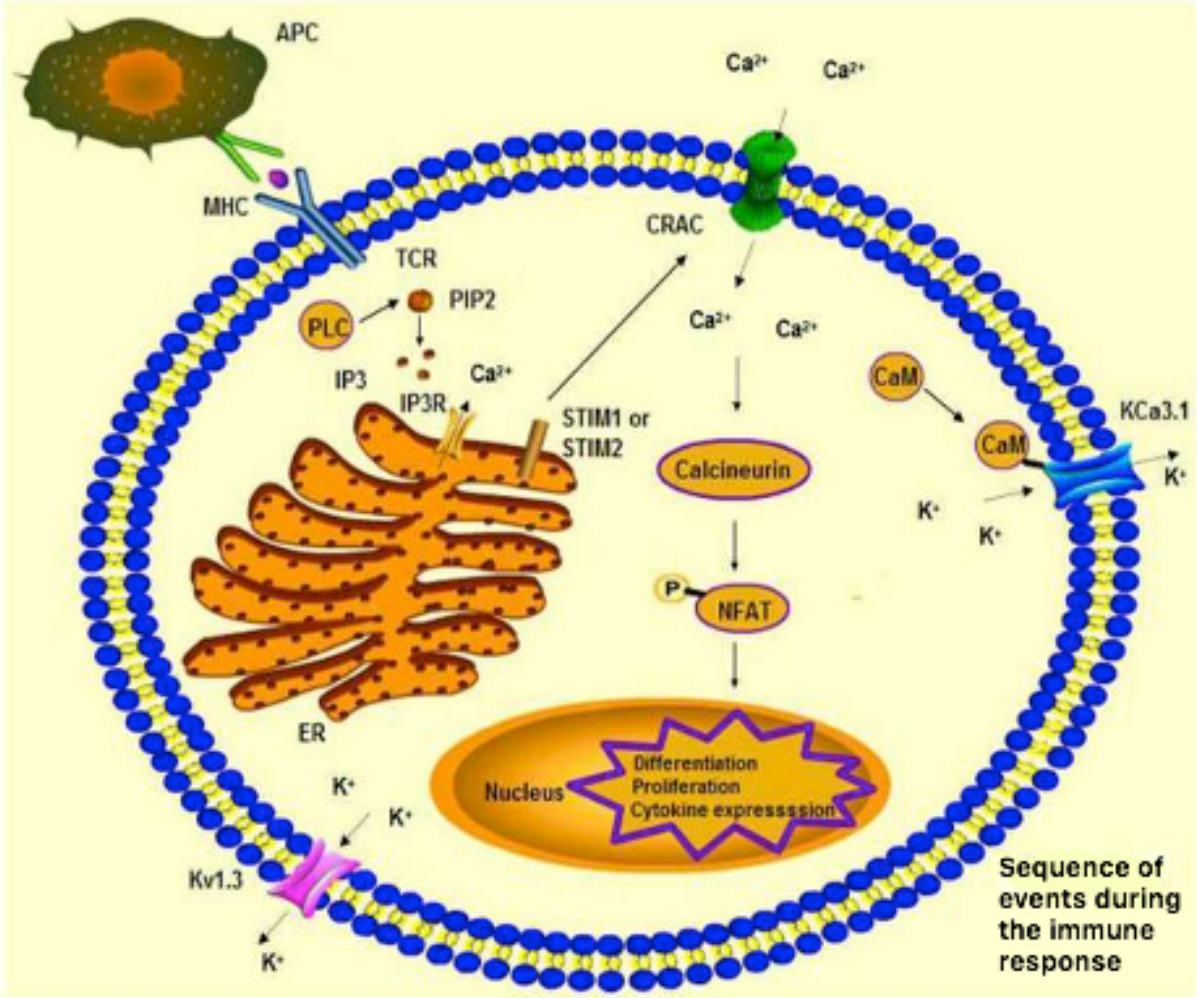

Figure 7. Sequence of events during the immune response in memory T cells (Image modified from Zhao Y. *et al.,* 2015). The engagement of APC cells with TCR expressed on T cells, initiate the cascade of events that result in the activation of the voltage-gated K^+ channels Kv1.3 and the KCa3.1 channel that counterbalance the increase in $[Ca^{2+}]_i$.

Both Kv1.3 and Kca3.1 channels have been found at the Immunological Synapse (IS) (Nicolaou S.A. *et al.,* 2007 (a); Nicolaou S.A. *et al.,* 2007 (b)). The first organization of an immunological synapse has been described in 1998 for $CD4^+$ T cells and antigen-presenting B cells (Monks *et al.,* 1998). Specifically, the immunological synapses are described as highly organized region of contact between T cell and cell presenting antigen, APC (Lin J. *et al.,* 2005; Nicolaou S.A. *et al.,* 2009). Structurally, they are organized in two compartments or regions: a central region, *c-SMAC*, formed by T cell receptor (TCR) and associated signalling molecules such as CD2, CD28, PKC-O, LcK, Fyn, CD4 and CD8 (Huppa and Davis, 2003), and

peripheral region, *p-SMAC*, containing the leukocyte function-associated molecule-1 (LFA-1) and the scaffolding protein talin (Lin J. *et al.,* 2005).

The contribution of Kv1.3 and Kca3.1 channel to the intracellular Ca^{2+} concentration differs in the different subset of memory T cells and depends on their level of expression. Quiescent T_{CM} and T_{EM} cells exhibit a similar K^+ channels expression level, however this changes during activation. In effector T_{EM} cells ($CD4^+$ or $CD8^+$ $CCR7^-$ $CD45RA^-$), Kv1.3 channels are significantly upregulated (about 1500 channels/cells); whereas in effector T_{CM} cells ($CD4^+$ or $CD8^+$ $CCR7^+$ $CD45RA^-$), Kca3.1 channels are upregulated (Cahalan M.D. and Chandy K.G. 2009). Because of this differential upregulation of the two channels in the two subset of T cells, it is possible to achieve a selective pharmacological modulation, so that KCa3.1 inhibitors preferentially suppress $CCR7^+$ naïve and central memory T cells (T_{CM}), and Kv1.3 inhibitors suppress $CCR7^-$ effector memory T cells (T_{EM}) (Chandy K.G and Norton R.S., 2017). T_{EM} cells are the mainly involved in autoimmune diseases, hence why blockers that can preferentially suppress Kv1.3 without affecting naïve and T_{CM} cells, are regarded as a desirable therapy for the treatment of these diseases (Cahalan and Chandy 2009; Chandy and Norton, 2017; Devarajan and Chen, 2013; Wulff *et al.,* 2003, a).

1.5 Potassium channels pharmacology

K^+ channels pharmacology is characterized by sensitivity to three main categories of inhibitors: venom-derivate peptides, organic small molecules and metal ions (Pérez-García M.T. *et al.,* 2018; Wulff H. and Zhorov B.S., 2008). At present, isoform-specific antibodies that specifically act on a certain number of ion channels, have also been added to the classification of the K^+ channels inhibitors (Gómez-Varela D. *et al.,* 2007). Based on the mechanisms of action, K^+ channels ligands are identified into two main classes: the pore blockers and the modulators (Kuzmenkov A.I. *et al.,* 2015). Ligands belonging to the pore blockers class, are able to block the ion flux by binding to the pore region of the channels (Mackinnon R. and Miller C., 1989). Inhibitors that act by modulating channel gating properties through the binding to the voltage-sensor domain or auxiliary subunits, are commonly identified as modulators (Perez-Garcia M.T. *et al.,* 2018; Swartz K.J., 2007; Swartz K.J. and Mackinnon R., 1997 a, b). TEA and 4-AP have been the widest organic small molecules used for pharmacological studies on K^+ channels, displaying a very potent inhibitory effect and specificity on the channels. Venom-derived toxins are considered the largest family of ion

channel blockers (Wang X. *et al.,* 2020). They are highly potent peptides found in the venom of various species, comprising sea anemones, scorpions, spiders, snakes, insects, cone snails and worms. Their structure consists of a variable number of aminoacidic residues, between 18-60 amino acid residues, cross-linked by disulphide bridges (Mouhat S. *et al.,* 2004).

Animals use venom for different purposes, including self-defence and predatory behaviours. Although the composition of the venom may vary from animal to animal, the composition of the most comprehend inorganic salts, low molecular weight organic molecules, peptides (2-10 KDa) and enzymes (< 10 KDa) (King G.F., 2011). Venom-derived toxins are able to block ion channels with very high affinity and selectivity and nowadays their application have been found successful for the treatment of several conditions, including pain, epilepsy and cardiovascular diseases, and some venom-derived peptides are currently in clinical development for tumor imaging (for example, Chlorotoxin, from the venom of the stalker scorpion *Leiurus quinquestriatus hebraeus*) (Pennington M.W. *et al.,* 2018). Furthermore, venom-derived peptides found a wide application not only in the pharmaceutical area but also in the cosmetic area, as well as in agricultural applications (Pennington M.W. *et al.,* 2018). In general, toxins fall into two categories based on their mechanism of action (Figure 8). Toxins from scorpions, sea anemones, snakes and cone snails are defined "*pore blockers*" because they bind to the outer vestibule of K^+ channel, thereby blocking the ion conducting pore by inserting a critical residue into the channel pore (Mouhat S. *et al.,* 2004; MacKinnon R. and Miller C., 1989; MacKinnon et *al.,* 1990). An important structural and functional feature conserved among these toxins, is certainly the "*functional dyad*", typically constitute by a lysine (*Lys*) residue plus aromatic (*Tyr* or *Phe*) or aliphatic (*Leu*) aminoacidic residues, separated by 6.6 Å (Dauplais M. *et al.,* 1997; Gasparini *et al.,* 1998). An intriguing observation to raise from this point, is that the dyad is well conserved among structurally unrelated proteins; this is strictly related to the pivotal role of both Lys and aromatic neighbouring residues in the toxin binding (Dauplais M. *et al.,* 1997). Analysis on scorpion toxins revealed that the positively charged ammonium groups of the Lys may mimic the K^+ ions entering the pore, thus occluding the ion pathway (Goldstein S.A. and Miller C., 1993; Giangiacomo K.M. *et al.,* 1992; Park C.S. and Miller C., 1992). A similar mechanism has been proposed also for sea anemone-derived toxins (Dauplais M. *et al.,* 1997). Regarding the aromatic residues, they have been addressed to two main roles: 1) promoting local hydrophobic interactions between the toxin and the channel; 2) sustain the crucial Lys when this plugs into the pore, by promoting the protrusion of the residue outside the toxin surface (Dauplais M. *et al.,* 1997). Despite the

importance of the functional dyad, is interesting to note that some toxins lacking this conserved feature, are still able to block Kvs channels (Mouhat S. *et al.,* 2004). An example is given by the scorpion toxin Tc32, which does not bring a functional Lys within the amino acidic sequence and does not contain any aromatic amino acids (Batista C.V. *et al.*, 2002).

Differently, toxins that act by binding to the voltage sensor domain (VSD) of the Kvs channels, cause a modification of the kinetic behaviour, thus affecting the gating properties (Swartz K.J. and MacKinnon R., 1997 a,b; Swartz K.J., 2007). Toxins that act in such way have been classified as gating modifier toxins (GMTs) and a great percentage of those is represented by spider-derived toxins (e.g. Hanatoxin (HaTX) from the Chilean tarantula *Grammostola spatulata*). At presents, toxins and peptides acting on K^+ channels are the most studied and this is in agreement with the concept that K^+ channels, by presenting a broad structural and functional diversity, are considered a very valuable therapeutic target (Lewis R.J. and Garcia M.L., 2003). Nevertheless, an increasing number of venom-derived toxins are emerging as sodium channels inhibitors and this is particularly important considering their involvement in pain sensations.

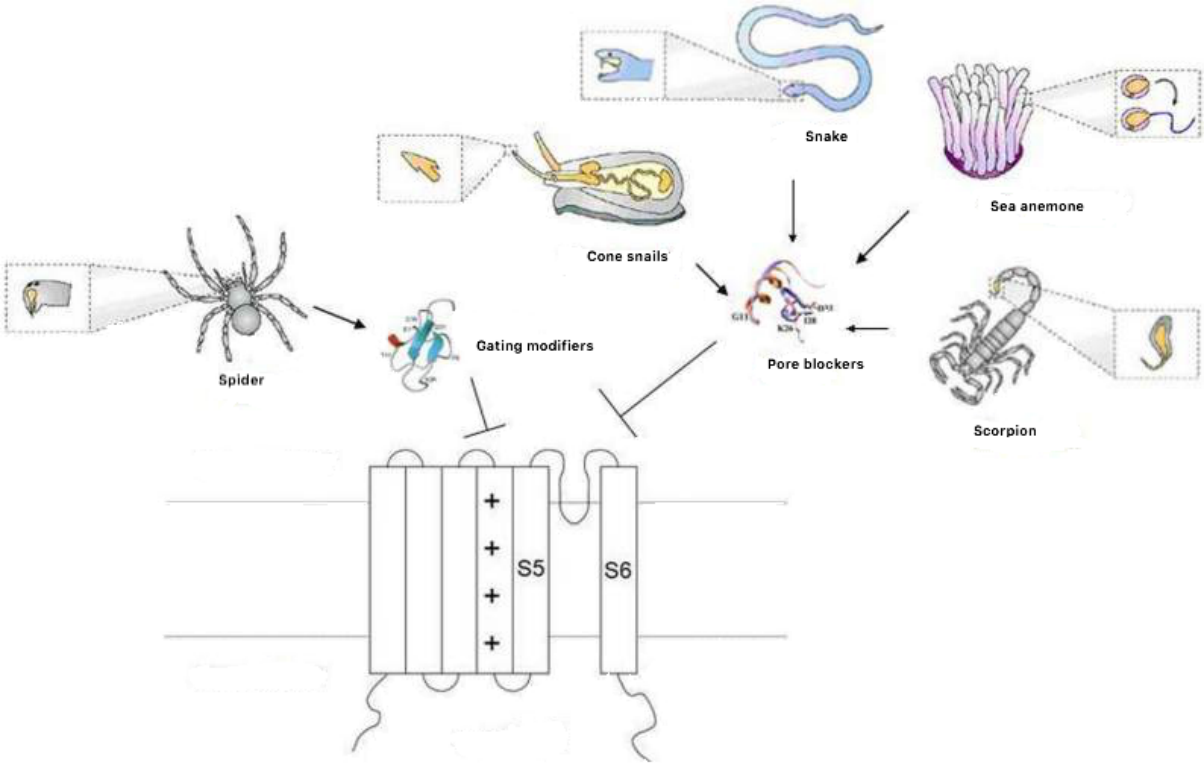

Figure 8. Representation of the mechanism of action of toxins on K^+ channels. The two main category of toxins, the pore blockers and the gating modifiers are represented. Spider toxin acts mainly by binding the segment S4, known to be the sensor of the voltage, whilst toxins derived from scorpions, sea anemones, snakes and cone snails block the central pore of the channel, preventing K^+ transport (Image modified from Yipeng Zhao *et al.,* 2015).

1.5.1 Kv1.3 Pharmacology

Considering the pivotal role in T cell physiology and is implication in the pathogenesis of several autoimmune diseases mediated by T_{EM} cells, selective block of Kv1.3 has become an attractive potential tool for the treatment of autoimmune diseases such as multiple sclerosis (MS), rheumatoid arthritis (RA), type I diabetes mellitus (T1DM) and many more, as well as neuroinflammatory diseases (Wang X *et al.,* 2020; Wulff H. and Zhorov B.S., 2008; Zhao Y. *et al.,* 2015). The widest and most representative group of toxins that act on K^+ channels and therefore can block Kv1.3, are obtained from the venom of sea anemones and scorpions. Both groups of toxins have been extensively studied in the years and represent a rich source of peptides and toxins active on ion channels and receptors. *ToxProt* database (Jungo F. and Bairoch A., 2005), counts 236 peptides or protein toxins isolated from 45 different sea

anemones species (Prentis J.P. *et al.,* 2018). *UniProt*, reports a large number of ligands that act on K^+ channels from scorpion venom (Mouhat S. *et al.,* 2008), as well as *Kalium* database, that contains all known scorpion toxins, reports a list of 174 molecules in total that act on K^+ channels (Kuzmenkov A.I. *et al.,* 2016).

1.5.2 Sea anemone toxins

Sea anemones are considered a group of exclusively predator marine animals belonging to the phylum *Cnidaria*, class *Anthozoa*, subclass *Hexacorallia*, order *Actinaria* (Geller J.B. *et al.,* 2005). Sea anemones from the family *Aliciidaea* are dangerous to human. In particular, the venom from *Phyllodiscus semoni* has been linked to acute renal failure (Mizuno M. *et al.,* 2000) and the venom-derived protein toxin, PsTx-115, have been shown to cause several kidney damages in rat model (Mizuno M. *et al.,* 2007). Sea anemones possess specialized stinging cells, cnidocytes, furnished with organelles called nematocysts (cnidae), that contain a complex blend of toxins that the animal can use for predatory or defence purposes (Fautin D.G., 2009). Once expelled from the nematocysts, toxins can penetrate the epithelium of the victim, ultimately leading to paralysis (Honma T. and Shiomi K., 2006). Nematocysts present differences among sea anemones, according to their differential specialization. Sea anemones also produce toxins in a second type of cells, an ectodermal gland cells (Moran Y. *et al.,* 2012; Columbus-Shenkar Y.Y. *et al.,* 2018). The venom composition includes a mixture of proteins, peptides and non-peptidic compounds (Madio B. *et al.,* 2019). Among the non-peptidic compound, two small molecules, caissarone and bunodosine 391, have been identified and characterized from the venom of the Brazilian sea anemones *Bunodosoma caissarum* (de Freitas J.C. and Sawaya M.I., 1989) and *Bunodosoma cangicum*, respectively (Madio B. *et al.,* 2019), but other non-peptidic components still remain unknown.

Anemone toxins can be classified into 15 known families. Of those, the four most common families are: *Actinoporin family*, sea anemone superfamily; *Sea anemone Na^+ channel inhibitory toxin family*: type I subfamily; *Sea anemone type 3 (BDS) K^+ channel toxin family* and *Venom Kunitz-type family*, sea anemone type 2 K^+ channel toxin subfamily (Prentis J.P. *et al.,* 2018). A very potent inhibitor of Kv1.3 and probably the most representative, is *ShK* toxin, isolated from the sea anemone *Stichodactyla heliantus* (Castañeda O. *et al,* 1995).

ShK is a peptide of 35 amino acidic residues, with a characteristic motif comprising six cysteine residues connected by three disulphide bridges as Cys3-Cys35; Cys12-Cys28 and Cys17-

Cys32 (Pohl J. *et al.,* 1995). Two main residues, indicated as the Lys22 and the neighbour Tyr23, are fundamental for the toxin to bind to all the four subunits of the channel. The residues interact with the shallow vestibule at the outer entrance of the channel pore, with the Lys22 protruding and occluding the pore following the classic "*cork in a bottle*" model, whilst Tyr23, seals the binding (Chang S.C. *et al.,* 2018). The two residues, Lys22 and Tyr23, form the so-called "*functional dyad*" (Kalman K. *et al.,* 1998; Pennington M.W. *et al.,* 1996; Pennington M.W. *et al.,* 2009; Chandy K.G. and Norton R.S., 2017; Lanigan M.D. *et al.,* 2002; Rauer H. *et al.,* 1999), a characteristic arrangement conserved also in other voltage-gated K^+ channel inhibitors derived from different species (Duplais M. *et al.,* 1997; Honma and Shiomi, 2006). Although this distinctive arrangement functional dyad plus neighbouring aromatic or aliphatic residue (Chandy K.G. and Norton R.S., 2017; Gilquin B. *et al.,* 2005) is shared by many peptides, some types of toxins present a slightly different organization, with the critical Lys in a different position within the peptide sequence (Chandy K.G. and Norton R.S., 2017; Gilquin B. *et al.,* 2005). An example is given by BgK from the sea anemones *Bunodosoma granulifera*, which displays the functional lysine in position 25.

ShK present a very high affinity (K_i ~10 pM) for Kv1.3 but also display high pM affinity for Kv1.1, Kv1.4 and Kv1.6 which are expressed, respectively, in cardiac tissues and in the brain, and also for Kv3.2 and KCa3.1 (Chang S.C. *et al.,* 2018; Kalman K. *et al.,* 1998). Due to this affinity for other K^+ channels, several modifications have been tempted on ShK in order to make the peptide more specific for Kv1.3 over other close-related K^+ channels, leading to the design of a series of ShK analogues (Table 1). Among all the analogues that have been produced, a particular mention is dutiful towards ShK-186, at present *Dalazatide*, a 37 amino acid residues synthetic peptide, the first Kv1.3 inhibitor tested in clinical trials for the treatment of autoimmune diseases (Tarcha E.J. *et al.,* 2017). Dalazatide completed Phase 1a and 1b in trials in 2016 (Prentis P.J. *et al.,* 2018).

Name	Modifications	Target	References
ShK-Dap^{22}	Lys 22 is replaced with 1,3 diaminopropionic acid (Dap)	> 20-fold selectivity for Kv1.3. Kv1.1-Kv1.2 heterotetramers	Kalman K. *et al*., 1998; Lanigan M.D. *et al*., 2002; Middleton R.E. *et al*., 2003
ShK-F6CA	Fluorescein-6-carboxyl (F6CA), is attached to the N-terminus of the peptide via a hydrophobic AEEA linker (2-aminoethoxy-2-ethoxy acetic acid; mini PEG)	100-fold selectivity for Kv1.3 over Kv1.1	Chang S.C. *et al.,* 2018; Beeton C. *et al.,* 2003
ShK-170	L-phosphotyrosine is attached to the N-terminus of the peptide via an AEEA linker	ShK-170 shows 100-1000-fold specificity for Kv1.3	Chang S.C. *et al.,* 2018
ShK-186	Similar to ShK-170 in the N-terminus but the C-terminus is replaced by an amide	Similar specificity of ShK-170 towards Kv1.3	Chang S.C. *et al.,* 2018;
ShK-192	L-phosphotyrosine (N-terminus), is replaced by a non-hydrolyzable paraphosphonophenylalanine (Ppa) and Met21 with non-natural amino acid norleucine	High specificity towards Kv1.3, over 100-fold selectivity over other close-related channels	Chang S.C. *et al.,* 2018; Pennington M.W. *et al.,* 2009;
ShK-EWSS	The AEEA linker and L-phosphotyrosine are replaced by the residues glutamic acid (E), tryptofan (W) and two serines (S)	High selectivity towards Kv1.3 over close-related channels	Chang S.C. *et al.,* 2015; Chang S.C. *et al.,* 2018
ShK-[K18A]	K 18 is substitute with Alanine.	High selectivity towards Kv1.3 over Kv1.1	Rashid M. H. *et al.,* 2013; Chang S.C. *et al.,* 2018
ShK-amide	Additional Lys and amide on the C-terminus of the peptide	Improved selectivity towards Kv1.3	Pennington M.W. *et al.,* 2012

Table 1. Table depicting the main ShK analogues with relative chemical modifications and targets.

1.5.3 Scorpion toxins

Scorpions, class *Arachnida*, phylum *Artropoda*, are considered one of the ancient groups of animals that inhabited the earth (Cao Z. *et al.,* 2014). They are classified into 18 subfamilies, most of which belong to the genera *Buthidae* and constitute around the 25% of the world biodiversity (Prendini L. and Wheeler C., 2005). Scorpions possess a venom apparatus used for capturing the prey and/or for defence from predators. Scorpion represent a public health problem in some part of the world, where a significant number of envenomation cases from different scorpion species are reported every year, some of which are fatal for humans (Chippaux J.P. and Goyffon M., 2008). The most dangerous species for human are from the genus *Androctonus*, *Buthus* and *Leiurus* in North Africa and Middle East; *Centruroides* and *Tityus* in America; *Mesobuthus* in Asia and *Parabuthus* in South Africa (Caliskan F. *et al.,* 2013). Scorpion venom is an heterogenous blend of inorganic salts, free amino acids, heterocyclic components, peptides, proteins and enzymes (such as phosphodiesterases, phospholipases, glucosaminoglycans and bio-chemicals such as histamine, serotonin, tryptophan and many more) (Quintero-Hernández V. *et al.,* 2013). The number of components in the venom of scorpions varies, reaching over 600 different components in certain genus. Considering the composition and the presence of a variable amount of different toxins (such as neurotoxins, cardiotoxins, nephrotoxins and hemotoxins), scorpion venom is a valid source of ion channels inhibitors and/or modulators (Oliveira I.S. *et al.,* 2019). The amount of toxins present in the scorpion venom is only a small fraction of the total composition, generally spacing between 0.01-0.5 % of the venom (Miller C., 1995). The first peptide described for its inhibitory effect on K^+ channels in the electrophysiological preparation of the squid giant axon, was Noxiutoxin (NTX) isolated from the venom of the *Centruroides noxious* in 1982 (Carbone E. *et al.,* 1982; Possani *et al.,* 1982). Charybdotoxin (ChTX) from *Leirus quinquestriatus,* characterized soon after NTX toxin, represent one of the most extensively studied scorpion peptide and was widely used as a probe for structural studies aimed at understanding the structure-functional properties of K^+ channels (Sugg E.E. *et al.,* 1990; Miller C., 1995). Other examples of scorpion toxins well characterized are *Iberiotoxin* (IbTX) (Galvez A. *et al.,* 1990), *Margatoxin* (MgTX) (Garcia-Calvo M. *et al.,* 1993), *Kaliotoxin* (Crest M. *et al.,* 1992), and many more. These toxins share a common three-dimensional folding, comprising a short α-helix segment and a β-sheet of two or three strands, stabilized by three or four disulphide bridges in conserved position (Possani D.L. *et al.,* 1999). Most of the known toxins show a common structural motif stabilized by three disulphide bridges, with some exception

represented by Pi1 toxin from *Pandinus imperator*, and HsTX1 toxin from *Heterometrus spinnifer*, that present an additional disulphide bridge to stabilize the structure (Olamendi-Portugal T. *et al.,* 1996; Delepierre M. *et al.,* 1997; Lebrun B. *et al.,* 1997). The most predominant components of scorpion-venom affecting Kvs channels are peptides that adopt a characteristically CS α-β (cysteine-stabilized α-helical and β-sheet) fold (Gao B. *et al.,* 2013).Of these peptides, the largest family is represented by the α-KTx toxins (Tytgat *et al.,* 1999; Rodriguez de la Vega R.C. and Possani L.D., 2004). This group of toxins includes peptides of 23-42 residues, six cysteines residues motif and three or four disulphide bridges (Quintero-Hernàndez V. *et al.,* 2013). These toxins further fall at least into three subfamilies: *Charybdotoxin-like-toxins* (subfamily 1) that potently inhibit BK channels; *Noxiustoxin-like-peptides* (subfamily 2) and *Kaliotoxin-like-peptide* (subfamily 3) that act on Kvs channels (Miller C., 1995). Other than α-KTx toxins, a second family, β-KTx toxins, and a third family, γ-KTx toxins, are included in the group of KTXs toxins.

β-KTXs family, includes toxins with aminoacidic sequences of 45-68 residues (Diego-García E. *et al.,* 2008); whereas the γ-KTXs family, comprises peptides with similar size and three-dimensional structure showed by the α-KTXs family peptides, but different selectivity and binding region. Indeed, they are selective for hERG channels and interact with the turret region more than the pore (Zhang M. *et al.,* 2003; Xu C.Q. *et al.,* 2003). Other minor components of scorpion venom are represented by peptides that have different folds. Of those, an interesting category is given by peptides that share a common motif, the ICK (inhibitory cysteine knot)-type toxins. ICK is a conserved structural motif shared by a large number of polypeptides found in different phyla, animal, plant and fungus. Toxins that have the ICK motif, are highly conserved at both gene structure and precursor organization level, despite presenting a very low sequence similarity (<30%) (Zhu S. *et al.,* 2003).

Toxins can act by two different mechanisms: "*pore plugging*" and "*intermediate mode*". The pore plugging toxins act by binding to specific residues in the external vestibule of K^+ channels, occluding the conduction pore (Anderson *et al.,* 1988; Mackinnon and Miller, 1988; Miller 1988; Park and Miller, 1992a; Giangiacomo *et al.,* 1992). In this model, toxin locks into the channel selectivity filter with the Lys residue, establishing a strong interaction (Oliveira I.S. *et al.,* 2019). The most important residues involved in the interaction toxin-channel and conserved among the different scorpion toxins acting on Kv1 channels (Tytgat *et al.,* 1999), are represented by K27, M29 and M30. K27, the key residue for the toxin binding, slightly protrude

into the K^+ conduction pore, and corresponds to the residue K22 in ShK toxin. Mutagenesis analysis have demonstrated that the substitution of K27 with an arginine, destabilized the toxin over 1000-fold (Miller C., 1995), underlying the fundamental role of the lysine in the protein-protein interaction. Some toxins present a lysine in a different position within the peptide sequence (Chen R. *et al.,* 2011; Cerni F.A. *et al.,* 2014). Alternatively, toxins that bind to the KCa2 channels, can interact with a negatively charged extracellular loop of the channel via a patch of basic residues, according to the well characterized "*intermediate mode*" (Rodriguez de la Vega *et al.* 2013; Andreotti et al., 2005).

Because of their relevance as therapeutical tool for blocking ion channels and for their clinical relevance as neurotoxins, scorpion toxins have been evaluated for the treatment of several diseases such as immune diseases (e.g. Kaliotoxin (KTX) from *Androctorus mauretanicus* (Crest M. *et al.,* 1992) and OSK1 from *Orthochinus scrobiculosus* (Chen R. and Chung S.H., 2012), neurological diseases, cancer and others (BenNasr Hmed *et al., 2013*). Of the latter, a remarkable example is given by toxins like BmK AGAP derived from the venom of the scorpion *Buthus martensii* and Chlorotoxin from the venom of the deathstalker *Leiuurus quinquestriatus*. Both toxins show anticancer activity towards glioma cells (Baby J. and Jency G., 2012). In particular, Chlorotoxin, by exhibiting a specific-inhibitory effect towards small conductance chloride (Cl^-) channels (DeBin J.A. and Strichartz G.R., 1991), represent an important tool for early detection of glioma cancer cells (Lyons A. *et al.,* 2002). Another example is given by Bengalin from the Indian scorpion *H. bengalensis,* that shows antiproliferative, cytotoxic and apoptogenic activity against human leukemic cells (Das Gupta S. *et al.,* 2006).

1.5.4 Spider toxins

Spiders show an extensive biological and ecological diversity, with more than 49.007 species, update at the writing date, diffused all over the world (G.Corzo and P.Escoubas, 2003; Catalog, W.S. World Spider Catalogue). Spiders dangerous for human are limited to few taxa only, including the mygalomorph Australian funnel-web spiders (*Atrax* sp. and *Hadronyche* sp.), the araneomorph recluse spiders (*Loxosceles* sp.), widow spiders (*Latrodectus* sp.) and armed spiders (*Phoneutria* sp.) (Nentwig W. and Kuhn-Nentwing L., 2013). The venom is produced in specialized venom glands and released into the glandular lumen (Langenegger N. *et al.,*

2019). The composition varies between different species, as well as in individual of the same species and is affected by age, gender or geographic (Escoubas P. *et al.,* 2008; Zobel-Thropp, P.A *et al.,* 2018). Generally, the venom components are divided into four categories: 1) small molecular mass compounds (SMMCs) that include ions, organic acids, nucleotides, nucleosides, amino acids, amines and polyamines (Kuhn-Nentwig, L. *et al.,* 2011); 2) antimicrobial peptides (AMPS) also known as cytolytic or cationic peptides; 3) peptide neurotoxins; 4) proteins and enzymes (Langenegger N. *et al.,* 2019). From a structural point of view, most venom-derived peptides share an ICK (inhibitory cysteine knot) motif, constitute by a triple stranded antiparallel β-sheets, containing six cysteines motif stabilized by, at least, three disulphide bridges, with C1-C4, C2-C5, C3-C6 connectivity (Langenegger N. *et al.,* 2019; Dongol Y. *et al.,* 2019). All spider venom derived peptides, with very few exceptions, (e.g. Atracotoxins) share ICK motif with three disulphide bridges (Dongol Y. *et al.,* 2019). However, the diversity of peptides that display ICK motif is particularly wide with the result that some of the peptides, do not show a β-sheets structural arrangement (Agwa A.J. *et al.,* 2017 (a); Henriques S.T. *et al.,* 2016; Minassian N.A. *et al.,* 2013). Furthermore, some peptides display other structural motifs, however with less frequency compared to ICK motif (Langenegger N. *et al.,* 2019). A second important structural characteristic shared among the ICK motif peptides, is the presence of hydrophobic patch surrounded by charged amino acids, on the toxin's surface. (Agwa A.J. *et al.,* 2017 (b); Bosmans F. *et al.,* 2006). These charged amino acids include Trp, Tyr and Lys, which frequently participate in the peptide-lipid bilayer interaction (Killian J.A. and von Heijne, 2000). This structural feature is thought to contribute to the potency and selectivity of the peptides towards the target (Wang J.M. *et al.,* 2004; Lawrence N. *et al.,* 2018; Murray J.K. *et al.,* 2015; Smith J.J. *et al.,* 2007; Liu Y. *et al.,* 2012; Luo J. *et al.,* 2014; Cardoso F.G. *et al.,* 2015; Klint J.K. *et al.,* 2015; Henriques S.T. *et al.,* 2016; Minassian N.A. *et al.,* 2013).

Spider-venom derived peptides act on a broad *spectrum* of ion channels and receptors, including transient receptor potential (TRP) channels, acid sensing ion channels (ASICs), mechanosensitive ion channels (MSICs), ionotropic glutamate receptors (GluRS), G-protein coupled receptors (GPCRs), voltage-gated sodium channels (Na_v), voltage-gated potassium (K_v) channels, voltage-gated calcium (Ca_v) channels and calcium-activated potassium (K_{ca}) channels (King G.F. and Hardy M.C., 2013; Cardoso F.C. and Lewis R.J., 2019; Dongol Y. *et al.,* 2019). These peptides act, mainly, by modulating the gating mechanism of the channels, thus modifying the kinetics behaviour by controlling the movement of the paddle motif,

constitute by S3-S4 segments, when this translocate from one side to the other of the membrane (Bosmans and Swartz, 2010; Ruta *et al.,* 2003; Swartz and Mackinnon 1995; Swartz and Mackinnon 1997 (a) and (b); Agwa A.K. *et al.,* 2017 (a)). For such properties, they are included in the category of the gating modifier toxins (GMTs) (Agwa A. J. *et al.,* 2017 (b)). Gating modifiers toxins can act differently on the gating mechanism of the channel, according to the site where the peptide binds to the channel (Agwa A.K. *et al.,* 2017 (a)). Although a great fraction of the peptides derived from spiders modulate sodium channels, several of those are able to inhibit potassium channels. A great example is given by Hanatoxin (HaTX1 and HaTX2) from the venom of a Chilean tarantula *G. spatulata* (Swartz and Mackinnon, 1995). Below a table that summarize spider-venom peptides that act on K^+ channels mainly by modify the channel gating (except HpTX 1-3 toxins) (Table 2).

Name	Origin	Target	References
Hanatoxin	*Grammostola spatulata*	Kv2.1 and Kv4.2	Swartz K.J. and MacKinnon R., 1995
SGTX1	*Scodra griseipes*	Kv2.1	Marvin L. *et al.,* 1999; Lee C.W. *et al.,* 2004
GxTx1E (Guangxitoxin)	*Plesiophrictus guangxiensis*	Kv2.1	Herrington *et al., 2006*
ScTx1 (Stromatoxin)	*Stromatopelma calceata*	Kv2.1, Kv2.2 and Kv2.1/Kv9.3	Escoubas P. *et al.,* 2002
HmTx1,2 (Heteroscondratoxins)	*Heteroscondra maculate*	Kv2 and Kv4	Escoubas P. *et al.,* 2002
PaTX 1,2 (Phrixotoxins)	*Phrixotrichus auratus*	Kv4.3/ Kv4.2	Diochot *et al.,* 1999
HpTx1-3 (Heteropodatoxins)	*Heteropoda venatoria*	Kv4	Sanguinetti *et al.,* 1997; Zarayskiy *et al.,* 2005
TLTX1-3	*Theraphosa leblondi*	Kv4	Ebbinghaus *et al.,* 2004
VSTX1	*Grammostola spatulata*	K_VAP	Ruta *et al.,* 2003; Ruta, MacKinnon, 2004

Table 2. Table summarizing the main spider-derived toxins that target K^+ channels.

Although spider-venom peptides represent a valid potential therapeutic lead for treating ion channel-related diseases, there are still some limitations in their application. Firstly, peptides often show ability to block other ion channels (Bosmans *et al.,* 2006; Bosmans and Swartz, 2010; Middleton *et al.,* 2002), thus determining less selectivity for the target and often determining opposite effect on the gating properties (Navarro M. *et al.,* 2019). One example is Hanatoxins (HaTX) that blocks Kv2.1 (Swartz and Mackinnon, 1997 (b)), but activates Kv1.2 (Milescu M. *et al.,* 2013). Hanatoxin is also able to act on certain subtypes of voltage-activated calcium (Ca_v) channels, as well as voltage-activated sodium (Na_v) channels (Bosmans F. *et al.,* 2008; Li-Smerin Y. and Swartz J.K., 1998). One possible strategy to enhance the selectivity of the peptides towards the target, would be to attempt modifications on the peptide to create analogues, that could potentially show more selectivity, mimicking the efforts made in creating analogues for other channel-blockers peptides (i.e. *ShK* analogues). In this regard, there is an significant body of evidences that suggest how increasing the interaction between the peptides and the membrane lipids, could lead to the enhancement of the inhibitory potency of the peptides (Agwa A.J. *et al.,* 2017 (c); Henriques S.T. *et al.,* 2016). Work carried on from *Agwa et al.,* demonstrate that an engineered analogue, gHwTx-IV, derived from the spider peptide toxin HwTx-IV, exhibits higher ability to interact with lipid membranes thus enhancing its potency against hNav1.7 channel (Agwa A.J. *et al.,* 2017 (c)). However promising, there is still *ongoing* work in this direction. Other limitations to take into account, regard primarily the rapid degradation of the peptide that may limit the use in *in vivo* experiments, as well as the challenging clinal use of the peptides, due to the biochemical instability that may limit the oral intake (Bosmans F. and Swartz J.K., 2010).

At present, spider-venom derived peptides are an excellent tool to elucidate the structural and functional mechanism of voltage-gated ion channels, with a particular regard to Na_v channels, extensively studied for their involvement in pain sensation (Ma RSY *et al.,* 2019; Bosmans F. and Swartz K.J., 2010).

1.5.5 Snake toxins

Snakes venom represents a good source of proteins that act as toxins on several physiological systems. Snake's venom, produced in specialized venom glands, is a cocktail of proteins and peptides that the animal delivers through bites (Doley R. and Kini R.M., 2009). The venom composition varies between individuals of different species (Fry B.G. *et al.,* 2008; Tasoulis T. *et al.,* 2017) as well as in individuals of the same species, and is influenced by several factors including age (Dias G.S. *et al.,* 2013), gender, (Menezes M.C. *et al.,* 2006; Zelanis A. *et al.,* 2016), location (Durban J. *et al.,* 2011; Goncalves-Machado L. *et al.,* 2011) and season (Gubensek F. *et al.,* 1974). Snakes venom toxins affect mainly the central nervous system (CNS) (Neurotoxins and Dendrotoxins), the cardiovascular system (Cardiotoxins), the muscular and vascular system (Koh D.C. *et al.,* 2006). Potassium channels inhibitors are small molecule extracted mainly from the venom of the mambas, African snakes belonging to the elapid family (Harvey A.L., 2001). Potassium channels inhibitors have been found in the venom of the black mamba (*Dendroaspis polylepis*), the Eastern green mamba (*Dendroaspis angusticeps*) and the Western mamba (*Dendroaspis viridis*) (Berndt K.D. *et al.,* 1993; Harvey A.L. and Anderson A.J., 1985), and subsequently named Dendrotoxins (DTXs).

DTXs are molecules of 57-60 amino acids, comprising a Kunitz-type fold, six cysteines motif and three disulphide bridges (Berndt K.D. *et al.,* 1993). They are specific inhibitors of the voltage-gated K^+ channel of the *Shaker* family, with α-dendrotoxin acting on Kv1.1, Kv1.2 and Kv1.6 in the nanomolar range, and K-dendrotoxin blocking preferentially Kv1.1 (Harvey A.L., 2001). Dendrotoxins homologues have also been found in other species, such as the sea *anemone Anemonia sulcata* (Schweitz *et al.,* 1995).

These toxins share a common and conserved arrangement typical of the voltage-gated K^+ channels blockers, known as "*functional dyad*", constitute by functional Lys and close hydrophobic residues (Leu, Tyr or Phe) important for the toxin to bind to the channel (Duplais M. *et al.,* 1997; Gasparini S. *et al.,* 1998; Alessandri Haber N. *et al.,* 1999). Other than Dendrotoxins, few other snake venom-derived toxins have been reported to act on potassium channels. In this regard, β-bungarotoxin, sarafotoxin and natrin are interesting examples (Dutertre S. and Lewis R.J., 2010). Work carried by *Wang et al*., demonstrated the inhibitory effect of natrin on Kv1.3 channel in the nanomolar range (1-200 nM). Interestingly, natrin, derived from the snake venom of *Naja naja atra* and reported as BK_{ca} channel blocker, is able to block the channel although lacking the functional dyad (Wang F. *et al.,* 2006). At present,

snake toxins found a good application as therapeutic agents (like Captopril, a potent inhibitor of the angiotensin converting enzyme (sACE)) (Cushman D.W. *et al.,* 1977; Cushman D.W. and Ondetti M.A., 1999) and also, for diagnostic purpose (Textarin: Ecarin test used to detect Lupus Anticoagulant (LA)) (Triplett D.A. *et al.,* 1993).

1.5.6 New insight into the worm peptides

In the past years, an increasing number of researches pointed out the presence of a large number of peptide toxins in worms, emphasizing the importance of this specie as a new and rich sources of ion channel-targeting proteins. *SMART* database (a Simple Modular Architecture Research Tool) (Letunic I. *et al.,* 2020), to date, reports the presence of 13,829 ShKT domains, of which 7.329 proteins are found in worms. The largest family of ShK-related peptides and domains is found in nematodes, trematodes and cestodes (Chhabra S. *et al.,* 2014). These parasitic worms are able to secrete numerous toxins and proteins that target several ion channels, including sodium channels (Na_vs) and potassium channels (K_vs). Work carried out by Chhabra *et al*., identified two peptides from human-infecting (*Ancylostoma ceylanicum*) and dog-infecting (*Ancylostoma canium*) hookworms (AcK1) able to block the voltage-gated potassium channel Kv1.3 with nanomolar-to-picomolar potency and high specificity (Chhabra et *al.,* 2014). Recently, a novel family of peptides have been isolated from the epidermal mucus of the "bootlace worm" *Lineus longissimus* (Jacobsson E. *et al.,* 2018). These peptides contain 31 amino acids, three disulphide bridges and a characteristic ICK motif (Jacobsson *et al.,* 2018). Of this family of cysteine knot peptides, α-1 is the most abundant and show selectivity for the invertebrate voltage-gated sodium channel at low nanomolar concentration (Jacobsson et al., 2018). In 2020, investigations conducted by Chu *et al*., lead to the identification of several peptide toxins in the venom of centipedes that act on voltage-gated sodium channels (Na_vs), voltage-gated potassium channels (K_vs), voltage-gated calcium channels (Ca_vs) and TRPV1 channels (Chu Y.Y. *et al.,* 2020). These peptides display novel structural arrangements, characteristic disulphide bridges patterns and a variable number of cysteine residues (Chu Y.Y. *et al.,* 2020). The mechanism of action of these peptides is linked to inhibition or activation of channels current. Although this line of research is promising, lot more work is required, as only twelve toxins have been currently tested on ion channels (Chu Y.Y. *et al.,* 2020). Below, a summary of the novel centipede toxins that block potassium channels (Table 3).

Peptide Toxin (name)	Structure	Bioactivity	References
κ-SLPTX-Ssm1a	51 amino acids, 6 cysteines, 3 disulphide bridges	Inhibits Kv currents in DRG. IC50= ~ 44.2 nM	Yang S. *et al*., 2012
κ-SLPTX-Ssm2a	31 amino acids, 6 cysteines, 3 disulphide bridges	Inhibits Kv currents in DRG. IC50= ~ 570 nM	Yang S. *et al*., 2012
κ-SLPTX- SSm3a	68 amino acids, 4 cysteines, 2 disulphide bridges	Inhibits Kv currents in DRG (not fully inhibits peak Kv current)	Yang S. *et al*., 2012
κ-SLPTX$_{15}$-Ssd2a	72 amino acids, 6 cysteines	Irreversibly blocks Kv currents. IC50= ~ 10nM	Liu Z.C. *et al*., 2012
SSTX	53 amino acids, 4 cysteines, 2 disulphide bridges	Blocks Kv7 (IC_{50} values of 2.5 μM for Kv7.4; 2.8 μM for Kv7.1; 2.7 μM for Kv7.2 and 2.7 μM for Kv7.5). Also inhibits Kv1.3 with IC50= 5.26μM	Luo L. *et al*., 2018 Du C. *et al*., 2019
SSD609	47 amino acids, 6 cysteines, 3 disulphide bridges	Inhibits I_{Ks} current. IC50= 652.7 nM	Liu Z.C. *et al*. 2012; Sun P. *et al*., 2015
SsTx1	36 amino acids, 4 cysteines, 2 disulphide bridges	Inhibits Kv current in DRG. IC50= 200nM Also blocks Kv2.1 in human embryonic kidney 293 cells with IC50= 41.7 nM	Chen M. *et al*., 2014 Wang Y. *et al*., 2017

Table 3. A summary of the novel centipede toxins that act on K^+ channels with specifications on structure and bioactivity.

1.6 Conclusions and Remarks

Venomous animals have evolved thorough the years developing potent characters beneficial for survivors. The production of venom is beneficial for the animal for defence, competition or predatory strategies. During the years, some animals have evolved specialized glands for the production of venom, whilst other contains various toxic substances in different tissue within the body (Utkin Y.N., 2015). The composition of the venom varies among different species and contains several components including inorganic ions, proteins, nucleotides and enzymes, and can induce numerous effects such as haemorrhage, necrosis or neurotoxicity, once expelled from the specialized apparatus (Fry B.G. *et al.,* 2009; Utkin Y.N., 2015).

History has conveyed to us several examples of the usage of venom in the ancient world, where its powerful properties were used for medical benefits but also as biological weapons. Ancient Greeks were among the first population to describe the benefits of snake venom, and among the first to use the venom as weapons against enemies during the battles by using poisoned arrows and swords, but also to poison food, water and air (Major A., 2003). Appian, the Roman historian of Greek origin, described one of the first administration of the venom from the steppie vipera (*Vipera ursinii*), as a natural remedy to save Mithradates life by stopping his bleeding (Bhattacharjee P. and Bhattacharyya D., 2014). Mithradates, also known as the "Poison King", was the ruler of the kingdom of Pontus and also an expert in toxicology and poisons. Since his father died of poisoning, Mithradates was interested in reaching immunity to poison and, to do so, he started to ingest small quantity of venom from plants and animal regularly. He is also known for the formulation of the universal antidote "*Antidotum Mithridaticum*" (Major A., 2010). When his empire fell over Pompey, Mithradates tried to kill himself by drinking some venom but the amount left, after giving some to his two daughters first, was not enough to provoke his death, due to his immunity. He will die, instead, pierced by the blade of the sword inflicted on him by one of his friends, Bituitus, according to Appian descriptions. In Roman age, venom was also used to produce drugs to treat smallpox, leprosy and fever, but also for wound healing (Utkin Y.N., 2015). Studies around venom properties, began in the 17th and 18th centuries by the pioneering works of two Italian scientists, Francesco Redi and Felice Fontana. The two scientists contribute to the description of the toxicity of snake venom and the discovery of the snake venom glands, respectively (Redi F., 1664; Utkin Y.N., 2015).

Although the therapeutic use of venom dates back to ancient times and have been used for centuries in Chinese, as well as Indian medicine culture (El-Aziz T.M.A. *et al.,* 2019), more

detailed studies around the venom composition started in the late 1980s and early 1990s (King G.F. *et al.,* 2008, a). Work carried out by several groups, revealed that the lethal composition of the venom represents only a small fraction of the total composition, and the non-lethal part includes proteins and peptides with a plethora of bio-properties (Oliveira B.M., 1997; Possani L. *et al.,* 2000; Adams, 2004), useful as research tools (Adams et *al.,* 1993; McIntosh *et al.,* 1999; King G.F., 2007; King G.F., 2008 (b)), pharmaceutical agents (Harvey, 2002; Lewis and Garcia, 2003) and insecticides (Tedford *et al.,* 2004; Bosmans and Tytgat, 2007).

Thanks to the advancement of new technologies, it was possible to characterise the venom composition of several species revealing that, some components are conserved among certain species, thus indicating a common ancestral origin. Contemporary use of toxin-based drugs started with the introduction of Captopril (Capoten®; Anakena), the first angiotensin converting enzyme (ACE) inhibitor for the treatment of hypertension (Cushman D.W. *et al.,* 1977; Lewis L. and Garcia R., 2003). At present, six venom-derived drugs have been approved by the FDA for the treatment of several conditions, whereas others are on clinical trials and in preclinical development (King G.F., 2011; Pennington M.W. et al., 2018). Toxins represent an attractive tool for the development of drugs due to the high potency and often selectivity towards their targets. Nevertheless, the production and subsequently use of these peptides in the common medical practice is highly challenging and present several limitations. Indeed, still nowadays, although huge efforts in the discovery, isolation and modification of several venom compounds, a significant number of candidates fail the clinical trials, preventing the introduction in the drug market. Limitations presented by peptides and toxins are numerous. Firstly, is dutiful to mention firstly the limitation in terms of quantity. Obtaining a large amount of venom and purified toxins is a quite challenging task, especially when they are extracted from small animals, such as scorpions and/or spiders. Among the terrestrial animals, snakes produce the highest amount of venom (Bordon K. *et al.,* 2020), and this could justify why a large number of peptide-based drugs are obtained from snake venom. Together with quantity limitation, the isolation of specific toxins and peptides, due to the heterogeneous nature of venoms, is a quite challenging task to perform (Bordon K. *et al.,* 2020). In addition, the structure of most of the peptides, rich in disulphide bridges (ranging from two to four, or more in certain types), makes the chemical synthesis not only expensive, but also difficult in the final product (Chen N. *et al.,* 2018). Furthermore, several peptides and toxins need to undergo structural and chemical modifications to improve biostability, bioavailability and selectivity (Clark G.C. *et al.,* 2019). The main challenges to overcome are also related to the short

circulation half-life, poor membrane permeability (because most of the peptides are not able to cross the BBB) and poor oral availability (Chen N. *et al.,* 2018). For the administration, at the moment, the main way is parental administration (Ibraheem D. *et al.,* 2014; Duskey J.T. *et al.,* 2017). Several strategies to enhance the circulating half-life of the peptides have been attempted, such as genetic fusion to proteins or protein domains (immunoglobulin, human serum albumin (HSA) and antibody FC domain) and chemical conjugation to synthetic polymers (PEG) (Chen N. *et al.,* 2018). Although valid, these modifications, determine a reduction of the biological activities of the peptides, such as protein-target affinity (Chen N. *et al.,* 2018). All those reasons, combined with expensive and long last pre and clinical trials, significatively limit the translation of several candidates in drugs, although the toxin-derived drugs market is rapidly growing. Also, several candidates failed the clinical trials for adverse effects, lack of efficacy and dose-limiting toxicity (Harvey A.L., 2014; Lewis R.J., 2015).

We have explored the fascinating world of venomous species, with a main focus on the Animalia kingdom, examined the most relevant discoveries in the field, and considered *pro et contra* of those peptides. The usage of toxins in the medical practice space from the ancient world to the modern era, but there is still a huge amount of work to be done in this direction. The tremendous progresses in science and technology, significantly contributed to expand the knowledge in this interesting field, reinforcing the pivotal role of nature as source of compounds important for humans.

1.7 Aims

The aims of this study are to investigate the pharmacological properties of a novel class of Kv1.3 peptide-blockers from the parasitic nematode *Heligmosomoides polygyrus.* The two novel peptides, SXCL-1 and SXCL-6, share the *ShK-like* domain typically found in toxins that inhibit the voltage-gated K^+ channel, Kv1.3. Therefore, these peptides are indicated to be promising and potent channel inhibitors.

I aim to address my research by investigating the effect of the novel *ShK-like* peptides, SXCL-1 and SXCL-6 on Kv1.3 channel, and by elucidating the potential channel-peptides interaction sites (Chapter 3). To do so, I investigated whether site-specific mutations occurring within aminoacidic residues at the pore region of the channel, can determine a variation of the inhibitory effect of the peptides, therefore reducing the inhibitory effect (Chapter 3). Furthermore, to investigate the selectivity of the peptides towards Kv1.3 over other close-related voltage-gated K^+ channels, investigations were conducted on other members of the *Shaker*-related superfamily including Kv1.1, Kv1.2 and Kv1.5 and the *Shab*-related member, Kv2.1 (Chapter 4).

A part of my investigations was also focused on the characterisation of a *de novo* variant in KCNB1 gene, encoding the voltage-gated K^+ channel Kv2.1, found in a young patient by a group of clinicians in America (California). The aim of our collaborative work was to characterise the electrophysiological implications that the novel variant determines on the channel properties. To do so, I used the well-known Kv2 blocker, Guangxitoxin-1E (GxTx-1E) to investigate the functional and electrophysiological implications of the mutation on Kv2.1 channel's activity. Electrophysiological characterisation was obtained using the whole-cell patch clamp technique on tSA201 cells, transiently expressing the channel (Chapter 5).

In the final chapter, I investigated the activity of the peptides in naturally expressing Kv1.3 cells, Jurkat T cells. I aim to address this by a combination of electrophysiology and immunological assay. This chapter is to be considered a "short" piece of work and I intend to address as preliminary data for further studies (Chapter 6).

Chapter 2: Material and Methods

The characterisation of novel peptides from the parasitic nematode *Heligmosomoides polygyrus* (*H.polygyrus*) on voltage-gated potassium channels from the *Shaker*-related and *Shab*-related subfamilies was conducted using the whole-cell and perforated patch-clamp technique on transiently transfected modified human embryonic kidney cell line (tSA201 cells) and on an immortalized human T lymphocyte cell line (Jurkat T cells), respectively.

2.1 Cell culture

Cell culture procedure was performed using a Biosafety Class 2 laminar flow hood with High Efficiency Particulate Air (HEPA) filters (HeraSafe, Heraeus), using aseptic techniques. All procedures were performed in accordance with the designated standard operating procedures and risk assessments specific to the work being performed. All cell culture products were purchased from Sigma (UK) and consumables from Fisher Scientific (UK), unless otherwise stated.

2.1.2 Cell lines

tsA201 cells, a modified human embryonic kidney cell line (HEK293), were used to perform most of the experiments. Cells were purchased from the European Collection of Cell Culture (ECACC) (catalogue number: 85120602) through Sigma-Aldrich. tsA201 stably expressing SV40 temperature-sensitive T-antigen, express high level of recombinant proteins as the result of their modification (Graham F.L. and Eb A.J., 1973; Graham F.L. *et al.,* 1977). Cells present an epithelial-like morphology with a pyramidal or rhombic shape (Figure 9, see also Mathie A. *et al.,* 2021)**.** In addition, electrophysiological experiments were conducted on Jurkat cells, an immortalized line of T-lymphocytes, a kind gift from Dr. Vadim Sumbayev (University of Kent, Medway School of Pharmacy, UK).

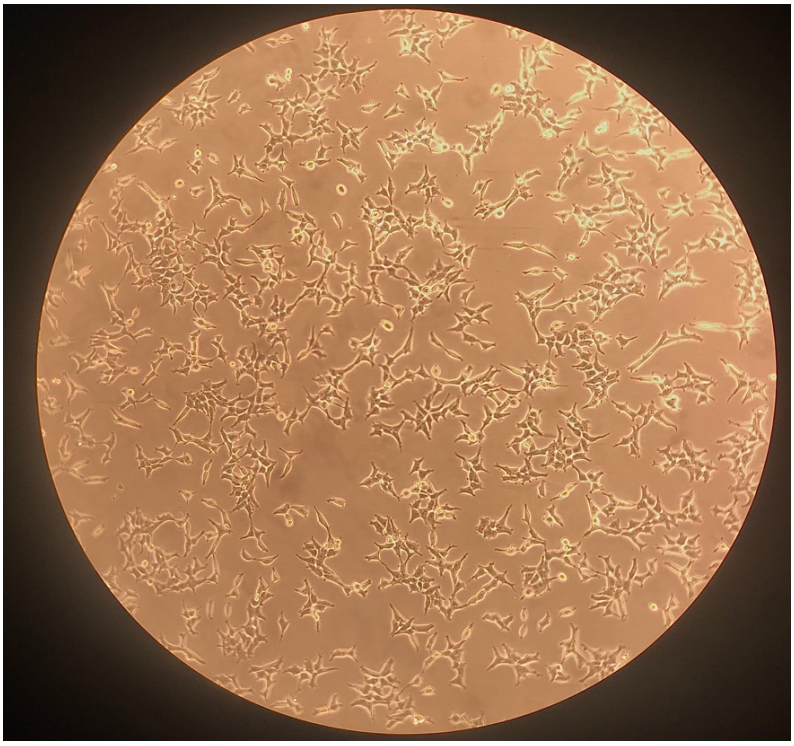

Figure 9. Untransfected tSA201 cells. Image of tSA-201 cells cultured in our laboratory at passage number 16 (unpublished picture). Cells were visualised using a Nikon TMS microscope (Made in Japan) and picture was taken using a Dual 12PM camera (Apple, California). Cells present an epithelial-like morphology with a pyramidal or rhombic shape

2.1.3 tSA201 Cell passage

Cells were cultured in growth media containing 88% (v/v) Dulbecco's Modified Eagles Media (DMEM), 10% (v/v) heat-inactivated fetal bovine serum (HIFBS), 1% (v/v) non-essential amino acid solution (NEAA), 2mM L-Glutamine and 1% (v/v) penicillin (10,000 $U{\cdot}mL^{-1}$) and streptomycin (10$mg{\cdot}mL^{-1}$), using monolayers 25cm^2 or 75cm^2 vented tissue culture flasks. Cells were passaged when flasks reached 70% - 80% of confluency. Cells were separated from the flask surface using Trypsin-EDTA solution (ethylenediaminetetraacetic acid) (10X, 0.5% trypsin, 0.2% EDTA) in quantity of 1 mL or 2 mL, according to the flasks dimension (25 cm^2: 1 mL; 75m^2: 2 mL). Flask was then mildly agitated and incubated at 37°C for 2-4 minutes, according to the dimension of the flask. After this time, the flask with the content was gently tapped on the side to ensure that all cells are dissociated from the bottom of the flask. 5 mL of fresh media was then added to the flask and pipetted up and down repeatedly to disperse cell clumps. 5 mL of cells were then transferred to a falcon tube and centrifuged for 3 minutes at 800 rpm. After centrifugation the supernatant was removed, and cells were re-suspended in 5 mL of fresh media by pipetting up and down to thoroughly resuspend the cells. Cells were then counted. 100 µL was taken for cell counting on *FastRead 102* slide (Immune Systems Ltd,

UK). The appropriate amount of cell suspension was calculated to seed new flask at a density of 1.5 X 10^5 cells/ mL and made up to 5 mL for the 25cm^2 flask or 20 mL for the 75cm^2 flask. The remaining cell suspension was then used to prepare plates (section 2.1.4) for electrophysiological experiments or sometimes for cryopreservation (section 2.1.6). New flasks were then incubated within a humified atmosphere of 95% oxygen and 5% carbon dioxide (CO_2) at the temperature of 37°C and passaged again when they reached 70% - 80% of confluency.

2.1.4 tSA201 cell plating for electrophysiology

For electrophysiology experiments, resuspended cells at a density of 7 X 10^4 cells/ mL were transferred onto 13 mm circular glass coverslips coated with poly-L-lysine solution (PLL, 0.5 mg/mL) to ensures good cell adhesion. 0.5 mL of cells were added to each well of the plate (2 mL in total for 4-well plate). To ensure that each coverslip was covered by cells, a light and gentle tap was applied to each coverslip in each well. Cells were then incubated until the following day, ready to be transiently transfected.

2.1.5 tSA201 cell transfection

For electrophysiological purposes, cells were transiently transfected using a modified calcium-phosphate protocol (Chen C. and Okayama H., 1987; Batard P. *et al.,* 2001), with both the cDNA of a voltage-gated potassium channel (Kv) of interest and the cDNA of a reporter gene, green fluorescent protein (GFP), to help identify cells that had been successfully transfected. Transfection of one 4-well plate was conducted as follows. Two Eppendorf tubes were required, labelled *A* and *B*. Tube *A* contained 0.5µg of either hKV1.1, hKV1.2, hKV1.5 and hKV2.1, or 0.3 µg (hKV1.3) of the cDNA of interest and 0.5 µg or 0.3 µg of the reporter protein GFP; 22.5 µL of $CaCl_2$ (2M) and ddH_20 up to 100 µL of volume in total for all four wells (25 µl/ well). Tube *B* contained 100 µL of phosphate-free HEPES buffered saline (280 mM NaCl, 50 mM Hepes, pH 6.9 using NaOH) and 1.8 µL Phosphate buffer (Na_2HPO4, 100nM). Each tube was then vortexed and spun down briefly; the content of tube B was transferred dropwise to tube A, and then incubated at room temperature for 5-15 minutes, to allow the establishment of the $CaPO_4$/DNA precipitate. The content of the tube was then gently mixed by pipetting slowly up and down and 50 µL was transferred to each well. Cells were

incubated for a range of time between 4-6 hours at 37ºC in 5% CO_2. After the incubation, the media was removed and each well washed twice with 1 mL of warmed phosphate-buffered saline (PBS) and then 0.5 mL of warmed culture media was added to each well. Plates were then placed back in the incubator overnight, ready for electrophysiology experiments the following day (Figure 10).

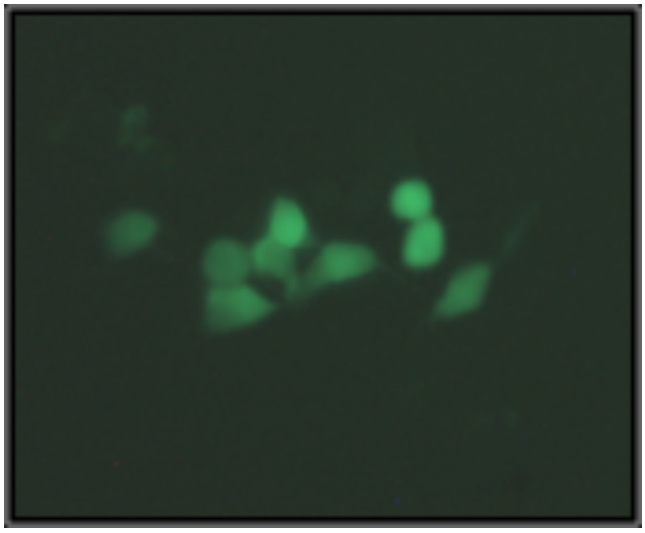

Figure 10. tSA201 cells transfected with GFP. Transfected tSA201 cells with GFP suitable for whole-cell electrophysiological recording (unpublished). After transfection cells maintained their healthy shape (Philip Thomas, Trevor G. Smart, 2005) and the characteristic green colour reports the cells that have been successfully transfected.

2.1.6 tsA201 cell freezing procedure

Transfection and patching efficiency of tsA201 cells have been shown to decrease with repeated passages over time (~30 passages). Thus, on receiving a new batch of cells, it is good practice to freeze down some of the low passage cells for future experiments or in case of infection, incubator failure etc. When a large flask (75 cm^2) reached the 70-80% of confluency, the supernatant was removed and 2 mL of trypsin-EDTA was added. The flask is gently agitated and incubated for 3-5 minutes in a 5% CO_2 incubator. After this short incubation, cells were dissociated from the bottom of the flask applying gentle agitation and 10 mL of media was then added pipetting up and down repeatedly to ensure that cells are thoroughly

resuspended, and the trypsin had been quenched. 10 mL of resuspended cells were then transferred to a 15 mL falcon and centrifuged at 800 rpm for 4 minutes. After centrifugation, all supernatant was removed using a sterile Pasteur pipette and the pellet was resuspended in cryogenic media (90% HIFBS, 10% dimethylsulfoxide (DMSO)), in appropriate volume to obtain a cell concentration of 2-4 X $10^{6.}$ mL. Subsequently, 1 mL of resuspended cells was transferred to each cryogenic vial, properly labelled with cell line name, passage number and date, and placed into Mr Frosty box (Sigma-Aldrich), containing isopropyl alcohol and placed in -80°C freezer overnight. The following day, the ampoules were transferred to the vapour phase of a liquid nitrogen vessel and left until needed.

2.1.7 tSA201 cells resuscitation

Resuscitation process must be done very quickly in order to avoid the risk of toxicity from DMSO. The cap of the frozen ampoule was turned a quarter turn to release any residual liquid nitrogen. When doing this, a tissue soaked in 70% ethanol, was wrapped around the cap. Cap was re-tightened and the ampoule was quickly transferred to a 37°C water bath for 1-2 minutes, avoiding the complete immersion of the ampoule in the water. The content of the ampoule was slowly transferred into a 15 mL falcon tube, containing 5 mL of pre-warmed media, using a sterile Pasteur pipette. Cells were then centrifuged at 800 rpm for 3 minutes to remove any cryoprotectant. The supernatant was then discarded, and cells were resuspended in 5 mL of media. Resuspended cells were then transferred into a 25 cm^2 filtered capped flask and placed into 5% CO_2 incubator overnight. The following day cells were assessed. A mixture of mainly adherent and some floating cells is an indication of successful resuscitation. The old media was then carefully discarded and replaced with 5 mL of fresh new media. Cells were placed back into 5% CO_2 incubator and left until they reached the 70 - 80% confluency. At this point, cells were passaged as described above (see 2.1.3).

2.2 Jurkat cells passage

Jurkat T cells, an immortalized line of human T lymphocyte cells, were provided by Dr. Vadim Sumbayev (University of Kent, Medway School of Pharmacy, UK) (Figure 11). Cells were cultured in Roswell Park Memorial Institute (RPMI) (1X) media, enriched with GlutaMAX™ growth media containing 10% (v\v) heat-inactivated fetal bovine serum, 1.5% (v\v) penicillin (10,000 UmL^{-1}) and streptomycin (10$mgmL^{-1}$). Cells were sub-cultured when flasks reached enough confluency. Cells were transferred from 75 cm^2 flask into a 50 mL falcon tube and centrifugated for 5 minutes at 1200 rpm at temperature not exceeding 25 °C. After

centrifugation, cells were re-suspended in 10 mL of fresh RPMI media. 2.5 mL of resuspended cells were then diluted in 27 mL of fresh media by pipetting up and down carefully and placed back in the 5% CO_2 incubator until required. Cells were passaged when an adequate confluency was reached.

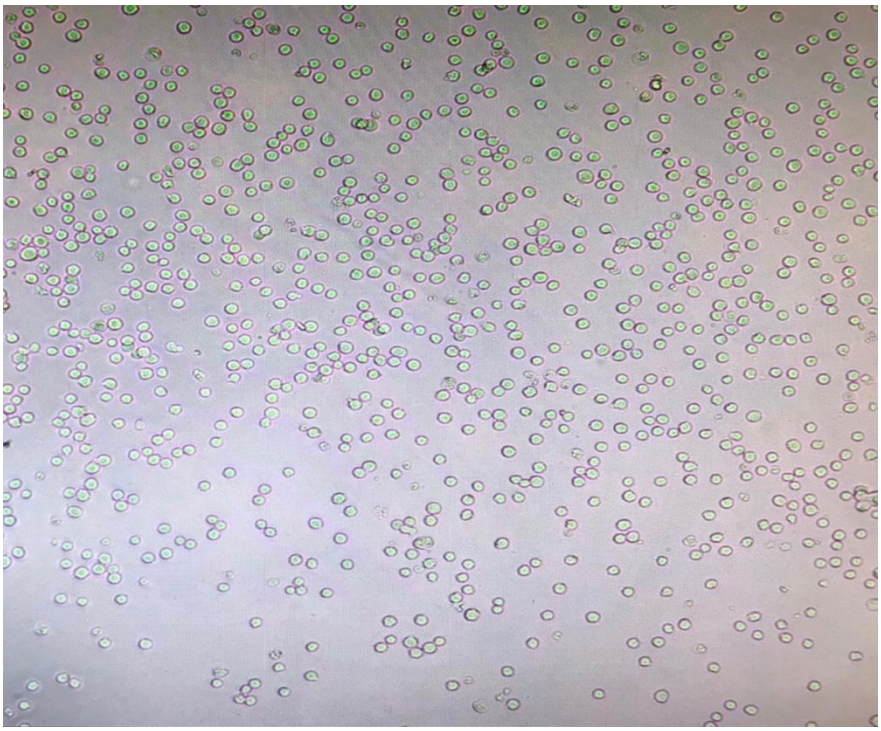

Figure 11. Jurkat T cells. Image was taken using Leica microscope DM5500B (Leica Microsystems, CMS GmbH, Made in Germany). Jurkat cells presented a circular shape and are non-adherent when in the flask.

2.2.1 Jurkat cells plating

After centrifugation, 0.5 mL of resuspended cells were transferred into a fresh falcon tube containing 8.5 mL of fresh RPMI media. Content was pipetted up and down carefully to fully resuspend the cells. 1 mL of cells were then transferred to a fresh Poly-L-lysine (PLL) plate and placed back in the 5% CO_2 incubator. Cells were ready to be used for electrophysiological experiments after a minimum of 1 hour from their preparation. This time were sufficient to ensure that a good number of cells would adhere on the coverslips. All PLL plates used to conduct experiments on Jurkat T cells, were prepared fresh 24 hours before the experimental day.

2.2.2 Jurkat cells freezing procedure

When reached a good confluency, cells where centrifuged for 5 minutes at 1200 rpm not exceeding 25°C and then resuspended in 10 mL of cold RPMI media. 2 mL of resuspended cells was then transferred to each cryogenic vial, properly labelled with cell line name, passage number and date. Cryogenic vials were then transferred for a period of time ranging from 30 minutes up to 60 minutes in the -20 °C freezer, before being transferred in the -80°C until required.

2.2.3 Jurkat cells resuscitation procedure

20 mL of RPMI media was poured into a 50 mL falcon tube and left to worm up for about 20-30 minutes. In the meantime, a cryogenic vial containing Jurkat cells was removed from the -80 °C freezer and left to defrost. When defrosted, the content of the cryogenic vial was quickly transferred to a falcon tube containing pre-warmed RPMI media, and centrifuged for 5 minutes at 1200 rpm, not exceeding 25°C. After centrifugation the supernatant was discarded, and the pellet was resuspended in 30 mL of fresh media. Flasks were then prepared following the routine procedure (2.2), placed back in the 5% CO_2 incubator until required. Cells were passaged when an adequate confluency was reached.

2.3 Electrophysiology

Electrophysiological investigations on tSA201 and Jurkat T cells, were attained using the patch clamp technique. The technique enables the recording of ionic currents from an isolated patch of the membrane using a glass pipette filled with an appropriate electrolyte solution pressed against the cell surface. By applying suction, the pipette and the cell membrane enter in direct contact and a seal is formed (Ogden D. and Stanfield P., 1999). The patch of the sealed membrane is then ruptured by applying quick suction so that electrical access to the cell is ensured (Linley J.L., 2013) (Figure 12). For all experiments, a voltage-clamp method was used. In such a way, the membrane voltage can be set by the investigator as command voltage (V_{CMD}) or holding voltage (V_{HOLD}) and the transmembrane current required to maintain this voltage can be measured. This is achieved by using a negative feedback that produce a current equal and opposite in charge to the current flowing through the open channels. The whole-cell patch or whole-cell recordings allow to record the ionic current generated from the movement of ions across the whole membrane.

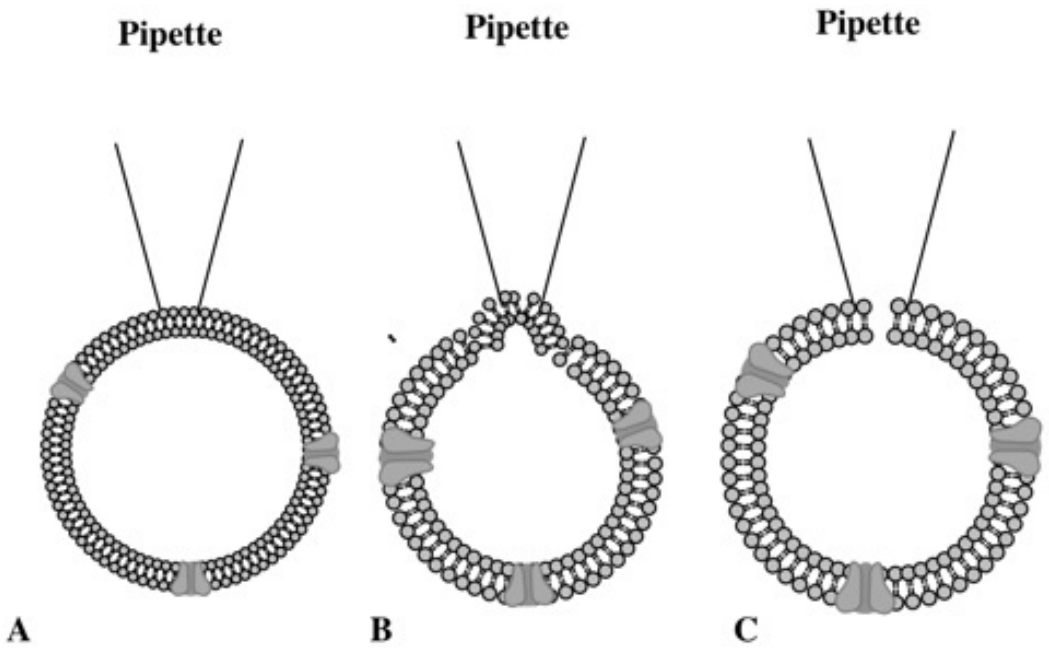

Figure 12. Sequence to reach the whole cell configuration. **A:** Pipette approaches the cell. **B:** Suction is applied to form a seal between the membrane and the tip of the pipette (gigaseal). **C:** Whole cell configuration is reached.

In figure 13, is presented a typical rig set-up for electrophysiological purpose. Microscope, head stage and manipulator were placed on an air table (Technical Manufacturing Corporation) to create an isolation system; as such, the components can be protected from external sources of vibration that can affect the recordings. To further increase the protection from sources of noise, the set-up is encased in a Faraday cage. Glass coverslips with the cells prepared as indicated above (see 2.1.5) were placed into a double-chambered Perspex bath and assessed upon an inverted, fixed stage microscope (Olympus CKX41). The microscope has both a standard light source and a fluorescence source (X-Cite 120Q, Excelitas technologies), so that it is possible to observe the cells after being transfected. When performing experiments, the bath chamber was filled with either external solution (see section 2.5) or with external solution containing one of the toxins. The external solution fills both wells of the bath chamber, that are connected via a tight channel, for a total amount of approximately 2 mL. The separation of the two wells within the bath chamber determine the separation of the recording section from the suction section, allowing a reduction of the noise to the recording system. The coverslip containing cells is placed in the first chamber whilst a ground electrode, comprising a silver chloride pellet connected through a cable to the headstage amplifier (CV 203BU, Axon

Instruments) is placed in the second chamber. Borosilicate micropipette, prepared from borosilicate glass capillaries (Harvard Apparatus, UK), with an outer diameter of 1.5 mm and internal diameter of 1.17 mm, were used for all electrophysiological experiments. The micropipettes were prepared using a vertical puller (PC-10, Narishige) that generate two micropipettes with an average resistance of 5-10 MΩ and 1-2 μm tip diameter. The micropipettes were filled with an internal solution (see section 2.5) using a microneedle injector, in a way that the end of a silver wire was immersed. A silver wire was encased in HL-U holder (Axon Instruments), attached to the headstage amplifier (CV 203BU, Axon Instruments). The silver wire was chlorinated in bleach for about twenty-thirty minutes, in order to provide a coat of AgCl, important to create a stable electrode. Usually the silver wire was bleached every few weeks and re-mounted on the holder to be used. The coating of the silver wire determines the following reversible reaction:

$$Ag + Cl \rightleftharpoons AgCl + e -$$

This reaction determines the transduction of a current consisting in ions in solution to a current involving electron in a silver wire that can be measured.

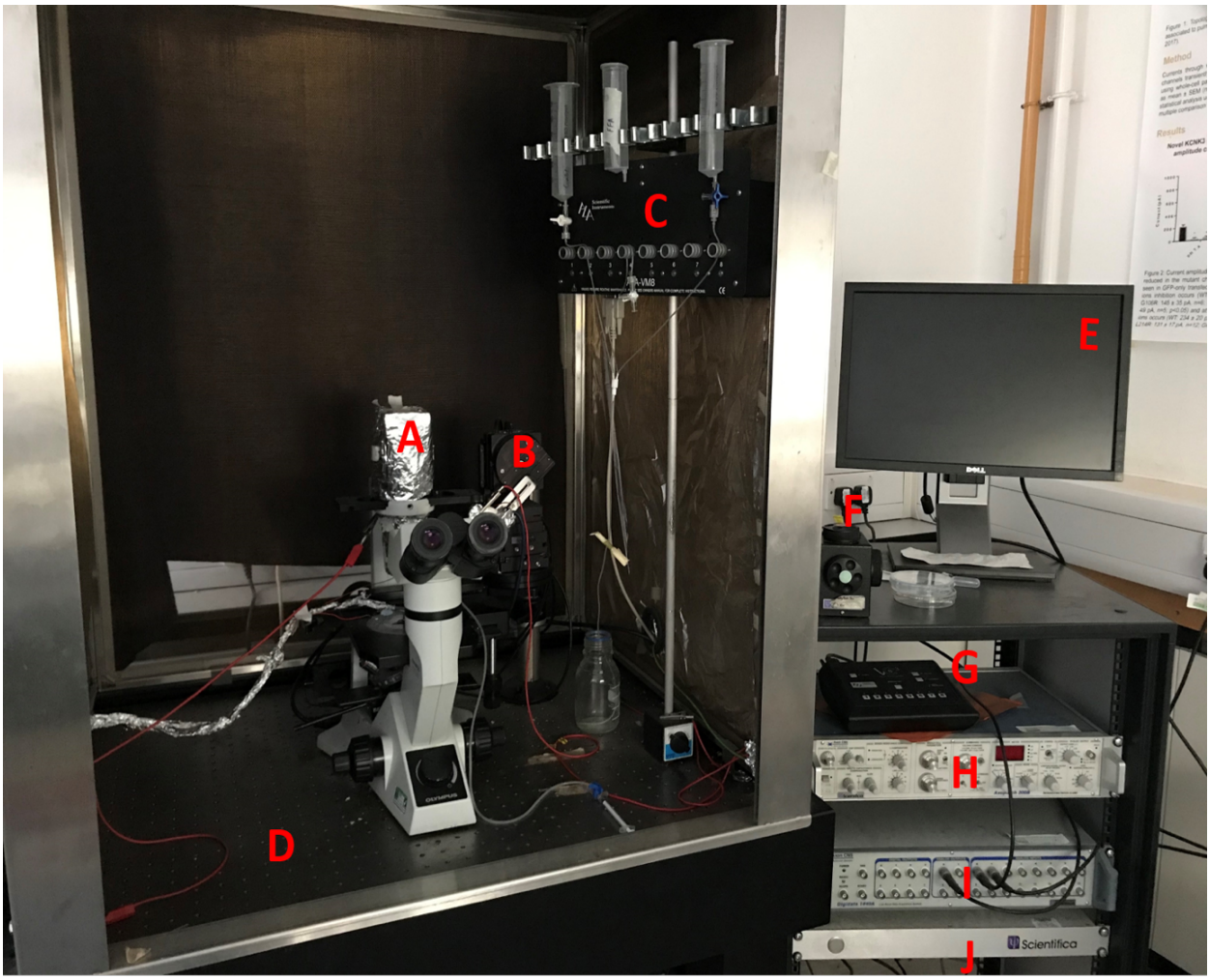

Figure 13. Rig set up. A) Inverted microscope (Olympus CK X41); **B)** Amplifier headstage; **C)** Gravity Perfusion system (ALA-VM8, ALA Scientific Instruments); **D)** Air Table (Technical Manufacturing Corporation); **E)** Computer Screen (Dell); **F)** Micromanipulator controller (Scientifica); **G)** Perfusion Channel Controller (ALA Scientific Instruments); **H)** Axopatch 200B Amplifier (Molecular Devices); **I)** Digidata 1440A digitizer (Molecular Devices); **J)** Micromanipulator power source (Scientifica)

The micropipette was connected to a headstage amplifier (CV 203BU, Axon Instruments), in turn connected to an Axopach 200B amplifier (Axon Instruments).

The headstage amplifier works as a differential amplifier, mounted with a feedback resistor (Rs). The amplifier has two inputs (non-inverting input (+) and inverting input (-)) and generates an output (V_0), proportional to the difference between the two input signals.
In figure 14, is shown a schematic representation of the mechanism of a differential amplifier, contextualized in a patch clamp application. The micropipette is connected to the inverting input of the amplifier, essentially a current-to-voltage convertor, thereby the current that flows through the pipette (i_p), flows into the current-to-voltage convertor. The second input that goes into the non-inverting inputs of the amplifier, is the command voltage (V_{CMD}) set by the experimenter. The output generated by the amplifier, is proportional to the difference between the two inputs, so that:

$$V0 = V\ CMD54 - V(P)$$

The Rs, works by taking some fractions of the output signal (V_o) and feed it back to the input, generating a current I_F so that the membrane voltage (V_m) is kept as close as possible to the command voltage (V_{CMD}). The feedback system basically maintains:

$$Vm = V(CMD)$$

The amount of current required to keep the two voltages in range of value as close as possible can be measured and recorded, as an indication of the ion channels activity. The signal was further processed by the Axopatch 200B amplifier (Axon Instruments) via a 4-pole Bessel low-pass filter set at 5 KHz, so that all frequencies above 5 KHz are excluded from the signal output. The signal is now ready to be conveyed to the digitizer (Digidata 1440A, Axon Instruments) that converts the analogic signal into a digital signal that can be transmitted to the computer and registered using the pCLAMP 10 software (Axon Instruments).

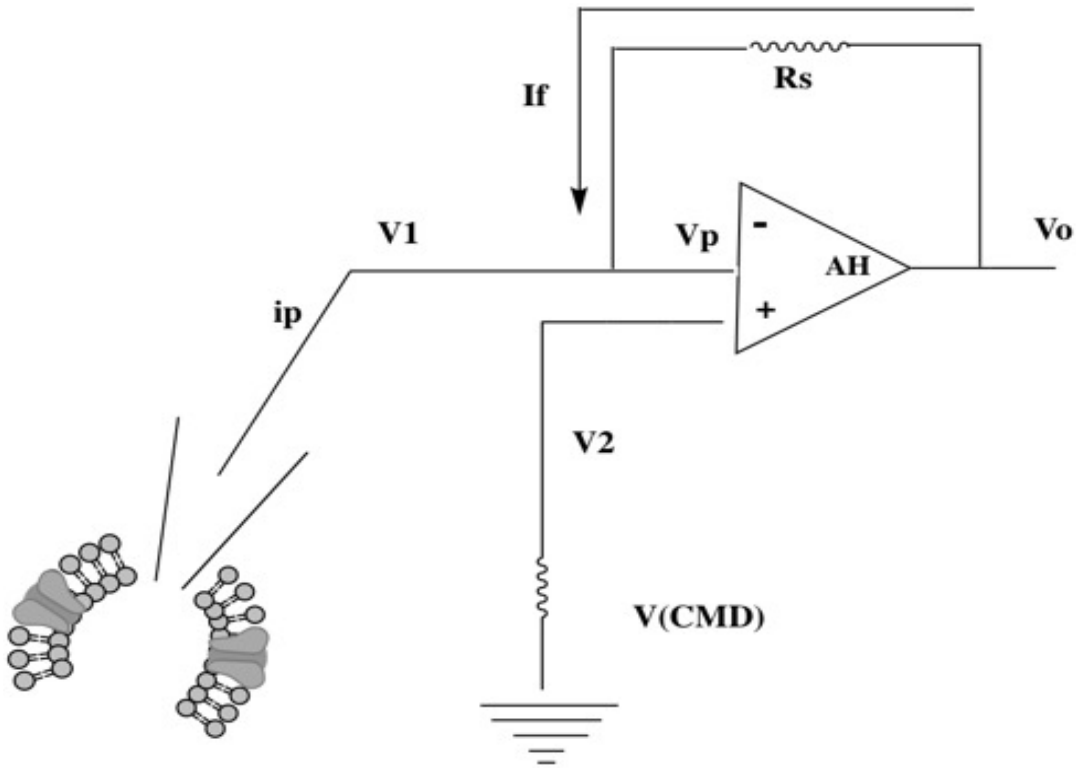

Figure 14. A schematic representation of a differential amplifier. The first input (V1) that goes into the inverting input of the amplifier (AH) is generated by the micropipette registering the current at the cell membrane. The second input (V2) is set by the experimenter (VCMD). The current IF generated by the feedback resistor (Rs) keeps the membrane voltage as close as possible to the command voltage (V_{CMD}).

2.3.1 Whole cell patch clamp recordings

At the start of the recording, a micropipette filled with an internal solution, is manoeuvred into the bath chamber, containing the external solution, and micropipette movements were controlled using a PatchStar micromanipulator (Scientifica, UK). Isolated and green fluorescent cells, as the channel was co-transfected with GFP protein, were the cells usually selected for recordings. A fluorescence illuminator (X-Cite 120Q), containing a mercury bulb and set at a wavelength of 395 nm, was used to view the fluorescent cells. Once cells were selected, the micropipette was fully immersed into the chamber and maneuverer in direction of the cells, until a contact between the micropipette and the cell was created. Contact between the micropipette and cells can be seen on the computer screen, as an increase in the micropipette resistance is recorded. At this point, a negative pressure is applied to the micropipette using a

10 mL suction syringe, in order to generate a seal between the micropipette and the cell membrane. Alternatively, negative pressure could be created by mouth suction. The seal has a resistance within the giga Ohm (GΩ) order and therefore defined "*giga-Ohm seal*". The seal can be created quickly, or in certain circumstances, it requires a while to be formed. A new fresh pipette was used each time when attempting to create a seal. Once the giga-seal was created, rupture of the membrane below the pipette tip, was reached by applying further negative pressure "pulses". As an indication of the rupture of the membrane, a large capacity transient at the leading and trailing edges of the pulse can be seen (Figure 15). At this stage, the contents of the interior of the cells are in diffusional equilibrium with the solution in the micropipette. This conventional whole-cell configuration allows to measure the current from all open ion channels within the cell membrane.

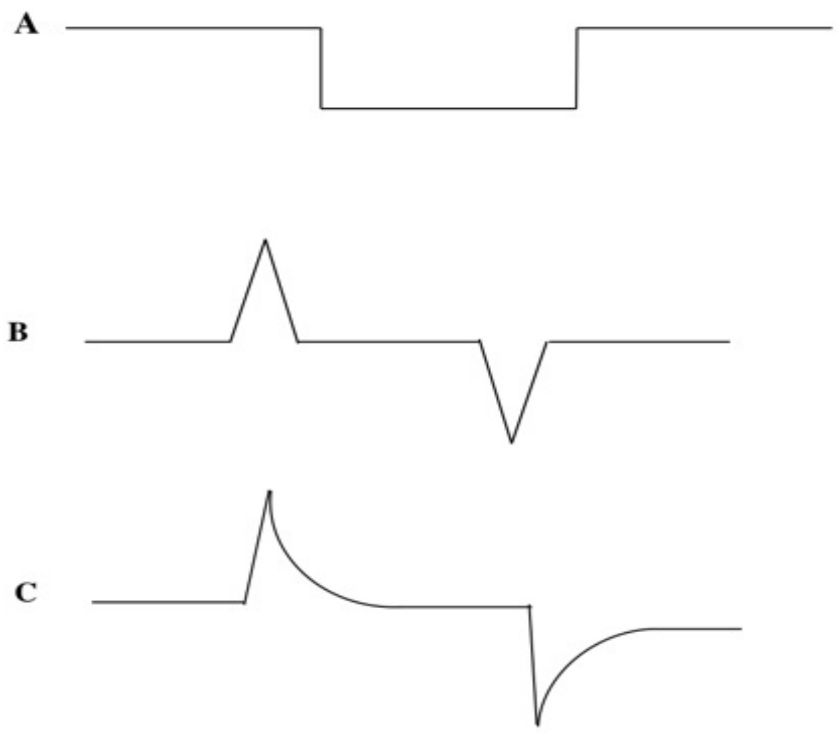

Figure 15. Initial sequence of steps during patch clamp recordings seen on the computer on pCLAMP. A: Pipette is placed correspondence of the cell membrane. Suction is applied to form a seal **B:** Giga seal is formed, and negative pressure is further applied to break through the membrane **C:** Whole cell is reached and transients at the leading and trailing edges can be noticed. Recording can now start.

2.3.2 Perforated patch clamp recordings

Perforated patch clamp technique was used to obtain electrophysiological recordings for Jurkat T cells using amphotericin B (A9528, Sigma-Aldrich, UK). The technique is a variation of the conventional whole-cell patch clamp and was first described by *Horn* and *Marty* (Horn R. and Marty A., 1988). Perforating patch clamp allows to measure the ionic flux through the membrane by perforating, instead of rupturing (as in the whole-cell), the patch of the sealed membrane (Linley J.E., 2013; Lippiat J. D., 2008). Membrane is perforated by using pore-forming antibiotics, that are added to the solution filling the patch pipette, at an appropriate concentration. The most common pore-forming antibiotics are nystatin (Horn R. and Marty A., 1988) and amphotericin B (Rae J. *et al.,* 1991) but, in some occasion, gramicidin can be used (Rhee J.S. *et al.,* 1994). These pores formed within the membrane are permeable to small monovalent ions, but are inaccessible to impermeable ions, such as Ca^{2+} and other molecules of larger molecular weight (Lippiat J.D., 2008). Perforated patch-clamp technique is commonly used in experiments aimed at studying the regulation of ion channels by intracellular signalling pathways as the cytosolic component are maintained integral, as well as the endogenous concentration of Ca^{2+} (Linley J.E., 2013).

2.4 Data analysis

Electrophysiological recordings were obtained using pCLAMP software (Clampex 10.2, Axon Instruments) installed on Window 7 computer. Recordings were acquired using a specific voltage protocol, in accordance with the kinetics properties of the channel.

To measure the current passing through the channels, a *"+50 mV continuously"* protocol was used to evoke the currents through the voltage-activated K^+ channels (Kvs) (Figure 16, A). Cells were held at -60 mV before stepping down to -80 mV for 500 milliseconds (ms); this was then followed by a step up to +50 mV for 500 ms and then back down to -80 mV for 500 ms, returning to the holding potential of -60 mV. The protocol was applied once every 15 seconds with a total of 30 sweeps recorded for each cell. Of those, a minimum of 5 sweeps were then averaged for any given current value measured at +50 mV using Clampfit (Clampfit 10.2, Axon Instruments) and Excel (Microsoft Corporation, USA). To determine I-V relationships for the channels a different voltage protocol was used (Figure 16, B). Cells were held at -60 mV and currents were recorded from +50 mV to -90 mV in 10 mV steps for 500 ms, followed by 500 ms step back to -90 mV and then returning to the holding potential of -60 mV. One sweep occurred every 15 second for a total of 15 sweeps. The current at each voltage was plotted using Clampfit (Clampfit 10.2, Axon Instruments) and Excel (Microsoft Corporation, USA).

The acquired data was then transferred to GraphPad Prism 8 (GraphPad Software Inc., CA; USA) to create graphics and to perform statistical analysis. Data are expressed as mean ± 95% Confidence Intervals of the mean of the mean peak current (pA) measured at +50 mV in the absence and presence of toxin. *'n'* represented the number of cells used for experiments and each group of experiments had an *n* of at least 5 (n=5). All measurements were conducted at room temperature (21-23ºC).

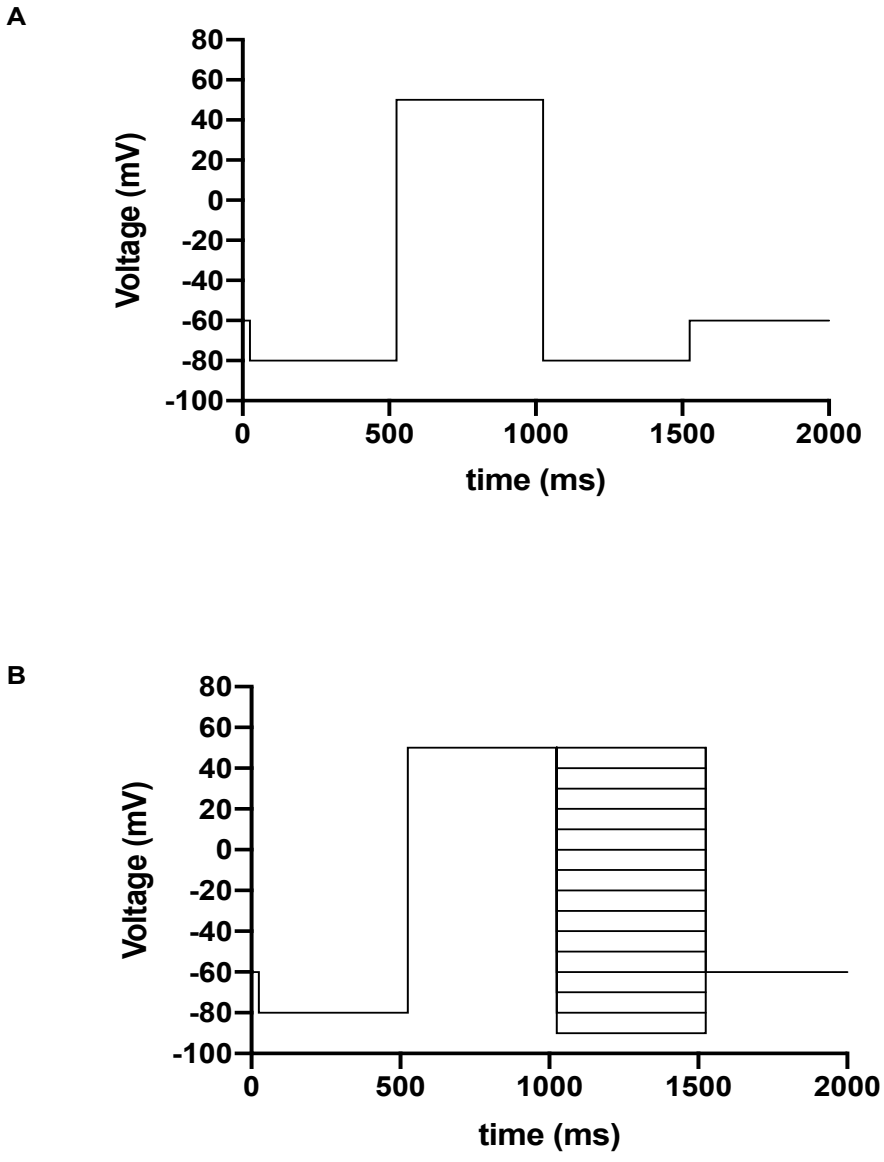

Figure 16. Representation of the protocols used to evoke Kv currents in electrophysiological experiments. A) "+ 50 mV continuously" protocol used for Kv channels recordings. **B)** "+50 mV to -90 mV" protocol to determine I-V relationship.

2.4.1 Statistical Analysis

Statistical analysis were performed using GraphPad Prism 8 software (GraphPad Software Inc., CA; USA). Raw data traces were an average of all cells recorded either in control or in the presence of a toxin. Data were expressed as the mean current measured at +50 mV± 95% Confidence Intervals (CI) and *n* represents the number of individual cells. Statistical analysis was performed using either a one-way ANOVA with a post-hoc Dunnett's multiple comparisons test or an unpaired Student's t-test. Data was considered statistically different if $p < 0.05$ (*), $p < 0.01$ (**), $p < 0.001$ (***). Percentage (%) of inhibitions were calculated from the difference of the current at +50 mV of a particular channel in control conditions compared to that same channel incubated in a particular concentration of the toxin. Data from cells expressing channels incubated in toxin were recorded either simultaneously to those cells incubated in control solution or around the same calendar period and cell batch.

2.5 Solutions and compounds

Electrophysiological experiments on cells were conducted using an external solution comprising 145 mM NaCl, 2.5 mM KCl, 2 mM $MgCl_2$, 1 mM $CaCl_2$ and 10 mM 4-(2-hydroxyethyl)- 1-piperazineethanesulfonic acid (Hepes). Solution was adjusted at pH 7.4 using NaOH and stored at 4°C. The internal solution included: 150 mM KCl, 3 mM $MgCl_2$, 5 mM EGTA and 10 mM 4-(2-hydroxyethyl)- 1-piperazineethanesulfonic acid (Hepes). Solution was adjusted at pH 7.4 using KOH and filtered using 0.2 µM cellulose acetate filter (Sartorius). Solution was then aliquoted in 1.5 mL Eppendorf tubes and stored at -20 °C. For perforated patch recordings, a 60 mg/mL stock of amphotericin B solubilized (A9528, Sigma-Aldrich, UK) was prepared by dissolving in DMSO. The stock was stored at -20°C until required. The same day of experiments, amphotericin B was added to 0.5 mL of internal solution to a final concentration of 240 µg/mL. The tube was vortexed until a weak yellow colour was predominant, and the amphotericin B had dissolved. It was then used to fill the micropipette as required. Both internal and external solutions are adjusted at pH 7.4 to recreate physiological conditions.

2.5.1 Toxins preparation

A commercial *Sthicodactyla heliantus* (ShK) toxin, was purchased from Alomone Lab (Israel). The toxin was prepared in stock of 10µM in DMSO, aliquoted in Eppendorf tubes (50 µL each

tube) and stored at -20 °C until required. SXCL-1 (Imperial College, London, UK) expressed in HEK cells and SXCL-6 (Imperial College, London, UK) expressed in yeast *Pichia pastoris*, were prepared in a similar way to ShK toxin. Stock is 10 µM (diluted in DMSO) and tubes were kept at -20 °C until required. A commercial Guangxitoxin 1E (*Plesiophrictus guangxiensis*) was purchased from Tocris (Bio-Techne Ldt, Abingdon, UK), and prepared in stock of 10 µM in distilled water as specified in the safety datasheet, aliquoted in Eppendorf tubes containing 50 µl each and stored at -20 °C until required. On the experimental day, aliquots of the toxins were diluted directly into the external solution according to the concentration required and used the same day. Before use, aliquots were defrosted thoroughly.

2.6 Computer Modelling

A model of human (h) Kv1.3 channel was kindly gifted from Professor Raymond Norton (Monash University, Melbourne, AU) and Professor George Chandy (Lee Kong Chian School of Medicine, Nanyang Technological University, Singapore). The model, referred as *Kv1.3 Norton-Chandy*, comprises the regions of the channel involved in the binding, so that the amino acidic residues forming the selectivity filter (374-491; hKv1.3 sequence UniProt, entry code: PP22001), the segments S5-S6 and the pore region (416-456 hKv1.3 sequence UniProt, entry code: PP22001) are included in the model. This can be considered a shortened model, that includes the pore domain of the channel but exclude the voltage-sensor domain (VSD) and reports a difference of 70 amino acidic residues when compared to hKv1.3 sequence in UniProt (hKv1.3 sequence UniProt, entry code: PP22001).

Computer modelling predictions were performed using the online software ZDOCK (Pierce B.G. *et al.,* 2014). The final output generated by the software included more than 500 complexes of which, the top 10 were visualised using PyMOL 2.4 (Schrodinger, Inc.). Toxins used to perform computer modelling were: SXCL-1 and SXCL-6. The two novel peptides templates were created using the online software SWISS-MODEL (Biozentrum, University of Basel, The center for Molecular Life Science) (Waterhouse A. *et al.,* 2018). The sequence of the two peptides SXCL-1 and SXCL-6 were provided by Professor Murray Selkirk (Imperial Collage, London, UK).

2.7 Computational Alanine Scanning

Computational Alanine Scanning analysis was performed using the webserver PP Check (Sukhwal A. and Sowdhamini R., 2013). Each of the top 10 PDB protein-protein complexes

result from ZDOCK analysis, was uploaded on the server and residues involved in the binding, were mutated into alanine (A). Amino acids were then screened based, primarily, on two criteria: difference in free energy (ΔG) and frequency among the complexes. In such way, a final list of aminoacidic residues with high energy difference (ΔG) and high frequency within the complexes was stipulated, and the top 3 residues were considered for site-direct mutagenesis analysis (see also Chapter 3, section 3.5).

2.8 Molecular Biology

2.8.1 Mammalian Expression Plasmids

Human (h) wild-type (WT), voltage-gated channel, *Shaker*-related subfamily, member 1, Kv1.1 (KCNA1, Genbank™ NM_000217.1), member 2, Kv1.2 (KCNA2, Genbank™ NM_004974.4), member 3, Kv1.3 (KCNA3, Genbank™ NM_002232), member 5, Kv1.5 (KCNA5, Genbank™ NM_002234) and human potassium voltage-gated channel, *Shab*-related subfamily, member 1, Kv2.1 (KCNB1, Genbank™ NM_004975) cDNA clones were purchased from Cambridge Bioscience (Cambridge, UK) and provided in the mammalian expression vector pCMV6-XL4. Green fluorescent protein (GFP) was inserted in pcDNA3.1 vector and was a kind gift of Helen Meadows, GlaxoSmithKline, UK.

2.8.2 Site-directed Mutagenesis

Point mutations were introduced by site-directed mutagenesis into pCMV6-XL4 encoding Kv1.3 cDNA and Kv2.1 cDNA, using the QuikChange II Site-Directed Mutagenesis Kit (Agilent, CA, USA). A pair of complementary oligonucleotide primers (25-35 bases) incorporating the intended mutation (aspartic acid (D) 449 to an alanine (A) (D449A); histidine (H) 451 to an alanine (H451A); and valine (V) 453 to an alanine (V453A)) for Kv1.3 and (proline (P) 17 to a threonine (T)) for Kv2.1, were synthesised (Eurofins MWG Operon, Ebersberg, Germany). Full primer sequences are shown in the appendix (figure 105).

QuikChange utilises a three-step protocol that allows the introduction of site-specific mutations into double-stranded (ds) plasmids using the polymerase chain reaction (PCR) and PfuTurbo® high-fidelity DNA polymerase (Agilent, CA, USA). The first step of the process is the denaturation of the plasmid template and annealing of the complimentary oligonucleotide primers, containing the desired mutation, to opposite strands of the plasmid. Annealing temperatures for each PCR reaction were determined by the GC-content of the oligonucleotide

primers. The PCR product is then digested with *Dpn-I* endonuclease (10 U/µL), which is specific for methylated and hemi-methylated DNA. *Dpn-I* digestion is used to digest any remaining, non-mutated parental DNA template and to select for mutation-containing synthetized DNA (Nelson M. and McClelland M., 1992). The *Dpn-I* digested PCR reaction is then transformed into XL1-Blue super competent cells (Agilent, CA, USA) using a heat-shock protocol. 50 µL aliquots of XL1-Blue super competent cells were defrosted in ice to which 3 µL of the *Dpn*I-treated DNA was added. Transformation reactions were mixed gently and then incubated on ice for 30 minutes (min). The transformation reaction mixture was then heat-shocked at 42°C for 45 seconds (s) and placed immediately on ice for 2 min. Following this incubation, 500 µL of preheated (42°C) NZY^+ broth (Sigma, UK) was added. It was then incubated at 37°C for 1 hour with shaking (225-250 rpm). The transformation mixture was then plated onto LB agar plates containing the appropriate antibiotic (ampicillin (50 mg/mL) Sigma, UK) and incubated overnight at 37°C allowing only those cells containing the plasmid vector (therefore with antibiotic resistance) to proliferate.

2.8.3 Preparation of DNA

Single colonies were used to inoculate 5 mL LB broth (Sigma, UK) cultures containing the appropriate antibiotic. After overnight incubation at 37°C, with gentle agitation, the bacterial cultures were spun down, lysed and purified using a DNA Miniprep kit (Sigma, UK) and stored at -20°C until required. The purity and concentration of the prepared DNA was determined using a Nanodrop spectrophotometer (Implen, Germany). All WT and mutated constructs were fully sequenced before use (MRC/PPU, School of Life Sciences, University of Dundee, Scotland).

2.9 Enzyme-linked immunosorbent assay (ELISA)

ELISA-based assays kit was used for the detection of Interleukin-2 (IL-2) (R&D System, Abindgon, UK) and was kindly provided by Dr. Vadim Sumbayev (Medway School of Pharmacy, University of Kent). The experimental procedure was as following.

2.9.1 Treatment of Jurkat cells with ShK, SXCL-1 and SXCL-6

Stage 1: Phorbol 12-myristate 13-acetate (PMA) and toxins preparation. In order to perform the ELISA assay for detecting the level of IL-2, cells were pre-treated with PMA. PMA was prepared the day before the experiment, diluted in filtered PBS (concentration 50 μM) and kept in the -20°C freezer until required. Toxins (ShK, SXCL-1 and SXCL-6) were prepared before the experimental day, diluted in filtered phosphate-buffered saline solution (PBS) (toxin concentration 0.5 nM) and kept in the -20°C freezer until required.

Stage 2: Plates Preparation and cell treatments. Usually this stage occurs at day 1 of the experiment. Cells were transferred into a 50 mL falcon tube and centrifuged for 5 minutes at 1200 rpm, not exceeding 25°C. Supernatant was removed and pellet was resuspended in 20 mL of fresh RPMI media, previously warmed up. At this point, 0.5 mL of resuspended cells were transferred into a 15mL falcon tube and 20 μL were then used for cell counting using the *FastRead 102* slide (Immune Systems Ltd, UK). Subsequently, 1 mL of resuspended cells were added to each well of the 4-wells plates. Wells were then labelled according to the experimenter scheme. Subsequently, 2 μL of PMA was then added to each well, followed by 5μL of the toxins, previously prepared as indicated above to make up the appropriate concentration. Plates were gently agitated and placed in the 5% CO_2 incubator at a temperature of 37°C overnight.

Stage 3: Sample collection. After the overnight incubation, samples were collected and placed in a fresh Eppendorf tube. Tubes were centrifuged for 5 minutes at 3000 rpm. After centrifugation, supernatant was collected and poured into a new tube. According to the experimenter, samples can be directly used for ELISA-assay or placed in the -20°C freezer until required.

2.9.2 Enzyme-linked immunosorbent assay (ELISA) procedure.

The 96-well microplate, coated with Poly-D-Lysine (PDL), was incubated overnight at room temperature, with 100 μL of capture antibody, previously diluted in PBS. After the overnight

incubation, the "blocking buffer stage" started. 100 µL of ELISA blocking buffer (PBS/Bovine Serum Albumin (BSA) 1%) was added to each well and incubated for 1 hour at room temperature. After the incubation, samples were loaded. Following the scheme designed by the experimenter, 100 µL of sample were added to each well and incubated at room temperature for two hours. This stage of the procedure is defined "samples loading". Subsequently, wells were washed for a total of three times with 1X Tris-buffered saline, 0.1% Tween 20 (TBST) buffer. 100 µL of specific biotinylated detection antibody, previously diluted in PBS/BSA 1%, were added to each well and incubated for 2 hours at room temperature. After the 2 hours incubation, cells were washed for three times using 1X TBST buffer. After this passage, 100 µL of streptavidin conjugated with horseradish peroxidase (HRP) were added to each well and incubated for 30 minutes at room temperature, avoiding direct contact of the plate with the light. After the 30 minutes incubation, wells were washed with 1X TBST buffer and 100 µL of substrate solution were added to each well for a maximum of 10 minutes. Substrate solution contained: 0.2% H_2O_2; 56 mM of *o*-phenylenediamine (OPD). Briefly, HRP/H_2O_2- catalysed oxidation of OPD leads to the production of the yellow emitting 2,3-Diaminophenazine (DAP) (Mekler V.M. and Bystryak S.M., 1992; Fornera S. and Walde P., 2010). DAP UV-vis *spectrum* absorption varies according to the pH values (Hinterberger V. *et al.,* 2018). When the colour of the solution is changed, 100 µL of 1.8 M of H_2SO_4 was added to each well. Results were acquired using Tecan ELISA reader (JENCONS-PLS) and absorbance was measured at 492 nm. Data were then prepared and processed for statistical analysis.

2.9.3 Statistical analysis

ELISA for the detection of Interleukin-2 (IL-2) analysis was performed using Excel (Microsoft) and graphical representations were obtained using GraphPad Prism 8 (GraphPad Software Inc., CA; USA). Statistical analysis were performed using one-way ANOVA (multiple comparisons Dunnette's test) and data are expressed as mean ± SEM.

Chapter 3: Electrophysiological and functional characterisation of the two novel *ShK-like* peptides, SXCL-1 and SXCL-6 on Kv1.3 channel

3.1 Introduction

Heligmosomoides polygyrus (*H. polygyrus*), originally known as *Nematospiroides dubius* and/or *H. bakeri*, is a parasitic worm able to establish chronic infection in mice (Johnston C.J. *et al.,* 2015) by triggering several immunomodulatory mechanisms that, ultimately, suppress the host's immune responses (Mishra P. *et al.,* 2013). Helminth infections occur especially in developing countries, whereas are less common in developed countries, where a combination of factors, including the sanitation process and the improvement of the hygiene conditions, have dramatically reduced the contact between pathogens and hosts. Several researches are aiming to unravel the use of helminth parasites or their products as therapeutic tools that can offer protection against autoimmune diseases (White M.P.J. *et al.,* 2020). In a matter of fact, helminths are able to induce many regulatory pathways during their cycle in the mammalian host, by inducing a strong Th2 immune response that includes release of cytokines, typically interleukins (IL-4 and other TH_2-type cytokines) and Immunoglobulin E (IgE), as well as activation and mobilization of mast cells, eosinophils and basophils (Maizels R.M. *et al.,* 2004). Work carried by *Correale* and *Farez,* also revealed a strong correlation between persistent helminth infection and responsiveness to inflammatory diseases such as Multiple Sclerosis (MS) (Correale J. and Farez M.F., 2007; Correale J. and Farez M.F., 2010).

H. polygyrus is a widely used model to investigate the interactions between the helminths and their hosts (Pelly V.S. *et al.,* 2016) and has been previously used to elucidate the role of Th2 immunity in reducing the severity of inflammatory diseases in experimental autoimmune encephalomyelitis (EAE) model, a mouse model of MS (White M.P.J. *et al.,* 2020).

The parasitic worm has a direct lifecycle in the host, predominantly wild mouse, that occur after ingestion of infective L3 larvae. The ingested larvae undergo several developmental stages before emerging as adult worm in the gut lumen. Eventually, adult worms mate and female produce eggs that are released into the environment through the feces. Whilst in the feces, larvae undergo two further developmental stages (L1 and L2) before becoming infective at stage L3. At this point, the L3 larvae can infect another host and start the cycle over again (Reynolds L.A. *et al.,* 2012) (Figure 17).

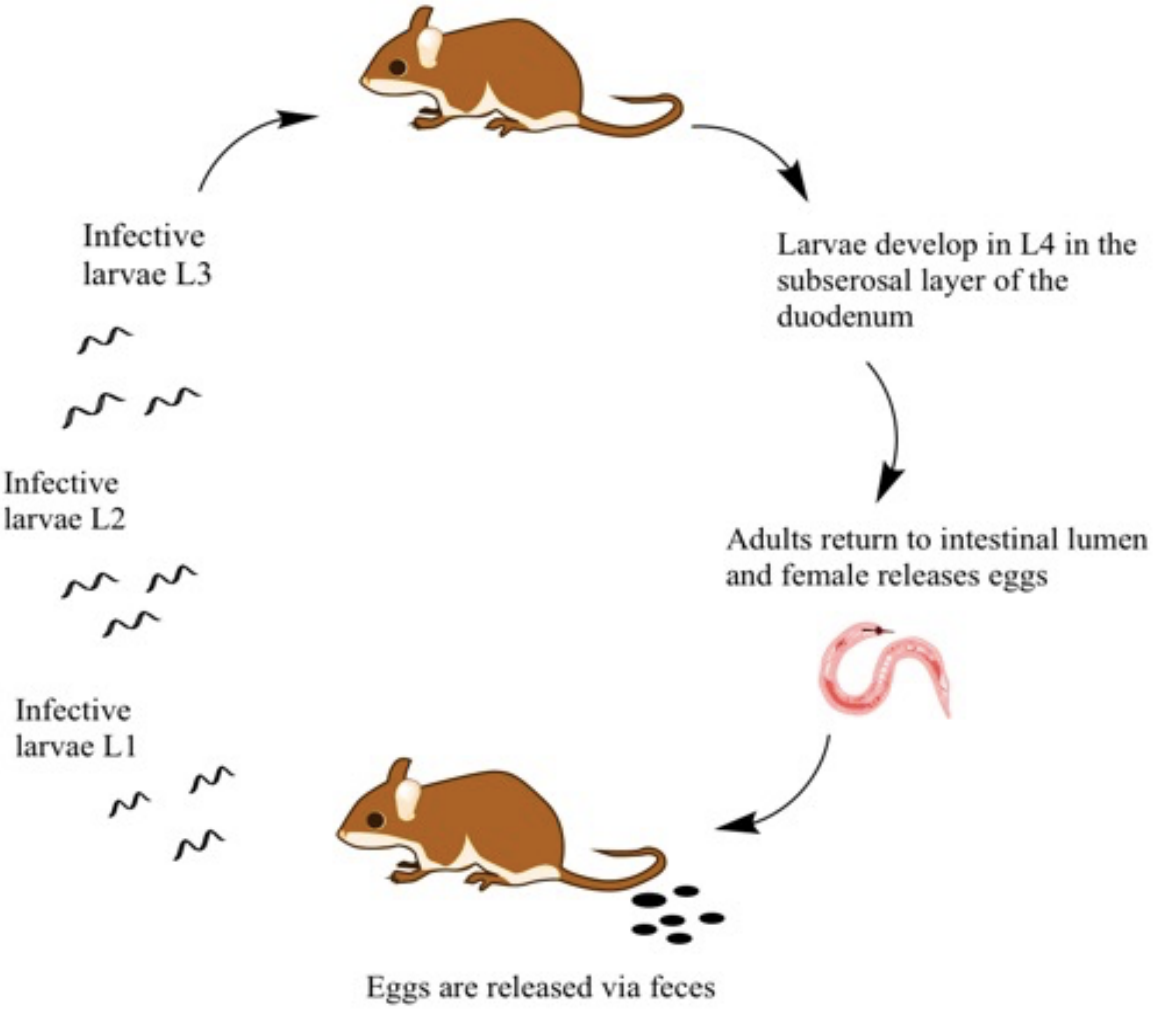

Figure 17. *H. polygyrus* lifecycle in the host. Infective larvae at stage 3 (L3), infect the host by ingestion. In laboratory experiments, the lifecycle of *H. polygyrus* is recreated by administration of the infective L3 larvae by gavage in mice (Johnston C. J. *et al.,* 2015). Larvae develop into adult that releases eggs. Eggs are then expelled via feces and infective larvae develop.

During the adult stage, the worm secretes an abundant number of proteins that collectively are named "HES products" (Adult excretory-secretory products). The most abundant secrete have been identified as VAL/ASP-like products (Hewitson J.P. *et al.,* 2011). Those proteins released by the worm, play a pivotal role in sustaining the helminth immune evasion of the host immune system and are attractive as immunomodulatory tools (Hewitson J.P. *et al.,* 2011).

Recent investigations conducted by our collaborators at Imperial College (London, UK), identified several proteins that share the characteristic *ShKT-like* domain, a hallmark domain conserved among toxins that are able to selectively block potassium channels, in the products

of adult *H. polygyrus.* This family of novel peptides have been named SXCL-*like* proteins, or alternatively, *ShK-like* peptides and comprises peptides with aminoacidic sequence of 41-49 residues, 6 cysteines domain and candidate functional lysine (K) within the aminoacidic sequences. So far, nine of those peptides have been identified (SXCL-1-9).

As reported above (see Introduction, section 1.5.6), an increasing number of studies are pointing out the relevance of worm peptides, especially within the nematodes, cestodes and trematodes *phylum*, as novel potential immunomodulators that have a phylogenetical relationship with the sea anemones toxins and can selectively target potassium channels (Chhabra S. *et al.,* 2014). Therefore, the hypothesis underlying our study is aimed at investigating the proprieties of two novel peptides belonging to the SXCL-*like*/*ShK-like* proteins family, that could potentially represent novel therapeutical tools for the treatment of several conditions including, but not limited to, autoimmune diseases that involve the voltage-gated potassium channel, Kv1.3. These peptides are named SXCL-1 and SXCL-6 and share the characteristic *ShK-like* domain found in other toxins able to inhibit ion channels.

3.2 *ShK-like* domain

Toxins and peptides that act as inhibitors of K^+ channels, have been found to share a functional and highly conserved domain, known as ShKT, or ShK-*like* domain. Originally, this domain was found in ShK toxin, isolated from the sea anemone *Stichodactyla heliantus* and soon after was identified in other toxins derived from both animal and plant kingdom (Prentis P.J. *et al.,* 2018). ShKT domain usually comprises 36 to 42 aminoacidic residues, 6 cysteines motif and conserved residues within the aminoacidic sequence. Generally, the structure is stabilized by disulphide bridges, variable in numbers, but the typical architecture includes three disulphide bridges that connect the cysteine residues (SMART database, Heidelberg). Single ShK-*like* domain, as found in sea anemones and more recently in nematodes, represent the simplest architecture that these domains can adopt, although some proteins can contain multiple Shk-*like* domains (Gerdol M. *et al.,* 2019). A long line of researches focused the attention on revealing the potential role of ShKT toxins as therapeutic tool to treat human diseases that involve an alteration of the normal function of ion channels. Since ShK toxin, at present Dalazatide, showed great results in specifically target Kv1.3 channels, involved in the development of a large number of autoimmune diseases, ShKT toxins have been evaluated as potent blocker not only of Kv1.3 channels but also other potassium channels, and are regarded

as good candidates to treat autoimmune, as well as other disorders. The mechanism of action of those toxins on K^+ channels varies and predominantly involves either the block of the pore region or the modification of the gating properties of the channel.

3.2.1 SXCL-1

The *ShK-like* peptide SXCL-1, expressed in HEK cells, is a peptide of 42 amino acidic residues, 6 cysteines residues and a candidate functional lysine thought to be in position 21 (K21). SXCL-1 is the most abundant peptide secreted by adult *H. polygyrus* during its lifecycle in the host, as HES adult product. Analysis conducted using the SWISS-model software (see Material and Methods, sections 2.6 and 2.7), have conveyed to the identification of the model structure of the peptide, via comparison with other already known peptides sequences. In figure 18, is showed the template for SXCL-1 structure based on the homology model of the sea anemone toxin OspTx2b from *Oulactis sp.,* an isoform of OspTx2a that blocks Kv channels (Krishnarjuna B. *et al.,* 2018; Sunanda P. *et al.,* 2018).

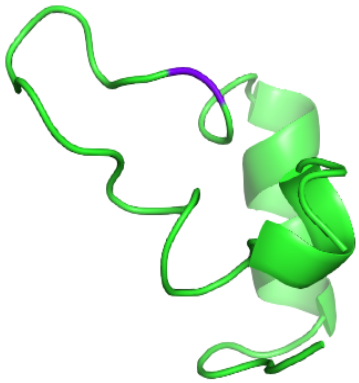

TCRDNVNRGICAMHKANGRCKQDYSDWMFIMKNQCAKTCGFC

Figure 18. SXCL-1 peptide. A) Model structure of SXCL-1 with functional Lys highlighted in violet (K21). **B)** Aminoacidic sequence of SXCL-1 with Lys (K21) in violet.

3.2.2 SXCL-6

The *ShK-like* peptide SXCL-6, expressed in the yeast *Pichia pastoris*, presents a slightly longer aminoacidic sequence than SXCL-1, comprising 48 residues, 6 cysteines pattern and candidate functional lysine in position 28 (K28). SXCL-6 model was created using the SWISS-model software (for further details see Material and Methods, sections 2.6 and 2.7) based on the sequence homology between SXCL-6 and already existing peptides. In figure 19, is showed the representative model of SXCL-6, obtained using as a template BgK toxin, from the sea anemone *Bundosoma granulifera*, a known and characterized toxin that inhibit Kv channels (Cotton J. *et al.,* 1997).

AYDVCKDRAQPSVCQRHKEKGRCDGEDKDWKYIMKLNCKKTCGFCTAY

Figure 19. SXCL-6 peptide. A) Model of SXCL-6 with candidate functional lysine coloured in violet (K28). **B)** Amino acidic sequence of SXCL-6 peptide with lysine (K28) in violet.

3.3 Objectives

SXCL-*like* proteins, SXCL-1 and SXCL-6, presenting the characteristic ShKT domain within the sequence with functional lysine in position 21 and 28, respectively, are valuable candidates as potent inhibitors of the voltage-gated K^+ channel, Kv1.3. To investigate the properties of the peptides, I performed electrophysiological investigations using the whole-cell patch clamp technique, aimed at testing the peptides at different concentrations within the nanomolar range (nM). The main purpose was to delineate the pharmacological profile of the two peptides, using as a positive control the well characterized ShK toxin from the sea anemone *Stichodactyla heliantus.*

I then applied a combination of computer modelling and computational alanine scanning (see Material and Methods, sections 2.6 and 2.7) to predict the potential interaction sites between the two novel *ShK-like* peptides and Kv1.3 channel. From the investigation, three main aminoacidic residues resulted to be involved in the channel-peptides interaction. Therefore, I investigated whether mutations affecting these three important binding sites located at the channel pore, can cause a reduction of the affinity channel-peptides, therefore limiting the ability of the peptides to bind to the channel. Residues considered for site-directed mutagenesis analysis were: Asp449, Val453 and His451.

3.4 Results

3.4.1 Electrophysiological characterisation of ShK

Kv1.3_WT channel currents were recorded using whole-cell patch clamp technique on tsA201 cells, transiently transfected with hKv1.3 DNA. Currents were evoked using a "+ 50mV continuously" protocol as described previously (see Material and Methods, section 2.4) and then analysed at +50 mV as peak current (pA).

First investigations were focused on the characterisation of the effect of a well-known and effective Kv1.3 blocker, the ShK toxin, from the sea anemone *Stichodactyla heliantus* (Castraneda O. et *al.,* 1995). The toxin was purchased from AlomoneLab (Israel) and tested at various concentrations (nM range). In figure 20, is showed Kv1.3_WT in control conditions. The channel presents an average peak current of 4699 pA (95% CI 1073: 8326 n=5). To note, tSA-201 cells, express some background currents that is possible to record using the same approach reported above. Below, in figure 20 (in red), untransfected cells show an average peak current of 563 pA (n=4).

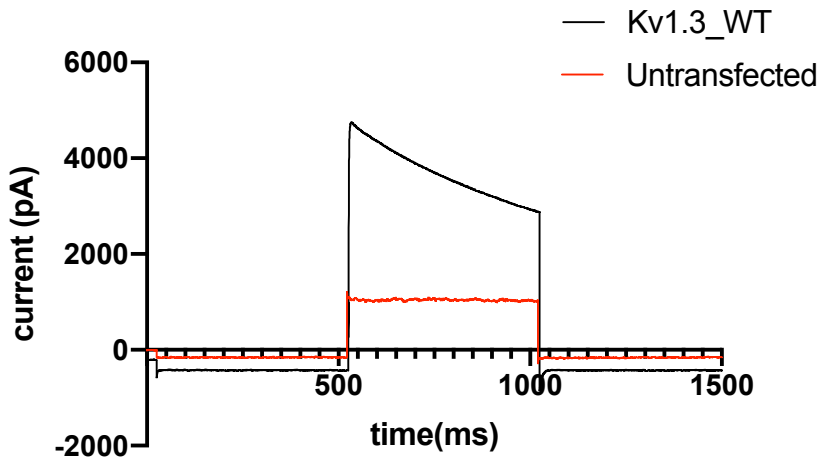

Figure 20. Representative trace of Kv1.3_WT. Average peak current of Kv1.3_WT in control conditions was equal to 4699 pA (n=5). To note, in red, untransfected cells average current was equal to 563 pA (n=4).

Following the data sheet information available from AlomoneLab, we went on and tested different concentrations of the toxins in the nanomolar range, including 5 nM, 1 nM, 0.5 nM and 0.1 nM. Investigations were conducted by incubating Kv1.3_WT with ShK toxins at different concentrations, for 20 minutes in 5% CO_2 incubator. ShK is a potent Kv1.3 blocker, therefore, incubation of the channel with 5 nM, 1 nM, 0.5 nM and 0.1 nM, determined a reduction of the average Kv1.3_WT peak current from 4699 pA to 1484 pA (95% CI 542: 2427 n=7) (Figure 21 and representative trace Figure 22, A); 2068 pA (95% CI 1148: 2988 n=6) (Figure 21 and representative trace Figure 22, B); 3565 pA (95% CI 784: 6346 n=5) (Figure 21 and representative trace Figure 22, C) and 6070 pA (95% CI 4005: 8133 n=6) (Figure 21 and representative trace Figure 22, D) respectively.

To note, 5 nM of the toxin significantly inhibits the average peak current of the channel by 68% ($P<0.05$ using one-way ANOVA, Dunnett's multiple comparisons test).

A dose-responses curve was then plotted to establish the IC50 of the toxin for our investigations. ShK shows an IC50 of 0.5 nM with sigmoidal course (Figure 23.).

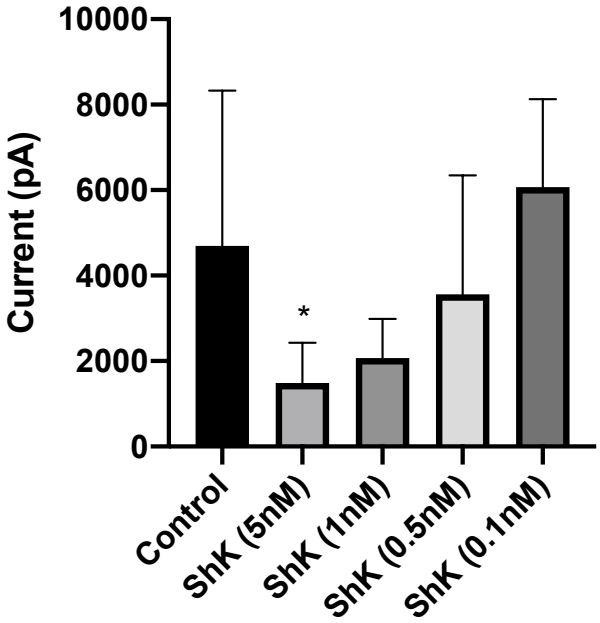

Figure 21. Peak current graphic of Kv1.3_WT in control and with different concentrations of ShK. Bars are indicative of 95% Confident Intervals (CI) of the mean. ShK at 5 nM, significantly inhibit the channel currents by 68% (p=0.0236).

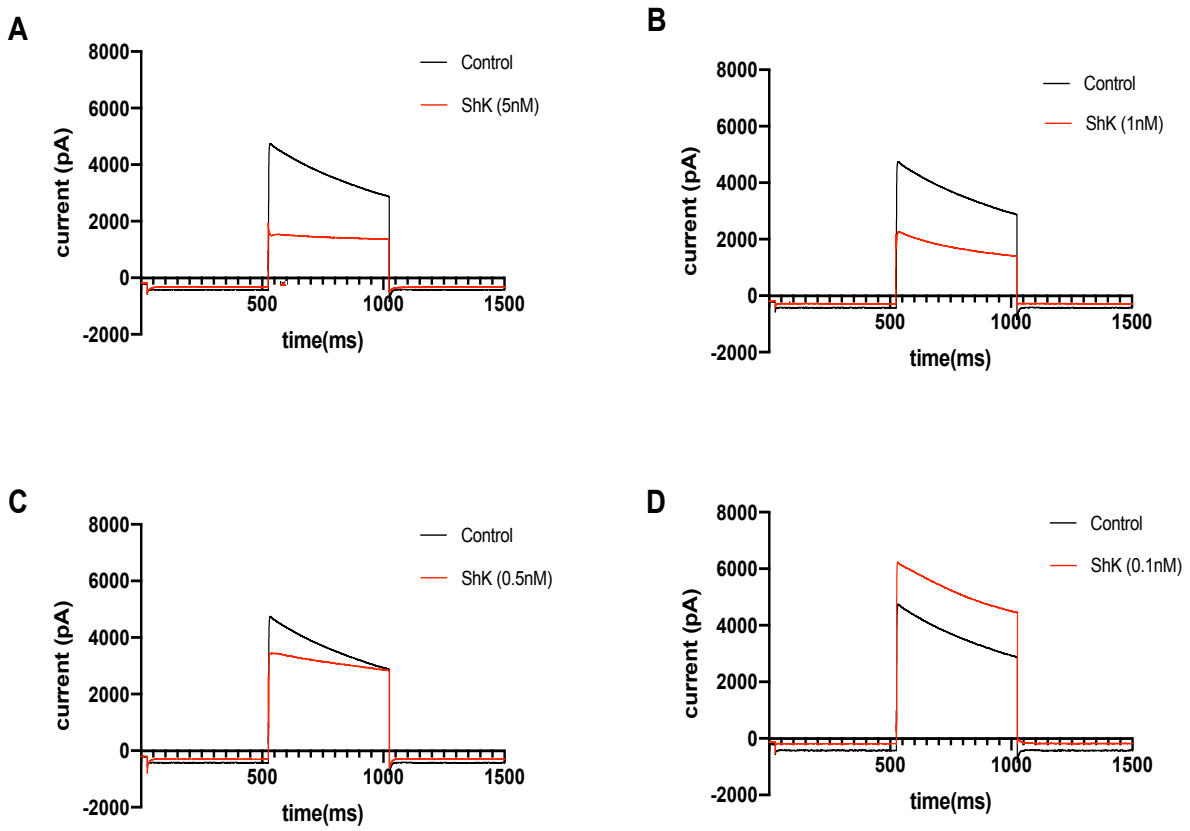

Figure 22. Layout panel representative of Kv1.3_WT in control and with different concentrations of ShK toxin. Representative traces Kv1.3 in control conditions (in black) and in presence of various concentration of ShK toxin (in red). **A)** Kv1.3 in control and ShK at 5 nM; **B)** Kv1.3 in control and ShK at 1 nM; **C)** Kv1.3 in control and ShK at 0.5 nM; **D)** Kv1.3 in control and ShK at 0.1 nM.

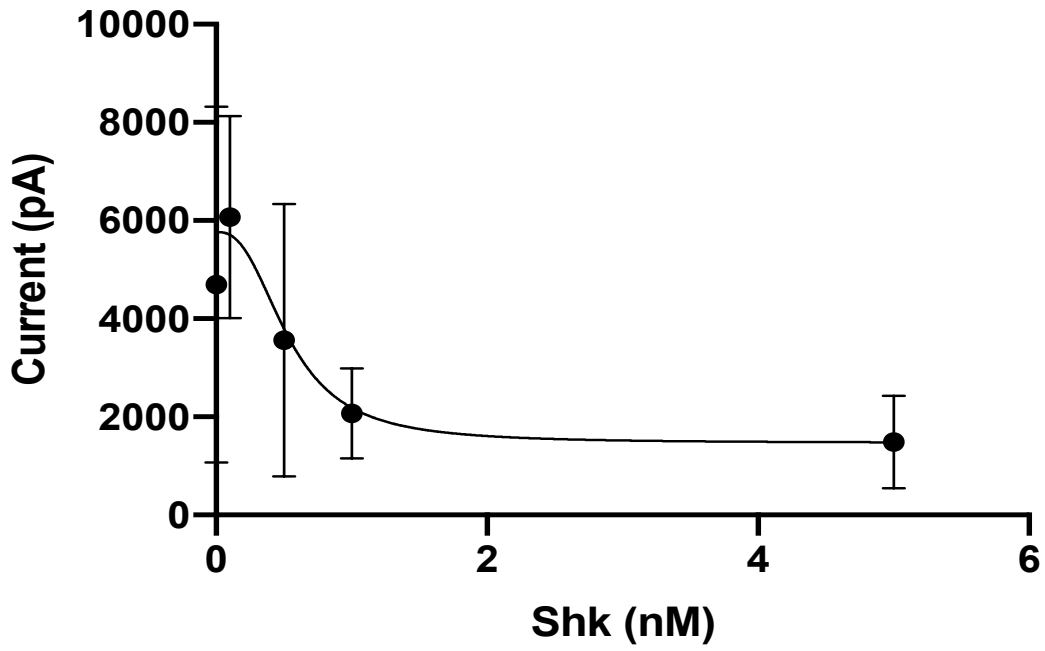

Figure 23. Dose-responses curve of ShK. The toxin presents an IC50 of 0.5 nM with sigmoidal course. Concentrations included in our investigations were 5 nM, 1 nM, 0.5 nM and 0.1 nM.

3.4.2 Electrophysiological characterisation of SXCL-1

Considering the results obtained from our investigations conducted using ShK toxin as a positive control, we determined an initial range of concentrations to test for our two novel *ShK-like* peptides, SXCL-1 and SXCL-6. As such, we started from concentrations spacing in the nanomolar range (nM) and we used a similar investigation method. Kv1.3_WT channel currents were recorded using whole-cell patch clamp technique on tsA201 cells, transiently transfected with hKv1.3 DNA. Currents were evoked using a "+50 mV continuously" protocol as described previously (see Material and Methods, section 2.4) and then expressed as average peak current (pA). Kv1.3_WT expression resulted in an average peak current expression resemble to 4875 pA, in control conditions (95% CI 3980: 5771 n=30) (Figure 24).

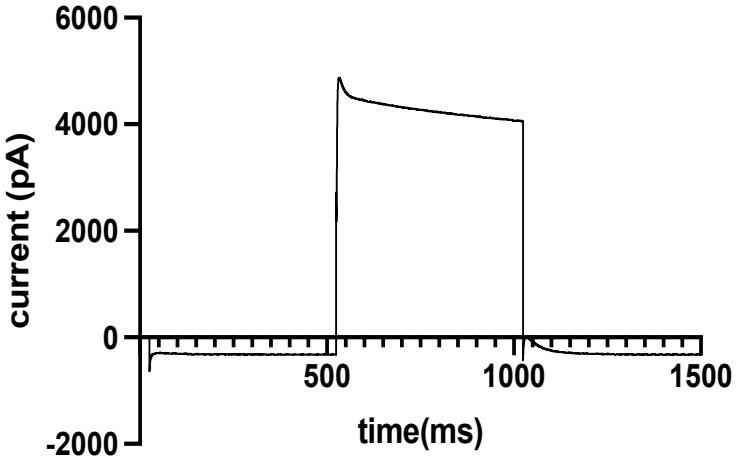

Figure 24. Electrophysiological profile of Kv1.3_WT channel in control conditions. Whole-cell currents are evoked at +50 mV. The average peak current is 4875 pA (n=30).

Kv1.3_WT was then incubated with SXCL-1 peptide using various concentrations of the peptide for each experiment, in a similar way to what showed for ShK. Concentrations tested were: 10 nM, 5 nM, 1 nM, 0.5 nM, 0.1 nM, 0.03 nM and 0.001nM.

Incubation of Kv1.3_WT with 10 nM of SXCL-1 determined an average peak current of 2224 pA (95% CI 872: 3576; n=7) (Figure 25 and representative trace Figure 26, A). Current significantly reduced by 55% in presence of the peptide ($P<0.05$ using one-way ANOVA, Dunnett's multiple comparisons test). 5nM of SXCL-1 determined an average peak current resemble to 1757 pA (95% CI 486: 3028; n=13) (Figure 25 and representative trace Figure 26, B). Also, at 5 nM was observed a significant current inhibition resemble to 64% ($P<0.05$ using one-way ANOVA, Dunnett's multiple comparisons test).

When 1 nM, 0.1 nM, 0.03 nM and 0.001 nM of the peptide were incubated with Kv1.3_WT channel, the resulting average peak currents were equal to 3026 pA (95% CI 2018 : 4034; n=7) (Figure 25 and exemplar trace Figure 26, C); 3607 pA (95% CI 2362 : 4852; n=7) (Figure 25 and exemplar trace Figure 26, D); 5398 pA (95% CI 2595 : 8200; n=6) (Figure 25 and exemplar trace Figure 26, E); 5708 pA (95% CI 3031 : 8386; n=6) (Figure 25 and exemplar trace Figure 26, F) and 4522 pA (95% CI 3259 : 5786; n=10) (Figure 25 and exemplar trace Figure 26, G), respectively, with no statistical significance ($P> 0.05$, using one-way ANOVA, Dunnett's multiple comparisons test).

Once determined the range of concentrations and the effect of each concentration on the average peak current of the channel, a dose-responses curve was plotted. SXCL-1 has an IC50 of 0.6 nM. The curve presents a sigmoidal course (Figure 27).

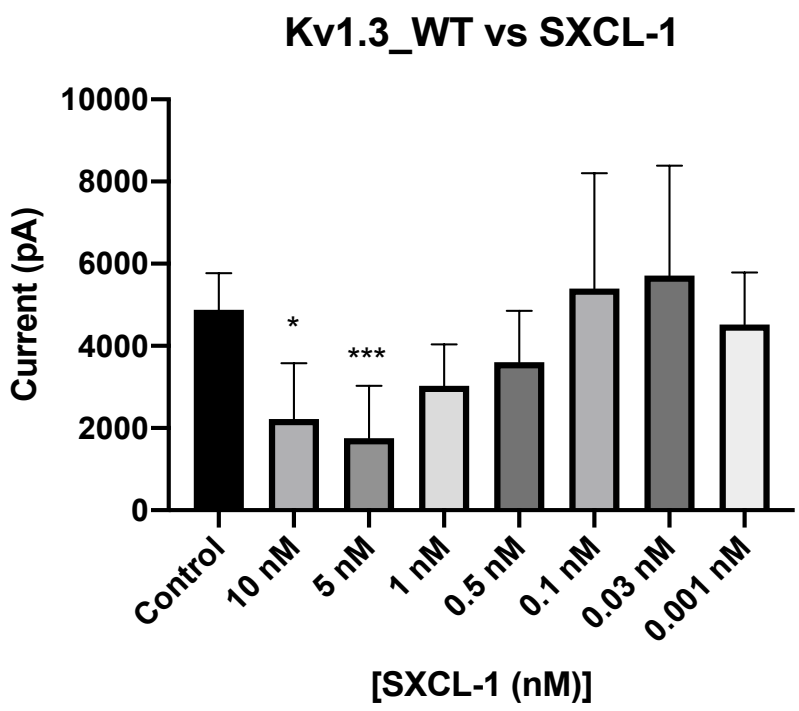

Figure 25. Peak current graphic of Kv1.3_WT in control conditions and with different concentrations of SXCL-1. Bars are indicative of 95% Confident Intervals (CI) of the mean. SXCL-1 at 10 nM (n=7) significantly reduces the channel current by 55% (p=0.0247). 5 nM (n=13) of the peptide significantly inhibit the channel currents (p=0.0002) causing a reduction of the average peak current resemble to 64%.

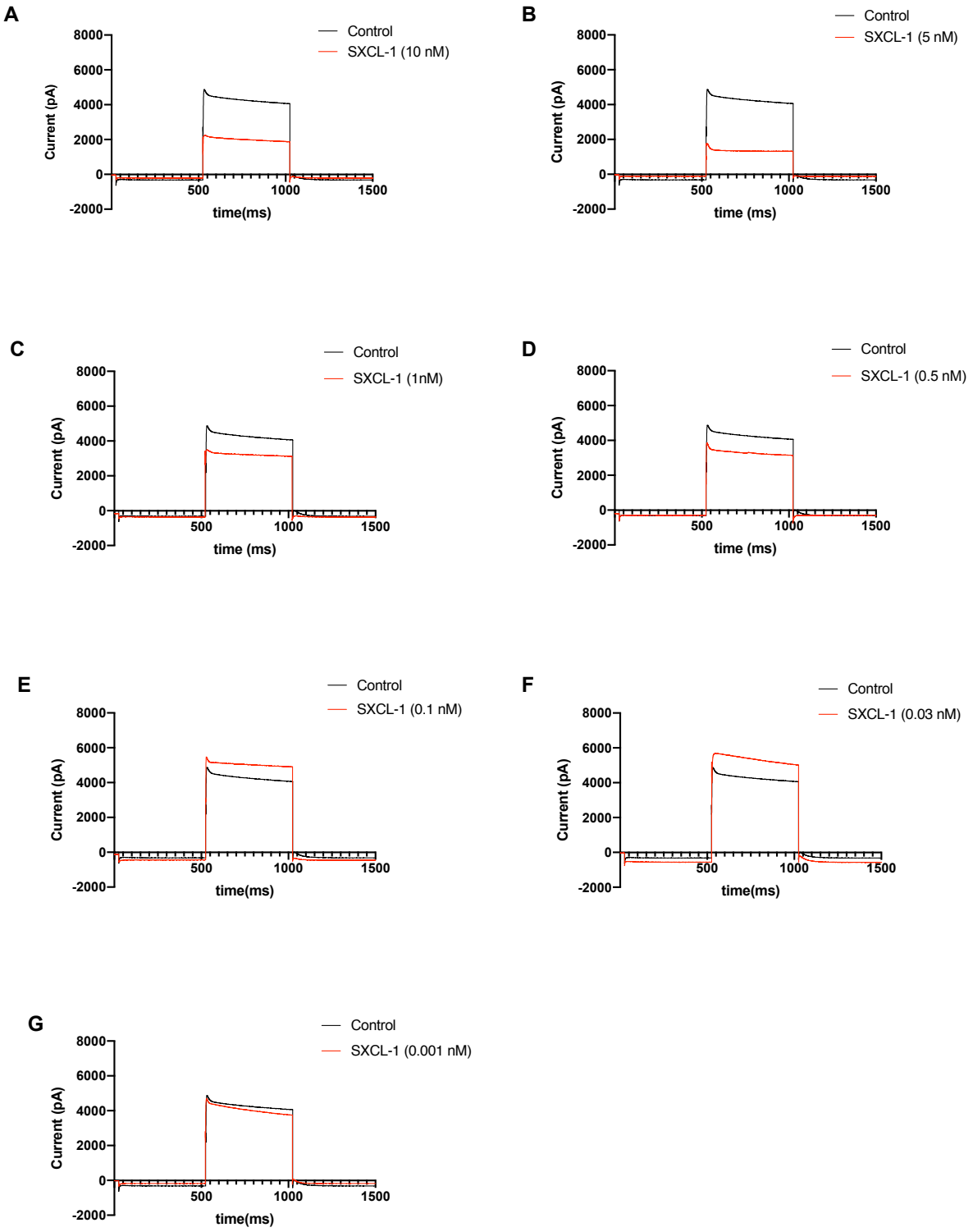

Figure 26. Representative layout figure of Kv1.3_WT in control conditions (in black) and with different concentrations of SXCL-1 peptide (in red). A) Kv1.3 in control and in SXCL-1 (10 nM); **B)** Kv1.3 in control and in SXCL-1 (5 nM); **C)** Kv1.3 in control and in presence of SXCL-1 (1 nM); **D)** Kv1.3 in control conditions and with SXCL-1 (0.5 nM); **E)** Kv1.3 in control and in SXCL-1 (0.1 nM); **F)** Kv1.3 in control and in SXCL-1 (0.03 nM); **G)** Kv1.3 in control and in SXCL-1 (0.001 nM).

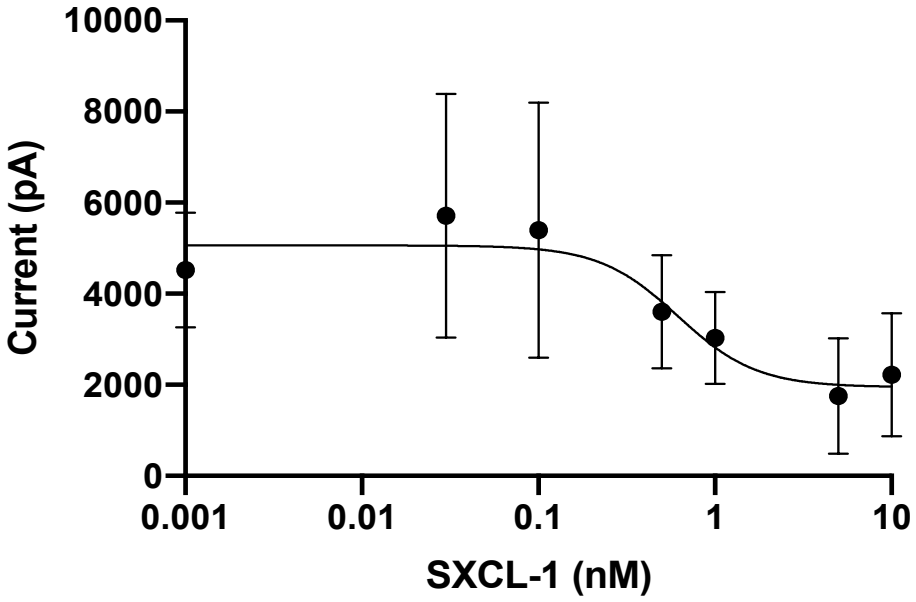

Figure 27. Concentration-responses curve for SXCL-1. The peptide presents an IC50 of 0.6 nM with a sigmoidal course. Range of concentrations plotted included 10 nM, 5 nM, 1 nM, 0.5 nM, 0.1 nM, 0.03 nM and 0.001 nM.

3.4.3 Investigation of the interaction sites between Kv1.3 and SXCL-1

Computer modelling analysis were performed to underpin the possible interaction sites between SXCL-1 and Kv1.3 channel. Previous studies have highlighted the importance of the pore region as the binding area on the channel for several Kv1.3-blockers that have in common the characteristic ShK-*like* domain, and the mechanism of action have been already elucidated. In particular, several evidences highlighted the importance of a residue, D449, located at the pore region, for the binding of toxin to the channel (Chen *et al.,* 2011). Therefore, this residue has been considered as the main input for our investigations when computer modelling analysis were performed using ZDOCK server (see Material and Methods, section 2.6). Together with this residue, Lys21 in SXCL-1 was considered for the investigation, as the second input for the server to work with.

In figure 28 and 29, is showed a proposed model of interaction between SXCL-1 on Kv1.3 channel. The peptide is coloured in yellow and the pore region of the channel is coloured in pink. According to the computer analysis and the electrophysiological investigations conducted in the laboratory, SXCL-1 seems to approach the pore region of the channel. Based on our hypothesis, the peptide could interact with residues at the outer entrance of the channel pore, mimicking the already know motion "cork-bottle" that is a common feature of pore-blocker peptides (Chandy K. G. and Norton R. S., 2017). The result is a significantly potent inhibition of the channel current at concentrations in the nanomolar (nM) range as showed in the previous result section (3.4.2)

Figure 28. Proposed model of interaction between SXCL-1 and Kv1.3. The pore region is highlighted in pink and the SXCL-1 in yellow. The peptide, in yellow, is approaching the pore region. (Image was created using PyMoL for evaluation only).

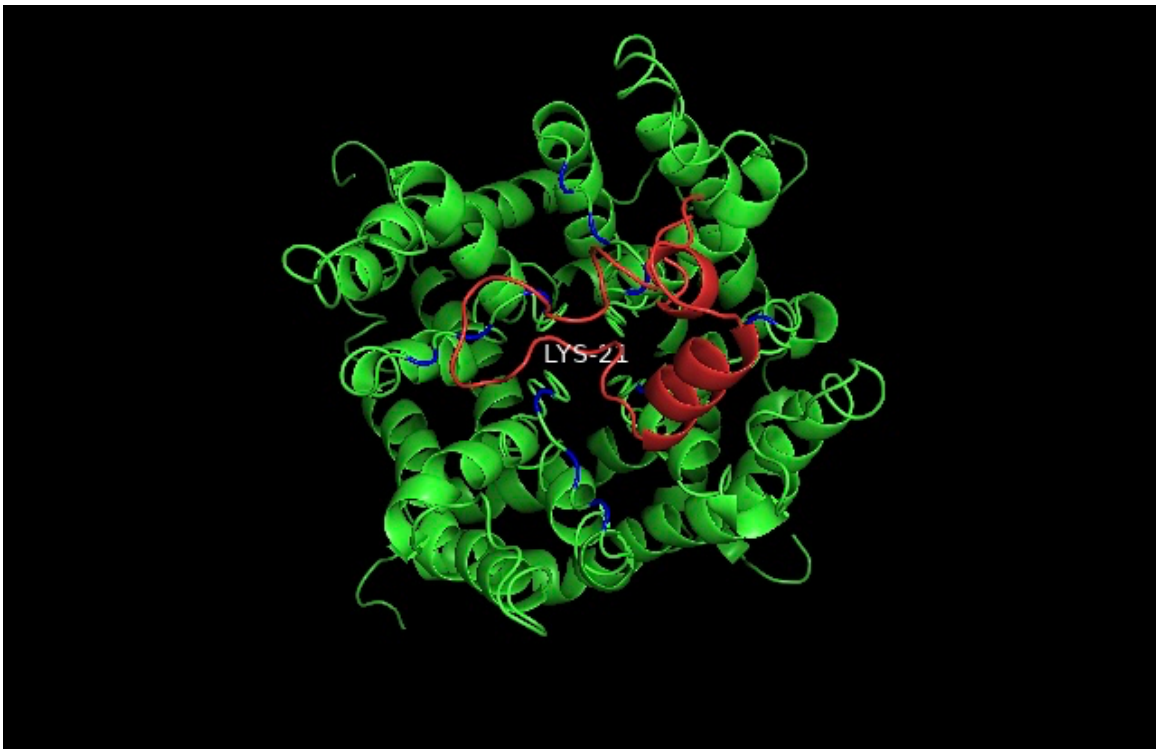

Figure 29. Top view of SXCL-1 approaching the pore region of Kv1.3. Lysine 21 is labelled. In blue are highlighted the residues withing the pore region considered important for the binding (H451, D449 and V453) (Image was created using PyMoL for evaluation only).

3.4.4 Electrophysiological characterisation of SXCL-6

Electrophysiological characterisation of SXCL-6 was conducted using a similar approach to SXCL-1 and the same range of concentrations. Kv1.3_WT was incubated with SXCL-6 peptide for 20 minutes in 5% CO_2 incubator, with different concentrations of the peptide for each experiment (10 nM, 5 nM, 1 nM, 0.5 nM, 0.1 nM, 0.03 nM and 0.001 nM).

Incubation of Kv1.3_WT with 10 nM, 5 nM, 1 nM, 0.5 nM, 0.1 nM, 0.03 nM and 0.001 nM, determined an average peak current of 2065 pA (95% CI 1055: 3074 n=7); 4500 pA (95% CI 2046: 6953 n=8); 5381 pA (95% CI 2910: 7853 n=7); 6093 pA (95% CI 3928: 8258 n=8); 6837 pA (95% CI 4741: 8933 n=7); 4805 pA (95% CI 3768: 5841 n=8) and 4311 pA (95% CI 2238: 6384 n=6), respectively (Figure 30 and representative trace Figure 31 A-G).
To note, incubation with 10 nM of SXCL-6 determines a significant inhibition of the channel current of 57% when compared to the average peak current of Kv1.3_WT equals to 4875 pA (95% CI 3980: 5771 n=30) ($P<0.05$ using one-way ANOVA, Dunnett's multiple comparisons test).

In a similar way to what showed for ShK and SXCL-1, a dose-response curve was fitted for SXCL-6. The peptide presents an IC50 of 6 nM, with sigmoidal course (Figure 32).

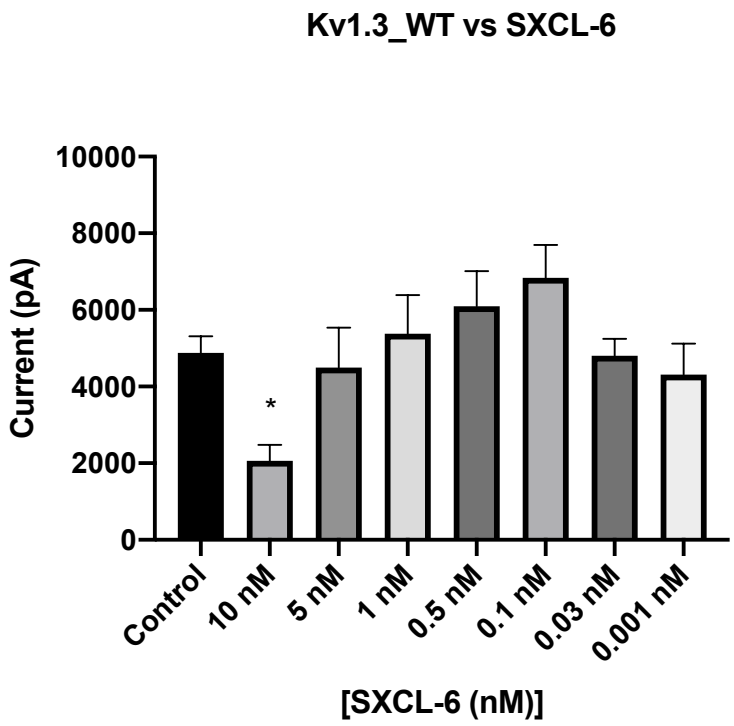

Figure 30. Peak current graphic of Kv1.3_WT in control conditions and with different concentrations of SXCL-6. Bars are indicative of 95% Confident Intervals (CI) of the mean. SXCL-6 at 10 nM, significantly inhibit the channel currents (p=0.0315)

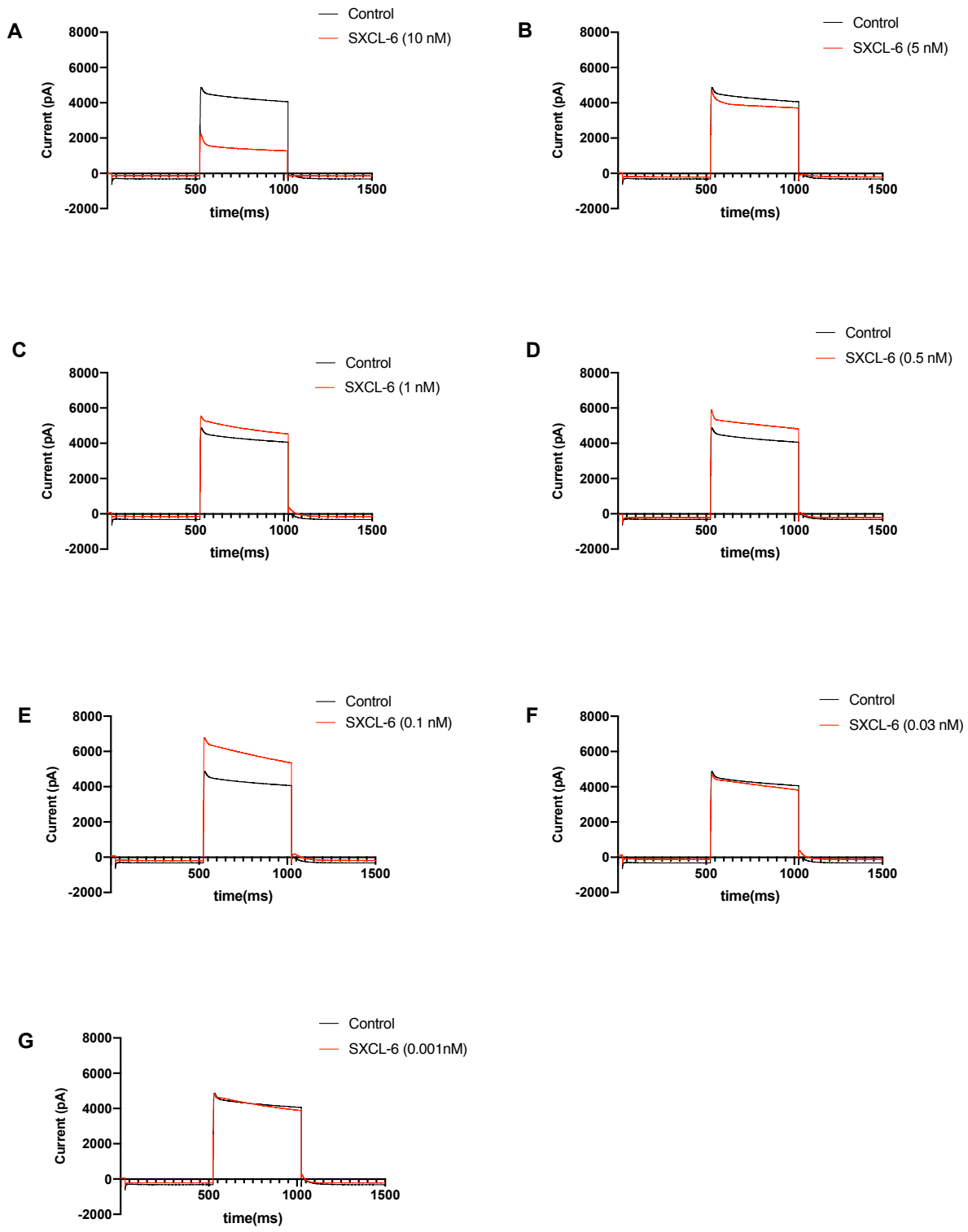

Figure 31. Layout panel representative of Kv1.3_WT in control conditions (in black) and in presence of various concentrations of SXCL-6 (in red). A) Kv1.3 in control and in SXCL-6 (10 nM); **B)** Kv1.3 in control and in SXCL-6 (5 nM); **C)** Kv1.3 in control and in SXCL-6 (1 nM); **D)** Kv1.3 in control and in SXCL-6 (0.5 nM); **E)** Kv1.3 in control and in SXCL-6 (0.1 nM); **F)** Kv1.3 in control and in SXCL-6 (0.03 nM); **G)** Kv1.3 in control and in SXCL-6 (0.001 nM).

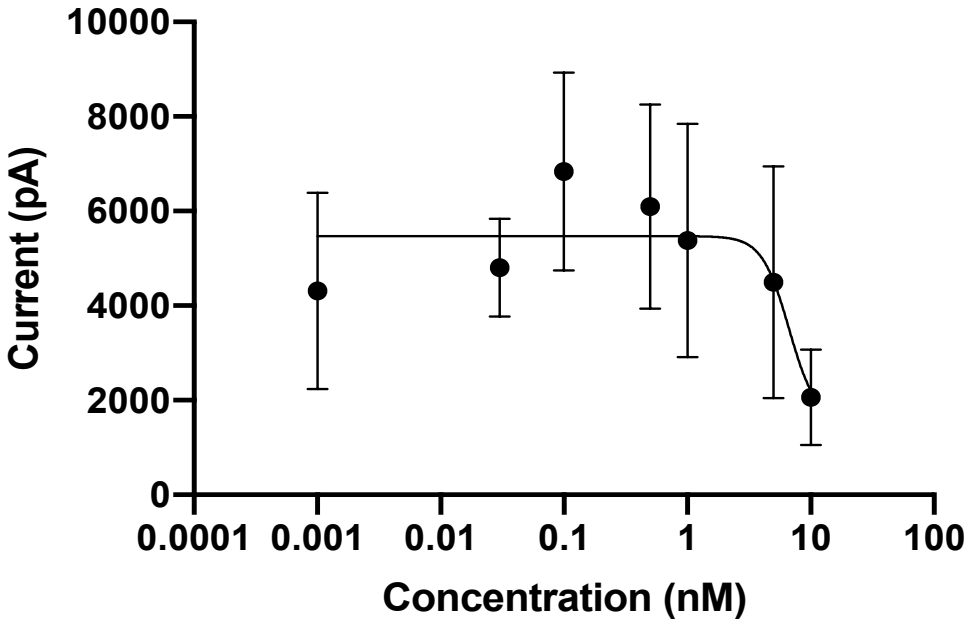

Figure 32. Dose-responses curve for SXCL-6 peptide. The peptide shows an IC50 of 6 nM, fitted in a sigmoidal course.

3.4.5 Investigation of the interaction sites between Kv1.3 and SXCL-6

SXCL-6, presents the characteristic *ShK-like* domain, with 6 cysteines motif and functional lysine that we speculate could be in position 28 (K28). As such, computer modelling analysis were conducted to predict the potential interaction sites between the peptide and Kv1.3 channel. In a way similar to SXCL-1, investigations were based on the assumption that the peptide, by sharing the conserved domain and the functional lysine (K28) within the aminoacidic sequence, might act as pore blocker and inhibiting the channel current by interacting with the pore region of Kv1.3 channel. In a work from *Chen et al.,* D449 is considered a critical residue for toxins to bind the channel (Chen *et al.,* 2011). In our investigations, we used D449 as input for the computer modelling predictions, together with the critical lysine, that we predicted to be at position 28 within the amino acidic sequence of the peptide. In figure 33, is showed a prediction of the binding site of SXCL-6 (in blue) on the channel pore (in pink). The prediction shows that the peptide might interact with the pore region of the channel, presumably by establishing interactions with residues located at this region. In figure 34, is showed a top view of the pore region and the peptide approaching the channel. Residues that we speculate are involved in the binding, are coloured in blue and are: H381, D379 and V383 that correspond to H451, D449 and V453 in hKv1.3 sequence.

Figure 33. Predicted binding mode of SXCL-6 on Kv1.3 channel. The pore region of the channel is highlighted in pink. SXCL-6 peptide is coloured in blue. To note, the peptide in the motion to approach the pore, could act by interacting with residues that are located in the pore region (Image was produced using PyMoL for evaluation only).

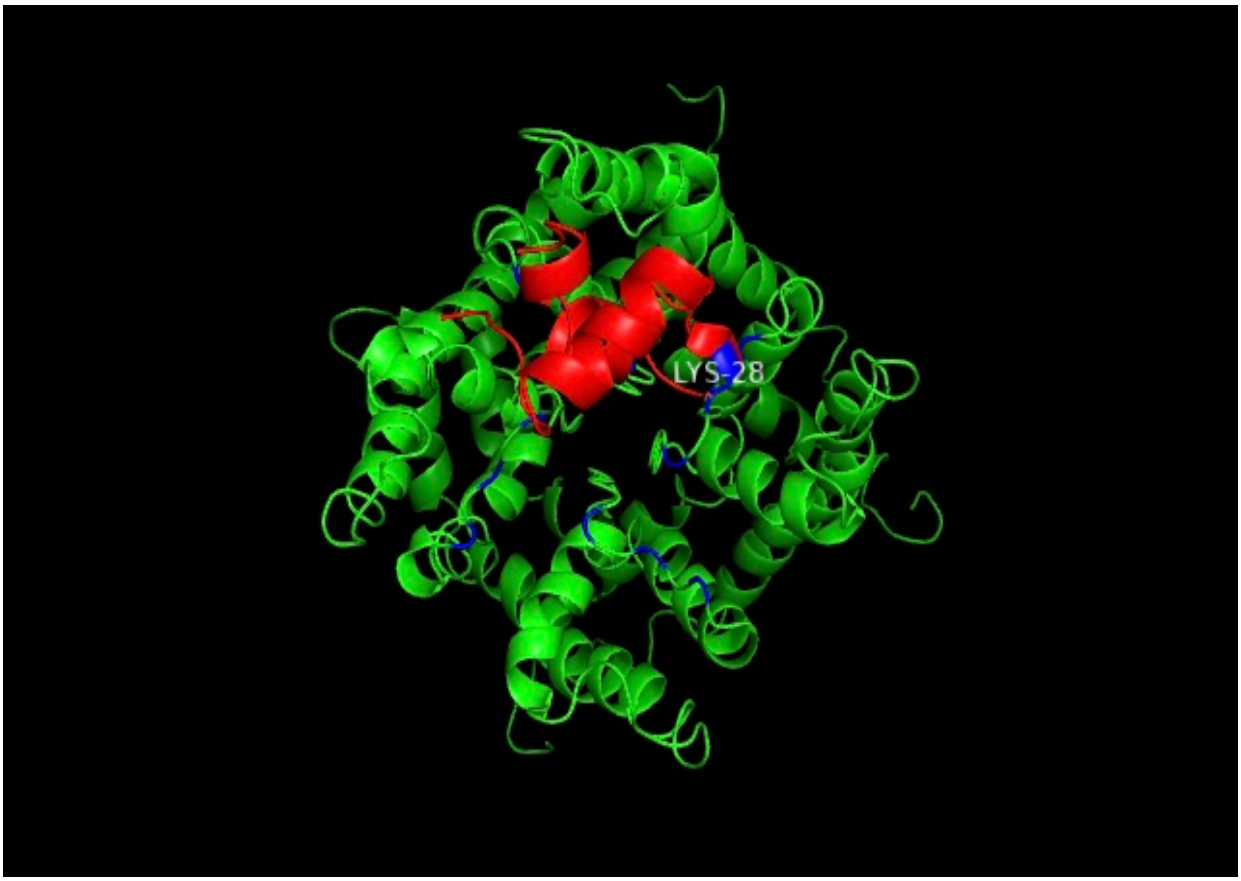

Figure 34. Kv1.3 channel and SXCL-6 top view. The peptide is coloured in red and predicted functional lysine is highlighted in blue (LYS-28). Residues within the pore region that resulted to be involved in the binding of the peptide to the channel, are coloured in blue and correspond to H451, D449 and V453. To note, the model is defined as "truncated" and report a difference of 70 amino acidic residues when compared to the hKv1.3 sequence. Therefore, all calculations are made respecting the nature of the model. (Image was produced using PyMoL for evaluation only).

3.5 Investigating the effect of three mutations in the pore region of Kv1.3 channel in the binding of ShK and *ShK-like* peptides, SXCL-1 and SXCL-6.

Computer modelling investigations suggested that it is likely to happen that the two peptides, acting as pore blockers, interact with residues located at the pore region, thus blocking the flux of ions through this region. Electrophysiological investigations, have confirmed that SXCL-1 and SXCL-6, are able to significantly reduce Kv1.3_WT current with an IC50 of 0.6 nM and 6 nM, respectively. We were then interested in understanding what aminoacidic residues were involved in the interaction between peptides-channel, when those are approaching the channel, and consequently, we asked whether mutations, involving those amino acidic residues, could affect the binding of the two peptides, thus abolishing their inhibitory effect. To answer these questions, computational alanine scanning analysis were performed on the top 10 complexes obtained from ZDOCK analysis. Evaluations were based on two main criteria: difference in free energy (ΔG) and frequency within the different complexes.

The free energy of the binding (ΔG), is an important parameter that defines the stability of protein-ligand complexes; only when the free energy of the system is negative, the protein-ligand binding can occur spontaneously (Du X. *et al.,* 2016). The level of the negative energy changes during the interaction between protein and ligand, therefore affecting the stability of the system. The second parameter considered during the evaluation was the frequency of the residues within the complexes. It is important to point out that several complexes are formed during the process of molecular recognition. Those are formed by the establishment of non-covalent interactions between biological molecules that interact with each other, or alternatively, with other small molecules (Janin J., 1995). As a result, more than 100 complexes Protein (P)-Ligand (A) were formed during the computational analysis using ZDOCK. Of those, the top 10 were used for analysis. Frequency within the complexes is an important parameter that indicates how often the residues were involved during the interaction protein-ligand.

A table summarising the results of the computational alanine scanning is showed below (Table 4).

Aminoacidic residues	Difference in energy (ΔG)	Complex and Frequency
P346VAL	0	1 (5)
P350GLU	0.51	5 (3,5,6,7,9)
P353ASP	-0.21	5 (3,5,6,7,9)
P354PRO	0.19	4(5,6,7,9)
P355SER	0.16	5(3,5,6,7,9)
P356SER	0	5(2,5,6,7,9)
P358PHE	0.09	5 (3,5,6,7,9)
P359ASN	0.07	3 (5,6,7)
P360SER	0.01	3(5,6,7)
P362PRO	0	1 (5)
P363ASP	0.66	3(5,6,7)
P366TRP	5.6	4 (2,5,6,7)
P375VAL	0	1 (7)
P377TYR	0.15	7 (2,3,5,6,7,8,9)
P379ASP	-47.85	7 (2,3,5,6,7,8,9)
P380MET	0.78	7 (2,3,5,6,7,8,9)
P381HSE	-8.95	6 (3,5,6,7,8,9)
P382PRO	0.01	6 (3,5,6,7,8,9)
P383VAL	-6.48	6 (3,5,6,7,8,9)
P384THR	0.23	6 (3,5,6,7,8,9)
P385ILE	0.42	5 (3,5,6,7,9)
P388LYS	-0.94	5 (3,5,6,7,9)
Top 3 Aa with highest score	**Interactions before mutation**	**Interactions after mutations**
P379ASP	A24ASP, A26GLU, A31LYS, A32TYR, A35LYS, A44PHE	A24ASP, A26GLU, A32TYR, A35LYS, A44PHE
P381HSE	A24AS, A25GLY, A26GLU, A27ASP, A30TRP, A31LYS, A32TYR, A35LYS, A25GLY, A26GLU, A27ASP, A28LYS	A26GLU, A27ASP, A30TRP, A32TYR, A25GLY, A26GLU, A27ASP, A28LYS
P383VAL	A29ASP, A30TRP, A31LYS, A32 TYR	A30TRP, A32TYR

Table 4. Results of computational alanine scanning analysis. ΔG in ASP379, H381 and V383 is highlighted in yellow. P indicates residues in the channel, A indicates residues in the peptide sequence.

According to the results, it was clear that three residues ASP379, H381 and VAL383, that correspond to D449, H451 and V453 in hKv1.3, were the most favourable amino acidic residues involved in the binding. The binding between the residue D379 on Kv1.3 channel and SXCL-6 peptide, is characterized by a value of ΔG equal to -47.85 *joules* and appears quite frequently, in 7 complexes out of the total 10 considered (Table 4).

The binding channel-peptide involving H381 and V453 show values of ΔG equal to -8.95 *joules* and -6.48 *joules*, respectively, and a frequency in 6 complexes out of 10 considered for both residues (Table 4). Interaction of the peptides with all three residues, by showing negative values of ΔG and high frequency among the complexes, are considered the most favourable to occur. In the latter part of the table, are indicated the aminoacidic residues for which the interaction is lost after the mutation of the residues in the channel to alanine (A) (Table 4, bottom). To note that after the mutation of each residue, D379, H381 and V453, a variable number of interacting residues within the amino acidic sequence of SXCL-6 are lost. Therefore, the peptide loses the ability to interact, mainly by establishing non-covalent interactions -van der Waals, hydrogen bonds, ion pairs and others- with the residues at the inner mouth of the pore region of the channel.

In figure 35, is showed a top view of the pore region of Kv1.3 with the three main residues labelled and coloured in different shades to give a pragmatic picture of where the residues are located in the pore region. In the picture, selectivity filter is also highlighted in yellow. All three residues are found to be located near the selectivity filter, with D449 being part of the signature sequence of the channel.

In light of the results obtained from the combination of computer modelling and computational alanine scanning, it is evident that all three residues might have a crucial role for the interaction of the peptides to the channel. We therefore investigated, via electrophysiological analysis, whether mutations involving those sites would reduce the affinity protein-ligand, thus decreasing the inhibitory effect of the peptides on Kv1.3 channel.

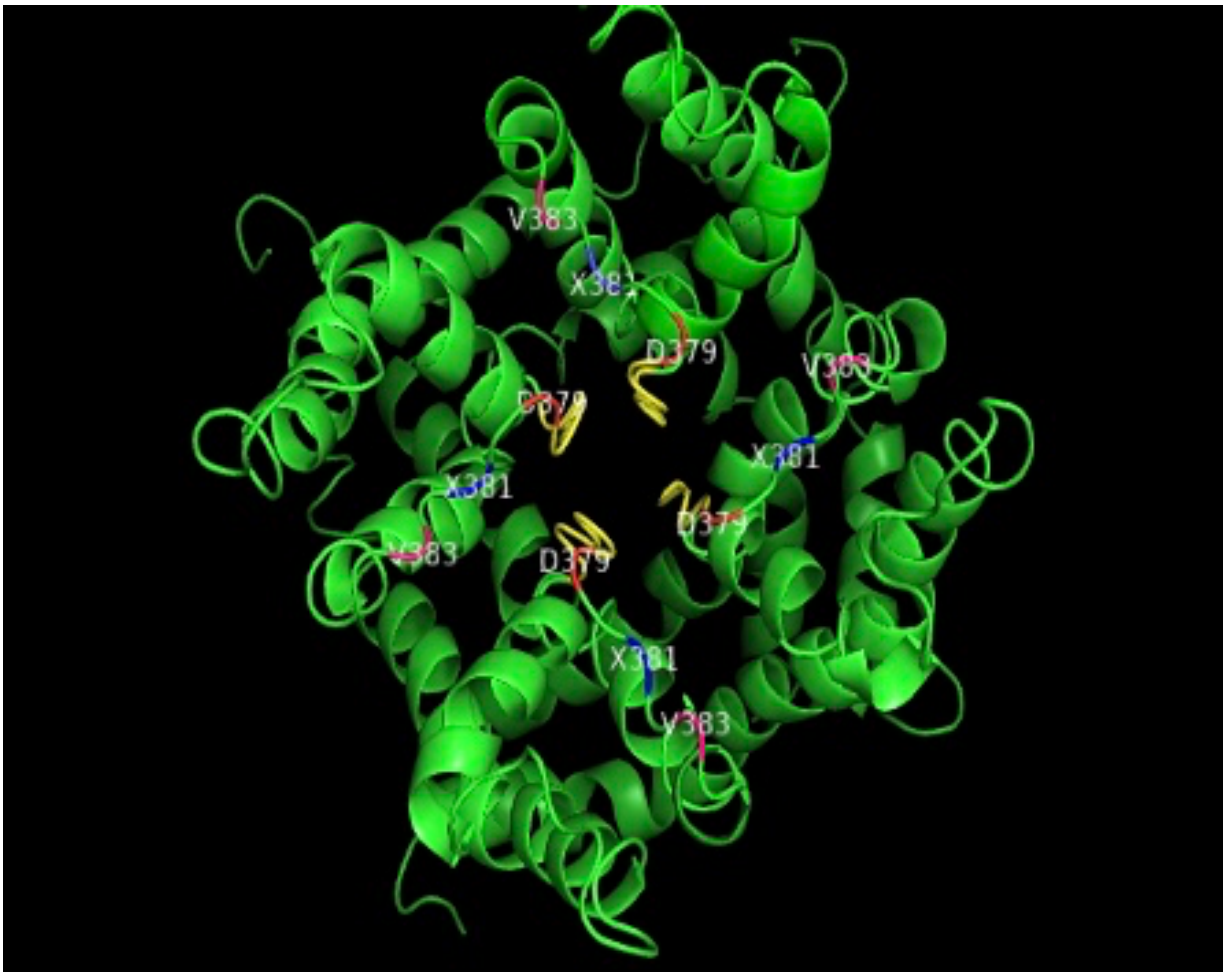

Figure 35. Kv1.3 model, top view with residues highlighted. In *yellow,* selectivity filter (374-379) which correspond to 444-449 in hKv1.3 sequence. In *red*, D379 (D449 in hKv1.3 sequence). In *blue,* H381 (H451 in hKv1.3 sequence). In *pink*, V383 (V453 in hKv1.3 sequence). All residues are found within the pore region of the channel, extended between aa346-aa386 (aa416-aa456 in hKv1.3 sequence). (Image was produced using PyMoL for evaluation only).

3.6 Functional characterisation of the mutation D449A and its implication for the channel-peptides interaction.

Site-directed mutagenesis was performed to obtain Kv1.3_D449A as previously described (see Material and Methods, section 2.8.2). Kv1.3_WT and Kv1.3_D449A currents were evoked at +50 mV and expressed as average peak current (pA). Below is showed a representative trace of Kv1.3_WT (in black) and Kv1.3_D449A (in red) (Figure 36). The average peak currents are 4524 pA (95% CI 2619: 6429 n=7) and 2029 pA (95% CI 1542: 2516 n=12), respectively. Mutation of the residue Aspartic acid (D) in Alanine (A), cause a significant inhibition of the channel currents resemble to 55%, as indicated in the peak current graphic below ($P< 0.05$, Unpaired t test) (Figure 37).

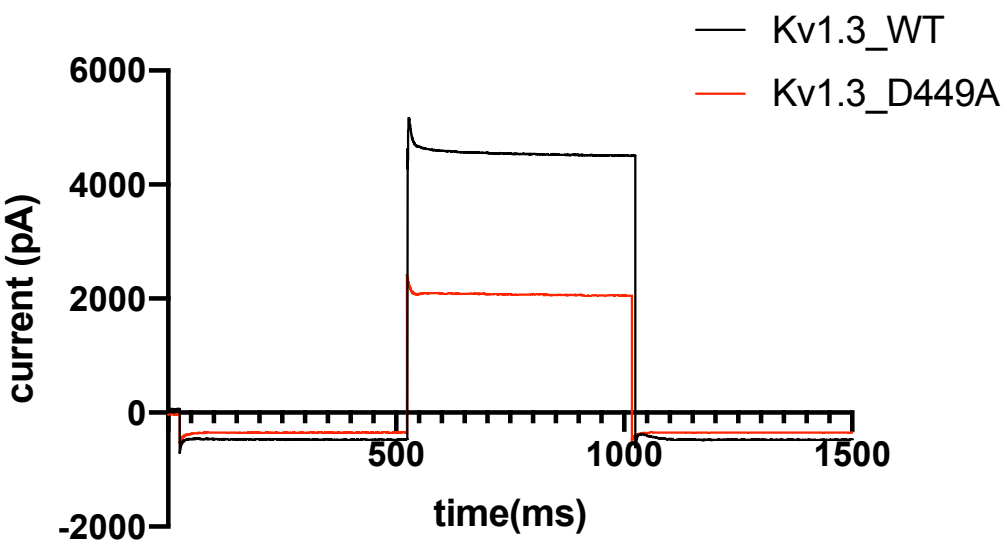

Figure 36. Representative trace of Kv1.3_WT and Kv1.3_D449A. In red is show the average peak current of Kv1.3 mutant compared to Kv1.3_WT, in black.

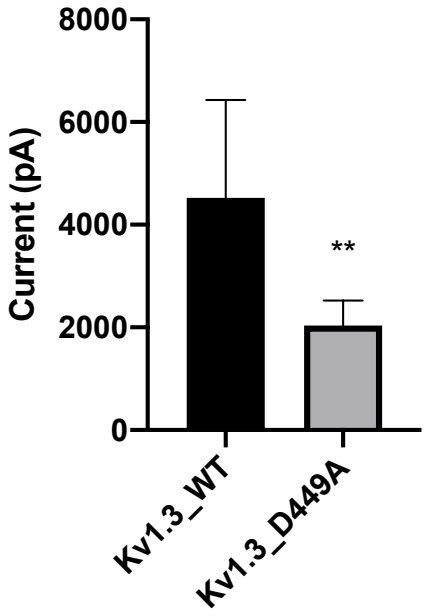

Figure 37. Peak current graphic of Kv1.3_WT and Kv1.3_D449A. Bars are indicative of 95% Confident Intervals (CI) of the mean. Kv1.3_D449A (n=12) current is significantly (Unpaired t test, adjusted P value p=0.0013) reduced compared to Kv1.3_WT (n=7).

3.6.1 Investigating the interaction between Kv1.3_D449A and ShK

Next, the effect of ShK on Kv1.3_D449A was tested by incubating the channel with 5 nM and then 10 nM of the peptide in 5% CO_2 incubator for 20 minutes.
Kv1.3_D449A in presence of 5 nM and 10 nM of ShK, present an average peak current of 1559 pA (95% CI 583.3: 2535 n=8) (Figure 38, A) and 1874 pA (95% CI 752: 2996 n=4) (Figure 38, B), respectively. In figure 39, a peak current graphic summarizes the results of the investigations with ShK at both concentrations. Data suggest a strong reduction of the interaction between the peptide and the channel, at concentrations of 10 nM and 5 nM of the peptides. Indeed, the peptide is only able to slightly reduce the average peak current of the channel by 23% at 5 nM, whereas a very small inhibition equal to 7% is observed when the concentration of the peptide is higher (10 nM). We found our results to be not statistically significant when one-way ANOVA (Dunnett's multiple comparisons test) was performed.

Taken together, these evidences are indicative of a critical role for the Aspartic acid at position 449, for the interaction between Kv1.3 and ShK.

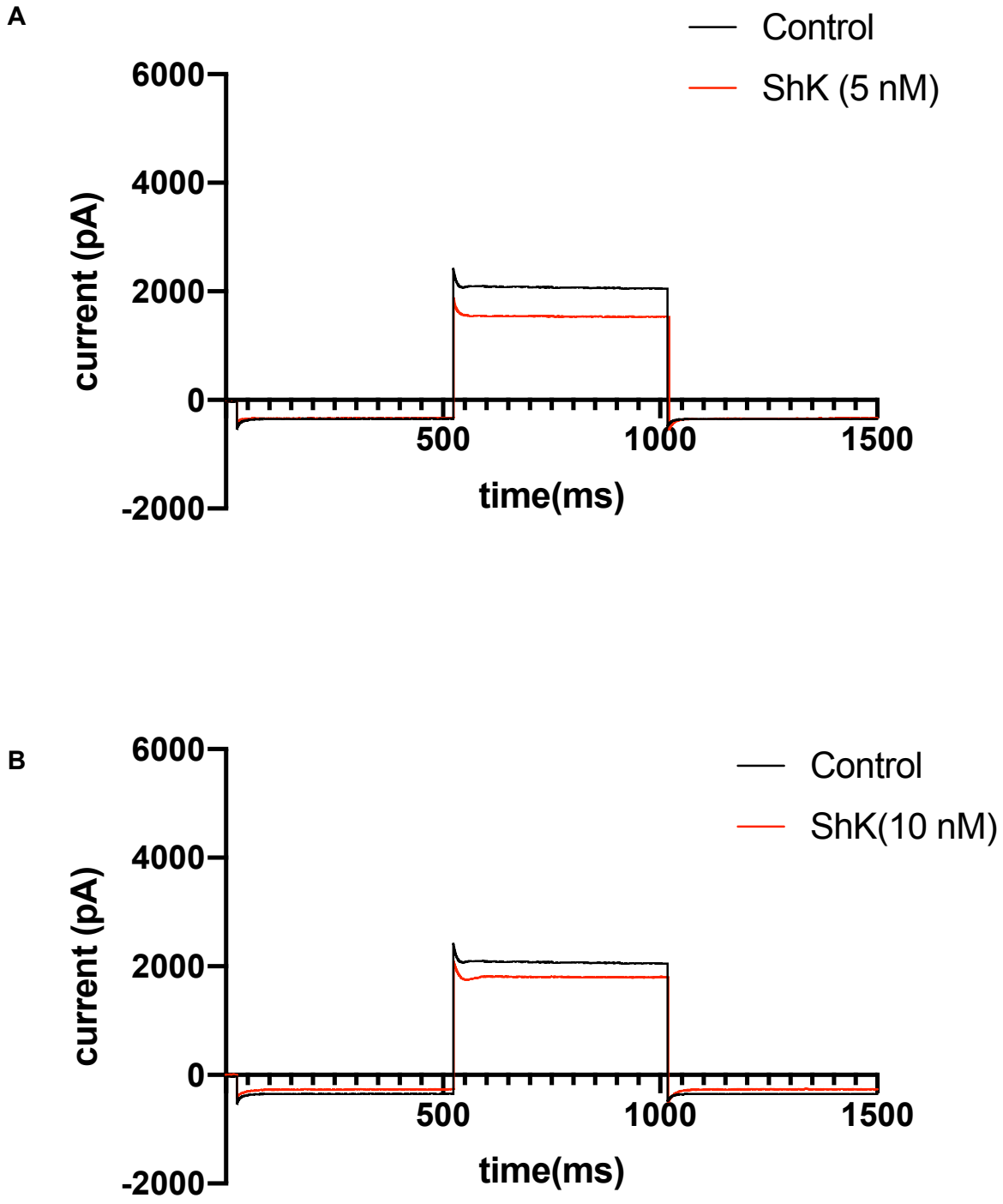

Figure 38. Layout representing Kv1.3_D449A in control conditions and in presence of 5 nM and 10 nM of ShK. A) Kv1.3_D449A in control (in black) and in ShK, 5 nM (in red); **B)** Kv1.3_D449A in control (in black) and in ShK, 10 nM (in red).

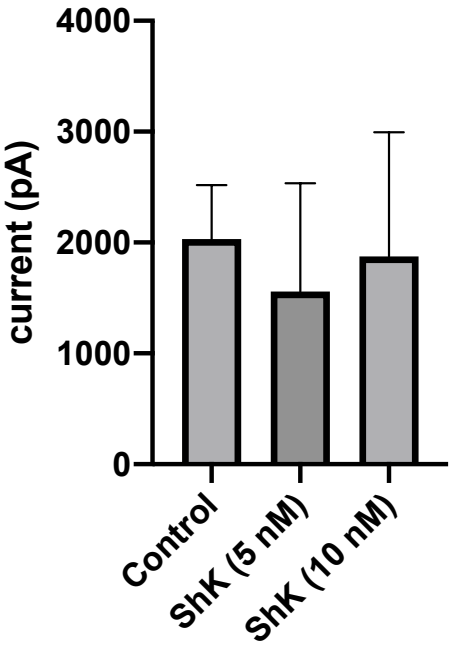

Figure 39. Peak current graphs representative for Kv1.3_D449A in control and with two concentrations of ShK. Bars are representative of 95% Confident Intervals (CI) of the mean. 5 nM (n=8) of ShK, only slightly reduced the channel currents by 23% (adjusted P value p=0.4539), whereas in presence of 10 nM (n=4) of the peptide the percentage of inhibition was reduced to 7% (adjusted P value p=0.9439).

3.6.2 Investigating the interaction between Kv1.3_D449A and the two novel *ShK-like* peptides, SXCL-1 and SXCL-6.

We then investigated whether the interaction of Kv1.3 with SXCL-1 and SXCL-6 was reduced following the amino acid substitution of the Aspartic acid (D) with Alanine (A).
Following 20 minutes of incubation in 5% CO2 incubator with 5 nM of SXCL-1, Kv1.3_D449A showed an average peak current (pA) of 1374 pA (95% CI 805: 1943 n=7) (Figure 40, A). The percentage of current inhibition was equal to 32% with no statistical significance (P>0.05 when using one-way ANOVA, Dunnett's multiple comparisons test). Incubation of the channel with 10 nM of SXCL-1 determined an average peak current resemble to 2415 pA (95% CI 2010: 2820 n=6) (Figure 40, B). At this concentration, no effect on the peak current of the channel was observed. When performed statistical analysis using one-way ANOVA (Dunnett's multiple comparisons test), results were found to be no statistically significant. In figure 41, a peak current graphic summarises the results of the investigations with SXCL-1.

Using the same approach, we investigated the effect of the mutation for the binding of SXCL-6. In figure 42, is showed a layout of representative traces of Kv1.3_D449A and SXCL-6 at 5 nM (Figure 42, A) and 10 nM (Figure 42, B). The average peak current of Kv1.3_D449A in presence of 5 nM and 10 nM of the peptide was equal to 1282 pA (506: 2058 n=5) and 1994 pA (95% CI 1374: 2614 n=6), respectively (P>0.05, one-way ANOVA- Dunnett's multiple comparisons test). In figure 43, a summary of the findings in the form of peak current (pA) graphic.

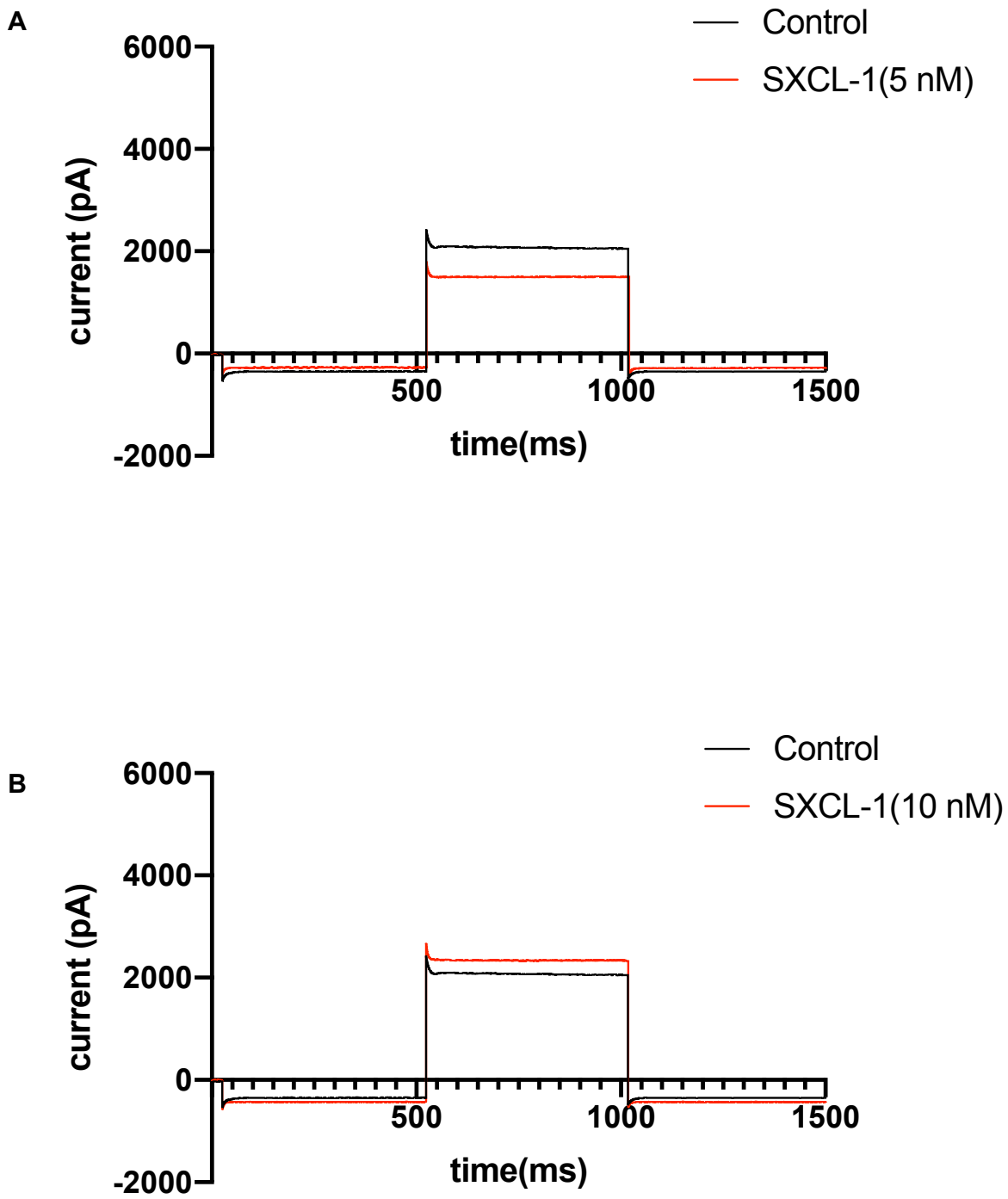

Figure 40. Layout representing Kv1.3_D449A in control and with 5 nM and 10 nM of SXCL-1. **A)** Kv1.3_D449A in control (in black) and in SXCL-1, 5 nM (in red); **B)** Kv1.3_D449A in control (in black) and in SXCL-1, 10 nM (in red).

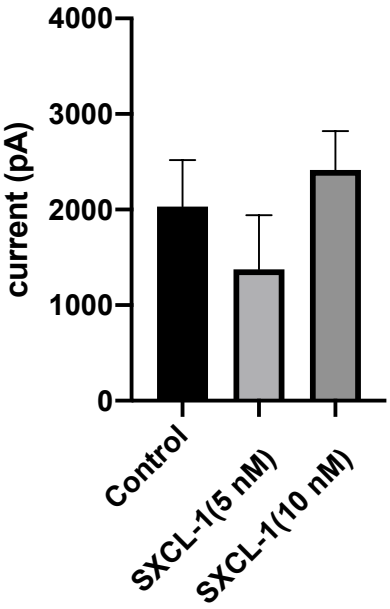

Figure 41. Peak current graphs representative for Kv1.3_D449A in control and with two concentrations of SXCL-1. Bars are representative of 95% Confident Intervals (CI) of the mean. 5 nM of SXCL-1 (n=7), reduced the channel currents by 32% (adjusted P value, p=0.0885); whereas in presence of 10 nM (n=6) of the peptide no effect was detected (adjusted P value, p=0.4213).

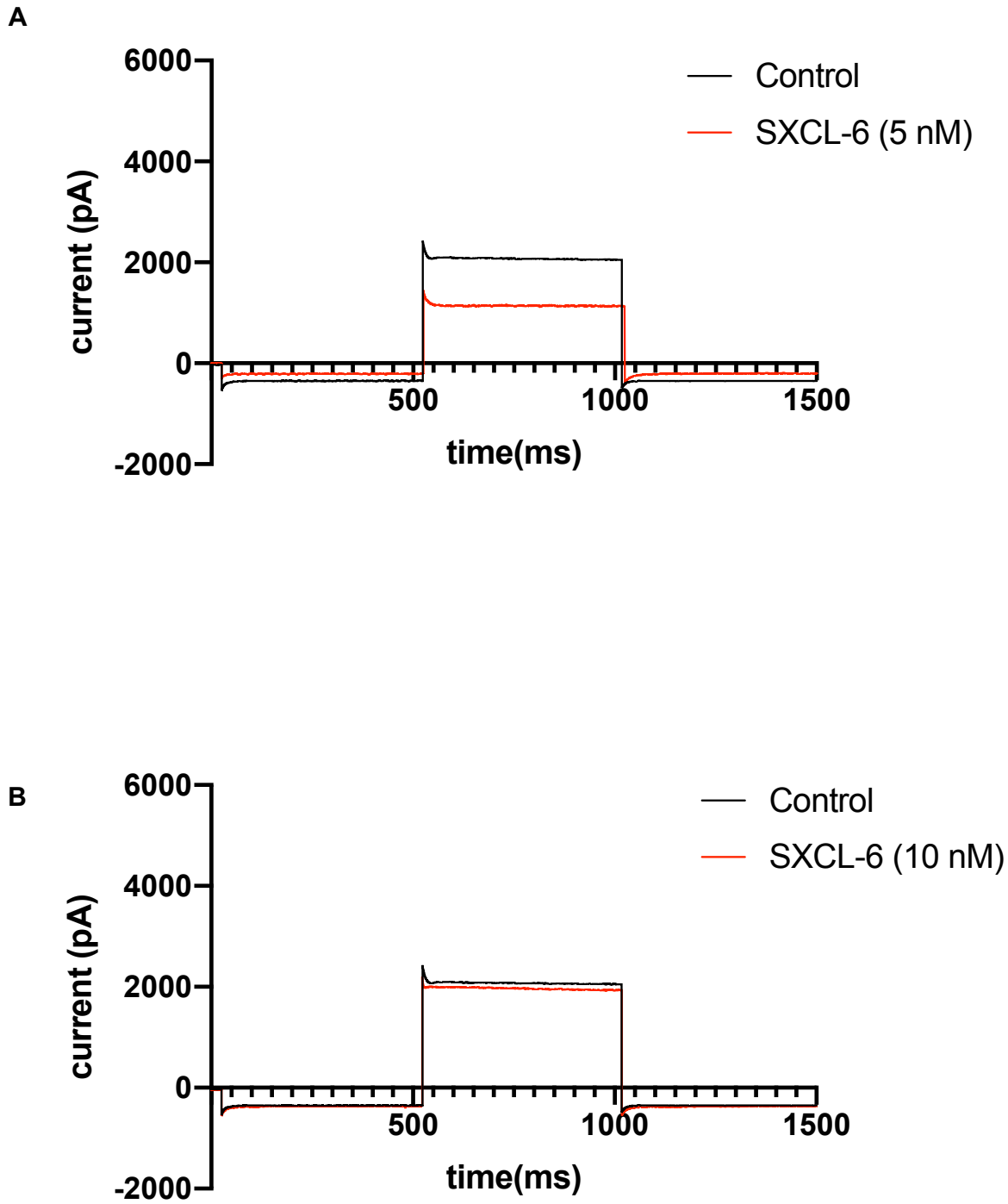

Figure 42. Layout representing Kv1.3_D449A in control and in presence of 5 nM and 10 nM of SXCL-6. A) Kv1.3_D449A in control (in black) and in SXCL-6, 5nM (in red); **B)** Kv1.3_D449A in control (in black) and in SXCL-6, 10nM (in red).

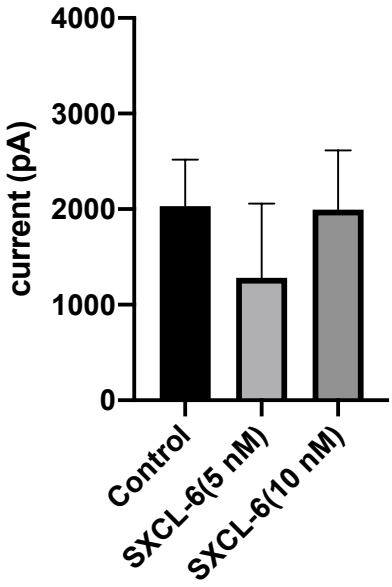

Figure 43. Peak current graphs representative for Kv1.3_D449A in control and with two concentrations of SXCL-6. Bars are representative of 95% Confident Intervals (CI) of the mean. 5 nM of SXCL-6 (n=5), reduced the channel currents by 37% (adjusted P value, p=0.1083); whereas in presence of 10 nM of the peptide (n=6) no effect was detected (adjusted P value, p=0.9934).

3.7 Functional characterisation of the H451A mutation and its implication for the channel-peptides interaction.

Site-directed mutagenesis was performed to obtain Kv1.3_H451A as previously described (see Material and Methods, section 2.8.2). Kv1.3_WT and Kv1.3_H451A currents were evoked at +50 mV and expressed as average peak current (pA).

Below is showed a representative trace of Kv1.3_WT (in black) and Kv1.3_H451A (in red) (Figure 44) and a peak current graphic (Figure 45). The average peak currents were 4524 pA (95% CI 2619: 6429 n=7) and 5572 pA (95% CI 4511: 6633 n=23), respectively. The average peak current (pA) is slightly higher for Kv1.3_H451A compared to the WT. Results were found to be not statistically significant (Unpaired t test, P>0.05).

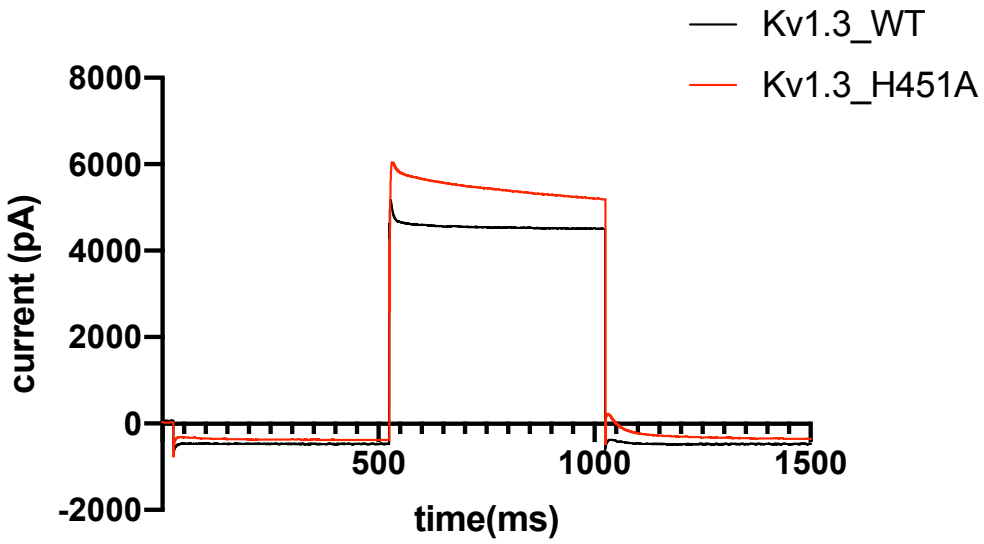

Figure 44. Representative traces of Kv1.3_WT and Kv1.3_H451A. In black is represented Kv1.3_WT and in red Kv1.3_H451A.

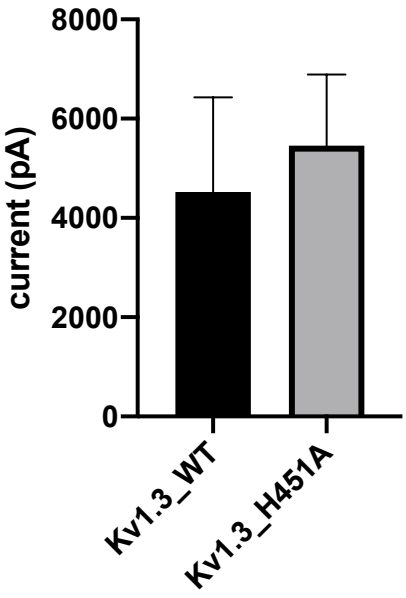

Figure 45. Peak currents (pA) graph representative of Kv1.3_WT and Kv1.3_H451A. Bars are indicative of 95% Confident Interval (CI) of the mean. Kv1.3_WT (n=7) and Kv1.3_H451A (n=23) are not significantly different (Unpaired t test, p=0.3152).

3.7.1 Investigating the interaction between Kv1.3_H451A and ShK

We then investigated whether the mutation in this specific site, could affect the binding of the ShK toxin, thus causing a reduction of the affinity channel-peptide. Therefore, 5 nM and 10 nM of ShK were incubated for 20 minutes in 5% CO_2 incubator.
Average peak currents (pA) of Kv1.3_H451A in presence of 5 nM and 10 nM of ShK were 4505 pA (95% CI 3590: 5419 n=10) (representative trace Figure 46, A) and 5648 pA (95% CI 2484: 8811 n=6) (representative trace Figure 46, B), respectively. In figure 47, a peak current graphic that summarizes the results of the findings.

Results from our investigations indicate that H451A mutation slightly enhance the current of Kv1.3 compared to the Kv1.3_WT, however we found our results to be not statistically significant. When the potent ShK toxin was incubated with Kv1.3_H451A, at both 5 nM and 10 nM, no significant peak current inhibition was observed (Figure 46 and 47). For both concentrations tested (5 nM and 10 nM), results were analysed performed one-way ANOVA (Dunnett's multiple comparisons test) and no statistically significant values were found ($P>0.05$).

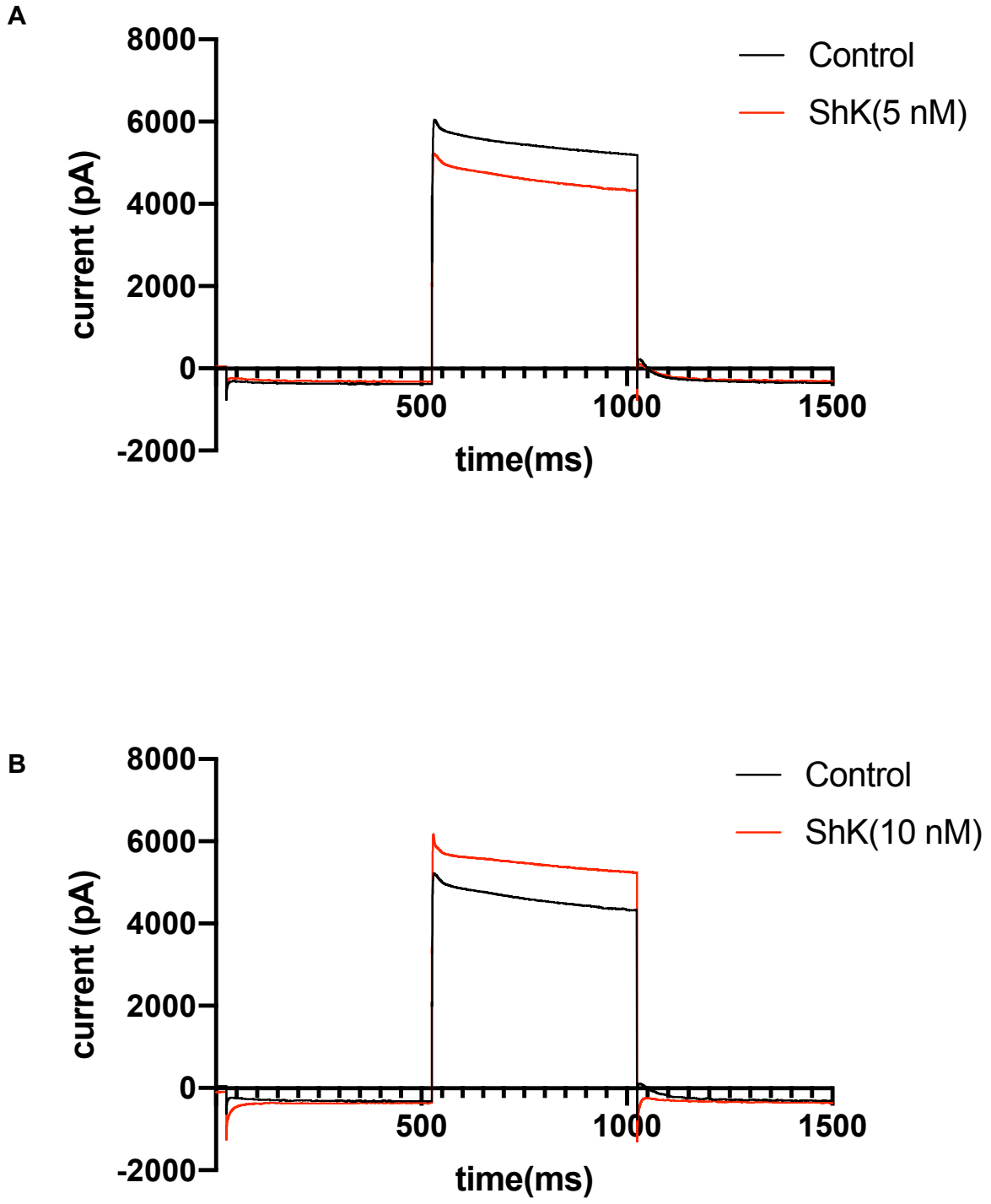

Figure 46. Layout representing Kv1.3_H451A in control and in presence of 5 nM and 10 nM of ShK. A) Kv1.3_H451A in control (in black) and in ShK, 5 nM (in red); **B)** Kv1.3_H451A in control (in black) and in ShK, 10 nM (in red)**.**

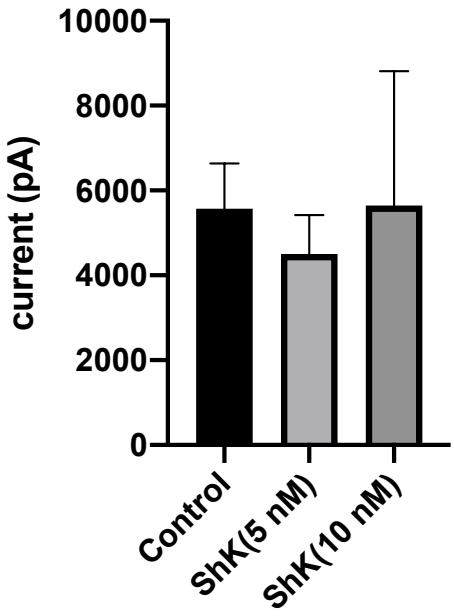

Figure 47. Current peak (pA) graph representative of Kv1.3_H451 in control and with ShK at 5 nM and 10 nM. Bars are indicative of 95% Confident Intervals (CI) of the mean. For both concentrations of toxin tested, (5 nM, n=10; 10 nM n=6) no effect in reducing the average peak current (pA) of the channel was observed (adjusted P values, p=0.3991 and p=0.9967, respectively).

.

3.7.2 Investigating the effect of H451A mutation in the interaction between Kv1.3 and the two *ShK-like* peptides, SXCL-1 and SXCL-6.

The effect of both *ShK-like* peptides, SXCL-1 and SXCL-6, were tested at 5 nM and 10 nM. Incubation with each concentration of each of the peptide, was conducted in 5% CO_2 incubator for a total of 20 minutes, as previously indicated.

In presence of SXCL-1, at 5 nM and 10 nM, the average peak current of Kv1.3_H451A was 4811 pA (95% CI 2571: 7051 n=6) (representative trace Figure 48, A) and 4723 pA (1969: 7478 n=5) (representative trace Figure 48, B), respectively. Compared to the value of the average peak current in control conditions [5572 pA (95% CI 4511: 6633 n=23)] no significant difference is found when both concentrations were tested (one-way ANOVA, Dunnett's multiple comparisons, P>0.05) (Figure 49).
Data suggest that the aminoacidic substitution determined a strong abolishment of the interaction between the peptide and the channel, suggesting a critical role for this residue in the binding. Indeed, when 5 nM and 10 nM of SXCL-1 were incubated with the channel, only a small inhibition of the average peak current, equals to 14% and 15% respectively, was detected.

Similar results were obtained also when SXCL-6 was incubated with Kv1.3_H451A. In presence of 5 nM of the peptide the average peak current was equal to 5083 pA (95% CI 3674: 6492, n=7) (representative trace Figure 50, A). Kv1.3_H541A in presence of 10 nM of SXCL-6 showed an average peak current of 6657 pA (95% CI 4047: 9267, n=6) (representative trace Figure 50, B). No significant inhibition of the average peak current of the channel was found when both concentrations were tested (one-way ANOVA, Dunnett's multiple comparisons, P>0.05) (Figure 51).

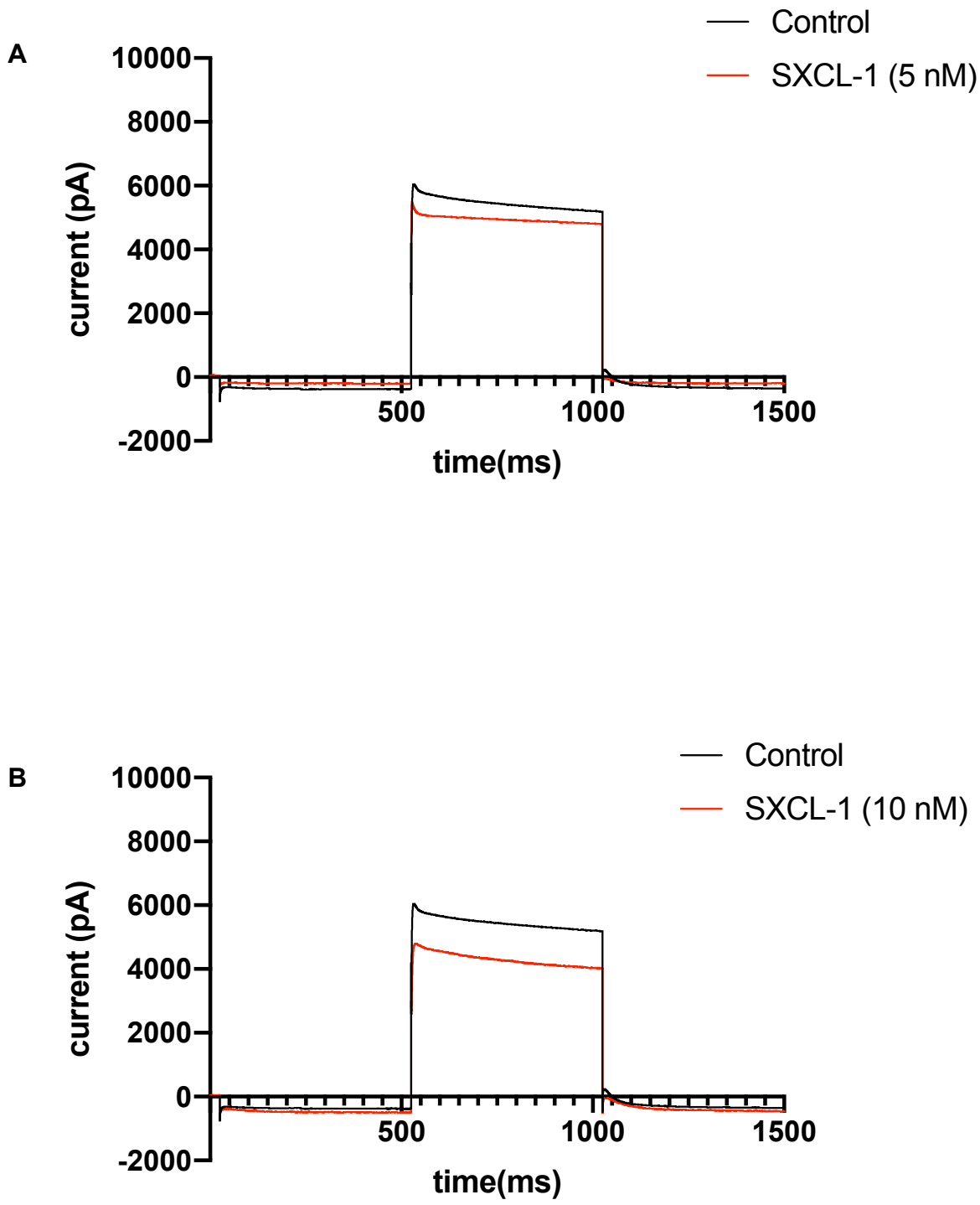

Figure 48. Layout of representative traces of Kv1.3_H451A in control and in presence of SXCL-1. A) Kv1.3_H451A in control (black trace) and in 5 nM of SXCL-1 (red trace). **B)** Kv1.3_H451A in control (black trace) and after 20 minutes incubation with 10 nM of SXCL-1 (red trace).

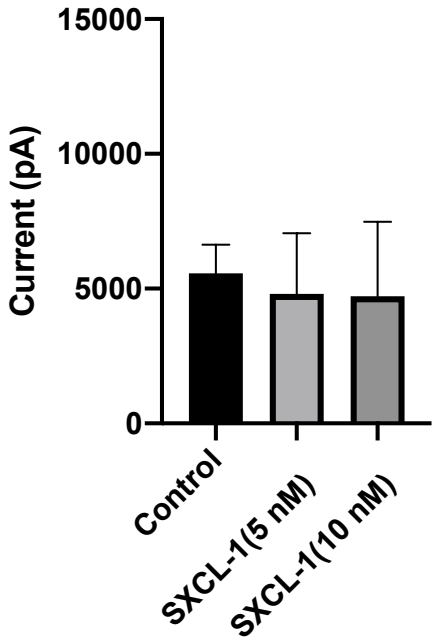

Figure 49. Peak current graphic representative of Kv1.3_H451A in control and with SXCL-1. No significant peak current reduction is observed when both concentrations of the peptide (5 nM, n=6; 10 nM, n=5) were incubated with the channel (adjusted P values, p=0.7331 and p=0.7172, respectively).

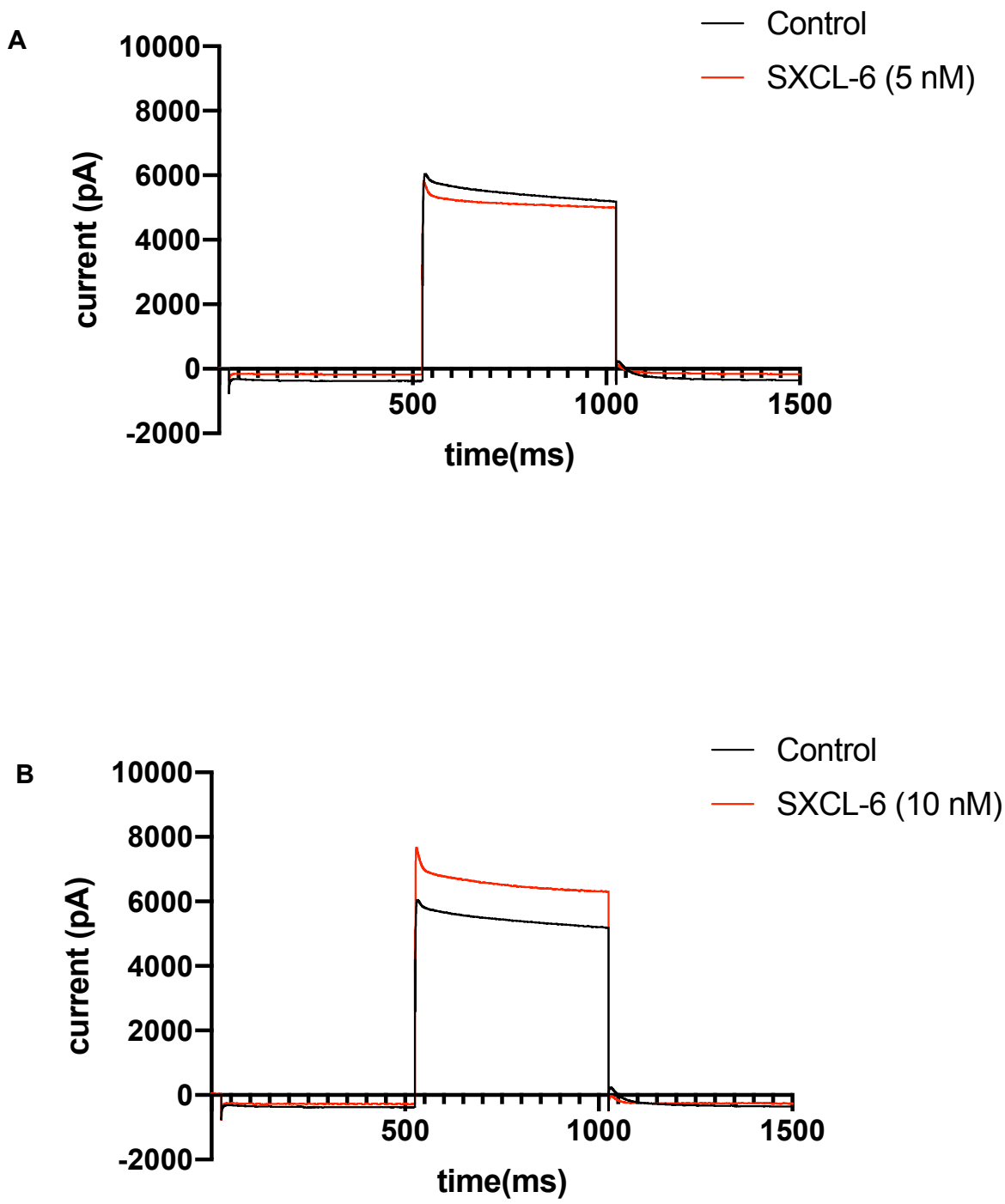

Figure 50. Layout of representative traces of Kv1.3_H451A in control and in presence of SXCL-6. A) Kv1.3_H451A in control (black trace) and after incubation with 5 nM of SXCL-6 (red trace). **B)** Kv1.3_H451A in control (black trace) and in presence of 10 nM of SXCL-6 (red trace).

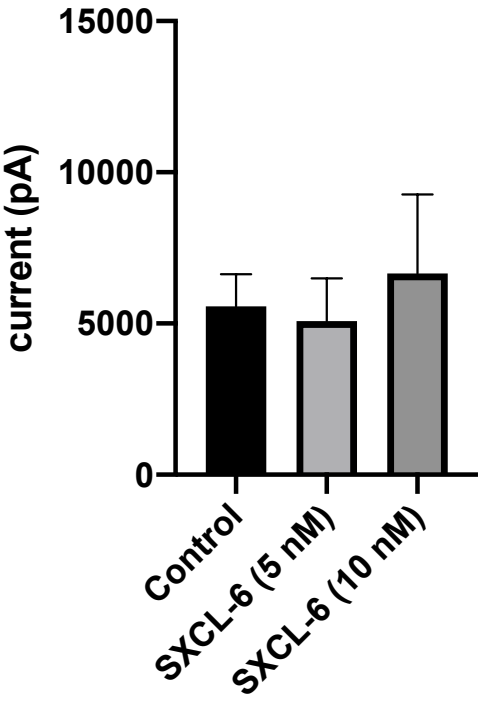

Figure 51. Peak current graphic of Kv1.3_H451 in control and with SXCL-6. Bars are representative of 95% CI of the mean. No inhibition is detected when 5 nM (n=7) (adjusted P value, p=0.8568) and 10 nM (n=6) (adjusted P value, p=0.5214) of the peptide were incubated with the channel.

3.8 Functional characterisation of V453A mutation and its implication in the channel-peptides interaction

Kv1.3_V453A mutant was created by site-directed mutagenesis as described previously (see Material and Methods, section 2.8.2). Whole-cell currents were evoked at +50 mV and expressed as average peak currents (pA).

In figure 52, are showed representative traces of Kv1.3_WT (in black) and Kv1.3_V453A (in red). Kv1.3_WT shows an average peak currents (pA) of 4524 pA (95% CI 2619: 6429 n=7), and Kv1.3_V453A has an average peak currents (pA) resemble to 2364 pA (95% CI 1857: 2871 n=15). The amino acid substitution of Valine (V) with Alanine (A), caused a significant reduction of the channel current, equal to 48% (Figure 53).

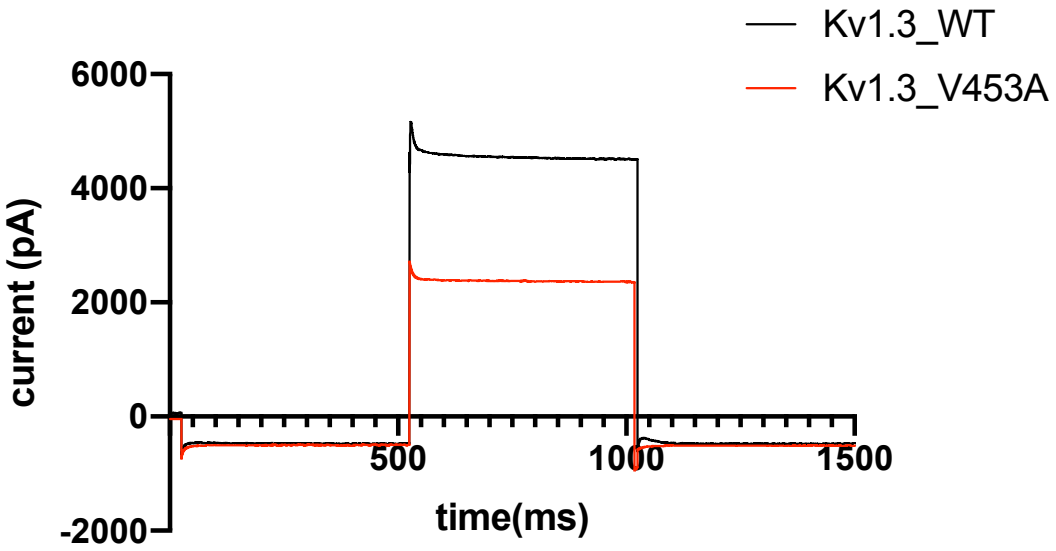

Figure 52. Representative traces of Kv1.3_WT and Kv1.3_V453A. Kv1.3_WT is represented in black and Kv1.3_V453A in red. The average peak current (pA) is reduced.

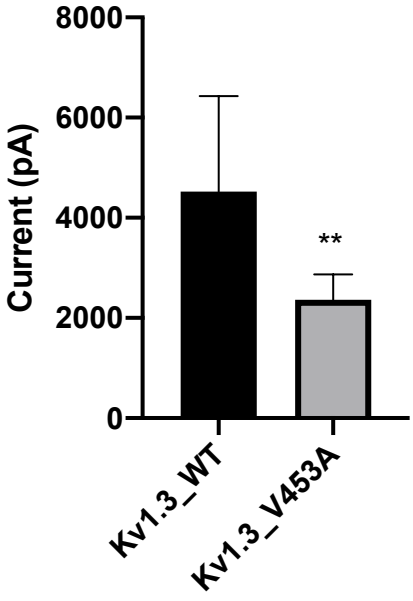

Figure 53. Peak currents (pA) graphic of Kv1.3_WT and Kv1.3_V453A. Bars are representative of 95% Confidence Interval (CI) of the mean. Kv1.3_V453A (n=15) current is significantly reduced (Unpaired t test, p=0.0025).

3.8.1 Investigating the effect of V453A mutation for the interaction between Kv1.3 and ShK

Then, we investigated the effect of the mutation on ShK by incubating Kv1.3_V453A with 5 nM and 10 nM of the toxin, in a similar way as described above for the other mutations.
In presence of ShK, the average peak current was resembling to 2006 pA (95% CI 870.5: 3142 n=6) and 1483 pA (1104: 1863 n=5) at 5 nM and 10 nM, respectively (Figure 54, A and B).
In figure 55, a peak current graphic summarises the results of the findings.

From our investigations, ShK slightly reduces by 18% the average peak current of the channel when 5 nM of the toxin are incubated. 10 nM of ShK are able to cause a reduction equal to 37%. Results are indicative of a reduction of the inhibitory effect of ShK at 5 nM when compared to the effect at 5 nM on Kv1.3_WT, yet at 10 nM the toxin is able to reduce the average peak current, however not at a significantly statistical level when one-way ANOVA, Dunnett's multiple comparisons test, was performed ($P>0.05$).

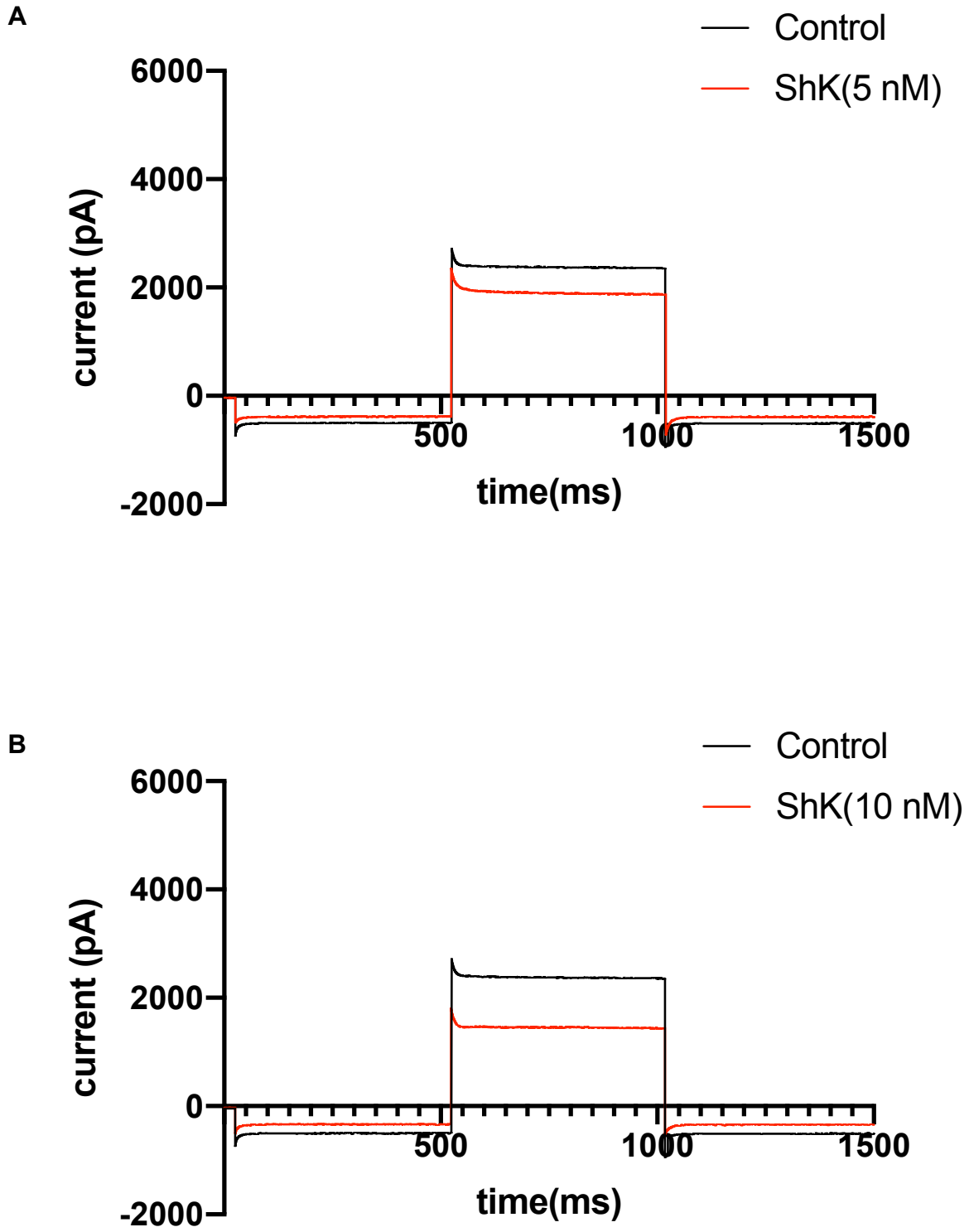

Figure 54. Layout representing Kv1.3_V453A in control and in presence of 5 nM and 10 nM of ShK. A) Kv1.3_H451A in control (in black) and with ShK, 5 nM (in red); **B)** Kv1.3_H451A in control (in black) and with ShK, 10 nM (in red).

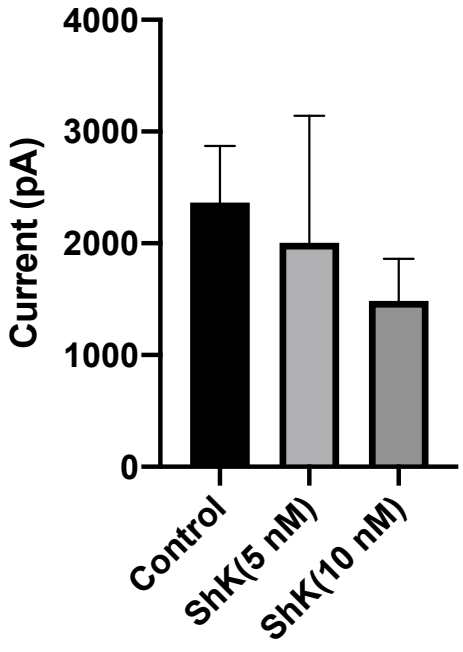

Figure 55. Peak currents (pA) graphic of Kv1.3_V453A in control and in presence of ShK (5 nM and 10 nM). Bars are indicative of 95% Confidence Interval (CI) of the mean. The average peak current (pA) of Kv1.3_V453A in presence of ShK (5 nM, n=6; 10 nM, n=5), is not reduced compared to the values calculated in control (adjusted P value, p=0.6395). ShK at 10 nM (n=5) reduces the average peak current by 37% (adjusted P value, p=0.1235).

3.8.2 Investigating the effect of V453A mutation for the interaction between Kv1.3 and SXCL-1 and SXCL-6

SXCL-1 and SXCL-6 were analysed at 5 nM and 10 nM to detect if any change in the interaction channel-peptides, would occur after the mutation.
A layout of representative traces for SXCL-1 is showed in figure 56. The average peak current of Kv1.3_V453A in presence of 5 nM and 10 nM of the peptide was equal to 1617 pA (95% CI 1176: 2058 n=10) (Figure 56, A) and 1826 pA (95% CI 1442: 2210 n=5) (Figure 56, B), respectively. 5 nM of SXCL-1 significantly inhibited the average peak current of Kv1.3_V453A (one-way ANOVA, Dunnett's multiple comparison test, $p<0.05$). A summary of the results is showed in figure 57.

For SXCL-6 investigations revealed that, after incubation with 5 nM of the peptide, the average peak current was equal to 2639 pA (95% CI 1031: 1939 n=5) (Figure 58, A); whereas at 10 nM, the average peak current was equal to 1485 pA (95% CI 1031: 1939 n=5) (Figure 58, B). A peak current graphic is showed in figure 69 as a summary of the investigations.

Data revealed that SXCL-1 reduced the average peak current of Kv1.3_V453A when in presence of both 5 nM and 10 nM of the peptide, whereas SXCL-6 did not inhibit the channel peak current at 5 nM, however reduced the average peak current by 37% when the concentration was increased to 10 nM, revealing a similar profile to ShK (10 nM) (section 3.3.14).

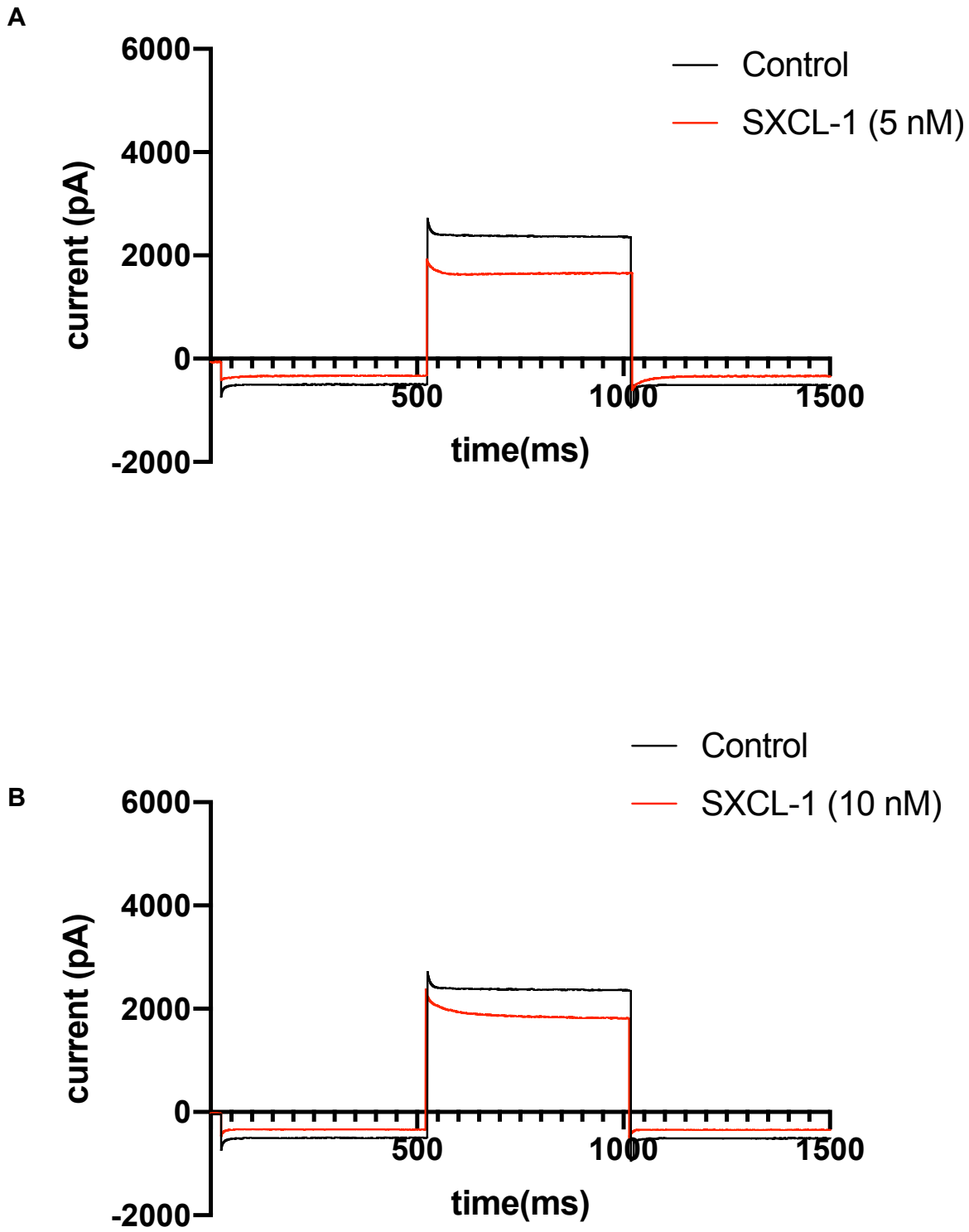

Figure 56. Layout of representative traces of Kv1.3_V453A in control and in presence of SXCL-1. A) Kv1.3_V453A in control conditions (black trace) and after incubation with 5 nM of SXCL-1 (red trace); **B)** Kv1.3_V453A in control conditions (black trace) and after incubation with 10 nM of SXCL-1 (red trace).

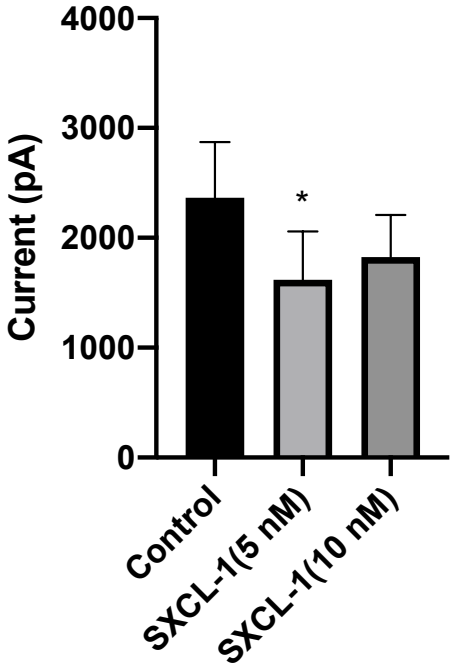

Figure 57. Peak current (pA) graphic of Kv1.3_V453A in control and with SXCL-1 (5 nM and 10 nM). Bars are representative of 95% CI of the mean. Average peak current was reduced by 32% ($p < 0.05$) when the channel was incubated with 5 nM of SXCL-1(n=10). Slightly inhibition is observed in presence of 10 nM of SXCL-1 (n=5) (adjusted P values, p=0.3158).

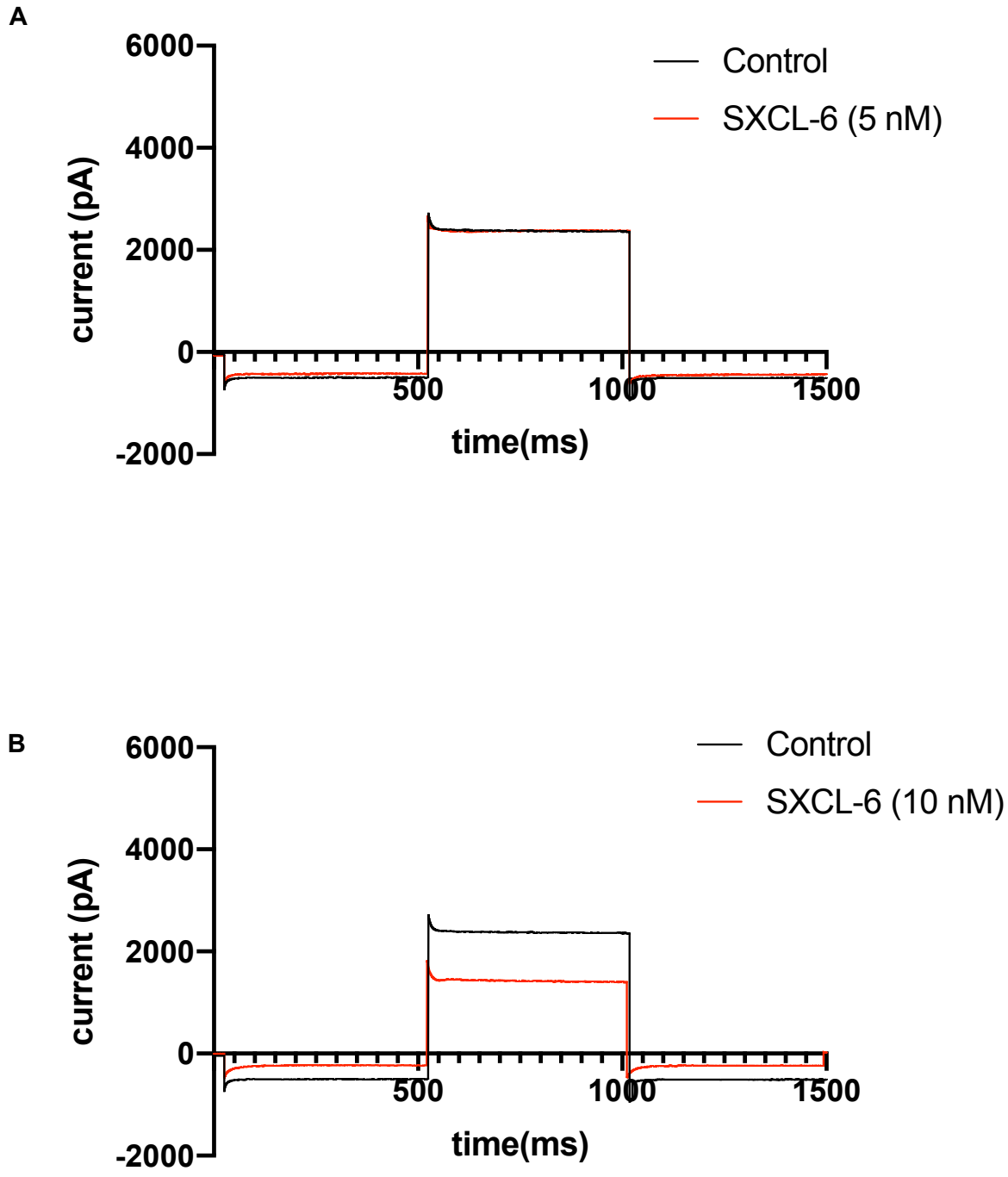

Figure 58. Layout of representative traces of Kv1.3_V453A in control and in presence of SXCL-6. A) Kv1.3_V453A in control conditions (black trace) and with 5 nM of the peptide (red trace). **B)** Kv1.3_V453A in control conditions (black trace) and with 10 nM of SXCL-6 (red trace).

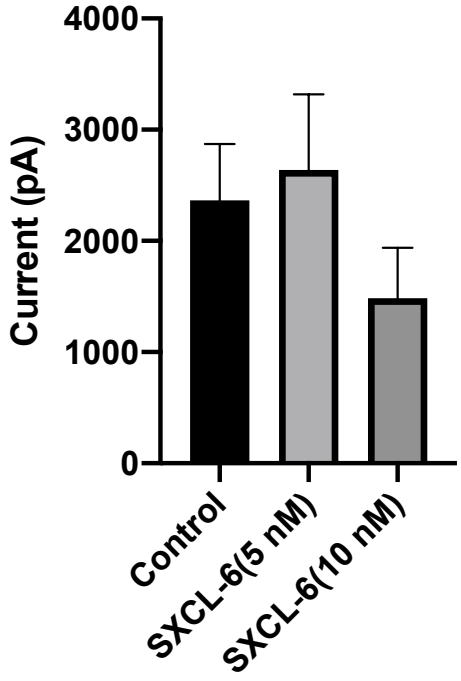

Figure 59. Peak current (pA) graphic representative of Kv1.3_V453A in control and with SXCL-6 (5 nM and 10 nM). Bars are representative of 95% CI of the mean. Average peak current was equal to 2639 pA in presence of 5 nM (n=5) (adjusted P value, p=0.6980) and 1485 pA (adjusted P value, p=0.0845) in presence of 10 nM of SXCL-6 (n=5).

3.9 Discussion

The intestinal parasitic nematode *Heligmosomoides polygyrus*, is typically used in research as a model to study chronic helminth infections, in order to reach a better understanding of the relationship between parasites infections and the host immune response (Robinson M. *et al.,* 1989; Behnke J. M. *et al.,* 2009; Harris N. L. *et al.,* 2014). Helminth infections represent a worldwide issue, as it is estimated that above a billion of people are infected with helminths (van Riet E. *et al.,* 2007). Of those infections, the higher prevalence is registered in developing countries, where a combination of factors including poor hygienic conditions, limited access to health care, low income as well as food and water scarce conditions, have conveyed to a higher number of infections compared to the number observed in developed countries (de Silva N. R *et al.,* 2003). Generally, the most common helminth infections are linked to geohelminth parasites, including *Ascaris lumbricoides*, *Trichuris trichiura* and hookworms (*Ancylostoma duodenale* and *Necator americanus*) (Bethony J. *et al.,* 2006). Helminth infections are responsible for malnourishment and compromised cognitive functions (van Riet *et al.,* 2007). Furthermore, helminths can cause chronic infection, as they can remain in the host for several months and can cause damage to different organs (van Riet *et al.,* 2007). Infection can occur via oral contact, direct contact with the skin or, alternatively, via bites delivered by an infected fly, *Onchocerca volvulus* (van Riet *et al.,* 2007). There is, however, a connection between helminth infections and protection against some diseases, in particular autoimmune and allergic disease (Ruyssers N. E. *et al.,* 2008; Cooper P.J., 2009). The base of this correlation is well explained by the "*hygiene hypothesis*", originally formulated by Strachan for hay fever (Strachan D. P., 1989) and subsequently extended to other diseases. This hypothesis postulate that the improvements of hygienic, economic and social conditions in certain countries, overall indicated as developed countries, determined a reduction in the natural exposure to parasites and others (Bloomfield S. F. *et al.,* 2006; Alexandre-Silva G. M. *et al.,* 2018;). These circumstances caused a suppression of several immunological mechanisms and circuits that contribute to the protection against those diseases (Elliott D. E. and Weinstock J. V., 2012). As a result of the lack of exposure, the risk of developing those diseases increases (Elliott D. E. and Weinstock J. V., 2012). In the case of helminths, they induce a TH_2-type response in the host, which determine an increase in the level of Interleukin-4 (IL-4), as well as IL-5, IL-9, IL-13 and IL-2 (commonly defined TH_2-type cytokines); IgE production and activation and mobilisation of $CD4^+$ TH_2 cells, eosinophils, mast cells and basophils, all of which contribute to reinforce the response against the parasite (Anthony R.M. *et al.,* 2007). The TH_2-type

response is the results of multiple interactions between the host immune cells and the products secreted by the parasite, which are a cocktail of several components (Zaccone, P. and Cooke A., 2013). Several researches highlighted the relevance of some helminth in offering protection against, for example, inflammatory bowel diseases (IBD), including Chron's disease (CD) and ulcerative colitis (UC) (Elliott D. E. and Weinstock J. V., 2012). The incidence of IBD is raising globally, however the aetiology is still partially unknown and is under investigations (Zhang Y. Z. and Li Y. Y., 2014). Environmental, genetic and immunological factors, together with the individual intestinal microbial flora, contribute to the development of the diseases (Scaldaferri F. and Fiocchi C., 2007). Several researches have demonstrated the benefits of using helminth-based therapy for the treatment of IBD in animal models of experimentally induced-colitis, including the tapeworm *Hymenolepis diminuta*, which ameliorated the ion transport parameters (Reardon C. *et al.,* 2001); the nematode *Trichinella spiralis* (Khan W. I. *et al.,* 2002), *Schistosoma mansoni* (Elliott D. E. *et al.,* 2003) and *Heligmosomoides polygyrus* (Elliot D.E. *et al.,* 2004). In the case of *H. polygyrus*, work by *Elliot* and co-workers, indicated a potent reduction of IFN-γ and IL-2 release in mice model of colitis, when treated with the helminth (Elliot D.E. *et al.,* 2004). Nevertheless, some harmful side effect derived from the usage of living worm as a therapeutical must be considered. Indeed, parasites might migrate to other tissues within the body and cause damage, as the reported case of *T. suis* invading the gastrointestinal tract (Kradin R. L. *et al.,* 2006) or infection (Ruysser N.E. *et al.,* 2008). They can also influence the natural intestinal motility by enhancing the propulsive activity at the level of the intestine, mucus and ion water secretion (Khan W. I. and Collins S. M., 2004). To overcome those limitations, a strategy was to identify the secreted products that are responsible for immunomodulation and that might be used for treatments instead of living worms (Ruysser N.E. *et al.,* 2008). Immunomodulator components were found to be important for the parasite to escape the immune system of the host by implementing several mechanisms (Zakeri A. *et al.,* 2018). In the specific case of *H. polygyrus*, these components are pivotal so that the parasite can remain in the host for several months. The HES products secreted by *H. polygyrus* during its lifecycle stages have been characterised (Hewitson J. P *et al.,* 2011; Moreno Y. *et al.,* 2011) and their immunomodulatory functions have also been investigated, revealing that are involved, for example, in the modulation of dendritic cells (Segura M. *et al.,* 2007; Massacand J. C. *et al.,* 2009) and cytokines release (Maizels R.M. *et al.,* 2012). Some of those products are stage-specific (Reynolds L.A. *et al,* 2012) as well as sex-specific (Adams J.H. *et al.,* 1988). The immunomodulatory products secreted by several helminths, could be used for example for

the treatment of certain pathologies, as encouraging results emerged from investigations in animal models of asthma (Yang J. *et al.,* 2007), type-1 diabetes (Zaccone P. *et al.,* 2003) and EAE (Lund M. *et al.,* 2016).

As for *H. polygyrus*, ES (excretory-secretory) products were tested for their potential use in the production of vaccine (Hewitson J.P. *et al.,* 2013). At stage L4 ES, VAL (Venom allergen/*Ancylostoma* secreted protein-like) proteins are the most abundant, including acethylcolinesterases 1 and 2 (ACEs), apyrase (APY-3), Val-7, lysozymes LYS-1 and LYS-2 and calreticulin (Hewitson J.P. *et al.,* 2013). Other than VAL proteins, the sushi-like domain proteins and ShK/SXC proteins are secreted. These two group of proteins, might have immunological properties that are helpful for the parasite to escape the immune system of the host during the infection (Hewitson J.P. *et al.,* 2013). Considering all the intriguing properties relative to the helminth's products and their potential translation into therapeutical usage for the treatment of several diseases, it is important to consider other eventual immunomodulatory properties of the ShK/SXC proteins. At present, it is reported that no other immunological properties other than the possible involvement in the blockade of the voltage-gated potassium channel Kv1.3 in T cells, have been described. This hypothesis is triggered by previous evidences relative to ShK, considered an SXC homologue protein -from which, by the way, these proteins are named after- that is able to potently inhibit the channel (Chi Vi. *et al.,* 2012; Hewitson J.P. *et al.,* 2013). Our investigations were focused on two of the nine ShK/SXC proteins (SXCL-1-SXCL-9), SXCL-1 and SXCL-6, from the L4 ES products of *H. polygyrus.* The two peptides showed a great effect in inhibiting the average peak current (pA) of Kv1.3 channel, expressed in tSA201 cells, with a pharmacological profile within the nanomolar (nM) range.

Results suggested that SXCL-1 at 5 nM and 10 nM determined a significant inhibition of the average peak current of the channel resembled to 68% and 64%, respectively. A similar pharmacological profile is seen for SXCL-6, however 10 nM of the peptide are required to reach a % of inhibition that equals 68%, significantly reducing the average peak current of Kv1.3 channel. The data acquired are only revealing a pharmacological inhibition lower than 100%, with a maximal concentration considered of 10 nM. Ideally, one would tend to examine a new drug/compound or, like this case, peptides and toxins, by investigating which concentration can determine a 100% or similar inhibition percentage. We considered our inhibition quite substantial and, by taking into account also time and products resources, we did not extend our investigations to higher nanomolar concentrations. Such investigations, however, could be undertaken in the near future, to expand the knowledges regarding the

pharmacological profile of the two peptides. Nevertheless, it is important to highlight that the inhibitory effect that we observed at 10 nM for both peptides and also at 5 nM for SXCL-1, are indicative of a strong effect. We also evaluated the half-maximal inhibitory concentration (IC50) to obtain a more detailed picture of the peptide's efficacy, with the result of IC50=0.6 nM for SXCL-1 and IC50=6 nM for SXCL-6.

Another important part of our investigations was to predict the interaction sites between Kv1.3 and SXCL-1 and SXCL-6. By using a combination of the protein docking server ZDOCK and the computational alanine scanning server, PP Check (for further details see Material and Method, section 2.6 and 2.7, respectively), we identified three important sites that contribute to the stability of the complex (protein-protein complex) established between Kv1.3-SXCL-1 and Kv1.3-SXCL-6. We then mutated those sites and investigated, by using an electrophysiological approach, the effect of those mutations on the channel-peptides interactions. The three sites that we evaluated for our experiments were: D449, H451 and V453. All three residues are located at the vestibule of the channel, with D449 within the selectivity filter, H451 and V453 slightly away from the latter, in proximity of the extracellular side of the channel. Our hypothesis was based on the observation that, these two novel *ShK-like* peptides, would act as pore blocker inhibitors, therefore in a similar fashion to other known pore-blockers peptides such as ShK (Lanigan M. D. *et al.,* 1996), ChTX (Stocker M. and Miller C.,1994; Hidalgo P. and MacKinnon, R., 1995), MgTx (Chen R. and Chung S. H., 2014), BmP02 (Wu B. *et al.,* 2016), and many more.
The idea was based on the mechanism of action of other already studied peptides, where the peptides, having a sequence rich in Lys which are positively charged at a pH values of 7, would be attracted to the negatively charged residues at channel vestibule (Wu B. *et al.,* 2016). We therefore proposed that the interaction would take place with a functional lysine locking into the pore of the channel, thus blocking the ion passageway, with a mechanism common to other peptides and previously elucidated as "cork in a bottle" (Bajaj S. and Han J., 2019). However, less is known about the structure of SXCL-1 and SXCL-6. One of the most important point is to define the residues, within the peptides sequence, that contribute to the binding. In our model, we proposed a functional Lysine at position 21 and 28 for SXCL-1 and SXCL-6 respectively, but no evidence is available to support this hypothesis. At the best of our knowledge at the moment, we suggest that a positively charged residue, such as Lys, is required to establish strong interactions with residues located at the channel surface. As the amino acidic sequences of both peptides is rich in Lys, another questions to address is whether one or more

lysines are involved in the binding to Kv1.3, as well as other residues that might play an important role for the binding. Elucidating the NMR structure or X-ray structure of the two peptides would help answering further queries that, unfortunately, we could not answer by simply performing electrophysiological investigations. Knowledges about the primary and secondary structure of SXCL-1 and SXCL-6 would be beneficial to understand also the peptides folding and whether they undergo conformational changes when binding to the channel. To address all those questions, would be advantageous to use a combination of docking approach, probably with more sophisticated server, and MD simulations, which are out of our research area. We refer at those strategies, in the light of future avenues to undertake for future investigations involving the two *ShK-like* peptides, SXCL-1 and SXCL-6.

In the results section 3.6, we demonstrated that the aminoacidic substitution of Aspartic Acid (D) at position 449 with Alanine (A), determined a significant reduction of the average peak current (pA) of the channel. Subsequently, when we did test 10 nM and 5 nM of SXCL-1 we did not see any effect at 10 nM, yet a reduction of the current resembled to 30% when 5 nM of the peptide was applied, however with no statistical significance (section 3.6.2, figure 40 and 41). This could underline that channel-peptides are still interacting however this interaction is weaker. When we investigated SXCL-6 (section 3.6.2, figure 42 and 43), we observed that, at both concentrations of 10 nM and 5 nM, the average peak current was reduced by 15% and 26%, respectively. Also, in this occasion, with no statistical significance. Results indicate that SXCL-1 (at 5 nM) and SXCL-6 (10 nM and 5 nM), interact with the channel, but those interactions could be weaker thus determining a lower % of inhibition on the average peak current of Kv1.3_D449A.

In section 3.8, we investigated the effect of the amino acidic substitution of Valine (V) at position 453 with Alanine (A), that significantly reduced the average peak current compared to Kv1.3_WT. We therefore examined the effect of this mutation for the binding of SXCL-1 (section 3.8.2). When both 10 nM and 5 nM of the peptides were incubated, separately, with the channel, we observed a reduction of the average peak current of Kv1.3_V453A resemble to 27% and 28%, respectively (section 3.8.2, figure 56 and 57). Overall, at both concentrations, we obtained a similar inhibitory effect, however reduced when compared to the inhibition that we observed in Kv1.3_WT. We could conclude saying that the interaction between Kv1.3_V453A and SXCL-1 is weaker due to the aminoacidic substitution at this specific site. In section 3.8.2, we also analysed the effect of the mutation on the inhibition determined by SXCL-6. When the channel was incubated with 5 nM of SXCL-6 we did not see any effect on

the average peak current (pA) whereas, when 10 nM of the peptide were incubated with Kv1.3_V453A, we did observe a greater inhibition of the channel current, equal to 40% (section 3.8.2, figure 58 and 59). No statistical significance was found when statistical analysis were performed.

Those observations are in agreement with what we observed in the WT channel, where 5 nM of SXCL-6 did not inhibit the average peak current of Kv1.3, however a significant inhibition was observed when the concentration was doubled (10 nM). In the case of Kv1.3_V453A, the aminoacidic substitution caused a reduction of the interaction channel-peptides, therefore for both SXCL-1 and SXCL-6, we did observe a disruption of the inhibitory effects, that might be related to the establishment of weaker interactions between the channel and the peptides.

Lastly, in section 3.7, we investigated the effect of the aminoacidic substitution that involved the Histidine (H) at position 451, generating the mutant channel Kv1.3_451A. We found that the average peak current of the mutant channel was slightly higher compared to the WT channel, but current were found to be no statistically different. We therefore went on to test the effect of the two *ShK-like* peptides on the mutant channel and we found that, after incubation with 5 nM and 10 nM of SXCL-1, a negligible effect on the average peak current of Kv1.3_H451A was detected (% of inhibition were equal to 14 and 15, respectively) (section 3.7.2, figure 48 and 49). Similar results were also obtained for SXCL-6; incubation of Kv1.3_H451A with 5 nM and 10 nM of the peptide did not determine any inhibitory effect on the average peak (section 3.7.2, figure 50 and 51). Our results suggest that the Histidine at position 451, might be a crucial residue for the peptide-channel interaction and therefore, when we tested both concentrations, we obtained results totally similar to the values in control. The results indicate that, most likely, both peptides lost their ability to interact with the channel following the mutation of the Histidine (H) into Alanine (A). This would be in agreement with the results obtained from the computational alanine scanning.

In the attempt to underpin the residues of the channel that are conserved among other voltage-gated K^+ channels and residues that varies, we show the sequence alignment of the pore region of hKv1.1, hKv1.2, hKv1.3, hKv1.5 and hKv2.1 obtained with Clustal Omega program in figure 60 (Uniprot entry code, Q09470: KCNA1_HUMAN; P16389: KCNA2_HUMAN; P22001: KCNA3_HUMAN; P22460: KCNA5_HUMAN; Q14721: KCNB1_HUMAN). In grey are indicated amino acids with high similarity among the channels, marked by asterisks (*); in light grey, amino acids with lower similarity in different grades (:) (.); and finally, in white, are indicated amino acidic residues that share no similarity. High similarity is noticeable in all channels at the region that contains the motif TXXTXGYG, known as the "*signature*

sequence" (Heginbotham L. *et al.,* 1994) and in the GYGD motif (in grey). The Aspartic Acid (D) is conserved in all five channels, with high degree of similarity (*). Histidine (H) is unique to hKv1.3 and is substitute by Tyrosine (Y) in hKv1.1; Valine (V) in hKv1.2; Arginine (R) in hKv1.5 and Tyrosine (Y) in hKv2.1 (residues are coloured in white). Valine (V) is shared by hKv1.1 and hKv1.3 and differs in the remaining channels (residues are in white). As showed below, we point out the attention to the Histidine 451, that is not conserved in any other channel, appear to be exclusive to Kv1.3 and at this site, no similarity is highlighted between the channels (white colour) (figure 60).

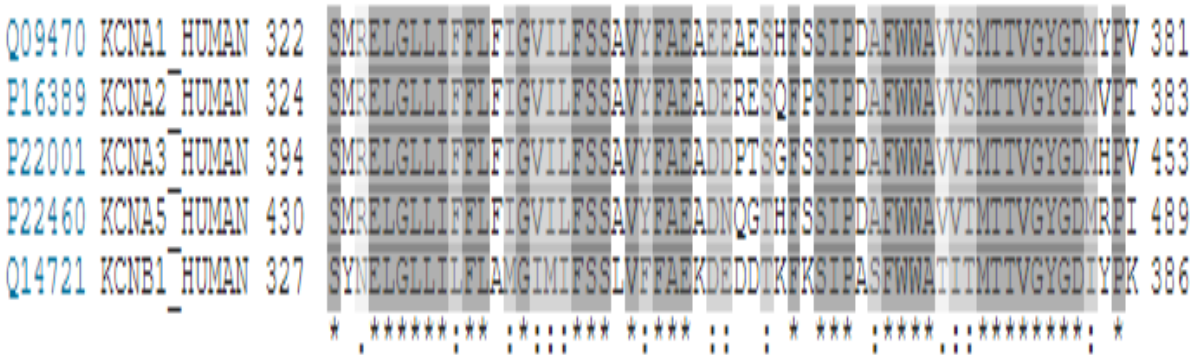

Figure 60. Voltage-gated K^+ channels (Kvs) sequence alignment. Alignment was obtained with Clustal Omega. Sequences of human Kv1.1 (KCNA1), Kv1.2 (KCNA2), Kv1.3 (KCNA3), Kv1.5 (KCNA5) and Kv2.1 (KCNB1) are reported in the following order. Residues with high similarity properties are coloured in grey (*); lower similarity properties are indicated by the light grey colour and marked by (:) and (.)

One assumption was that Aspartic Acid (D), vigorously interacts with a residue or more residues of the peptides, leading the peptides to bind to the channel and inhibiting the transit of ions through the pore. However, aspartic acid is conserved among other K^+ channels and considering only this residue as crucial for the interaction channel-peptides would be in disagreement with the other results of our studies. In literature was showed that mutations occurring at the selectivity filter, and in particular mutations that involve the Aspartic Acid (D), cause a significant disruption and destabilization of the selectivity filter itself, in some cases rendering the channel not responsive to electrophysiological experiments (Wu B. *et al.,* 2016). In our investigations, we were able to obtain responsiveness of the mutant channel,

however with a significant reduction of the functionality when compared to Kv1.3_WT (section 3.6). Aspartic Acid (D) is also highly conserved in other K^+ channel families, as it is part of the GYGD motif found within the pore region (Heginbotham L. *et al.,* 1994) with some exceptions in the Y and D positions for the two-pore domain channels (Chapman M. L. *et al.,* 2001). These considerations led to the observation that more residues at the channel surface might participate in reinforcing the binding peptide-channel. When we created Kv1.3_H451A mutant by substitution of histidine in position 451 at each α-subunit of the tetramer, our results suggested that, by replacement of the positively charged amino acid with a neutral amino acid (A), the binding affinity of the peptides dramatically dropped. The positive charge of H could be a crucial interaction site for the peptides when approaching the channel and therefore, when mutated, the affinity of both SXCL-1 and SXCL-6 for Kv1.3 severely decreased. These results would be in agreement with evidences from the literature that demonstrated the importance of the residue for the activity of other Kv1.3 blockers, including the scorpion toxin BmP02 (Wu B. *et al.,* 2016) and the β-adrenoreceptor antagonist carvedilol (Yang J. F. *et al.,* 2018). The evidence that H is a distinctive feature of Kv1.3, led to the conclusion that this residue might be extremely crucial in the interaction channel-peptides and might partially justify the selectivity towards this channel over other Kvs (for further evidences, see Chapter 5). Nevertheless, it remains to be established the degree of involvement of Aspartic Acid (D) and Valine (V) in the binding. Results suggest that both mutations result in a decreased affinity of Kv1.3-SXCL-1 and Kv1.3-SXCL-6, which underlines that both residues are important. Our results highlight that the pore region is the important area of contact for the peptides and that all three residues, with different degrees of involvement, might participate to the binding.

Our analysis took also into consideration the effect of those three site-specific mutations on the already known toxin, ShK. The mechanism of action of ShK is extensively known and it involves the occlusion of the pore of the channel through a critical lysine residue (K22) (Rauer H. *et al.,* 2000; Chen R. *et al.,* 2011). The results of our investigations revealed that mutation at position 449 that involves the Aspartic Acid (D), determined a slight reduction of the peak current of the channel when 10 nM and 5 nM of the toxin were applied (section 3.6.1, Figure 38 and 39). A similar effect is observed when the Valine was substituted with A (Kv1.3_V453A). In this case, ShK at 10 nM and 5 nM, was able to reduce the average peak current of the channel by 37% and 15%, respectively (section 3.8.1, Figure 54 and 55), demonstrating that there was still an interaction between the toxin and Kv1.3_V453A. The results obtained in both Kv1.3_D449A and Kv1.3_V453A follow a similar fashion for all three

peptides considered in our investigations. In the case of Kv1.3_H451A, we observed that 10 nM and 5 nM of ShK did not affect the average peak current of the channel (section 3.7.1, Figure 46 and 47), showing similar average peak current (pA) values.

Taken all together, those results indicate that in the case of the Aspartic Acid (D) and Valine (V) substitutions, is still possible to underline a weaker interaction between the channel and the peptides. The mutation occurring at D449, as suggested before, is thought to cause a strong destabilization of the selectivity filter (Wu B. *et al.,* 2016). In the case of Kv1.3_V453A, similarly to what we observed for SXCL-1 and SXCL-6, it is possible to point out a weaker interaction between the toxin and the channel; however the percentage of inhibition (in all three cases) was reduced compared to what we observed for the WT. To note, for Kv1.3_WT, 10 nM and 5 nM of SXCL-1, significantly reduced the average peak current of the channel by 64% and 68%, respectively. SXCL-6 at 5 nM did not exhibit any inhibition on Kv1.3_WT yet significantly reduced the average peak current of the channel by 68% at 10 nM.

Once again, for Kv1.3_H451A, the major disruption was observed when channel was incubated with 10 nM of ShK. Indeed, no inhibition on the average peak current (pA) of the channel was detectable. All three residues at the channel interface, seem to participate in the interaction with the peptides, however with different degrees of involvement. The H451 seems to play a major role for the binding of both SXCL-1 and SXCL-6, as well as ShK. Whereas, slightly less obvious is the involvement of D449 and V453. This might be also related to the functional effect of the mutation on the channel itself. In both cases, we can see that the current recorded through the channel was significantly reduced compared to the WT. In the case of Histidine, we can still see current flowing through the channel, followed by the absence of inhibition, or a very small inhibition, when peptides are applied at different concentrations. These evidences, together with the fact that Histidine is a distinctive tract to Kv1.3 and does not appear to be conserved in the other Kvs that we evaluated (Figure 60), suggest that the residue is one of the most frequently involved in the interaction with the peptides. Nevertheless, further investigation is required to address residual questions emerging from these evaluations, including the verification of which type of interactions are the most predominant between the residues of peptides and the residues at the channel surface. Most of the peptides that act as pore blockers, possess a functional dyad and establish strong hydrophobic interactions, however also hydrogen bonds interactions are found to be predominant for some Kv1.3 blockers (Wu B. *et al.,* 2016).

Although tremendous progresses have been made to improve the clinical usage of proteins and peptides for the treatments of diseases, there are still several challenges to overcome. Most of these challenges, are associated to the physic and chemical nature of these molecules including molecular weight and hydrophilic profile (in most of the cases). As a result, these molecules are characterised by poor oral bioavailability, poor membrane penetration and short half-life (Ibraheem D. *et al.,* 2014; Antosova Z. *et al.,* 2009). Oral administration of drugs in form of proteins and peptides, is limited by several obstacles that these molecules encounter during their route through the digestive tract (Pauletti G.M. *et al.,* 1996). First, proteins and peptides are the target of proteases, the enzymes located in the digestive tract that have the task of degrading proteins (Drucker D. J., 2020). This, together with the differences in the environment and pH level across the different sections of the digestive tract, contribute to limit the peptides bioavailability (Drucker D. J., 2020).

Next, the composition and arrangement of the intestinal epithelium, represent a physical barrier for the penetration of proteins and peptides, and more generally to drugs absorption (Hamman J.H. *et al.,* 2005; Gumbiner B., 1987). The intestinal epithelium is arranged in a single layer of cells, comprising enterocytes, Paneth cells and goblet cells (Hochman J. and Artursson, P., 1994), that allows only a paracellular pathway of absorption and is not accessible to hydrophilic molecules of large size (Pauletti G.M. *et al.,* 1996). For those molecules, the passage through the intestinal epithelium layer is restricted by the presence of the tight junctions, that form the so-called zonula occludens (ZO), and bound epithelial cells in correspondence of the apical domain (Gumbiner B., 1987; Madara J. L., 1989). Furthermore, peptides and protein have a very short half-life (Sarciaux J.M *et al.,* 1995); this imply various administrations to reach an adequate therapeutical level (Antosova Z. *et al.,* 2009), that might result in toxicity (Almeida A.J. and Souto E., 2007). Another point that must be considered, is the scarce ability of the peptides to cross the brain-blood barrier (BB) (Ibraheem D. *et al.,* 2014). Of course, all these factors influence the route of administration of drugs, including protein and peptides. Furthermore, several side effects derived from this administration way, must also be considered (Ibraheem D. *et al.,* 2014). Other non-invasive administration routes include: a) administration through the lungs (or pulmonary route), that has been considered, for example, in the case of the analogue of HsTX1, HsTX1[14], from the scorpion *Heterometrus spinnifer* (LeBrun B. *et al.,* 1997; Rashid M.H. *et al.,* 2014; Jin L. *et al.,* 2016); b) delivery via the buccal mucosa, evaluated for ShK-186 (Jin L. *et al.,* 2015), both *in vitro* and *in vivo*. Numerous researches are

now focusing on strategy aimed at globally enhance the bioavailability of the peptides, the plasma half-life and ensure protection from the activity of enzymes (Ibraheem D. *et al.,* 2014).

3.10 Conclusions and Remarks

SXCL-1 and SXCL-6 from the nematode *Heligmosomoides polygyrus* were the objectives of this research project, aimed at evaluating their pharmacological and functional properties on the voltage-activated K^+ channel, Kv1.3. The two novel *ShK-like* peptides showed a potent effect in inhibiting the average peak current (pA) of Kv1.3 channel, with a pharmacological profile within the nanomolar (nM) range, and a potent inhibitory effect > 60%.
Three interaction sites have been investigated, pointed out the importance of these residues for the binding of the peptides to Kv1.3. However, further investigations are required to answer different questions raised from our analysis that were discussed above (section 3.9).

In conclusion, our results indicate that the two *ShK-like* peptides, SXCL-1 and SXCL-6, represent a novel class of Kv1.3 channel inhibitors of worm origin and that might be considered for further studies in the future, aimed at investigating several other properties that remain, at the moment, uncovered.

Chapter 4: Electrophysiological characterisation of SXCL-1 and SXCL-6 on other members of the voltage-activated K^+ channel family

4.1 Introduction

The two *ShK-like* peptides, SXCL-1 and SXCL-6, have shown a clear inhibitory activity towards Kv1.3 channel, expressed in tSA201 cells, at concentrations including 10 nM, 5 nM, 1 nM, 0.5 nM, 0.1 nM, 0.03 nM and 0.001 nM, with SXCL-1 exhibiting a more potent effect at lower nanomolar concentrations of 5 nM compared to SXCL-6.

To further investigate the biological properties of the two peptides, we focused our attention in defining their selectivity towards Kv1.3 over other voltage-gated K^+ channels. In particular, investigations were conducted on other members of the *Shaker*-related family, aimed to uncover the activity of the peptides on Kv1.1, Kv1.2 and Kv1.5 channels. Furthermore, we investigated the biological properties of SXCL-1 and SXCL-6 on the voltage-gated potassium channel Kv2.1, a member of the *Shab*-family.

4.2 The delayed-rectifier K^+ channels, Kv1.1 and Kv1.2

The voltage-activated delayed rectifier K^+ channel Kv1.1, encoded by the gene KCNA1(on chromosome 12p13), belongs to the *Shaker*-related family member 1. The channel is constituted by four α-subunits and presents the characteristic six transmembrane topology, with each α-subunit containing the transmembrane segments S1-S6. Of those, S4 represent the voltage sensor and together with the segment S3 form the voltage sensor paddle, whereas the segments S5-S6 form the pore region, containing the selectivity filter. Both N-termini and C-termini are found at the intracellular side and contribute to the channel functions (Paulhus K. *et al.,* 2020) (Figure 61). For example, the N-terminus is involved in the inactivation process and subunit association (Hoshi T. *et al.,* 1990; Li M. *et al.,* 1992). Kv1.1 α-subunits can assemble with members of the same family to form heterotetramers- e.g. in the brain Kv1.1 α-subunits associate with Kv1.2 and Kv1.4 (Coleman S.K. *et al.,* 1999)- , or in addition, subunits can associate with auxiliary β subunits or interacting proteins (Trimmer J.S., 2015), a common feature of many potassium channels. Kv1.1 is also referred as low voltage-activated channel (LVA), as the activation requires a small depolarization of the membrane. Activation occurs rapidly and inactivation is slow (Dodson and Forsythe, 2004).

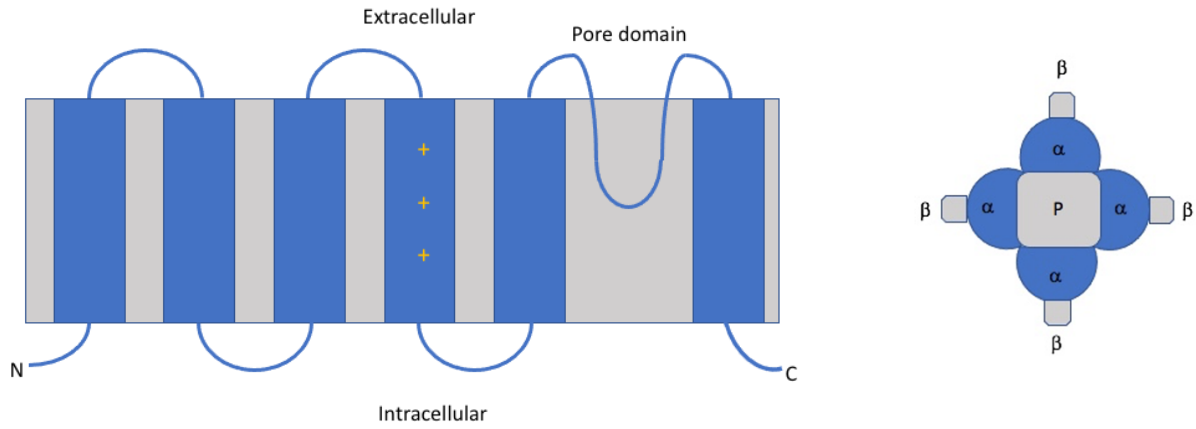

Figure 61. Kv1.1 transmembrane topology. Characteristic 6TM topology shared among the voltage-gated potassium channel. Pore domain is extended between segments S5-S6. Both N-terminus and C-terminus are intracellular. On the right is represented a schematic arrangement of 4 α-subunits assembled around a central pore and auxiliary β subunits.

The expression of Kv1.1 is extensively known in the brain, where the channel is found in both central (CNS) and peripheral (PNS) nervous system. In particular, Kv1.1 is found predominantly in the axon. In the brain, the channel contributes to the regulation of neuronal excitability by tuning the action potential (AP) shape and by contributing to the regulation of the membrane repolarization and firing properties (Jan L. Y. and Jan Y. N, 2012).

Mutations in KCNA1 gene, encoding Kv1.1 α-subunits, are involved in the development of a broad *spectrum* of channelopathies that cause a severe impairment of the channel normal functions. In particular, mutations are associated to Episodic Ataxia type 1 (EA1), epilepsy (in association or not with EA1) epileptic encephalopathy (in absence of EA1) and in some rare case can lead to hypomagnesemia, paroxysmal dyskinesia and myokymia (Paulhus K. *et al.,* 2020).

Episodic Ataxias (EAs) are a group of eight main rare neurological disorders with genetic component, characterized by an impairment of voluntary movements (Choi K. D. and Choi J. H., 2016). Furthermore, a ninth type, a "late onset" of episodic ataxia, have also been described (Damak M. *et al.,* 2009). In patients with EA1 (Episodic Ataxia type 1), a total of 47 mutations, of which most are missense and lead to a loss-of-function (LOF) of Kv1.1 channel, have been identified (Browne D.L. *et al.,* 1994). Mutations are widely spread and can affect several regions of the protein. The disorder is transmitted with autosomal dominant inheritance and

appears in childhood, with ataxia attacks variable in severity and frequency (VanDyke *et al.,* 1975). The phenotype of patients with EA1 is characterized by constant myokymia, ataxia and loss of motor coordination and balance, although over the years the phenotype spectrum has expanded (D'Adamo M.C. *et al.,* 2020). Therefore, Kv1.1 is regarded as essential candidate for the treatment of those and other neurological disorders that cause hyperexcitability. Although the expression of the channel is well characterized in the brain, an increasing number of researches are pointing out the importance of Kv1.1 in the heart. Kv1.1 expression is found in isolated atrial and ventricular myocytes from mouse heart, as well as in isolated human atrial myocytes (Glasscock E. *et al.,* 2015). Work carried out by *Glasscock et al.,* revealed a role for Kv1.1 channel and KCNA1 gene in regulating atrial repolarization and arrhythmia susceptibility (Glasscock *et al.,* 2015). Indeed, lack of Kv1.1 subunit impairs repolarization and could lead to an increased risk of atrial fibrillation (AF), due to an excessively prolonged atrial action potential (Si M. *et al.,* 2019). More recently, Kv1.1 has been recognised as important for normal ventricular functions. Indeed, the channel is involved in regulating ventricular arrhythmia susceptibility, contractility and repolarization (Trosclair K. *et al.,* 2021). Kv1.1 is also found in the kidney, where is expressed in co-localization with the Mg^{2+}-transporting channel transient receptor potential cation channel, subfamily M, member 6, (TRPM6), at the luminal membrane of the distal convoluted tubule (DCT) (Glaudemans B. *et al.,* 2009). The role of Kv1.1 in this compartment is to set the membrane potential, essential for Mg^{2+} reabsorption by TRPM6. Missense mutations in KCNA1 that lead to a loss of function of Kv1.1, are linked to autosomal dominant hypomagnesemia (Glaudemans B. *et al.,* 2009). Furthermore, Kv1.1 is found in pancreatic β cells, where it can influence the glucose- induced insulin release (Ma Z. *et al.,* 2011). A role for Kv1.1 in tumoral cells proliferation has been also elucidated in both human breast cancer cells and gastric epithelial cells (Ouadid-Ahidouch H. *et al.,* 2000; Wu W.K. *et al.,* 2006); as such, several evidences suggest that the channel could represent a potential target to treat cancer (Jeon W.I. *et al.,* 2012; Jang S.H. *et al.,* 2015). Together with a possible role as a target for cancer, Kv1.1 could be a potential candidate for the treatment of neuroinflammatory diseases, including multiple sclerosis (MS), stroke and trauma (Beraud E. *et al.,* 2006).

Taken together, all these evidences highlight the involvement of Kv1.1 in several channelopathies, most of which are related to mutations occurring in KCNA1. More researches are required to enlarge the number of blockers that can selectively target the channel and might be of potential help in ameliorating the diseases course. However, caution must be paid when

considering the pharmacological properties of Kv1.1 that are affected by the characteristic feature of the channel to form heterotetramers. This is evident especially in the brain, where the α-subunit of the channel is able to associate with α-subunits of other Kv channels. As such, selectivity is a paramount requirement for inhibitors directed towards the channel. At present, dendrotoxin κ (DTX-κ), from the venom of the mamba *Dendroaspias polylepis,* inhibits Kv1.1 alone and not other α-subunits (Wang F. *et al.,* 1999). Once again, animal venoms represent a valid and rich source of natural inhibitors for which specificity can be reached through chemical modifications of the structure if function and mechanism of action are well known.

The delayed-rectifier K^+ channel, Kv1.2, encoded by KCNA2 gene, is a member of the *Shaker*-related family and shares a similar structural arrangement with the other Kv1 members (see figure 61). Together with Kv1.1, the channel is defined a low voltage activated (LVA) channel and contributes to the regulation of excitability. The expression of the channel is prominent in the central nervous system (CNS), in correspondence of the soma, synaptic terminals and proximal dendrites, where other Kv1 α-subunits are also expressed, in particular Kv1.1 and Kv1.4 (Wang H. *et al.,* 1993, 1994; Coetzee W.A. *et al.,* 1999). Furthermore, Kv1.2 together with Kv1.1, is found at the juxtaparanodal region (JPX) close to the nodes of Ranvier (NORs), at the axonal initial segments (AIS), as well as at the pinceau region terminals of cerebellum basket cells (Robbins C.A. and Tempel B.L., 2012). The α-subunit of Kv1.2 channel is found also in dorsal root ganglion (DRG), where together with the α-subunit of Kv1.1 are the most abundantly expressed (Fan L. *et al.,* 2014). The association of Kv-α subunits is frequent in the central nervous system, with Kv1.1 and Kv1.2 subunits that often associate to form heterotetrametric channels (Coleman S.K. *et al.,* 1999). Mutations in KCNA2 gene, either gain-of-function (GOF) or loss-of-function (LOF) mutations, have been characterised in patients with epileptic encephalopathies (Syrbe S. *et al.,* 2015). The pharmacology of the channel is characterised by insensitivity to the common K^+ blocker tetraethylammonium (TEA) (Al-Sabi A. *et al,* 2013) and sensitivity to some venom-derived toxins such as Charybdotoxin (CTX) (Sprunger L.K. *et al.,* 1996) from the venom of the *Leiurus* scorpion, α-Dendrotoxin (DTX-α) (Wang F.C. *et al.,* 1999) and Urotoxin from the Australian scorpion *Urodacus yaschenkoi* (Luna-Ramírez K. *et al.,* 2014).

4.3 The voltage-gated K^+ channel, Kv1.5.

KCNA5 (on human chromosome 12p13.3), encodes for the *Shaker*-related voltage-gated potassium channel, member 5 (Kv1.5). The channel presents the typical structure shared among other members of the family, constituted by pore-forming α-subunit with six transmembrane domain topology (6TM) (see figure 61). Kv1.5 shows a rapid activation, sustained outward currents and slow inactivation, mediating the so-called 'ultra-fast delayed rectifier' (IK_{kur}) current. Channel properties can be further enhanced by the association with accessory β subunits (Kv β) (Martens J.R. *et al.,* 1999) and/or other channel subunits such as KCNE (Roepke T.K. *et al.,* 2008) or member of the K^+ channel-interacting proteins family (KChiP) (Li H. *et al.,* 2005). The role of Kv1.5 is pivotal in the heart, where its expression is predominant in human atria more than ventricle, at the intercalated disks and T tubles (Wang Z. *et al.,* 1993; Fedida D. *et al.,* 1993; Feng J. *et al.,* 1997) and where it contributes to the repolarization phase of action potential (AP). Targeting potassium channels expressed in the heart, and specifically Kv1.5 in the atria, is regarded as promising strategy for the development of novel anti-arrhythmic drugs that might contribute to treat certain types of conditions such as atrial fibrillation (AF) (Dorian P., 2003; Roden D.M., 2003). Atrial Fibrillation (AF) is a common form of arrythmia, with an estimated prevalence in the population that correlates with age (Miyasaka, Y. *et al.,* 2006). The pathophysiology underneath AF is complex and is linked to an abnormal activity of atrial cells (ectopic activity), that leads to an uncoordinated atrial activity and ventricular contraction. Uncoordinated atrial activity facilitates blood coat formation in the blind pouch atrial appendage, whereas ventricular contraction prevents cardiac contractile functions (Wakili R. *et al.,* 2011). Although AF is mainly a sporadic condition, a genetic component was identified.

In monogenic AF the higher number of mutations are loss-of-function (LOF) or gain-of-function (GOF) mutations born by genes encoding for ion channels subunits (Mahida S. *et al.,* 2011). Several mutations in KCNA5, encoding for Kv1.5, have been identified (Drolet B. *et al.,* 2005; Simard C. *et al.,* 2005; Olson T.M. *et al.,* 2006), revealing a hope for a possible ion channel-target therapy. The treatment of patience with AF is based on anti-pharmacological treatments and on the administration of anti-arrhythmic drugs. However, the use of anti-arrhythmic drugs remains the preferential treatment procedure, and this highlights the importance of discover novel compounds that carry less adverse effects in the ventricle compared to the Class III arrhythmogenic drugs at present in use (Tamargo *et al.,* 2009).

The rationale behind the strategy of using Kv1.5 blockers to treat this condition, is based on two main evidences: first, the channel is preferentially expressed in the atria and not in the ventricle; and second, targeting Kv1.5 currents is expected to determine an increase in the duration of the atrial AP and the refractory period of fibrillating atrium, which would be beneficial for patience with AF (Wetter and Terlau, 2014). However promising, Kv1.5 atrial-target therapy is quite complex and require drugs to be highly selective. At present, only few drugs are channel specific, whereas a vast number of them are able to act not only on other K^+ channels expressed in the heart, but also on Na^+ channels, making really difficult to promote drugs on clinical trials (Tamargo J. *et al.,* 2009). The significative challenge in discovery small molecules and compounds that can selectively act on Kv1.5 is also linked to the fact that the binding area of most Kv1.5 blockers is represented by amino acidic residues located at the pore region and lower S6 segments (Tikhonov D. B. and Zhorov B.S., 2014; Wu J. *et al,* 2009; Chen R. and Chung S. H., 2018). Some of those amino acids are highly conserved among different cardiac voltage-dependent channels (hERG, Kv1.1, KCNQ1, Kv1.7 and Kv1.3) and this intensify the challenges in finding specific Kv1.5 blockers (Tamargo J. *et al.,* 2009; Zhao Z. *et al.,* 2019) (Figure 62).

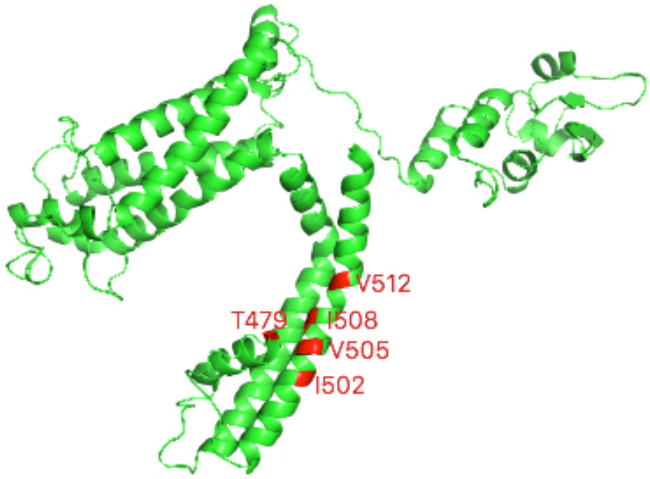

Figure 62. Kv1.5 homology model. Kv1.5 homology model was created using SWISS-MODEL. The channel is presented in monomeric state. Template used was **5wie.1. B** (crystal structure of a Kv1.2-2.1 chimera K^+ channel V406W mutant, in an inactivated state (Pau V. *et al.,* 2017). Sequence identity was 73.75%. Some residues interacting with Kv1.5 blockers are highlighted in red and are located at the pore region and segment S6.

Kv1.5 is also expressed in the immune system, in particular in macrophages, where it associates with Kv1.3 to form heterotetramers. The localization, as well as the kinetics and the pharmacological properties of the channelosome, are strictly related to the two channels ratio (Kv1.3/Kv1.5) (Vicente R. *et al.,* 2006; Villalonga N. *et al.,* 2007; Villalonga N. *et al.,* 2010). Furthermore, Kv1.5 is also found in macroglia, where it covers an important function in cell activation (Pyo H. *et al.,* 1997; Jou I. *et al.,* 1998). At present, the pharmacology of I_{kur} currents is characterized by insensitivity to TEA and Ba^{2+} but highly sensitive to 4-aminopyridine (4-AP) (Tamargo J. *et al.*, 2004; Fedida D. *et al.,* 1993; Snyders, D. J. *et al.,* 1993). When designing Kv1.5 blockers, although challenging, factors to take into account are the vast expression of the channel in other body tissues as well as the presence, in certain compartment, of heterotetramers that might alter the channel's pharmacology.

4.4 The voltage-gated K^+ channel, Kv2.1

The *Shab*-related superfamily member Kv2.1, encoded by KCNB1 gene in humans (chromosome 20q13.13), is responsible for a consistent quota of the delayed-rectifier K^+ (IK_{DR}) current in mammalian neurons expressed throughout the brain. In particular, Kv2.1 channels contribute to the majority of the IK_{DR} in pyramidal neurons of hippocampus and cortex (Du J. *et al.,* 2000; Guan D. *et al.,* 2007; Guan D. *et al.,* 2013; Liu P.W. *et al.,* 2014), where they participate to action potential repolarization (Liu P.W. *et al.,* 2014). Kv2.1 are also expressed as clusters at the cell body, proximal dendrites and axon initial segment of neurons (O'Connel K.M. *et al.* 2010; Fox P.D. *et al.,* 2013). Structurally, the channel presents a similar arrangement to other voltage-gated K^+ channels, with six transmembrane segments architecture (6TM). Both N- and C- endings are located at the cytoplasmatic side and contains functional domains that contributes to several processes (Barros F. *et al.,* 2012). One characteristic feature of Kv2.1, described also for Kv3.1 (Klemic K. G. *et al.,* 2001), is the U-shape inactivation, so-called because the inactivation-voltage relationship presents a characteristic U-shape (Klemic K. G. *et al.,* 1998). The U-shape inactivation represent a third type of inactivation that differ from the fast N-type (or "ball and chain") and the slow C-type inactivation (Hoshi T. *et al.,* 1990; Hoshi T. *et al.,* 1991). Indeed, U-shaped inactivation-voltage relationship is characterised by maximal inactivation at intermediate voltages and less marked inactivation at positive potentials, underlying a kinetic model for which the channel undergoes inactivation preferentially from a closed state (Klemick K.G. *et al.,* 2001). The U-shape inactivation is accelerated by extracellular K^+ or by K^+ channel blockers, such as TEA (Klemick K.G. *et al.,* 1998; Klemick K.G. *et al.,* 2001). At the N-termini, Kv channels presents a characteristic domain, the T1 domain also referred as cytoplasmatic tetramerization domain, constitute of 120 aminoacidic residues, that covers a fundamental role in the assembly of α-subunits ensuring subfamily-specificity (Kreusch A. *et al.,* 1998; Bixby A. *et al.,* 1999; Cushman S.J. *et al.,* 2000; Minor D.L. *et al.,* 2000) and is also important for the characteristic U-shape inactivation of the channel (Kurata H.T. *et al.,* 2002). Each of the Kv2α-subunit can associate with other modulatory α-subunits to form heteromeric channels, whose kinetics properties are different from the homomeric channels (Post M. *et al.,* 1996; Kramer J. *et al.,* 1998; Stocker M. *et al.,* 1999). The T1 domain is conserved among voltage-activated K^+ channels subfamilies, with some differences in the primary sequence for channels belonging to different subfamilies (Kurata H.T. *et al.,* 2002).

Alterations in KCNB1 gene, encoding for Kv2.1 α-subunits, are associated with the development of serious neurological disorders, including epileptic disorders. Epileptic encephalopathies (EE) are a group of disorders characterized by epileptic activity that significantly alters the normal cognitive and behavioural development (Jain P. *et al.,* 2013). Usually they appear in early life and during childhood and the course is variable. Some of the disorders included under the EE umbrella, have a genetic component found in mutations of genes encoding several potassium channels, including KCNB1 but not limited to. For examples, alterations in KCNA2 encoding hKv1.2 channel are also linked to epileptic encephalopathy, as discussed above in section 4.2 (Sachdev M. *et al.,* 2017), as well as mutations in KCND2 encoding hKv4.2, which are involved in the development of epilepsy and autism when mutations occur in the S6 segment of the protein (Lee H. *et al.,* 2014). Regarding Kv2.1, *De novo* mutations occurring at different sites of the channel, but mainly at the pore region, selectivity filter and voltage sensor domain (VSD), have been identified in several patients with EE (Torkamani A. *et al.,* 2014; Saitsu H., *et al.,* 2015; Thiffault I. *et al.,* 2015; de Kovel, C. *et al.*, 2017; Allen N. M *et al.*, 2016) and neurodevelopment disorders (Soden S.E. *et al.,* 2014).

4.5 Objectives

The objectives of this study are to assess the effect of SXCL-1 and SXCL-6 on other close-related K^+ channels: Kv1.1, Kv1.2, Kv1.5 and Kv2.1. To do so, the electrophysiological technique whole-cell patch clamp on tSA201 cells, transiently expressing the channel of interest, was used. Channel currents were characterised at +50 mV and expressed as peak current (pA), in presence and absence of each peptide at the of 5 nM, a concentration where SXCL-1 is able to inhibits the average peak current of Kv1.3, whereas SXCL-6 does not. As such, considering also the limitation in terms of quantity, that will be further explained in section 4.10, we chose to test this concentration and investigate whether the peptides have a biological effect on other voltage-gated potassium channels at this concentration. Only for Kv2.1, a different protocol was adopted. Currents were recorded using a step-voltage protocol, with currents expressed as peak currents (pA) and compared at +50 mV to allow similar conditions for all channel tested.

4.6 Results

4.6.1 Electrophysiological characterization of the voltage-gated channel, Kv1.1

Kv1.1_WT channel currents were recorded using whole-cell patch clamp technique on tsA201 cells, transiently transfected with human Kv1.1 DNA. Currents were evoked using a "+50 mV continuously" protocol as described previously (see Material and Methods, section 2.4) and then analysed at +50 mV as peak current (pA).

In figure 63 A, is shown an exemplar trace of Kv1.1_WT channel in a physiological extracellular solution under control conditions using a voltage-step protocol (Figure 63, B). The channel presents an average peak current of 2408 pA (95% CI 1836: 2979 n=8) at 50 mV.

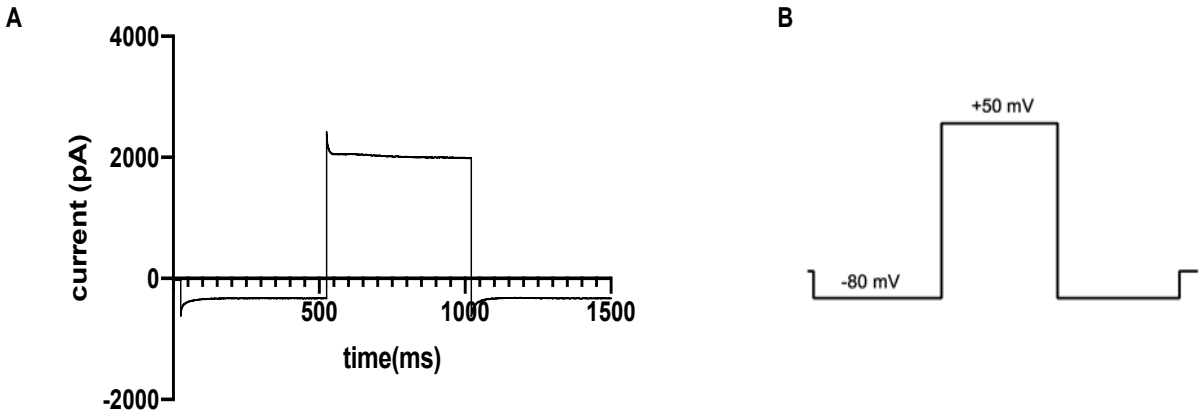

Figure 63. Representative trace of Kv1.1_WT. A) The channel in control conditions shows an average peak current of 2408 pA (n=8). **B)** Example of the protocol used for the electrophysiological recordings. Currents were recorded at +50 mV and expressed as peak currents (pA). To note, the "+ 50 mV continuously" protocol was used to characterise the current for all channels belonging to the *Shaker*-related family (Kv1.1, Kv1.2 and Kv1.5).

4.6.2 Electrophysiological characterization of the effect of the two novel peptides, SXCL-1 and SXCL-6 and ShK toxin on Kv1.1

As well as a potent blocker of Kv1.3, ShK has also been shown to exert inhibitory effects at subnanomolar concentrations on related Kv channel isoforms, including the Kv1.1 channel (Kalman K. *et al.,* 1998). As the two novel peptides, showed similar pharmacological profiles to ShK on Kv1.3, we wanted to test whether the peptides would also exert a similar inhibitory effect on the Kv1.1 channel. To test the effect of the two novel peptides, Kv1.1 was incubated with either 5 nM of SXCL-1, 5 nM of SXCL-6 or 5 nM of ShK diluted in the extracellular control solution, for 20 minutes in 5% CO_2 incubator prior the experiment. After 20 minutes, currents expressed from individual cells were measured using whole-cell patch clamp electrophysiology. Figure 64 shows a peak current graphic of Kv1.1_WT and in presence of 5 nM of each peptide.

The average peak current f Kv1.1 channel measured in the presence of 5 nM of ShK, SXCL-1 and SXCL-6 was equal to 1929 pA (95% CI 1836: 2979 n=8) (see Figure 64 and exemplar trace, Figure 65, A); 2024 pA (95% CI 1511: 2537 n=6) (Figure 64 and exemplar trace, Figure 65, B) and 2304 pA (95% CI 1947: 2661 n=7) (Figure 64 and exemplar trace, Figure 65, C), respectively. With an average reduction in current of 20%, 16% and 4%, respectively. For all of the peptides, no significant change was observed in channel current at 5 nM concentration when compared to the control currents [2408 pA (95% CI 1836: 2979 n=8)].

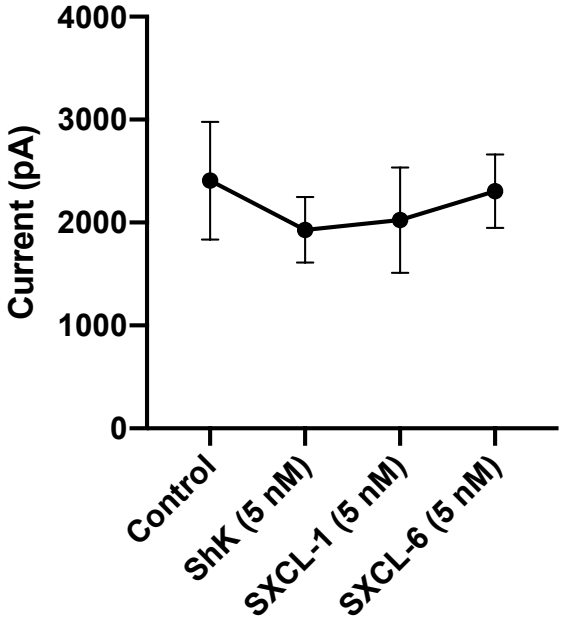

Figure 64. Kv1.1_WT peak current (pA) graphic in control and in presence of 5 nM of ShK, SXCL-1 and SXCL-6. Bars are representative of 95% CI of the mean. 5 nM of each peptide did not determine any significant reduction of the channel current. ShK determined a 20% current inhibition on Kv1.1 channel (1929 pA n=8; adjusted P value p=0.1472). SXCL-1 determine only 16% of current inhibition (2024 pA n=6; adjusted P value p=0.3911), whereas a 4% current reduction was detectable for SXCL-6 at the same concentration (2304 pA n=7; adjusted P value p=0.9619).

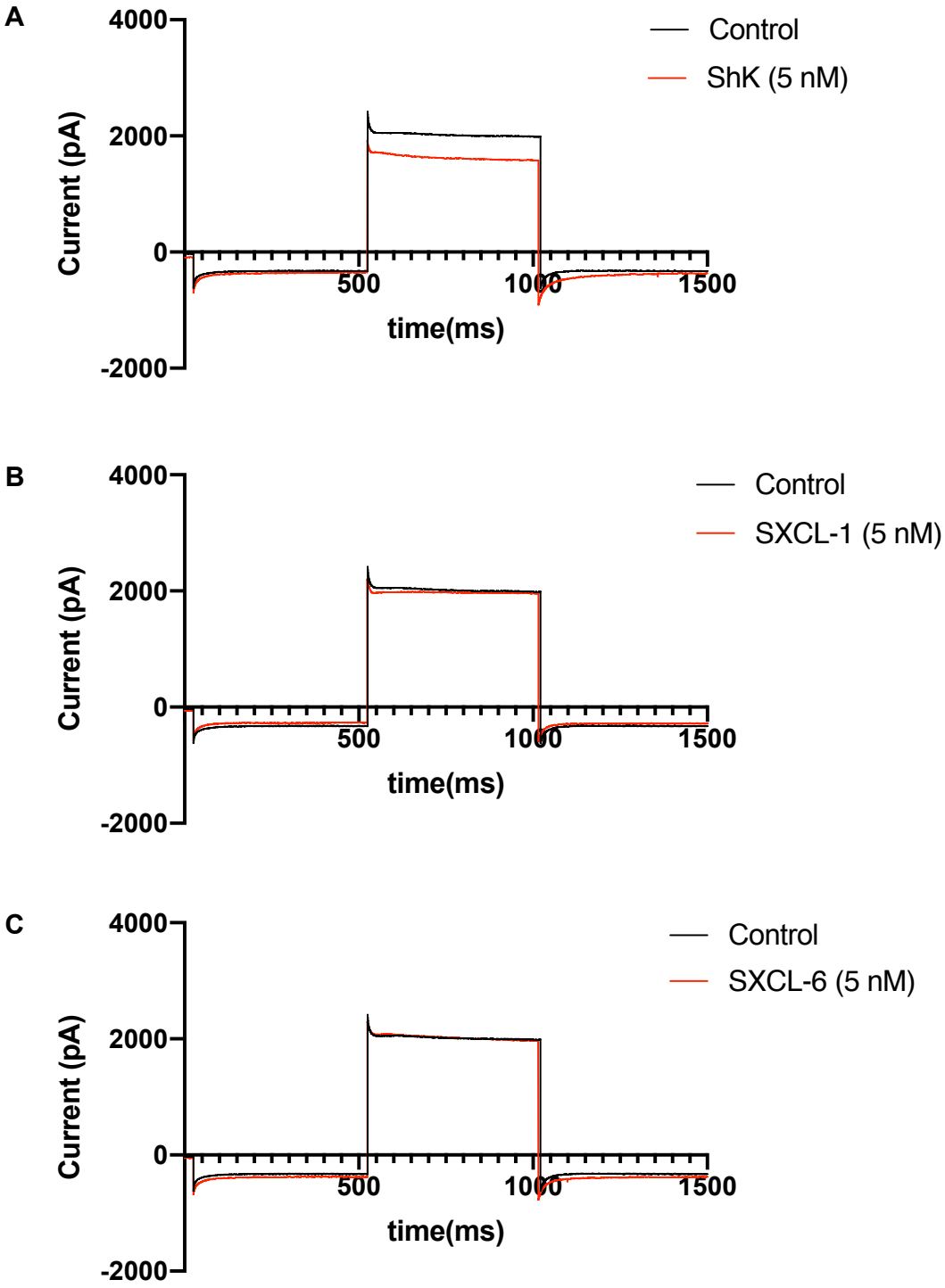

Figure 65. Layout of representative traces of Kv1.1_WT in control and in presence of 5 nM of each peptide. A) Kv1.1_WT (black trace) and 5 nM of ShK (red trace) **B)** Kv1.1_WT (black trace) and 5 nM of SXCL-1 (red trace) **C)** Kv1.1_WT and 5 nM of SXCL-6 (red trace).

4.7 Electrophysiological characterization of the voltage-gated potassium channel, Kv1.2

tsA201 cells were transiently transfected with hKv1.2 DNA and electrophysiological recordings on Kv1.2_WT were obtained using the whole cell patch clamp technique. Currents were evoked using a "+50 mV continuously" protocol as described previously (see Material and Methods, section 2.4) and then analysed at +50 mV as peak current (pA).

In the figure below (Figure 66, A), is showed a representative trace of Kv1.2_WT in a physiological extracellular solution under control condition using a voltage-step protocol (Figure 66, B). The average peak current measure at +50 mV was equal to 2305 pA (95% CI 1733: 2878 n=6).

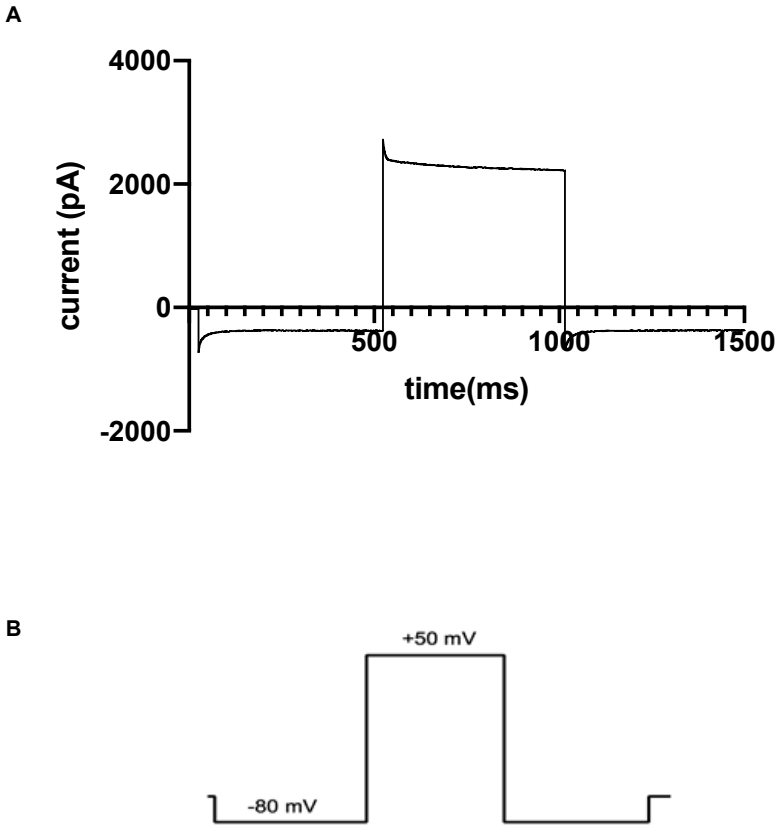

Figure 66. Layout of representative trace of Kv1.2_WT and protocol used for electrophysiological recordings. A) Representative trace of Kv1.2_WT. Average peak current was 2305 pA (n=6)**; B)** Example of the protocol used during the experiments (+50 mV continuously).

4.7.1 Electrophysiological characterisation of the two novel *ShK-like* peptides, SXCL-1 and SXCL-6 and ShK on Kv1.2

The effect of SXCL-1 and SXCL-6 were tested by using a concentration of 5 nM of each peptide and by incubating the cells expressing the channel for a total of 20 minutes in the 5% CO_2 incubator. Together with the two novel *ShK-like* peptides, ShK was also used in our investigations, in a similar way to SXCL-1 and SXCL-6.

Results from our investigations showed that in presence of 5 nM of ShK, SXCL-1 and SXCL-6, the average peak current of Kv1.2 was equal to 1626 pA (95% CI 1145: 2107 n=4, Figure 67 and representative trace in Figure 68, A), 2281 pA (95% CI 1926: 2635 n=5, Figure 67 and representative trace in Figure 68,B) and 2243 pA (95% CI 1619: 2867 n=5, Figure 67 and representative trace in Figure 68, C), respectively. Taken together, our investigations revealed that SXCL-1 and SXCL-6 did not determine any significant inhibitory effect on the average peak current (pA) of the channel when compared to the peak current in control conditions [2305 pA (95% CI 1733: 2878 n=6)]. For ShK, we did observe a 30% peak current inhibition, however with no statistical significance [1626 pA (95% CI 1145: 2107 n=4; adjusted P values p=0.0755].

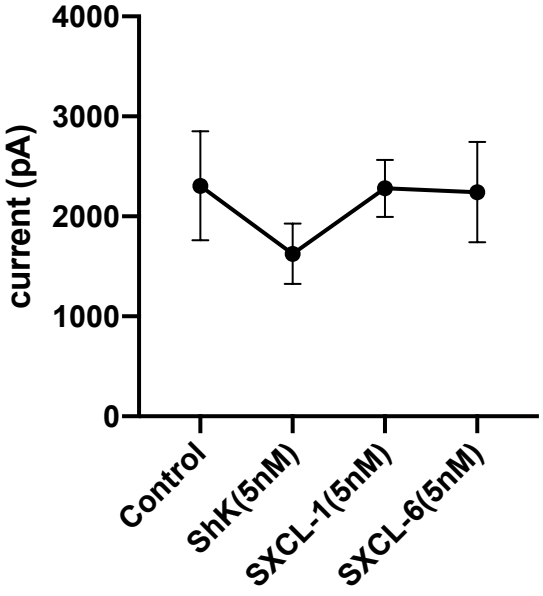

Figure 67. Peak current (pA) graphic of Kv1.2_WT in control conditions and in presence of 5 nM of ShK, SXCL-1 and SXCL-6. Bars are representative of 95% CI of the mean. Peptides were all tested at a concentration of 5 nM. No statistically significant difference was detected between peak current of Kv1.2_WT and after incubation with each peptide (adjusted P values were: p=0.0755 (n=4); p=0.994 (n=5); and p=0.9916 (n=5), respectively).

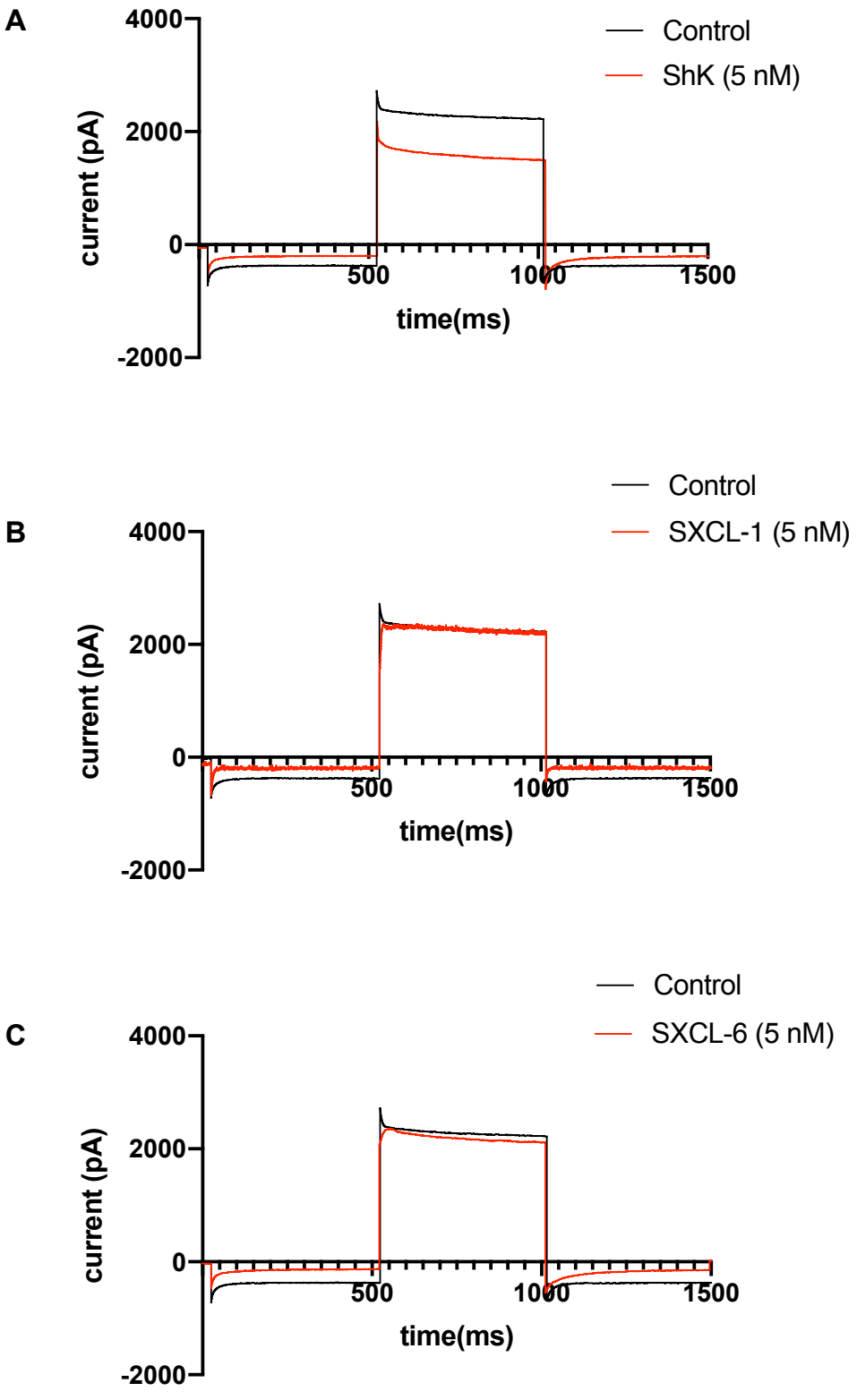

Figure 68. Layout of representative traces of Kv1.2_WT in control conditions and in presence of 5 nM of each peptide. A) Kv1.2 in control conditions (black trace) and with 5nM of ShK (red trace); **B)** Kv1.2 in control (black trace) and in presence of 5nM of SXCL-1 (red trace); **C)** Kv1.2 in control conditions (black trace) and after incubation with 5nM of SXCL-6 (red trace).

4.8 Electrophysiological characterization of the voltage-gated potassium channel, Kv1.5

tsA201 cells were transiently transfected with hKv1.5 DNA and electrophysiological recordings on Kv1.5_WT were obtained using the whole cell patch clamp technique.
Currents were evoked using a "+50 mV continuously" protocol as described in Material and Methods (section 2.4) and as previously shown for the characterization of other Kv channels. Currents were expressed as peak current (pA) at +50 mV.
Kv1.5_WT in control conditions presents an average peak current of 5426 pA (95% CI 3786: 7065 n=9) (Figure 69).

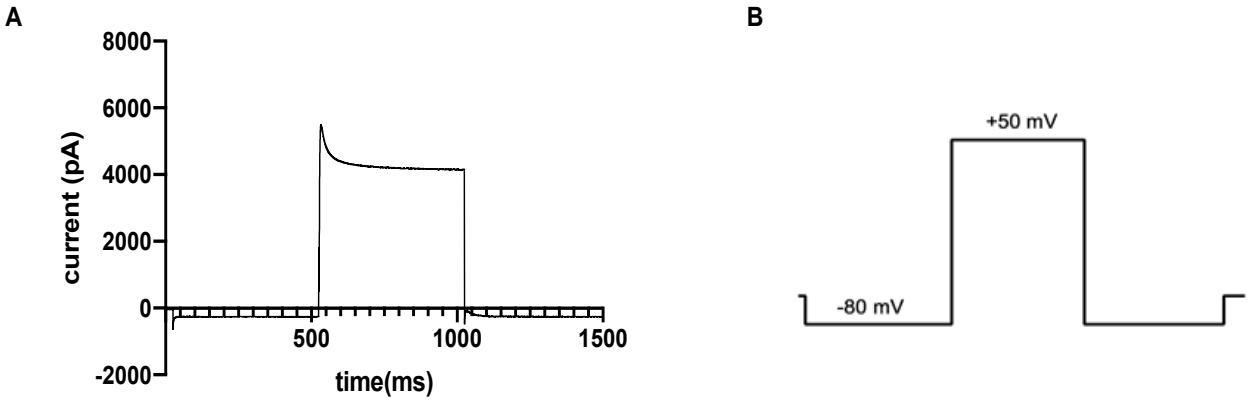

Figure 69. Electrophysiological profile of Kv1.5_WT channel. A) Kv1.5 in control conditions, the average peak current of the channel measured at +50 mV is equal to 5426 pA (n=9). **B)** Example of protocol used for electrophysiological recordings.

4.8.1 Electrophysiological characterisation of the effect of the two novel peptides, SXCL-1, SXCL-6 and ShK on Kv1.5

To uncover the effect of the two novel *ShK-like* peptides, SXCL-1 and SXCL-6, Kv1.5 channel was incubated with 5 nM of each peptide for 20 minutes in 5% CO_2 incubator, in a similar way to Kv1.1 channel and Kv1.2. Together with SXCL-1 and SXCL-6, the effect of the well-known ShK was also tested, by incubating the channel with 5 nM of the toxin in a similar way to SXCL-1 and SXCL-6. As showed in the average peak current graphic in figure 70, the two *ShK-like* peptides did not determine any significant effect on the channel average peak current. Kv1.5 in presence of 5 nM of SXCL-1 and SXCL-6 shows an average peak current of 6171 pA (95% CI 4791: 7552 n=6, Figure 70 and exemplar trace in Figure 71, B) and 5352 pA (95% CI 3813: 6892 n=6, Figure 70 and exemplar trace in Figure 71, C), respectively. ShK toxin, at 5 nM concentration, only slightly reduce the average peak current of Kv1.5, with an average peak current of 4097 pA (95% CI 2201: 5992 n=5) (Figure 70 and exemplar trace in Figure 71, A).

The two novel *ShK-like* peptides, SXCL-1 and SXCL-6, did not exhibit any statistically significant inhibitory effect on Kv1.5_WT [5426 pA (95% CI 3786: 7065 n=9)]. ShK toxin, only slightly reduced the channel current by 25% (Figure 70 and exemplar trace in Figure 71, A) with no statistically significance when analysed with One way-ANOVA, Dunnett's multiple comparisons test.

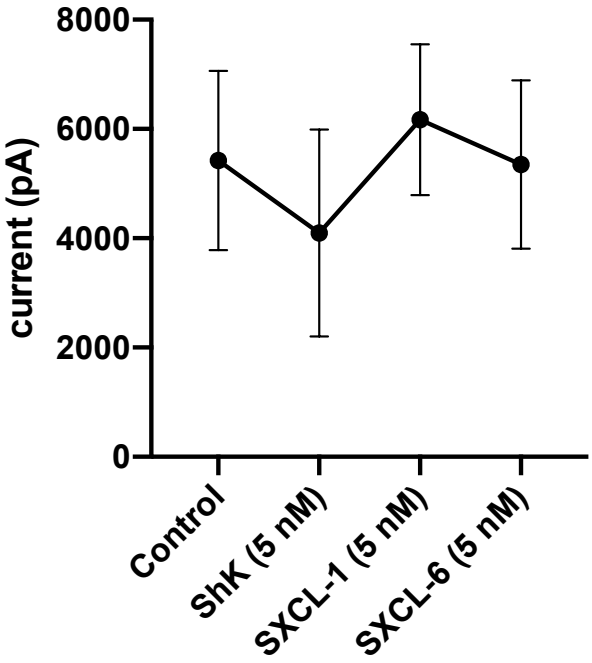

Figure 70. Kv1.5_WT peak current (pA) graphic in control conditions and with 5 nM of ShK, SXCL-1 and SXCL-6. Bars are indicative of 95% CI of the mean. Kv1.5_WT [5426 pA (95% CI 3786: 7065 n=9)]. Kv1.5 and ShK [4097 pA (95% CI 2201: 5992 n=5; adjusted P value p=0.4087)]. Kv1.5 and SXCL-1 [6171 pA (95% CI 4791: 7552 n=6; adjusted P value p=0.7700)]. Kv1.5 and SXCL-6 [5352 pA (95% CI 3813: 6892 n=6; adjusted P value p=0.9996)]. No statistically significance difference on the average peak current was detected after 20 minutes of incubation with each peptide at a concentration of 5 nM.

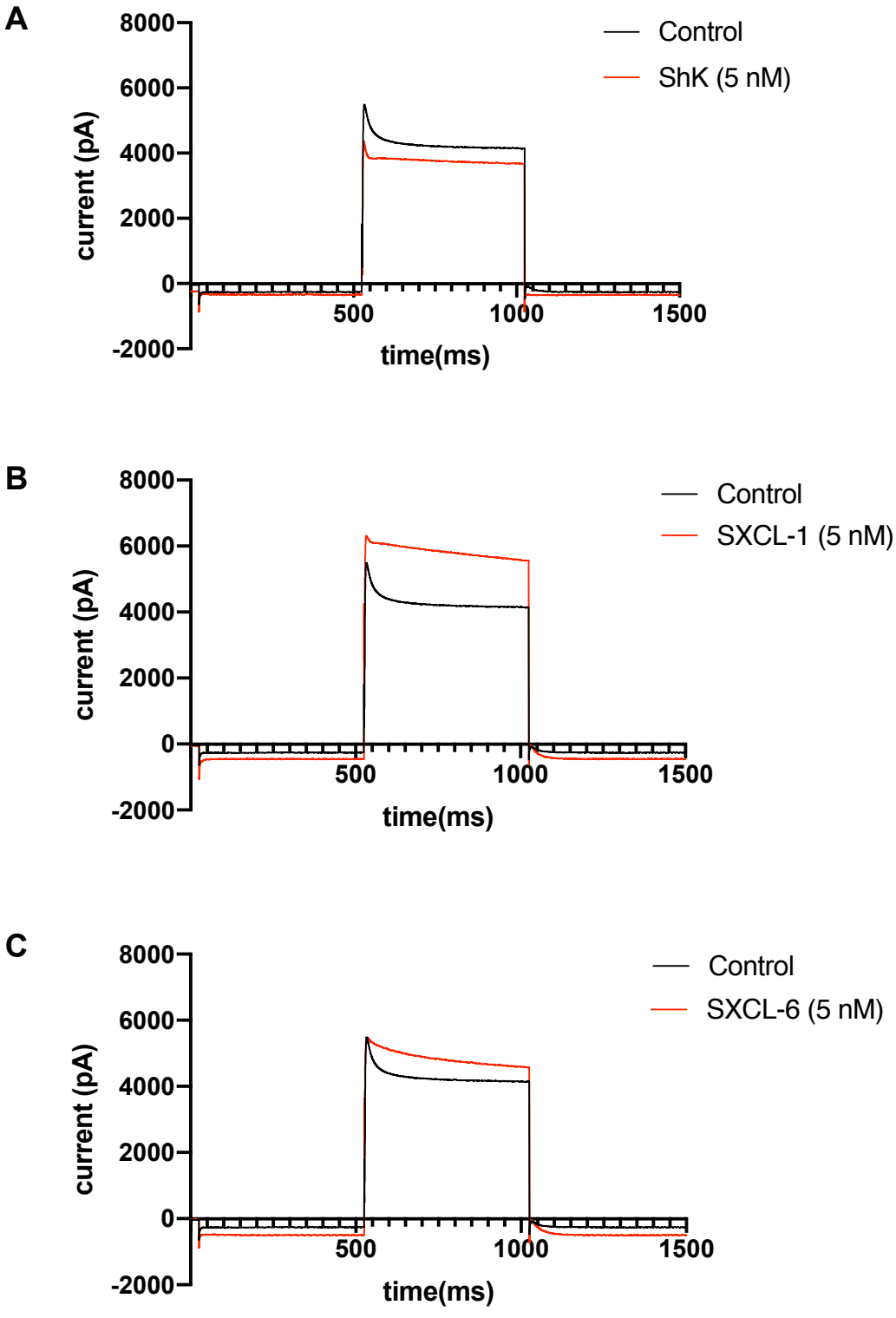

Figure 71. Layout of representative Kv1.5_WT traces in control conditions and in presence of 5 nM of each peptide. A) Kv1.5_WT (black trace) and ShK (red trace) **B)** Kv1.5_WT (black trace) and SXCL-1(red trace); **C)** Kv1.5_WT (black trace) and SXCL-6 (red trace).

4.9 Electrophysiological characterization of the voltage-gated potassium channel, Kv2.1

Kv2.1_WT was expressed in tsA201 cells, transiently transfected with hKv2.1 DNA. Electrophysiological characterization was obtained using whole cell patch clamp technique by evoking the channel current with a "+ 50 mV to -90 mV" protocol, with decreasing 10 mV intervals (see Material and Methods, section 2.4). Currents amplitudes were measured at +50 mV as before and expressed as peak current (pA). The average peak current (pA) for Kv2.1 in control conditions was 4948 (95% CI 3182: 6714 n=12) (Figure 72, A). The current-voltage relationship (I-V curve) was obtained by measuring the peak current (pA) at all different voltages from +50 mV to -90 mV and then plotted using GraphPad Prism 8 (Figure 72, B). Calculated reversal potential of Kv2.1_WT in control conditions was equal to -55.29 mV (95% CI -64.02: -46.56 n=12) (Figure 72, B).

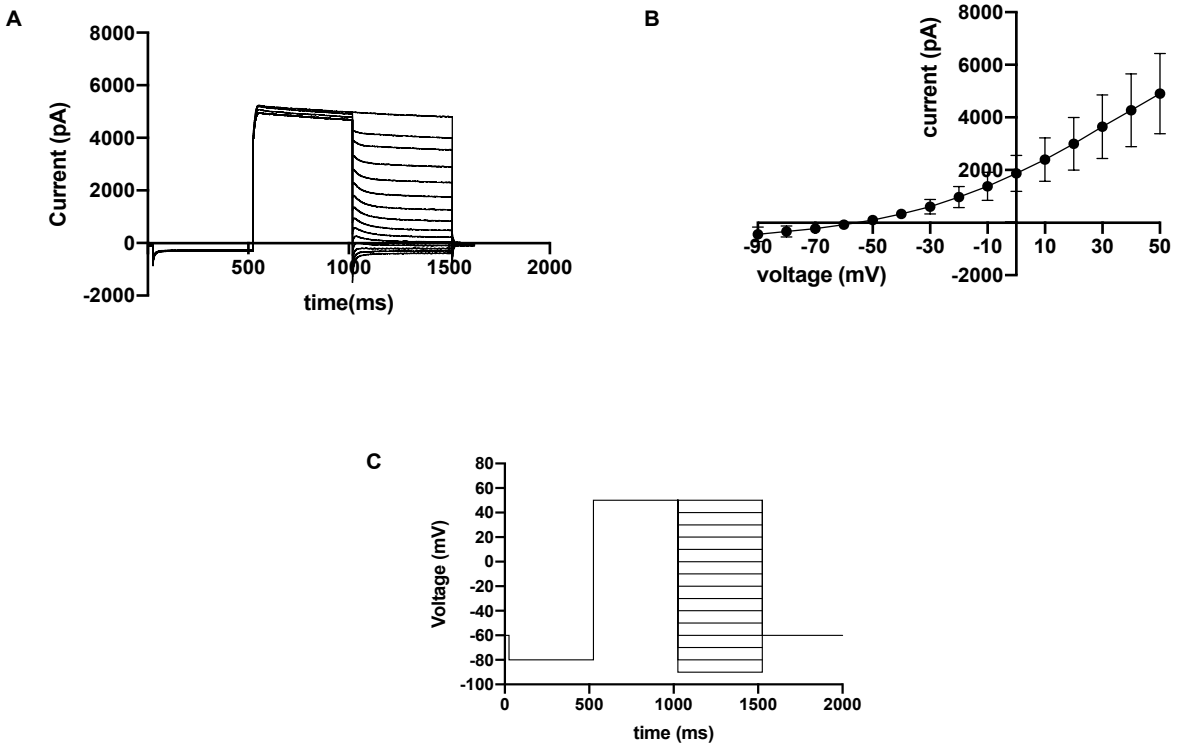

Figure 72. Electrophysiological characterization of Kv2.1_WT in control conditions. A) Representative traces of Kv2.1 at +50 mV. Average peak current equals to 4948 pA (n=12). **B)** Current-voltage relationship**.** The channel shows a voltage dependence resulting in a non-linear IV curve. **C)** Example of the protocol using for electrophysiological characterisation.

4.9.1 Electrophysiological characterisation of the activity of the novel *ShK-like* peptides, SXCL-1 and SXCL-6 and ShK on Kv2.1

Investigations to unravel the biological activity of the two novel *ShK-like* peptides, SXCL-1 and SXCL-6, were conducted by incubating the channel with 5 nM of each peptide for a total of 20 minutes, as previously described for Kv1.3 (chapter 3), Kv1.1, Kv1.2 and Kv1.5. Furthermore, investigations were conducted using ShK toxin as negative control, as the toxin is known to block Kv1.3 but not Kv2.1. Experiments were conducted in a similar way as previously described, so that the channel was incubated with 5nM of the peptides for a total of 20 minutes, in 5% CO_2 incubator.

Below, are showed layout panel of representative traces of Kv2.1 in presence of the two peptides, SXCL-1 and SXCL-6 (Figure 74, A; Figure 74, C) and ShK (Figure 74, E) and respective current-voltage (I-V) relationship curves (Figure 74, B; Figure 74, D; Figure 74, F). Currents are expressed as peak current at +50 mV, whereas I-V curves are representative of the average peak currents at every voltage from +50 mV to -90 mV. Incubation of the channel with 5 nM of SXCL-1 and SXCL-6, determined an average peak current (pA) of 3314 pA (95% CI 1503: 5125 n=5) and 2414 pA (95% CI 1299: 3529 n=5), respectively (Figure 73 and representative trace 74, A; Figure 73 and representative trace 74, C). Calculated reversal potential for Kv2.1_WT in presence of 5 nM of SXCL-1 was equal to -60.46 mV (95% CI -72.32: -48.60 n=5) (Figure 74,B); whereas value of the reversal potential for Kv2.1_WT in presence of 5 nM of SXCL-6 was equal to -60.32 mV (95% CI 66.44: -54.20, n=5) (Figure 74, D).

Application of 5 nM of ShK, determined a slight reduction of the average peak current of Kv2.1_WT that was equal to 3412 pA (95% CI 2591: 4233 n=8) (Figure 73 and representative trace 74, E). Calculated reversal potential for Kv2.1_WT in presence of 5 nM of ShK was equal to -53 mV (95% CI -57.35: -48.65 n=8) (Figure 74, F).

Indeed, both SXCL-1 and SXCL-6, at 5 nM concentration, determined an inhibition of the channel current resemble to 31% and 51%, respectively, with a particular emphasis on SXCL-6, that shows a more potent inhibitory effect towards the channel currents compared to SXCL-1. However, no statistic significant was found when statistical test (one-way ANOVA, Dunnett's test) was performed (adjusted P values are showed below in figure 73).

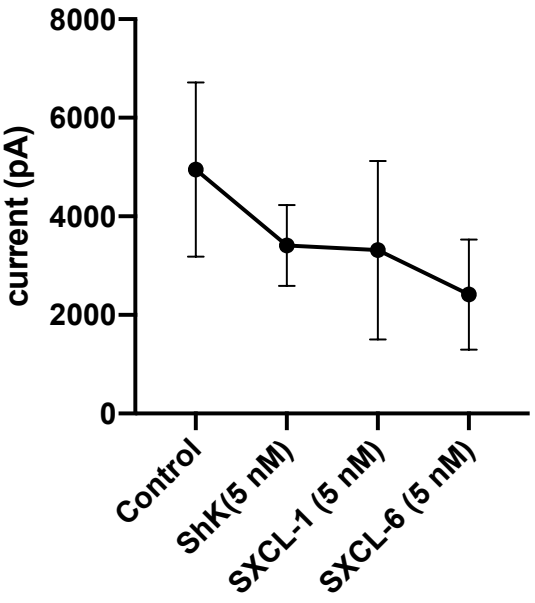

Figure 73. Peak current (pA) graphic of Kv2.1_WT in control conditions and in presence of 5 nM of each peptide. Bars are indicative of 95% CI of the mean. Kv2.1_WT [4948 (95% CI 3182: 6714 n=12)]. No significant peak currents (pA) inhibition was observed when 5 nM of ShK [3412 pA (95% CI 2591: 4233 n=8; adjusted P value p=0.8937)], SXCL-1[3314 pA (95% CI 1503: 5125 n=5); adjusted P value p=0.0987)] and SXCL-6 [2414 pA (95% CI 1299: 3529 n=5); adjusted P value p=0.4069)]. Only SXCL-6 was able to reduce the current by 51%, however with no statistical significance.

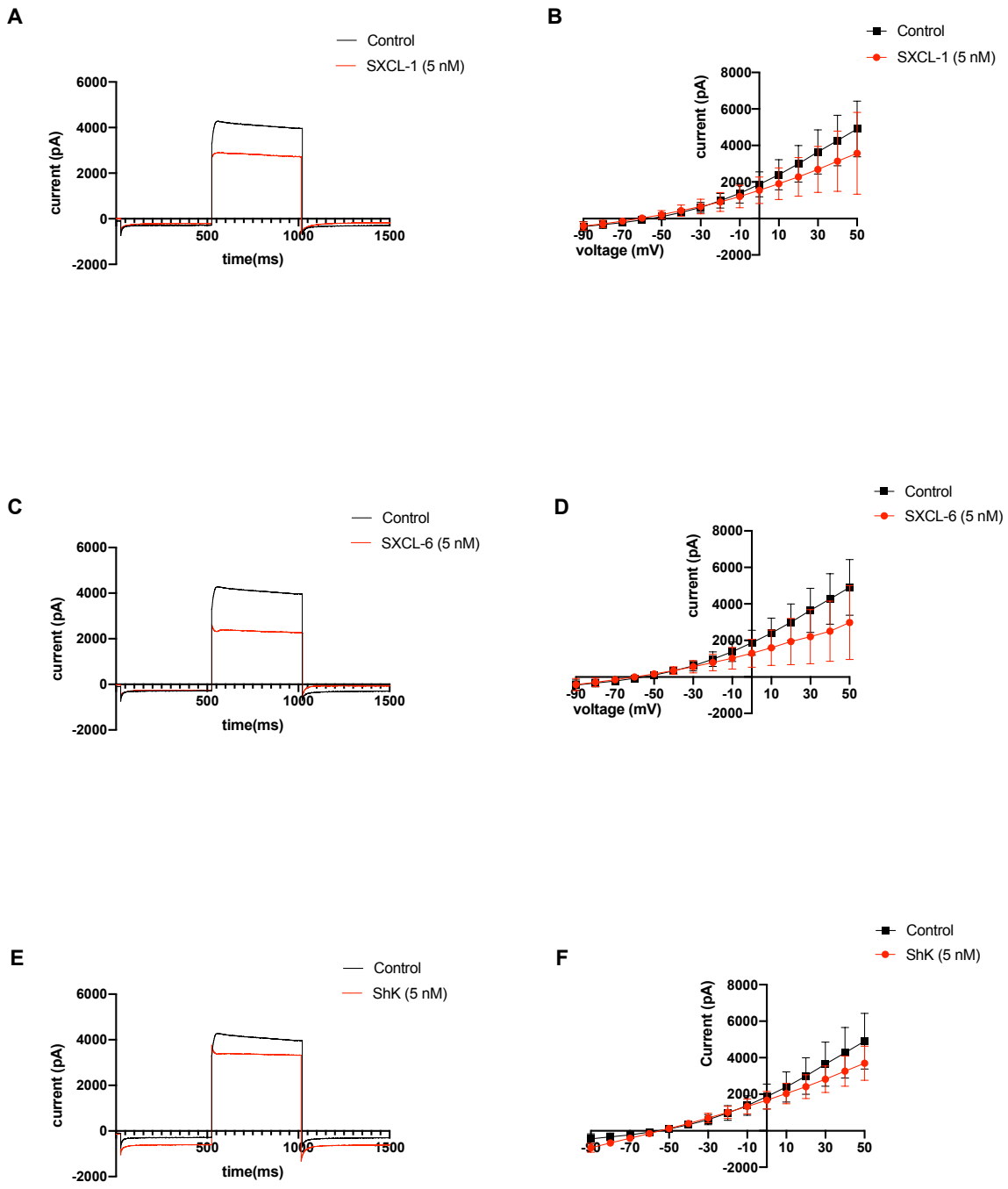

Figure 74. Layout panel of representative traces and current-voltage (I-V) curves. A) Representative trace of Kv2.1_WT (black trace) and in presence of 5 nM of SXCL-1 (red trace); **B)** Current-voltage relationship of Kv2.1_WT (black squares) and after application of 5 nM of SXCL-1 (red circles); **C)** Representative trace of Kv2.1_WT (black trace) and in presence of 5 nM of SXCL-6 (red trace); **D)** Current-voltage relationship plotted for Kv2.1_WT (black squares) and after application of 5 nM of SXCL-6 (red circles); **E)** Representative trace of Kv2.1_WT (black trace) and after incubation with 5 nM of ShK (red trace); **F)** Current-voltage relationship for Kv2.1_WT (black squares) and in presence of 5 nM of ShK (red circles).

4.10 Discussion

Venom from several animals, marine as well as terrestrial, represent an important source of toxins and peptides that have a great potential not only as therapeutic tools to treat human diseases but also as research tools, that help to reach a better understanding of the physiological properties of ion channels involved in a wide *spectrum* of diseases. The term "Channelopathies" is used to indicate an heterogeneous group of pathologies that affect several districts within the human bodies, linked to inherited or acquired factors (Kim J-B., 2014). The most common inherited factors occurring for channelopathies, are found in mutations of genes that encode for ion channels or accessory subunits and that lead to alterations of the channel's activity. At present, the list of channelopathies includes also some form of cancer (Pedersen S. F. and Stock C., 2013), leukaemia (Morelli M.B. *et al.,* 2013) and gastrointestinal diseases (Saito Y. A., *et al*., 2009). Mutations in genes encoding ion channels have been characterised in the nervous system, where they are linked to epilepsy, migraine, episodic ataxia, hyperkalemic and hypokalemic paralysis, and many more; in the cardiovascular system, where they are associated to Brugada syndrome, short QT syndrome, Atrial fibrillation (AF), congenital long QT syndrome (LQTS) and many more; as well as in the respiratory, endocrine and urinary system (Kim J-B., 2014). Human channelopathies have also been described in the immune system, where mutations in gene encoding ion channels such as ORAI1 (as well as the stromal interacting molecule 1, STM1), Mg^{2+} and Zn^{2+} transporters and many more, cause severe immunodeficiency and immune dysfunction (Vaeth M. and Freske S., 2018).
Considering the key role of ion channels in the physiology of excitable and non-excitable cells, is not surprising that mutations, that result in a reduction and/or enhancement of their activity, directly translates in the loss of the fine-tuned cellular functionality with clinical implications. Introducing target-specific therapies aimed towards ion channel using small compounds and peptides, is a promising route that several researches are focusing their attention on. Literature is fulfilled of small toxins and peptides, that successfully inhibits channels and are regarded as potential candidates for the treatment of several diseases. However promising, one of the limits that some of these peptides present, is given by their promiscuity in targeting several channels. A remarkable example is certainly given by ShK toxin from the sea anemone *Stichodactyla heliantus* that blocks Kv1.3 but shows also an inhibitory effect for the voltage-gated K^+ channels Kv1.1 (Beeton C. *et al.,* 2011) and Kv3.2, although at lower potency (Yan L. *et al.,* 2005), as well as for Kv1.2, Kv1.7 and KCa3.1 at nanomolar concentrations (Beeton C. *et al.,* 2011). If we consider the sea anemone world, which represent one the most profitable in terms

of channel-targeting peptides, also BgK from *Bundosoma granulifera* shows multiple selectivity towards Kv1 channels, as it is able to block Kv1.1, Kv1.2 and Kv1.3 (Cotton J. *et al.,* 1997). More examples can be found in Ts11 from the venom of the Brazilian scorpion *Tytus serratulus* that inhibits, although at low potency, Kv1.2, Kv1.3, Kv4.2, Kv10.1, hERG and Shaker IR (Cremonez C. *et al.,* 2016); conotoxins CPY-11 from the marine snail *Conus planorbis* and CPY-Fe11 from *Conus ferruginesus* that target, with different potency, Kv1.2 and Kv1.6 (Imperial J.S. *et al.,* 2008) and Urotoxin, obtained from the venom of the Australian scorpion *Urodacus yaschenkoi,* that potently blocks hKv1.2 but shows effect also on hKv1.1, hKv1.3 and hKca3.1 channels at lower potency (Luna-Ramírez K. *et al.,* 2014). These are only few examples of toxins that act on multiple targets. A huge effort has been made through the years aimed at limiting the "cross-selectivity" presented by the peptides. In this direction, tremendous progresses have been made in synthetizing analogues with enhanced selectivity towards a preferential target. Combinations of molecular dynamic and docking simulations, alanine scanning as well as electrophysiological recordings, have conveyed to the identification of the most important residues in these peptides for which mutations could enhance selectivity. Indeed, defining and understanding the biological activity of the peptides is pivotal and, ultimately translates in their potential introduction as drugs for the treatment of diseases. In this regard, the ultimately goal is to have peptides selective towards the channel for which alterations are at the base of the development of human pathologies, without compromising other channels normal functionality. K^+ channels are widespread in several organs and tissues, where they participate in numerous physiological processes, therefore their activity is essential for both excitable and non-excitable cells.

In chapter 3, we showed the inhibitory effect of the two novel *ShK-like* peptides, SXCL-1 and SXCL-6, towards Kv1.3 channel, expressed in tSA201 cells, in the nanomolar (nM) range. SXCL-1 exhibited a more potent effect at lower nanomolar concentrations compared to SXCL-6, following a similar fashion of the well know characterised *Stichodactyla heliantus* toxin (ShK). In this section, we concentrated our attention in investigating the biological activity of the two peptides towards other close-related K^+ channels. We considered the voltage-activated K^+ channels of the *Shaker*-family, Kv1.1, Kv1.2 and Kv1.5, and the voltage-gated potassium channel Kv2.1, a member of the *Shab*-family. We investigated their properties at a concentration of 5 nanomolar (nM) and compared their activity to what obtained for Kv1.3.

Results from the previous chapter, suggested that SXCL-1 acts more likely ShK, with an enhanced potency compared to SXCL-6, at lower concentration of 5 nM. Indeed, a similar inhibition on the channel current is reached when the concentration of SXCL-6 is doubled (10

nM). This evidence led us to a careful evaluation in terms of products source. One of the most difficult part of the toxin-based drug research, is represented by the limitations faced in obtaining a large amount of toxins from the venom of animals. Venom of animals is constituted by a cocktail of substances that have different biological properties. Isolation of a specific component in large scale, is often very challenging, especially when the component is found within the venom of small animals, for example spiders or scorpions, that overall produce a smaller amount of venom in their apparatus, compared to animals of larger size.

At present, most of the toxin-based drugs in use, and/or in clinical trials, are mostly derived from snakes (Bordon *et al.,* 2020). This is in accordance with the idea that snakes, being larger animals, produce a greater amount of venom in the specific glands, which translates into a larger amount of final product. In our specific case, the *ShK-like* peptides, are found within the HES (excretory-secretory) products of the nematode *Heligmosomoides polygyrus*, that are produced during the lifecycle of the parasite into the host. However, SXC-products are only a small fraction of the total amount of proteins that the parasite is able to yield during the different stages of the lifecycle and this certainly leads to challenges in terms of protein isolation. Therefore, when we talk about product source, we refer to all those challenges faced in obtaining a good amount of product that can be used for investigations *in vitro*, bearing in mind that *Heligmosomoides polygyrus*, is a very small sized parasite. Nevertheless, challenges are not only given by the fact that the SXC-products are only a fraction of the total amount of proteins that the peptides secrete, estimated to be approximately more than 300 in total, but also the time required to obtain the products. In laboratory setting, the lifecycle of the peptide into the host is recreated by administration of the larvae by gavage in mice. This necessitates culturing of the parasite, administration in mice models and then collection of the products, which turns into a time-consuming procedure, followed by the chemical isolation. All these factors lead to the fundamental purpose of maximise the usage of the obtained products. All those considerations, feed into the rationale of our investigations: potential new candidates for target-therapy, should act potently and at lower concentrations, when compared to potential competitors. In our case, the two peptides SXCL-1 and SXCL-6, could be considered as competitors. Following the idea that ShK is already well known for its potency against Kv1.3 over close-related channels, potency that is further enhanced by chemical modifications that led to the design of several peptide analogues, the purpose of our investigations was to determine not only the selectivity towards a preferential target (which in this case was Kv1.3), but also to determine whether the peptides showed an enhanced and/or reduced biological activity towards other channels at a concentration range where, the well-established toxin ShK

and the novel peptide SXCL-1, inhibit potently Kv1.3. Our interest was particularly strong towards SXCL-6, that showed no activity against Kv1.3 at 5 nM, but significantly inhibited the channel when concentration was increased by double (10 nM), reaching a similar effect observed for SXCL-1 at half concentration (5 nM).
What happens then, when that same concentration of the peptide is applied to other Kv channels? To address this question, we evaluated the effect of both SXCL-1 and SXCL-6, at the same concentration, on Kv1 and Kv2 members.

Data suggested that SXCL-6 (5 nM), did not produce any effect on the average peak current of Kv1.1, where the percentage of inhibition (%) was equal to 4, a similar trend to what we observed when the same concentration was applied to Kv1.3. We then tested the same concentration of the peptide on Kv1.2 and Kv1.5, obtaining similar results supportive of the idea that the peptide was not selective towards both channels. Nevertheless, intriguing results emerged from investigations conducted on Kv2.1 channel. Evidences suggested that SXCL-6 (5 nM), had an inhibitory effect on Kv2.1 channel. Indeed, the peptide was able to reduce the average peak current (pA) by 51%, an effect that, when the same concentration was tested for Kv1.3, was not seen. Data obtained for SXCL-6, however showed a reduction of the average peak current of Kv2.1 that was not statistically significant, are indicative of the fact that the peptide acts more potently towards Kv2.1 than Kv1.3 (% inhibition was equal to only 8), and shows a potent inhibitory effect that, at the same concentration of 5 nM, was not seen for Kv1.3. If we turn the prospective and we look at SXCL-6 as an inhibitor of other K^+ channels (e.g. Kv2.1) then, most likely, the peptide acts more potently in inhibiting Kv2.1 rather than Kv1.3 currents at same concentration. Few considerations could be done in this direction. Perhaps increasing the peptide concentration would determine an increase in the inhibitory effect towards Kv2.1 channel and this could mean that, at higher concentrations, the peptide could be more potent on Kv2.1 than Kv1.3. To confirm all these possibilities, further investigations are required. Our results highlighted an important pharmacological property of SXCL-6 on Kv2.1 channel that differs from the biological properties of ShK, that only slightly reduced the peak current of Kv2.1 channel (section 4.9.1). On the other hand, when we tested SXCL-1, at the same concentration of 5 nM, we observed that the peptide was also able to reduce the average peak currents of Kv2.1 channel, however at lower potency (inhibition % =33) when compared to SXCL-6. This suggests that SXCL-1 at 5 nM, inhibits the average peak current of both Kv1.3 and Kv2.1, with a reduced effect for the latter (section 4.9.1). We then tested the effect of 5 nM of SXCL-1 on Kv1.1 and we did observe a very small effect, with a % of inhibition equal

to 16, and no statistical significance. When we analysed ShK activity, we concluded that the toxin was able to reduce Kv1.1 average peak current by 20%, a percentage that is slightly higher than what was seen with SXCL-1. This brought us to outline another common feature between ShK and SXCL-1: high potency towards Kv1.3 channel yet, at lower potency, towards Kv1.1. Another shared feature between ShK and SXCL-1 is driven by the results obtained from the investigations on Kv2.1, that showed that ShK slightly reduce the peak current of Kv2.1 channel, with a similar inhibitory profile of SXCL-1. Lastly, investigations on Kv1.2 and Kv1.5 revealed that SXCL-1, similarly to SXCL-6, did not inhibit the channels current, supporting the idea that both peptides are not selective towards these channels. However, ShK at 5 nM, was able to reduce by 29% the peak current (pA) of Kv1.2, with no statistical significance.
Taken together, our evidence could open a novel route to explore in the future, with investigations on the activity of SXCL-1 and SXCL-6, that could be extended to the other member of the *Shab*-related family, Kv2.2. At the light of our evidences, we can conclude that SXCL-6, at 5 nM, was able to inhibit more potently Kv2.1 than Kv1.3. For the latter, no inhibition was recorded at 5 nM. SXCL-1 showed a significant inhibitory effect towards Kv1.3 at 5 nM yet was able to slightly reduce the peak current of Kv2.1 at the same concentration. This suggested that SXCL-1 is more potent and more selective towards Kv1.3 compared to SXCL-6 at the given concentration of 5 nM.

If we draw a line encompassing the activity of SXCL-1 and SXCL-6 towards Kv1.3, Kv1.1, Kv1.2, Kv1.5 and Kv2.1, we can see that SXCL-1 preserved its pharmacology, at a given concentration, overall on all three channels, with significant inhibitory effect towards Kv1.3 more than the others. Data for SXCL-6 suggested a different trend. In fact, at 5 nM, no effect is detected for Kv1.3, Kv1.1, Kv1.2 and Kv1.5 yet, at the same concentration, the peptide was able to inhibit the average peak current of Kv2.1. If we turn again the prospective of our speculations and we look at SXCL-6 as an inhibitor of other voltage-activated K^+ channels, then we could conclude that the peptide, could be seen as an inhibitor of Kv2.1 at low nanomolar concentration, with no cross-effect on the three other members of the Kv1 family, Kv1.1, Kv1.2, Kv1.3 and Kv1.5 included in our investigations. However, at 5 nM, we only observed a reduction of half current (with no statistical significance) and a question remains still open: what would happen if we would increase the concentration to reach a higher current inhibition? If we increase the concentration, then we might see an effect as well on Kv1.1 and, as demonstrated, a significantly potent effect on Kv1.3. However, from our investigations we can clearly see that SXCL-6, at low nanomolar concentration, showed pharmacological activity

on Kv2.1 and no inhibitory effect on Kv1 family channels. Our data suggest that both peptides are able to inhibit Kv2.1 current and this effect is stronger for SXCL-6 than SXCL-1. Conclusion is, if we turn our prospective and we look at SXCL-6 under a different light and we move our attention from Kv1.3, the peptide is able to determine, overall, an effect on Kv2.1 with low *cross-selectivity* with other Kv1 channels. What if we look at SXCL-1 as an inhibitor of Kv2 channels? In this case, inhibition is less than fifty percent, with *cross-selectivity* highly enhanced for Kv1.3 channel, which puts SXCL-1 in the position to be more potent towards the latter.

Our investigations are limited to Kv1.1, Kv1.2, Kv1.5 and Kv2.1 only and the reasons are mainly related to the conspicuous amount of the time that electrophysiological investigations require, together with the limitations in terms of products. Overall, our results highlighted striking pharmacological properties of the peptides on Kv1.1 and Kv2.1, that must be carefully considered. As mentioned above, *cross-selectivity* is one of the barriers that very often arises between the *in vitro* and *in vivo* studies, considering also that interactions toxin-target often could show incongruity when translated *in vivo* (Zhang Y., 2015). One of the major concerns, regard the ability of the peptides to act on Kv2.1 and, slightly for SXCL-1, on Kv1.1.
Kv1.1 channel covers a key role in the brain, where is expressed in neurons and regulate neuronal excitability and also in the heart, where is involved in the modulation of the repolarization of the AP. The channel is also known to form heterotetramers by assembling with other Kv1 subunits, and in particular with Kv1.2. Inhibition of Kv1.1 and/or Kv1.2 is associated with neurotoxicity in the brain (Coleman S.K. *et al.,* 1999; Wulff H. *et al.,* 2009) and can lead to cardiotoxicity as well. Kv2.1 is pivotal in the hippocampal and cortex neurons, where is involved in the modulation of neuronal excitability and alterations in the channel are linked to neurological disorders. It is evident that avoiding the targeting of those channels is fundamental to protect neuronal and cardiac functionality. The barrier of the *cross-selectivity* could be overcome by designing specific analogues that reach high selectivity towards a preferential target (in this case Kv1.3), by carrying chemical modifications within the sequence. These modifications can be induced as site modifications, in respect to specific residues within the sequence; as terminal -N or -C extensions or often, as a combination of both. These strategies represent a very promising route to reach the selectivity goal. Several analogues of the toxin ShK have been created, showing excellent property in terms of selectivity and potency. The first ever analogue created for ShK, Shk-Dap^{22}, carries a modification of the critical lysine at position 22 with the non-natural residue 1,3-

diaminopropionic acid (Dap^{22}) and shows lower affinity for Kv1.1, Kv1.2 and Kv1.4 and no effect on Kv1.5, Kv1.7, Kv3.1, Kv3.4 or KCa3.1 (Kalman K. *et al.,*1998). Another analogue, ShK-186 (known also as SL5), with a *L*-phosphor-tyrosine (*L-p*Tyr) attached to ShK-Arg^1 via hydrophilic linker (Beeton C. *et al.,* 2005), is currently on clinical trials for the treatment of a wide range of autoimmune diseases and is showing promising results (Tarcha E.J. *et al.,* 2017). The relevance that chemical modifications assume in terms of selectivity have been shown not only for ShK, but also for other toxins (e.g. scorpion toxins) with successful results (Rashid M. *et al.,* 2014). This process requires the combination of several techniques and a long-designing time, that ultimately lead to the validation of the results via electrophysiological experiments.
In the previous chapter, we have uncovered the residues at the pore region and selectivity filter of Kv1.3 channel, that appear to be critically involved in the interaction channel-peptides and we demonstrated that mutations occurring at those sites, strongly reduced the toxin-channel affinity. Our results are indicative of a pore blocking mechanism of action, suggesting the classification of SXCL-1 and SXCL-6 as pore blocker peptides, similar to ShK. However important to achieve an overall understanding of the mechanism of action, as stressed in the previous section, further investigations are required to attain a complete picture of residues, not only in the channel, but also in the peptide's sequences, that are involved in the binding. Indeed, little is known about the residues of the peptides that interact with those and, perhaps, other residues of the channel. Our initial assumption, started with the consideration that the peptides share the *ShK-like* domain, a common feature between toxins that act on Kv1.3 and/or are potential candidates, obtained from a wide range of species, including worms. The latter are known to secrete the largest family of ShKTs proteins (Chhabra S. *et al.,* 2014). To assess the similarity between our peptides and other ShK-domain proteins already deposited in Uniprot database, sequences were aligned using Blast (UniProt). Alignment of SXCL-1 (Figure 75, A) and SXCL-6 (Figure 75, B) are showed below. Regions with high similarity are indicated in grey and marked with asterisks (*). Sequences to include in the alignment were chose based on two main criteria: score and sequence identity. SXCL-1 sequence (Figure 75, A) was aligned with other three ShKT-containing protein sequences, obtained from phylogenetically linked nematode worms *Ancylostoma canium*, *Haemonchus placei* and *Teladorsagia circumcinta*. All those proteins share the ShK-domain at variable positions in their sequences. As showed by the grey colour, regions similarities cover the ShK-domain in all sequences, including SXCL-1. Sequence length is variable. To note that the ShK-like immunomodulatory peptide from the hookworm *Ancylostoma canium,* AcK1, has been evaluated for its immunomodulatory properties and the solution structure have been revealed

and is available on PDB (entry code: 2MD0) (Chhabra S. *et al.,* 2014). SXCL-6 sequence (Figure 75, B), was aligned with the sequences of ShKT-containing proteins obtained from *Nippostrongylus brasiliensis*, a gastrointestinal roundworm belonging to the phylum nematode, containing ShK-domain at variable positions. Conserved regions are highlighted in grey and include the ShK-domain. The length of the proteins is variable. As we can observe from this analysis, phylogenetically related species, in this specific case worm parasites from *phylum* nematoda, are able to secrete products that share a common feature, the ShK-domain, which in turn, is conserved among other species phylogenetically unrelated, indicative of a communal ancestral evolutionary pathway.

Together with the ShK-domain, another feature that appears recurrent from the alignment is the preservation of the triad K-T-C in all six sequences. In SXCL-1 this correspond to K37, T38 and C39; whereas in SXCL-6 to K40, T41 and C42. Several peptides extensively studied for their mechanism of action, including ShK, are known to determine their activity by binding to the target using conserved residues, that corresponded to the well know "functional dyad", constituted by K-T at variable positions within the amino acidic sequences. In the sequence of our peptides, is possible to point out the presence of several lysines, with SXCL-6 sequence enriched with 8 lysine residues and SXCL-1 with 5. However, the combination K-T, alternatively known as functional dyad, is visible only at the positions mentioned above. The peptides could use or could not use that specific combination of residues to bind to the channel.

A

```
B20210505216DA2B77BFBD2E6..   1   --------------------------------TCRDNVNRGICAMHKANGRCKQDYSDWM   28
A0A368EW09 A0A368EW09_ANCCA   1   MLLQV--------LCVFLLLNAF-TQDVAMAQGCRDRIPVNVCQQCKEKGNCKNQYTVE-   50
A0A0N4WSQ2 A0A0N4WSQ2_HAEPC   1   MQLPRLITHKNRFVSGWPINSVFHLVILIFFQRCMDEFPVERCLLHKKVGDCKYT-ETWQ   59
A0A2G9U4G2 A0A2G9U4G2_TELCI   1   --------MFFHLLCAMLIINAFARD-DVPLEECKDRGNERYCNSHKASGRCESE--NYK   49
                                                              * *.     *  :*  * *:

B20210505216DA2B77BFBD2E6..  29   FIMKNQCAKTCGFC-----------------------------------------------   42
A0A368EW09 A0A368EW09_ANCCA  51   -MMKMQCPKTCGFCQ----------------------------------------------   64
A0A0N4WSQ2 A0A0N4WSQ2_HAEPC  60   YLMKIKCAKTCGFCIILRKELPPNPLRSPTRAPPPRAPPRALPQTPPRTPPPSPSPTPSR   119
A0A2G9U4G2 A0A2G9U4G2_TELCI  50   FIMKTNCRKTCNLCDQ---------------------------------------------   65
                                   :** :* ***.:*

B20210505216DA2B77BFBD2E6..  43   --------------------   42
A0A368EW09 A0A368EW09_ANCCA  65   --------------------   64
A0A0N4WSQ2 A0A0N4WSQ2_HAEPC 120   SLPQNRSGSSLVIRNKNGTV   139
A0A2G9U4G2 A0A2G9U4G2_TELCI  66   --------------------   65
```

B

```
B20210505DA437993067D6F64..  1   -----------------AYDVCKDRAQPSVCQRHKEKGRCDGEDKDWKYIMKLNCKKTC   42
A0A158QXS4 A0A158QXS4_NIPBR  1   --MLAVLFCILLISSMAISDEPCKDRSPTAMCLRHKSVGRCTGDNGDWTSLMKMNCRKTC   58
A0A0N4YVN9 A0A0N4YVN9_NIPBR  1   --MLAVLFCILLISSMAISDEPCKDRSPTAMCLRHKNAGHCTSDDGDWVSIMKVNCRKTC   58
A0A0N4Y9F4 A0A0N4Y9F4_NIPBR  1   MKLLYVF-FFVALVMGAFAADVCKDRASQVRCDKNKAAGWCDGDQ-DRQAIMRQMCRKTC   58
                                 : : ****:    * ::*  * * .:: *   :*:  *:***

B20210505DA437993067D6F64.. 43   GFCTAY   48
A0A158QXS4 A0A158QXS4_NIPBR 59   EFCK--   62
A0A0N4YVN9 A0A0N4YVN9_NIPBR 59   EFCK--   62
A0A0N4Y9F4 A0A0N4Y9F4_NIPBR 59   GFC---   61
                              **
```

Figure 75. *ShK-like* peptides sequence alignment. A) SXCL-1 (code: B20210505216DA2B77BFD2E6) aligned with other three ShKT-domain proteins (entry code: ANCCA; HAEPC; TELCI) from parasites. **B)** SXCL-6 (code: B20210505DA437993067D6F64) aligned with other ShKT-domain proteins (NIPBR). Asterisks (*) are representative of region of similarity.

Referring back to the discourse relative to the design of analogues to enhance selectivity, knowledges about the structure and the residues that are involved in the binding are pivotal to serve this purpose. At the moment, we can only point out some strategies that might be helpful in guiding the analogues design process. For this, using a combination of scanning mutagenesis and electrophysiology, would be helpful to evaluate the strength of intermolecular pairwise interactions (e.g. protein-ligand complexes), aimed to identify and subsequently test the identified mutations *in vitro*. Several researches pointed out the use of thermodynamic mutant cycle analysis (Horovitz A., 1996) as an excellent technique to measure the strength of the interaction of protein residues, and its applications has been widely used for elucidating the interaction sites between channel-peptides (Ranganathan R. *et al.,* 1996; Hidalgo P. and MacKinnon R., 1995; Chang S.C. *et al.,* 2015). Computer docking together with MD simulations, are validated techniques that help to uncover several aspects around the relationship channel-inhibitors. All these valuations leave open the possibility for new future directions, that implicate the combinations of a wide array of techniques and a conspicuous amount of time in terms of research. Nevertheless, it is extremely important to stress that not always the production of derivates is successful. In some case, alteration of the structure of the peptide can lead to a reduction, more than an enhancement, in the selectivity towards a target, and/or to a reduction of the potency (Beeton C. *et al.,* 2005). Some modifications might render the peptide more susceptible to dephosphorylation, degradations, oxidation and hydrolysis and might affect the stability of the peptide at physiological value of pH (Beeton C. *et al.,* 2005; Beeton C. *et al.,* 2011). Another aspect that in our opinion is dutiful to raise, regards the eventual usage of the peptide derivates in *in vivo* studies. In the previous section, we evaluated some factors that need to be considered when proposing the usage of proteins and peptides as drugs for the treatment of diseases; these factors include safety in the administration, plasma level of the peptides, bioavailability and toxicity. Of course, we are not at that stage in our investigations, but it is important to add some considerations when talking about this eventuality. At present, we report that ShK analogues, have been successfully safely administrated both intraperitoneally (i.p.) and subcutaneously (s.c.), with very low toxicity (Beeton C. *et al.,* 2011). However, we also reported strong considerations relative to cross effect with helminths that might cause side effects when living peptides are administrated. Lastly, we would like to add some considerations regarding the pharmacological susceptibility of hERG channels to the two novel *ShK-like* peptides, SXCL-1 and SXCL-6. The blockade of hERG channels by several drugs as non-preferential target, is one of the major concerns for the production of drugs with a safe profile (Kalyaanamoorthy S. and Barakat K. H., 2018).

Therefore, is fundamental that novel candidate drugs are tested for their eventual effect on these channels. hERG channels, members of the *ether-à-go-go* family of voltage-gated K^+ channels, are fundamental in the heart, where they mediate the repolarization phase of cardiac action potential (AP) thus controlling the AP duration (APD) and QT interval (Sanguinetti M.C. and Tristani-Firouzi M., 2006). Loss-of-function (LOF) mutations in hERG channels result in prolonged repolarization of cardiac AP (Spector P.S. *et al.,* 1996), prolongation of the QT interval and therefore Long-QT Syndrome (LQTS) (Splawski, I. *et al.,* 2000; Paulussen, A. *et al.,* 2000; Laitinen, P. *et al.,* 2000), which predispose to cardiac arrhythmias (Curran M.E. *et al.,* 1995; Butler A. *et al.,* 2020). Furthermore, *Brugada and colleagues* showed that mutations in hERG channels, are also linked to an early repolarization of the AP, determining a short QT interval (Short-QT Syndrome- SQTS) (Brugada R. *et al.,* 2004; Campuzzano O. *et al.,* 2019; Hancox, J.C. *et al.,* 2019). In addition, hERG channels are blocked by several drugs that increase the risk of drug induced LQTS, with particular attention to the life-threatening *torsades de pointes* (TdP) (Hancox J.C. *et al.,* 2008; He F. Z. *et al.,* 2013). Torsades de pointes is a polymorphic ventricular arrythmia that can lead to ventricular fibrillation and death (Tamargo J., 2000). TdP represent a very concerning condition, as it can develop in patients that have already a predisposition, for example hypokalemia (Sanguinetti M.C. *et al.,* 1995), as well as in patients with no other medical conditions (Vandenberg J.I. *et al.,* 2001). hERG channels are also the target of animal toxins, mostly derived from scorpions of the genus *Centruroides* (Corona M. *et al.,* 2002). An example is given by Ergtoxin (ErgTX), a 42 aminoacidic residues peptides with 4 disulfide bridges isolated from the scorpion *Centruroides noxius* (Gurrola G.B. *et al.,* 1999; Scaloni A. *et al.,* 2000). ErgTX act on the channel with a pharmacological profile in the low nanomolar range (nM) and does not shown any effect on other K^+ channels such as Kv1.4, Kv4.2, Kv2.1 or KvLQT1 (Scaloni A. *et al.,* 2000). The binding site of ErgTX was described by *Pardo-Lopez and colleagues* and involves the outer vestibule of the channel, in particular residues located at the long S5-P linker and P-S6 linker (Pardo-Lopez L. *et al.,* 2002). Furthermore, hERG are also the target of a sea anemone toxin, APETx1, from *Anthopleura elegantissima* (Diochot S. *et al.,* 2003) that acts as a gating modifier toxin (Zhang M. *et al.,* 2007). For all those aspects, screening drugs for their potential effect in blocking hERG channel is a crucial parameter for pre-clinical studies. Several *in vitro* approaches have been proposed, including both electrophysiological and non-electrophysiological techniques (Hancox J.C. *et al.,* 2008; Vandenberg I. *et al.,* 2012). The latter includes mostly assays such as competitive binding assays with radioactively labelled blockers (Finlayson K. *et al.,* 2001), non-radioactive cell-based (Rb^+) efflux assay (Terstappen

G.C., 1999), fluorescence-based assays (Dorn A. *et al.,* 2005) and the novel antibody-based chemiluminescent assay HERG-Lite (Wible, B. A. *et al.,* 2005). Nevertheless, all those methodologies are characterised by several limitations thus rendering the electrophysiological approaches the most accurate for hERG screening (Hancox, J. C. *et al.,* 2008). In prospective, we report that such experiments aimed at evaluating an eventual secondary effect of both SXCL-1 and SXCL-6 on hERG channels would be beneficial to avoid any possible undesired cardiac side effect.

Overall, our results are indicative of a potential good chance of application of these peptides for further investigations. Revealing the residues that are responsible of the cross selectivity observed for other Kvs channels, is pivotal to convey the attentions towards a focus: deliver peptides that show potency at low concentration and for which activity can be enhanced by modifications. An absolutely striking result from our investigations was found in SXCL-6, that revealed a potent effect on Kv2.1. Application of 5 nM were enough to reach half current inhibition, with no effect on Kv1 channels. This is an interesting evidence that might move the focus from Kv1.3 to Kv2.1 for SXCL-6. In this direction, further investigations will be required to evaluate the effect of higher concentrations of the peptide and evaluate cross-selectivity with Kv1.3 that, at 10 nM, is significantly inhibited by the peptide.

4.11 Conclusions and Remarks

Our evidences support the idea that SXCL-1 and SXCL-6 are potent Kv1.3 inhibitors, however with a slightly different pharmacology trend. SXCL-1 showed a minor side activity on Kv1.1 and a slightly higher activity on Kv2.1 channel. SXCL-6, at the same concentration, was able to block Kv2.1 but did not have any effect on Kv1 channels. Certainly, more investigations are needed to elucidate the exact mechanism of action of the two peptides and therefore to reach a more complete understanding of how to enhance peptide's selectivity. Overall, our results are promising and indicative of natural resources for peptides that target ion channel.

Chapter 5: Functional characterisation of a *de novo* variant in KCNB1 gene using Guangxitoxin-1E

5.1 Introduction

In this chapter we investigated the electrophysiological implications of *a de novo* variant in KCNB1 gene (p.P17T; c 49 c>A; homozygous) found in a young patient by a group of clinicians in USA. Our work was aimed at characterising the electrophysiological implications of the mutation of the amino acid proline (P) to a threonine (T) at position 17, on the activity of the voltage-gated potassium channel Kv2.1, member 2 of the *Shab*-related family (Figure 76). The patient, that is turning five years old later this year, presents a clinical phenotype characterized by a severe speech delay, possible dysarthria or dyspraxia. At the moment, the patient is treated with occupational therapy (OT), physical therapy (PT) and speech therapy.

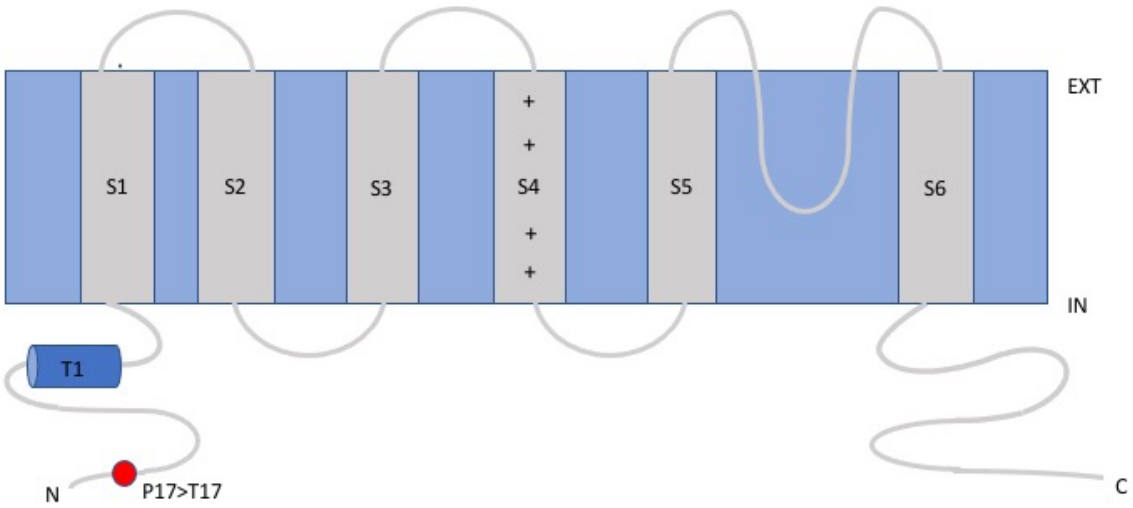

Figure 76. Transmembrane topology of Kv2.1 α-subunits. The channel is formed by four alpha subunits, each constitute by six transmembrane segments (S1-S6). Both N and C terminal are intracellular. In the picture, the site of the mutation of the amino acid proline (P) to a threonine (T) is represented by the red dot. Also, at the N terminus, the T1 domain is represented.

Loss-of-function (LOF) and missense mutations in KCNB1 gene encoding Kv2.1 have been associated with the development of epileptic encephalopathy (EE) (Torkamani A *et al.,* 2014). The majority of those mutations have been found within the ion channel domains, comprising the pore region (in particular missense mutations) and the voltage sensor domain (Torkamani

A. *et al.,* 2014; Srivastava *et al.,* 2014). Few mutations, occurring at the N- and C-terminal of the channel, have also been described in a lower number of patients (de Kovel C. *et al.,* 2017). Together with the localisation, several researches have focused their attention in analysing the effect of those mutations on the channel functions. In general, LOF mutations in potassium channels determine a reduction of the channel activity by either reducing the channel surface expression or their open probability; or by shifting the voltage-dependence of inactivation and activation (Nida Z. and Tzingounis A. V., 2018). Kv2.1 play a pivotal role in the regulation neuronal excitability by modulating the repolarization phase of the action potential (Liu P. W and Bea B. P., 2014) and by contributing to the regulation of neuronal activity, therefore defects occurring at gene level, can lead to severe neurological problems and the development of epileptic encephalopathies. For example, an interesting study published in 2015, described a *de novo* V378A variant, found in a young girl with infantile EE (Thiffault I. *et al.,* 2015), occurring at the pore region of Kv2.1, that caused a significant reduction of the selectivity of the channel for potassium ions (Thiffault I. *et al.,* 2015). The reduction of ion selectivity induces a reduction of Potassium (K^+) and gaining of Sodium (Na^+) ions. By gaining sodium the neuronal excitability would increase, as neurons would depolarise more rapidly. The study highlighted the important correlation between mutations that reduce the ion selectivity of the channel and the development of epileptic encephalopathies (Thiffault I. *et al.,* 2015). Earlier, an interesting paper published by *Torkamani* and colleagues, defined this correlation with a study on a wider number of patients with EE and mutations in KCNB1 gene (Torkamani A. *et al.,* 2014). It is important to point out that there is also a solid correlation between mutations and clinical phenotype. Indeed, LOF mutations seems to be linked to a less severe clinical phenotype, whereas missense mutations seem to have more severe clinical implications (de Kovel C. *et al.,* 2017). However, mutations in KCNB1 gene are characterised by a certain degree of heterogeneity; as such, same mutations can lead to more severe or weaker clinical manifestation in different patients (de Kovel C. *et al.,* 2017).

In our research case, we observed a partial loss-of-function mutation for Kv2.1. It can be referred as *"partial"* because the current is reduced by 30% compared to the WT (< 50%). The patient presents neurodevelopmental delay and is treated with OT, PT and speech therapy. The EKG is normal, and no seizures have been recorded so far. The location of the mutation at the N-terminal and the type of effect that has on the channel current (partial reduction the current) might be accountable for the milder phenotype that patient shows. In order to characterise the electrophysiological implications of the *de novo* KCNB1 mutations, we used a well-known Kv2.1 inhibitor, Guangxitoxin-1E.

Kv2 channels properties have been extensively studied by using toxins, mostly derived from spiders. Spider toxins are gating modifiers, as the mechanism of action and the consequently effect on the channel, are dictated by their ability to modify the channel kinetics by binding to the voltage sensor domains (VSDs) (Swartz K.J., 2007).This mechanism differs from the one observed in the pore blocking toxins that, conversely, act by binding to residues at the pore region of the channel (Miller C.,1995). The gating modifier toxins are regarded not only for their ability to target K^+ channels, but also for their potency on other voltage-gated channels (Catteral W.A. *et al.,* 2007), such as Ca^{2+} (McDonough S. I., 2007) and Na^+ channels (Gilchrist J. *et al.,* 2014). Furthermore, they are considered valid tools to evaluate the channel characteristics, both in wild-type and mutated system, other than for their pharmacological properties (Kalia J. *et al.,* 2015). Several studies have conveyed to the identification of the binding site of those peptides, that lays in correspondence of aminoacidic residues at the S3-S4 segments that constitute the voltage sensor domain (Swartz K.J. and MacKinnon R.., 1997 b; Winterfield J.R. and Swartz K.J., 2000; Bosmans F. *et al.,* 2008). The first toxin ever described for its effect on Kv2 channels is Hanatoxin (HnTx), from the Chilenean tarantula *G. spatulata*. The peptide shows high affinity for Kv2.1 and Kv2.2 channels yet is also able to inhibits Kv4 channels (Swartz K.J. and Mackinnon R., 1995). Another example is Guangxitoxin-1E (GxTx), isolated from the *Plesiophrictus guangxiensis,* that acts as a potent inhibitor of Kv2.1 channel more than Kv2.2 and Kv4 channels and does not have any effect on other channels. At present, GxTx-1E is considered, almost certainly, the most selective towards Kv2 channels (Tilley D.C. *et al.,* 2019). The two peptides, HnTx and GxTx-1E share some similarities in the mechanism of action, but present also some differences in the way they affect the gating of the Kv channels. Similarities can be found in the evidence that the two peptides share the same binding site on the voltage sensor and that the binding to the four subunits occurs independently (Tilley D.C. *et al.,* 2019). The plateau of efficiency is reached when the toxins are binding to all four a-subunits (Tilley D.C. *et al.,* 2019). Ultimately, the way they affect the gating is different. Hanatoxin act by stabilizing the voltage sensors in a state in between resting and full active conformation, whilst Guangxitoxin-1E stabilizes the voltage sensors in a fully resting conformation, so that the K^+ current inhibition results from a limitation in the chances of the channel pore to open, more than a complete impairment of the pore to open (Tilley D.C. *et al.,* 2019). This is in opposition with the effect seen in Hanatoxin that modifies the kinetic of the channel pore opening (Milescu M. *et al.,* 2013).

Considering the pivotal role of Kv2.1 in modulate neuronal excitability and its involvement in a wide *spectrum* of neurological disorders that found their foundations in altered neuronal activity, it is vital to characterise mutations occurring across the protein sequence that can lead to an impairment of the physiological activity of the channel.

5.2 Aims and Objectives

Here, we present a *de novo* mutation in KCNB1 gene that causes a light reduction of the channel currents, found in a patient with neurological impairments and we report the electrophysiological implications of the mutation P17T on the activity of the voltage-gated potassium channel, Kv2.1

The *de novo* variant was characterised by using whole-cell patch clamp on tSA201 cells transiently transfected with hKv2.1 DNA. Guangxitoxin-1E (GxTx), known as a potent blocker of Kv2 channels, was used to investigate the implications of the mutation on the channel properties.

5.3 Investigating the *De novo* variant in KCNB1 gene (p.P17T; c 49 c>A) found in a patient with neurological disorders.

Kv2.1_WT was expressed in tSA201 cells, transiently transfected with hKv2.1 DNA. Electrophysiological characterization was obtained using whole-cell patch clamp technique and channel currents were evoked using a "+ 50 mV to -90 mV" protocol (Figure 77, C) as described above (see Material and Methods section). Currents were analysed at +50 mV and expressed as average peak current (pA). Current-voltage (I-V) relationship was fitted by calculating the average peak current (pA) of the channel at every value of voltage, from +50 mV to -90 mV (Figure 77, B). The average peak current at +50 mV showed by Kv2.1_WT was 10406 pA (95% CI 6367: 14445 n=6) (Figure 77, A). The current-voltage (I-V) relationship (Figure 77, B) showed a non-linear progression. Calculated reversal potential for Kv2.1_WT was equal to -67.10 mV (95% CI -70.76: -63.43 n=6) (Figure 77, B).

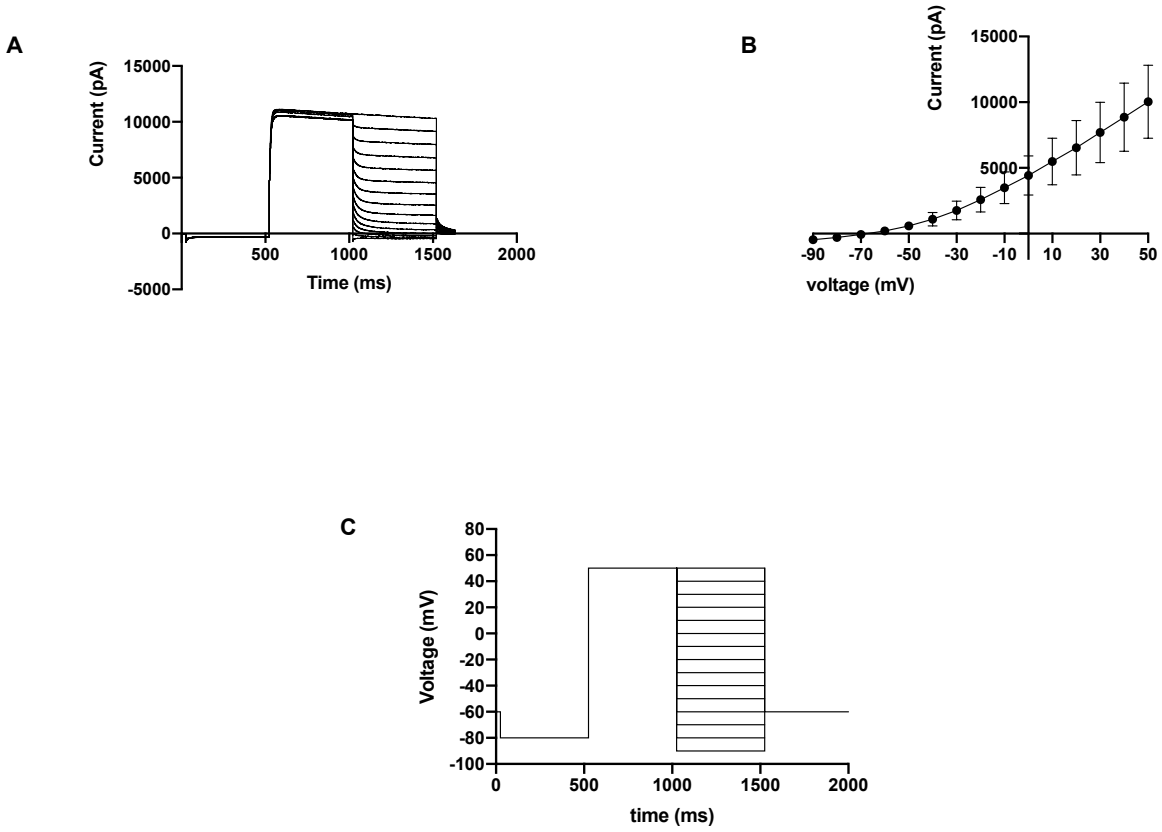

Figure 77. Layout panel representative of Kv2.1_WT. A) Kv2.1_WT in control conditions at voltages from +50 mV to -90 mV **B)** Current-voltage (I-V) relationship **C)** Example of protocol used for the electrophysiological investigations.

5.3.1 Electrophysiological characterization of Kv2.1_WT using Guangxitoxin-1E (GxTx-1E)

As might be expected, the ShK and *ShK-like* peptides were found to be less potent on the Kv2.1 channel, with SXCL-6 toxin exerting a more potent effect on the channel. For a comparison, we decided to test a known Kv2 channel inhibitor, Guangxitoxin-1E (GxTx-1E), from the tarantula *Plesiophrictus guangxiensis,* with reported IC_{50} values between 1 nM and 3 nM. As for the previous experiments the channel was incubated with the toxin over a range of concentrations (1 nM, 10 nM and 100 nM) using the same protocol of incubation for 20 minutes prior to experimentation. We found using our experimental systems that the most potent effect of the toxin was observed at 10 nM and 100 nM, which correlates with other evidences found in literature (Navarro A. *et al.,* 2019).

Incubation of Kv2.1 channels in 10 nM and 100 nM GxTx-1E resulted in average currents measured at +50 mV of 5142 pA (95% CI: 3504 to 6780, n = 7) (Figure 80, A and B) and 5551 pA (95% CI: 4294 to 6809, n = 6) (Figure 81, A and B) respectively, which were significantly different ($P < 0.05$, using a one-way ANOVA, followed by a Dunnett's multiple comparisons test) from WT controls of 10406 pA (95% CI: 6367 to 14445, n = 6, see Figure 77). Calculated reversal potential for Kv2.1 in 10 nM and 100 nM of GxTx-1E was equal to -61.97 mV (95% CI -64.96: -58.99 n=7) (Figure 80, B) and -66.62 mV (95% CI -72.76: -60.48 n=6) (Figure 81, B), respectively.

The significant inhibitory effect seen in Kv2.1_WT when incubated with 10 nM of GxTx-1E, was equal to a 50% reduction in current. Whilst for 1 nM GxTx-1E, only a small reduction in current was observed at +50 mV (8457 pA (95% CI: 5850 to 11245, n = 6) (Figure 79, A and B) which was not found to be significantly different from WT controls ($P > 0.05$, using one-way ANOVA, followed by a Dunnett's multiple comparisons test). Calculated reversal potential for Kv2.1 in 1 nM of GxTx-1E was equal to -68.02 (95% CI -74.38: -61.66 n=6) (Figure 79, B).

Showed below a current graphic that summarises the results of our findings (Figure 78).

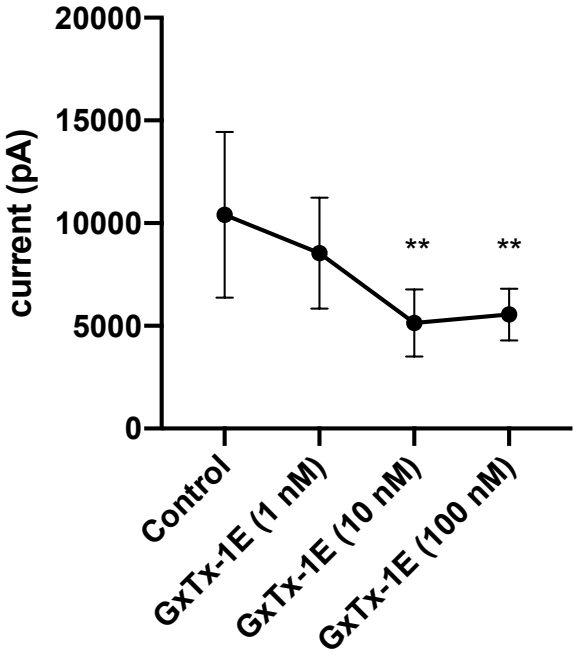

Figure 78. Peak current (pA) graph of Kv2.1_WT in control conditions and in presence of Guangxitoxin-1E (1 nM, 10 nM and 100 nM). Bars are representative of 95% CI of the mean. GxTx-1E at 10 nM and 100 nM significantly inhibits Kv2.1 average peak current (adjusted p values: p=0.021 and p=0.0026, respectively).

Demonstrated below in figure 79, 80 and 81 are representative traces of Kv2.1 and retrospective current-voltage plots for each toxin concentration in control conditions (black line) and in the presence of either 1 nM, 10 nM or 100 nM GxTx-1E toxin (red line).

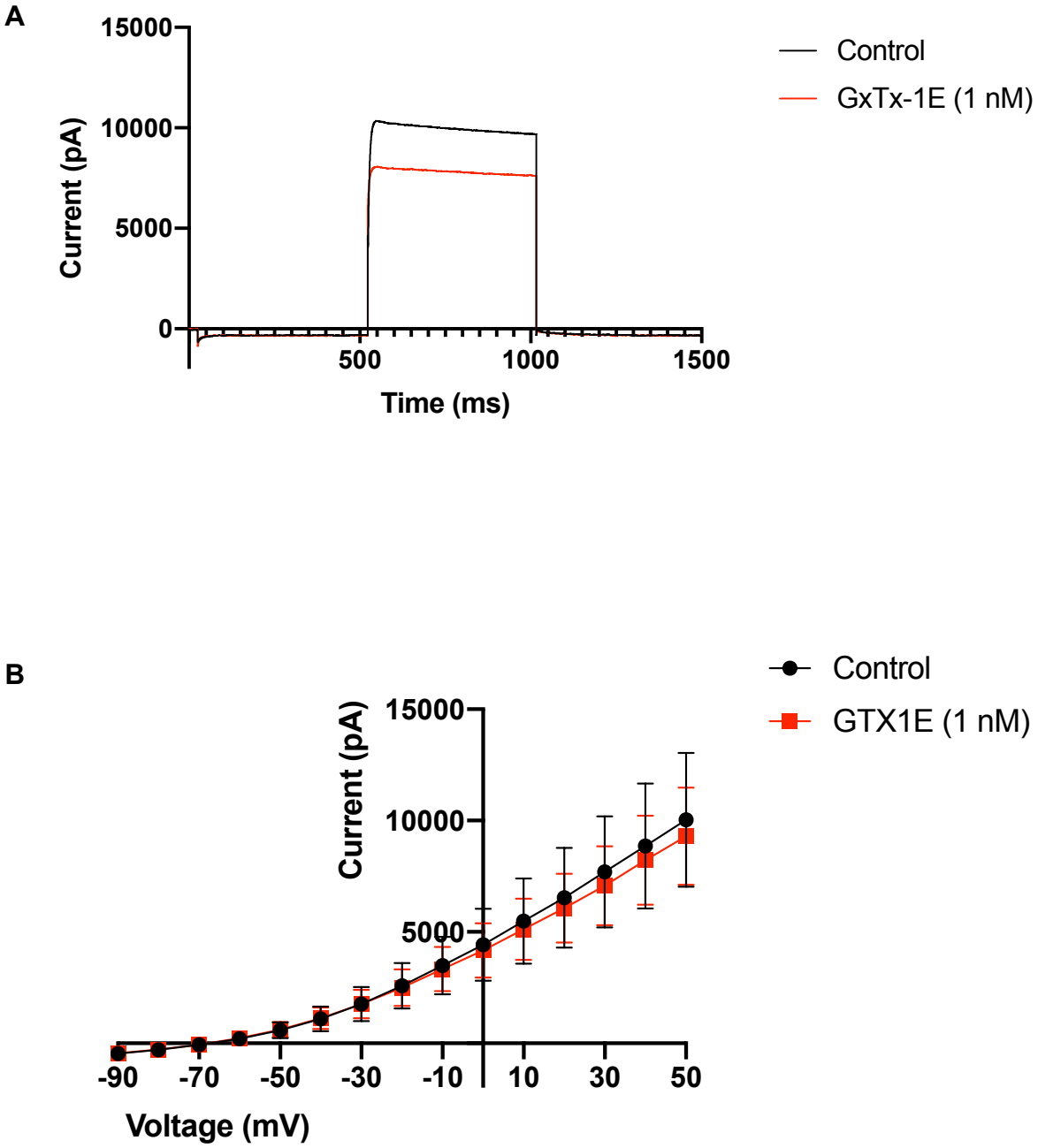

Figure 79. Kv2.1_WT in control and with 1 nM of GxTx-1E. A) Representative trace of Kv2.1 in control (in black) and Kv2.1 after incubation with GxTx-1E (red). Average peak current (pA) is calculated and represented at +50 mV. **B)** Current-voltage (I-V) relationship. Kv2.1_WT curve is showed by the black circles; red squares are representative of Kv2.1_WT with GxTx-1E (1 nM) curve.

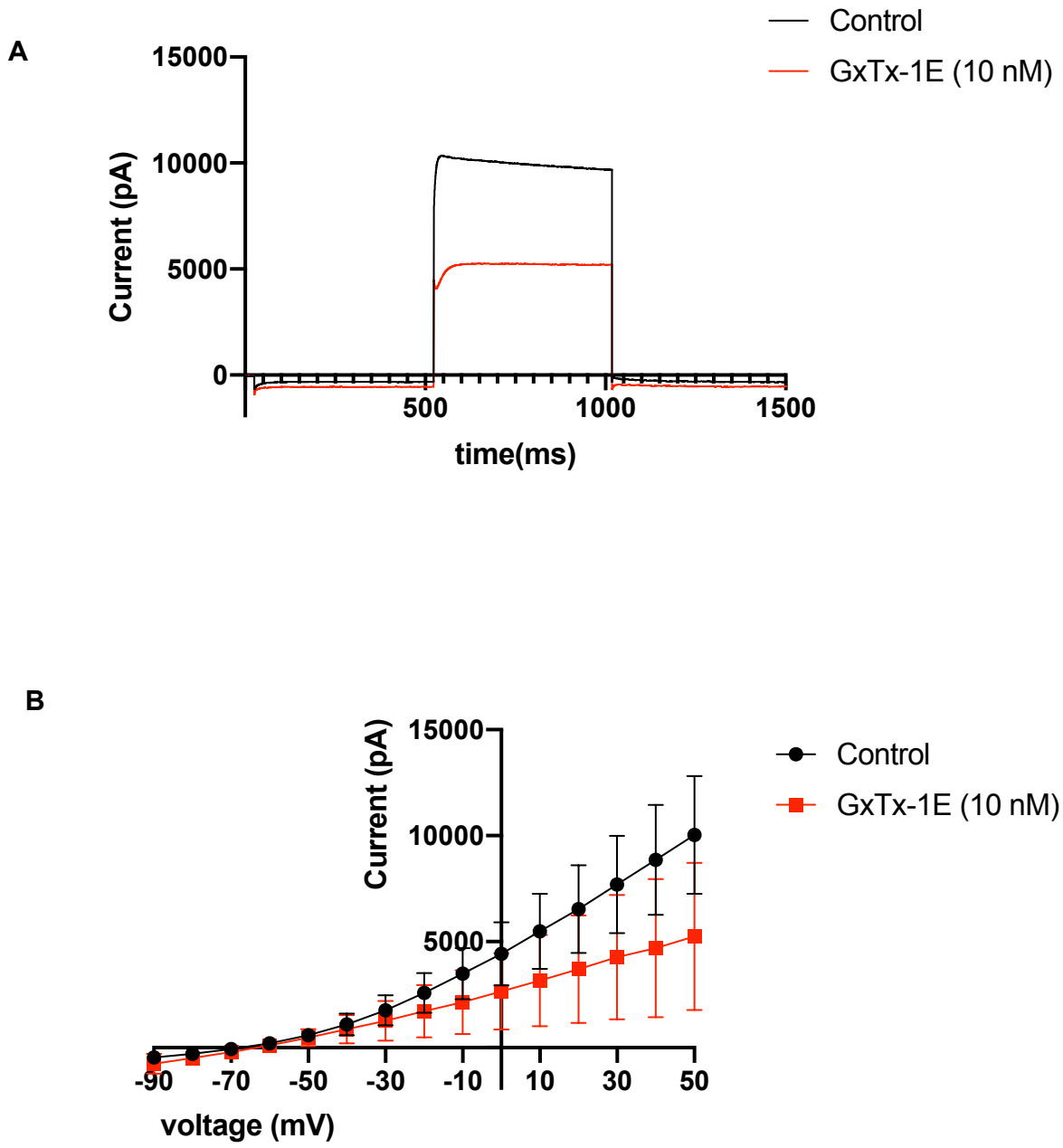

Figure 80. Kv2.1_WT in control conditions and with 10 nM of GxTx-1E. A) Representative trace of Kv2.1 in control conditions (in black) and Kv2.1 after incubation with GxTx-1E (red). Average peak current (pA) is calculated and represented at +50 mV. **B)** Current-voltage (I-V) relationship. Kv2.1_WT curve is represented by circles filled in black; red squares are representative of Kv2.1_WT with GxTx-1E (10 nM).

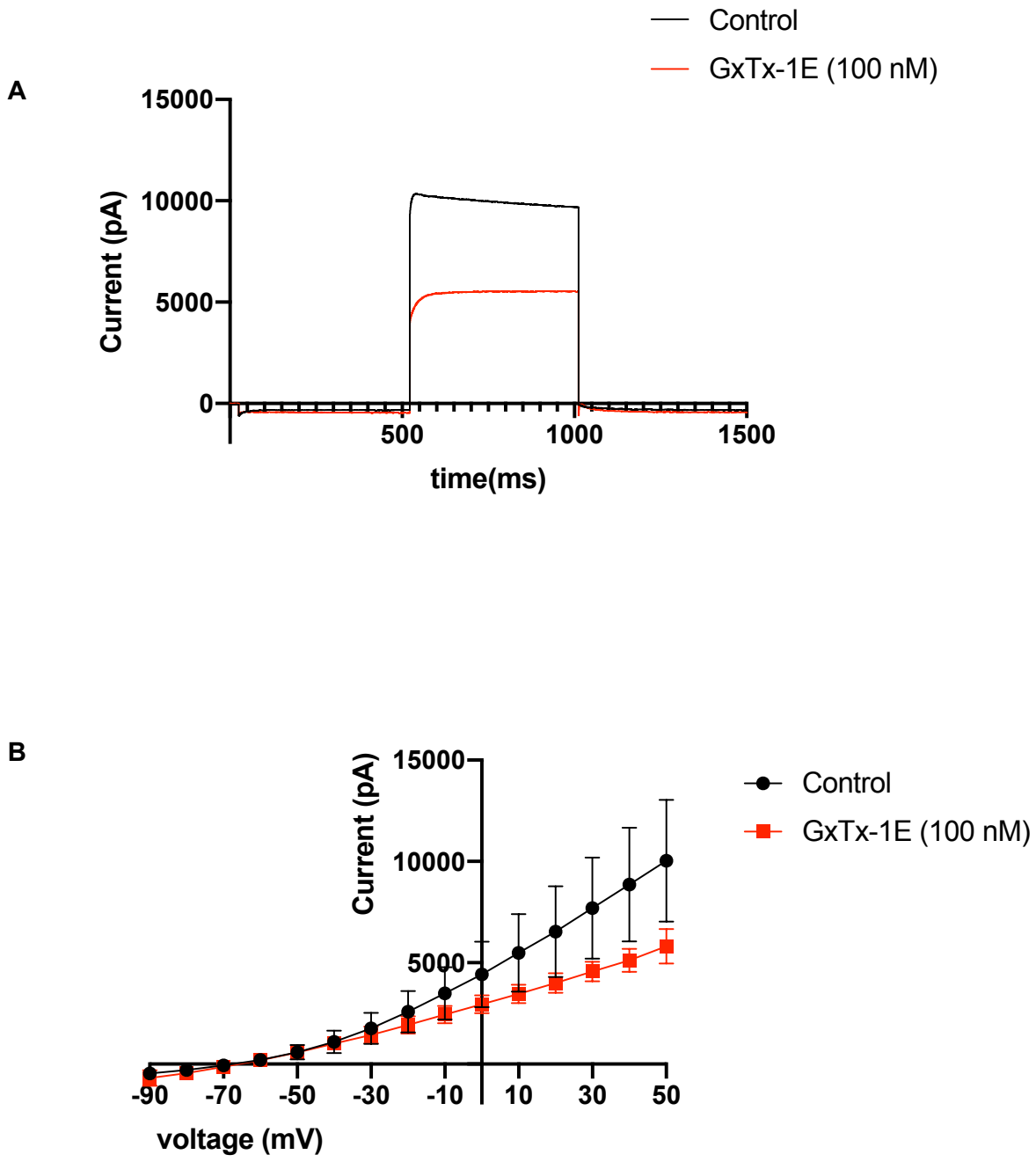

Figure 81. Kv2.1_WT in control conditions and with 100 nM of GxTx-1E. A) Representative trace of Kv2.1 in control (in black) and Kv2.1 after incubation with GxTx-1E (red). Average peak current (pA) is calculated and represented at +50 mV. **B)** Current-voltage (I-V) relationship. Black circles are representative of Kv2.1_WT curve red squares are representative of Kv2.1_WT with GxTx-1E (100 nM).

5.3.2 Electrophysiological characterization of the novel Kv2.1_P17T variant

Mutant Kv2.1 with the aminoacidic substitution P17T was obtained as previously described in material and methods section (Chapter 2, section 2.8.2). hKv2.1_P17T DNA was transiently transfected in tSA201 cells and electrophysiological characterization was conducted using a "+50 mV to -90 mV" protocol as described above for Kv2.1_WT. Currents are expressed as peak current (pA) measured at + 50 mV. Current-voltage (I-V) relationship was fitted by calculating the average peak current (pA) of the channel at every value of voltage, from +50 mV to -90 mV.

Kv2.1_P17T in control conditions showed an average peak current (pA) of 7369 pA (95% CI 5633: 9104 n=7) (Figure 82, A and B). Calculated value of the reversal potential for Kv2.1_P17T in control conditions was equal to -69.68 mV (95% CI -74.20: -65.16 n=7) (Figure 82, B). The average peak current is reduced by 29% when compared to the average peak current of the wild type (Figure 83, A and B). Statistical analysis revealed that the currents are not statistically different (Unpaired t test, P>0.05).

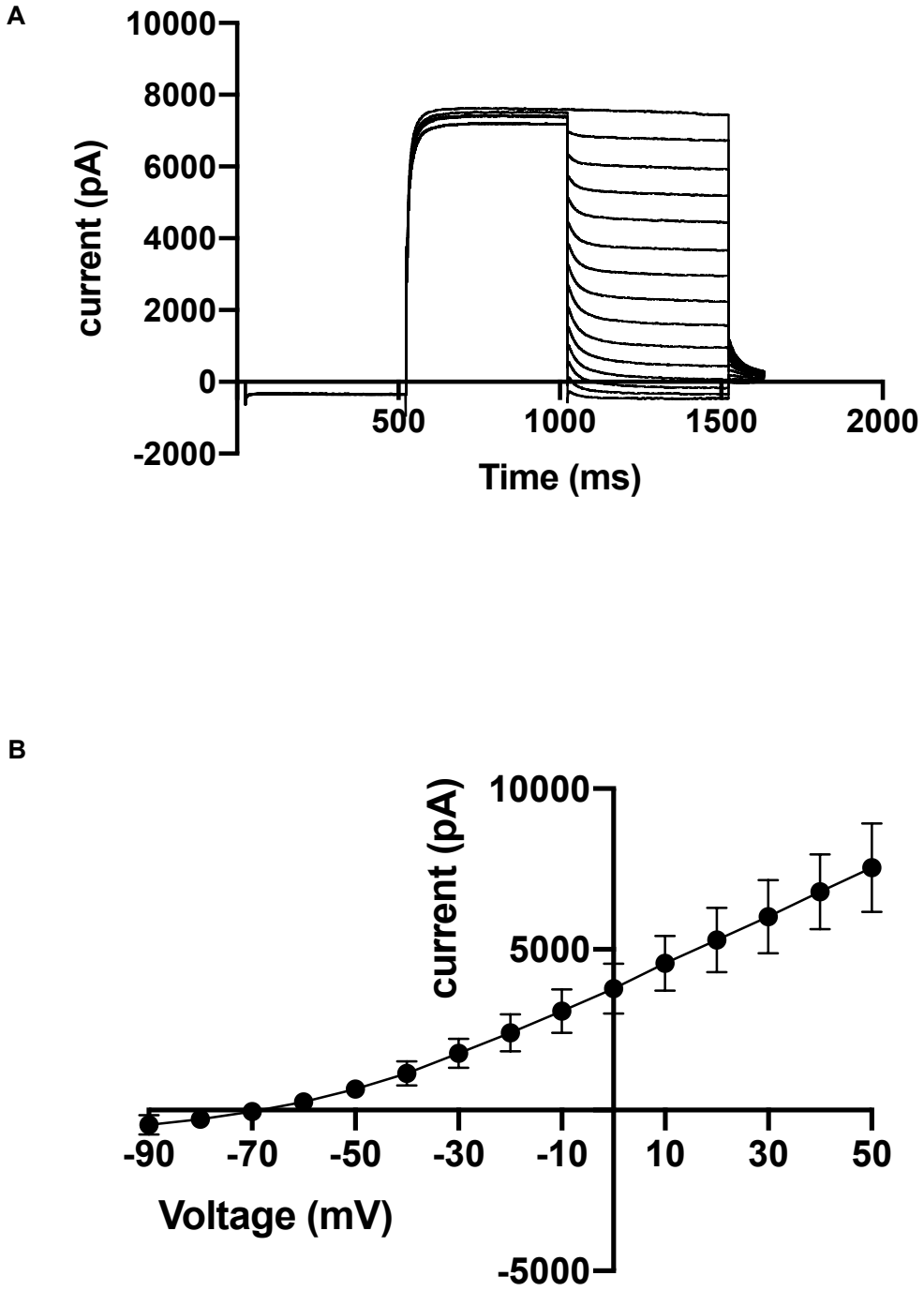

Figure 82. Layout panel representative of Kv2.1_P17T. A) Kv2.1_P17T in control conditions at voltages from +50 mV to -90 mV **B)** Current-voltage (I-V) relationship.

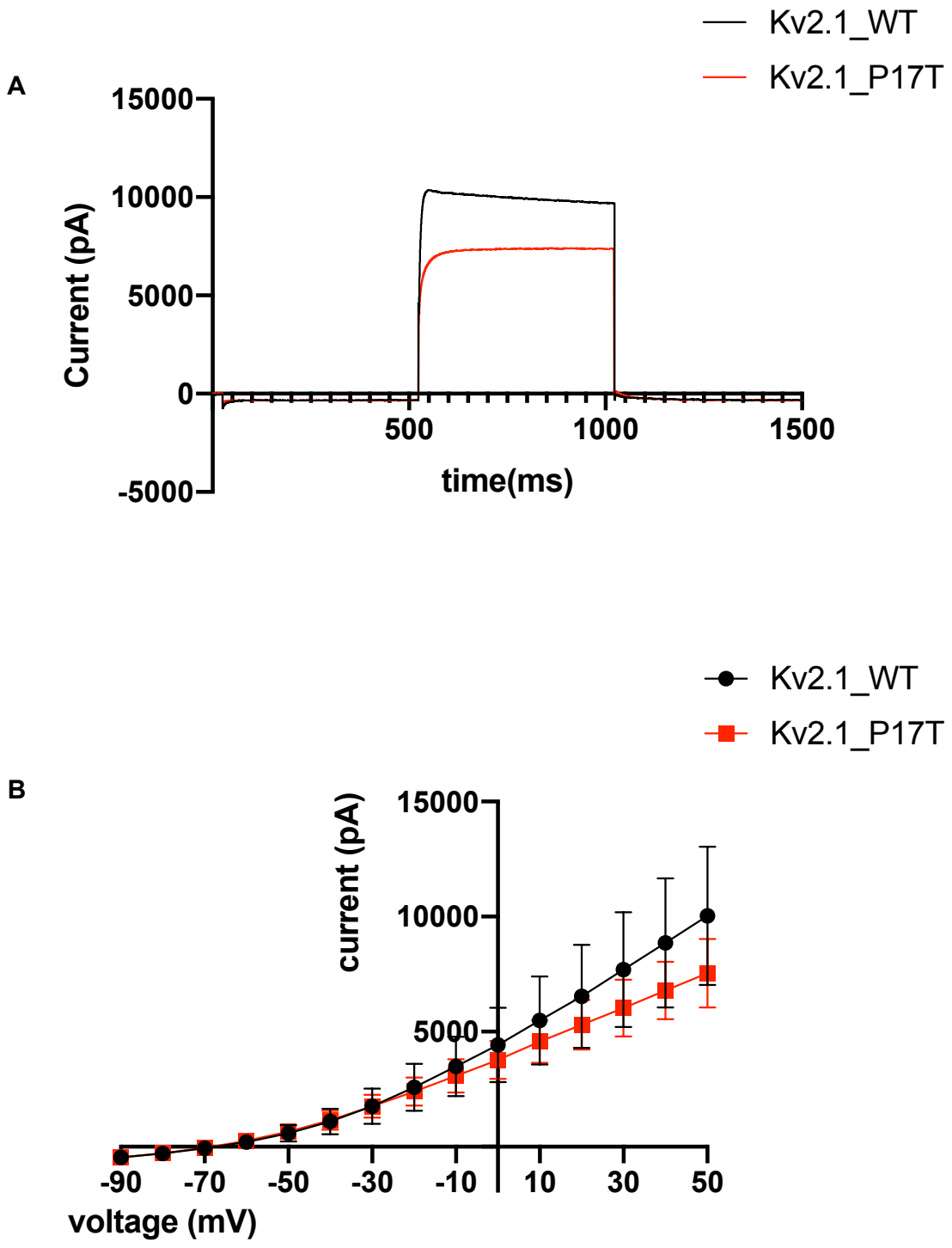

Figure 83. Layout panel of Kv2.1_WT and Kv2.1_P17T. **A)** Representative traces. Kv2.1_WT (black); Kv2.1_P17T (red). Currents are calculated and represented at +50 mV. **B)** Current-voltage relationship. Black circles: Kv2.1_WT; red squares: Kv2.1_P17T.

5.3.3 Characterisation of Kv2.1_P17T using the toxin Guangxitoxin-1E

Guagxitoxin-1E was used to detect the effect on Kv2.1_P17T in a similar way to the wild type channel. As we had found that a higher concentration of GxTx-1E was required to have a significant effect on the WT Kv2.1 channel, investigations on the mutant channel were conducted by incubating the channel with the toxin at 10 nM and 100 nM for a total of 20 minutes in 5% CO_2 incubator. The results are summarised in figure 84.
The average peak current of Kv2.1_P17T after incubation with 10 nM of GxTx-1E was equal to 7416 pA (95% CI 5670: 9162 n=9) (Figure 85, A). The I-V curve showed the course of the current at voltages between +50 mV and -90 mV. Current-voltage relationship showed a non-linear progression (Figure 85, B). In figure 86 (A), is showed a representative trace of Kv2-1_P17T after incubation with 100 nM of GxTx-1E. The average peak current was 5052 pA (95% CI 3065: 7039 n=6) ($P > 0.05$, using one-way ANOVA, followed by a Dunnett's multiple comparisons test). In figure 86, B is showed the I-V relationship. Calculated values of the reversal potential for Kv2.1_P17T in 10 nM and 100 nM of GxTx-1E were equal to -64.37 mV (95% CI -68.49: -60.25 n=9) (Figure 85, B) and -68.72 mV (95% CI -73.99: -63.45 n=6) (Figure 86, B).

The results suggest that the GxTx-1E toxin has a much less potent effect on the mutant Kv2.1 channel compared to the WT. Only at the highest concentration of toxin (100 nM) an inhibitory effect of 31% was measured on Kv2.1_P17T, compared to a 50% inhibition seen on WT channels at just 10 nM concentration. Whilst 10 nM of GxTx-1E did not determine any effect on the Kv2.1_P17T channel peak current.

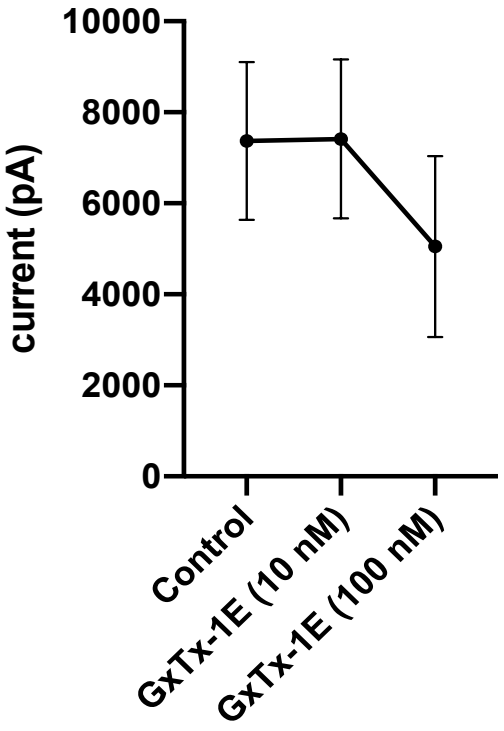

Figure 84. Kv2.1_P17T in control conditions and with Guangxitoxin-1E (10 nM and 100 nM) peak current (pA) graphic. Bars are representative of 95% CI of the mean. No significant effect is detected when 10 nM and 100 nM of the GxTx-1E are applied. GxTx-1E at 100 nM only reduce the channel current by 20%.

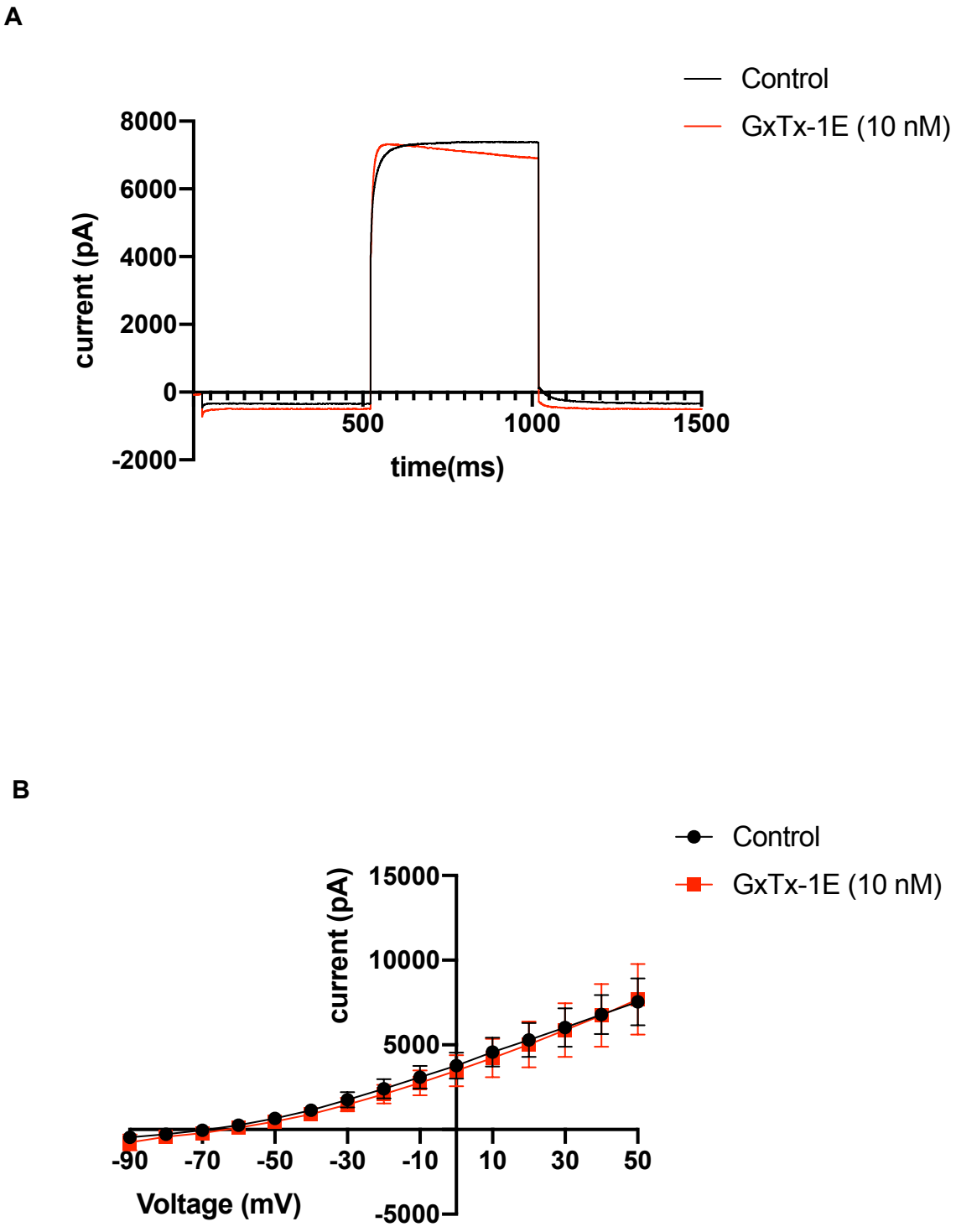

Figure 85. Kv2.1_P17T in control conditions and with 10 nM of GxTx-1E. A) Representative trace of Kv2.1_P17T in control conditions (in black) and after incubation with GxTx-1E (red). Average peak current (pA) is calculated and represented at +50 mV. **B)** Current-voltage (I-V) relationship. Black circles are representative of Kv2.1_P17T curve; red squares are representative of Kv2.1_P17T with GxTx-1E (10 nM).

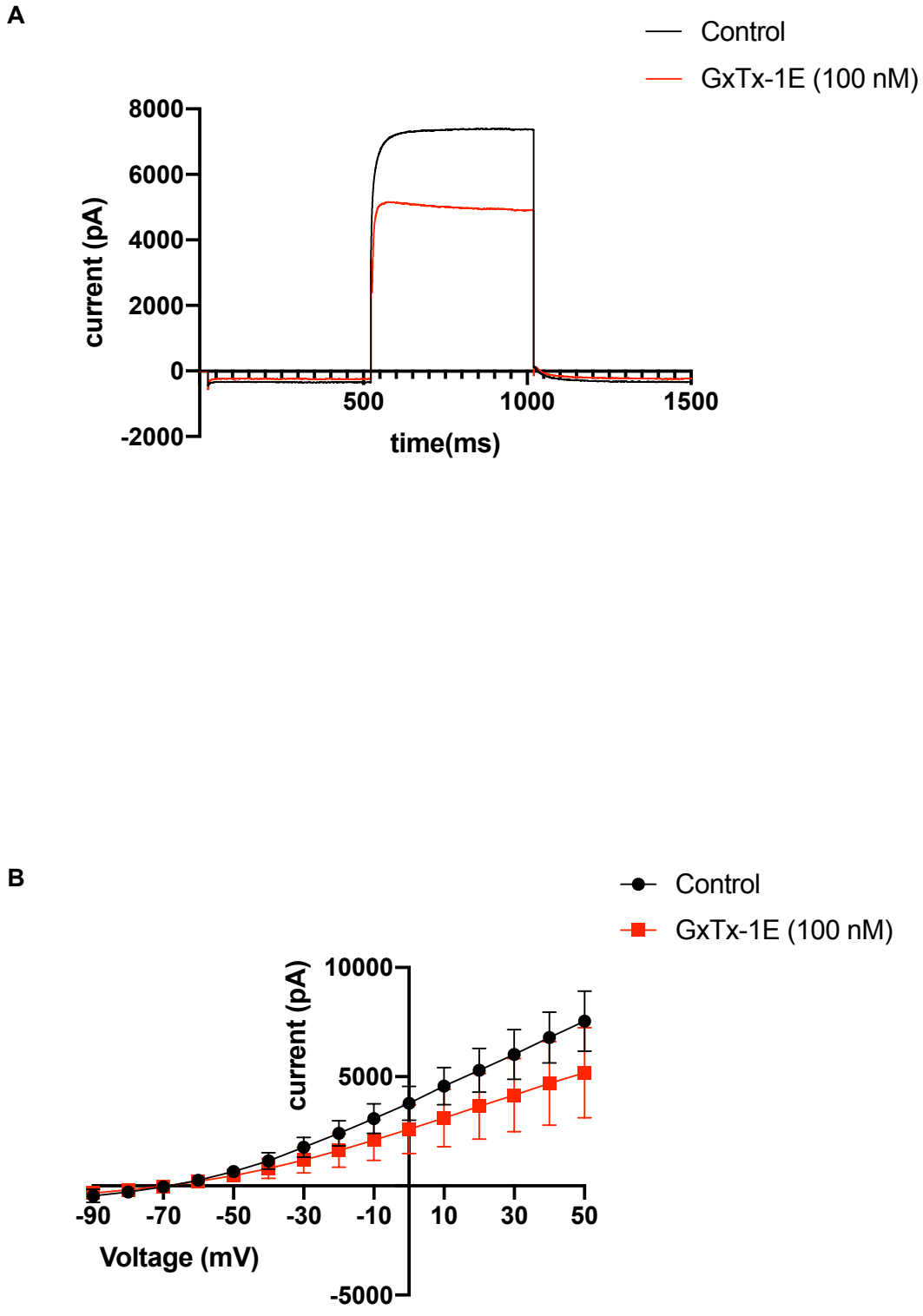

Figure 86. Kv2.1_P17T in control conditions and with 100 nM of GxTx-1E. A) Representative trace of Kv2.1_P17T in control conditions (in black) and after incubation with GxTx-1E (red). Currents are represented at +50 mV **B)** Current-voltage (I-V) relationship. Black circles are representative of Kv2.1_P17T curve; red squares are representative of Kv2.1_P17T with GxTx-1E (100 nM).

5.4 Discussion

Our investigations were focused on the characterisation of a *de novo* variant found in KCNB1 gene, encoding the voltage-activated K^+ channel, Kv2.1. The mutation is localised at the N-terminus of the channel. In particular, our interests were as following: first, to determine the effect of the mutation on the electrophysiological profile of Kv2.1 channel, seeking for an effect in terms of enhancement and/or reduction of the channel current, or no effect at all; second, by using a well-known and extensively studied Kv2 blocker, Guangxitoxin-1E, we were interested to see if the mutation, located at the site where the blocker is known to bind the channel, would shift and/or eliminate the potent inhibitory effect seen in the wild-type channel, or if the mutation, wouldn't affect the channel activity. Lastly, we wanted to prove that, selective toxins that act potently on one target, can be an excellent tool to study and characterise novel mutations occurring at different sites of the protein.

GxTx-1E from the Chinese tarantula *Plesiophrictus guangxiensis,* is the most potent Kv2 inhibitor and is known to act on the channel by binding the voltage sensors (Tilley D.C. *et al.,* 2019). In particular, the mechanism elucidated, expects that the toxin prevents the channel opening by binding the voltage sensors in a resting conformation, thus limiting its movement when the membrane depolarises (Tilley D.C. *et al.,* 2019). Interestingly, the peptide was much less effective on the mutant channel at concentrations that were active on the wild type, suggesting that the mutation does indeed affect the gating of the channel, preventing it from being pushed into a resting confirmation by the peptide. In our investigations, peak currents (pA) of Kv2.1_WT and Kv2.1_P17T were measured at +50 mV, in presence and absence of the toxin. In section 5.3.1, we tested three different concentrations of GxTx-1E in the nanomolar range (1 nM, 10 nM and 100 nM). Successfully, we demonstrated that, in presence of the toxin bound to the channel subunits, the channel peak currents were reduced in presence of 10 nM and 100 nM of the toxin. Incubation of the channel with 1 nM of the toxin, did not cause any significant inhibition of the channel's peak currents (pA), determining only a small percentage of inhibition, resemble to 18%. As for the *de novo* variant, P17T, the channel peak current was only slightly reduced compared to the WT channel, indicating that the mutation lightly affects the electrophysiological activity of the channel. A striking result obtained from our investigation, is represented by the lack of inhibitory effect of GxTx-1E on the mutant channel. High concentrations of the toxin, 10 nM and 100 nM, that in our investigations on the WT were sufficient to reach a good percentage of inhibition towards the channel current, were found to be not effective on Kv2.1_P17T. Indeed, the channel peak current in presence of 10

nM of the toxin was similar to the control (Control: 7369 pA; in 10 nM: 7416 pA), indicating that GxTx-1E lost the inhibitory effect on the channel. Even in presence of higher concentration of the toxin, 100 nM, the inhibition observed was lower that what we seen in the wild-type channel (WT: 47%; P17T: 31%). The shift in the current inhibition observed in Kv2.1_P17T could be explained taking into account the mechanism of action of the toxin. GxTx-1E is well known to bind the segment S3 of voltage sensor domain and to inhibit K^+ current by limiting the chances of the pore to open. This is reached by stabilizing the voltage sensor in a resting conformation (Tilley D.C. *et al.,* 2019). Mutations occurring upon a site that is, directly and/or indirectly, linked to the toxin's binding site, can disrupt the activity of the toxin either by disrupting the binding site itself or, alternatively, by reducing the chance of the toxin to bind to all α-subunits of the channel. In such way, higher concentration of toxin is required to reach the percentage of inhibition that in the wild-type channel is seen at lower nanomolar concentrations (10 nM). Evidence supports that the mutation not only reduced the current through Kv2.1 by 30 %, but also altered the electrophysiological properties of the channel. As such, higher concentration of the toxin is needed to increase the inhibition of the K^+ current.

Loss of function (LOF) and gain of function (GOF) mutations in genes that encode ion channels, are linked to a *plethora* of neurological disorders and in particular, mutations in KCNB1 encoding Kv2.1 have been linked to epileptic encephalopathies (Torkamani A. *et al.,* 2014). Interestingly, the patient expressing this clinical variant has so far not presented with any epileptic episodes. The *de novo* variant P17T, recently found in a very young patient, was reproduced in-house and characterised by electrophysiological investigations revealed that Kv2.1 channel, carrying the mutation in the N-terminal domain, showed a slightly lower current compared to the wild-type and altered pharmacological properties. All these observations might be helpful to understand deeply the clinical phenotype of the patient and address to a targeted therapy that might involve the selective target of the channel. More generally, the characterisation of mutations in gene encoding channels that are linked to the large group of channelopathies, is fundamental and provide a good way to extend our knowledges both, molecularly and therapeutically.

Chapter 6: Investigation of the properties of SXCL-1 and SXCL-6 on Kv1.3 expressed in Jurkat cells

6.1 Introduction

A vigorous and effective immune response is strictly dependent on Ca^{2+}(Trebak M. and Kinet J. P., 2019). Ca^{2+} signalling is vital not only for sustaining T cells activation and proliferation, but also for self-antigens tolerance and homeostasis (Fracchia K.M. *et al.,* 2013). For T cells, activation occurs after the engagement of T cells receptor (TCR), with the major histocompatibility complex-II (MHC-II), during antigen presentation. The subsequent activation of protein kinase (PKC) by phospholipase C (PLC), leads to the production of inositol (1,4,5)-trisphosphate [Ins (1,4,5) P3] that induces the release of Ca^{2+} from the store via the I_3PR receptor (Chandy K.G. *et al.,* 2004). The efflux of Ca^{2+} from the store causes a global increase of the internal concentration of Ca^{2+} that, in turns, induces the opening of the Ca^{2+}-release activated Ca^{2+} channel (CRAC) by the ER membrane protein STIM1. CRAC is a unique channel expressed in T cells and a few other cell types (Fracchia K.M. *et al.,* 2013).

The global rise of Ca^{2+} concentration observed after the antigen presentation, induces the binding of Ca^{2+} to calmodulin (CaM) that, after undergoing a conformational change, interact with the phosphatase calcineurin (Vetter S. W and Lecler E., 2003). This step is vital for the activity of the nuclear factors of activated T cells (NFAT) family members that, once dephosphorylated by calcineurin, re-locate into the nucleus where they start the transcription of the gene encoding the Interleukin-2 (IL-2) (Rao A., 1997) (Figure 87). More, c-JUN N-terminal kinase (JNK) and Ras, both activated by PLC, trigger the activation of additional transcriptional factors that, eventually, lead to T cell proliferation (Chandy K.G. *et al.,* 2004). The overall Ca^{2+} influx needs to be counterbalanced by the efflux of cations. Efflux of cations is mediated by K^+ channels. T cells express two main type of K^+ channels: the voltage-activated K^+ channel, Kv1.3 and the intermediate conductance Ca^{2+} activated K^+ (IKCa1) channel, that together orchestrate the calcium signalling sequence by controlling the membrane potential. The two channels contribute to maintain the membrane hyperpolarised, so that the driving force for Ca^{2+} entry is preserved (Chandy K.G. *et al.,* 2004). The two channels are differentially expressed in the different subsets of T cells, where their expression is strongly linked to both the activation state and the transition stage from naïve cells to memory cells (Wulff H. *et al.,* 2003 (a, b); Beeton C. *et al.,* 2003).

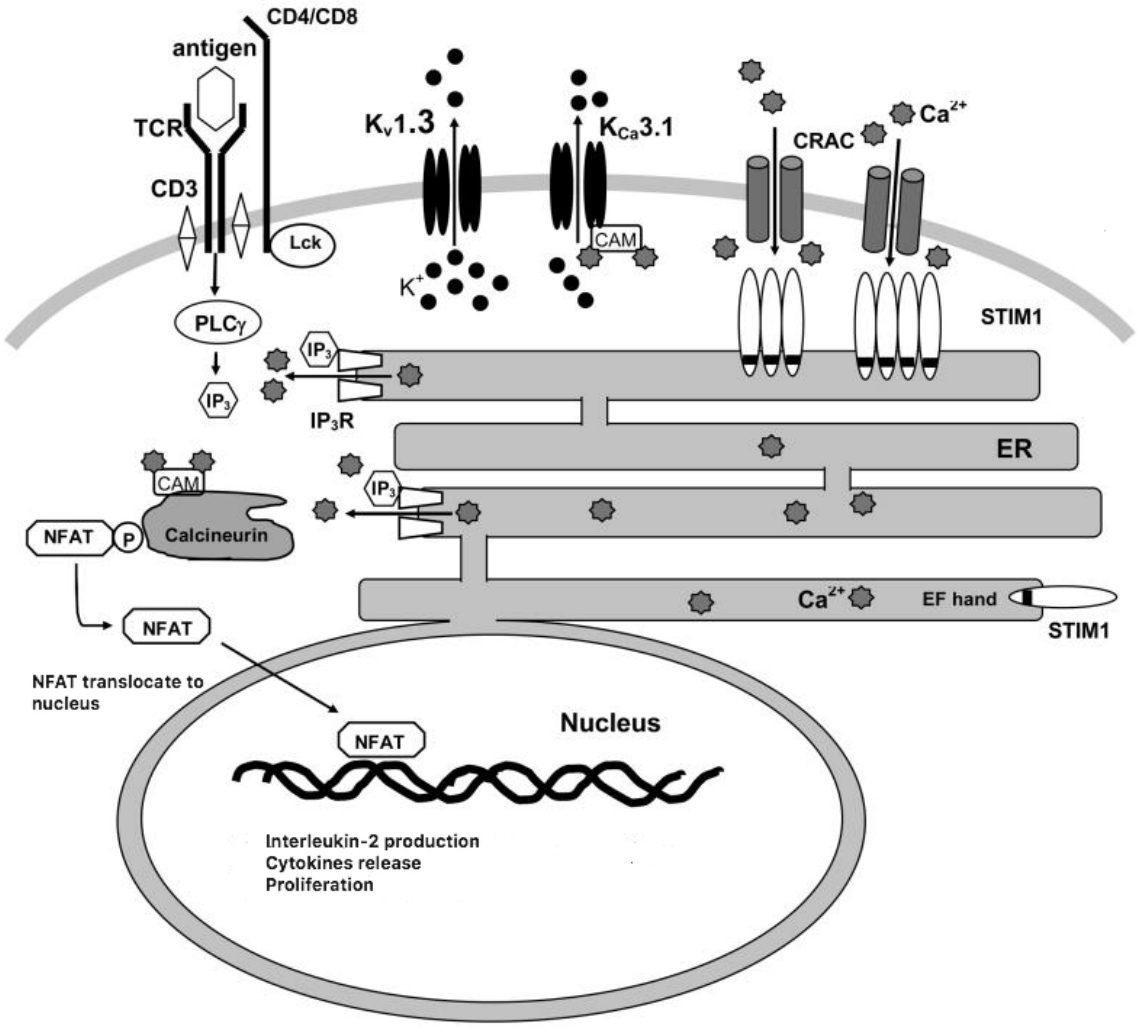

Figure 87. Schematic representation of the events in T cells after antigen presentation (Modified from Lam J. and Wulff H., 2011). Kv1.3 and Kca3.1 are found within the cell membrane and contribute to maintain the driving force for Ca^{2+} entry. Events Ca^{2+}-dependent lead, eventually, to the translocation of NFAT to nucleus and IL-2 production, cytokines release and proliferation.

IKCa1 and Kv1.3 channels are regarded as immunomodulators, with an intriguing potential for the treatment of autoimmune disorders. Autoimmune disorders develop from an alteration of the immune system, where immune cells present a compromised activity and target self-antigens. The treatment of patients with autoimmune diseases and inflammatory disorders involving T cells, implicates the use of drugs with immunosuppressant properties that inhibits T cells and other leukocytes (Yoon K. H., 2010; Coutinho A. E. and Chapman K. E., 2011). The most used immunosuppressant drugs include corticosteroids and cyclosporine (Kahan B. D., 1993; Stanbury R. M. and Graham E. M., 1998). Nevertheless, these drugs present several side effects, especially when used for prolonged period of time. Drugs and compounds able to act as selective immunomodulators rather than generic immunosuppressants, would be useful to treat all those diseases that involve T cells. Based on the channel expression's profile within the cell, it is possible to adopt strategies that aim at targeting Kv1.3, overexpressed in effector memory T cells (T_{EM}), without compromising the functionality of central memory T cells (T_{CM}) and vice versa, in diseases that implicate autoreactive T_{CM} cells. For example, diseases such as MS (Wullf H. *et al.,* 2003 (b)), rheumatoid arthritis (RA) type-1 diabetes mellitus (T1DM) (Beeton C. *et al.,* 2006), are characterised by autoreactive memory T lymphocytes, predominantly T_{EM}, with a high expression of Kv1.3 and low expression of IKCa1. In this scenario, a strategic therapy would aim at targeting Kv1.3, leaving uncompromised the activity of IKCa channel.

The expression of the two main potassium channels is detected in the three types of T cells, naïve T cells, T_{CM} and T_{EM}, that in the quiescent state, present a similar level of both channels (Cahalan M.D. and Chandy K.G., 2009). A quiescent state, indicates a catabolic state where the cell is not activated and therefore, is not able to perform effector functions and produce cytokines (Jones R. G. and Thompson C. B., 2007). However, activated T_{EM} cells upregulate Kv1.3 channel from about 300 channels in the resting state, to about 1500 channels/ cells when activated, whilst maintaining the number of Kca3.1 pretty stable. Conversely, T_{CM} cells upregulate IKCa channels to about 500 channel/cells when activated (Cahalan M.D. and Chandy K.G., 2009). The differential expression in the two different subsets of T cells, allow to selectively target the channels**.** Selective targeting of the channel with specific inhibitors causes the membrane to depolarize; consequently, membrane depolarization reduces the influx of Ca^{2+} and all the downstream events that depends on the increase of internal Ca^{2+}, such as cytokines production and cell proliferation.

Several peptides and small molecules, are now incorporated into the list of the channel inhibitors, acting with different potency and affinity. Channel inhibitors can be found in the form of toxins and peptides, the majority of which are derived from animals but not limited to this source. As previously discussed, Shk from the sea anemone *Stichodactyla heliantus* still remains one of the most potent inhibitors of Kv1.3 channel. Studies highlighted the beneficial inhibitory activity of ShK and analogue ShK- Dap^{22} in inhibiting the channel current in myelin antigen-activated T cells from patients with MS, with a potent inhibitory effect as well on cell proliferation of T_{EM} cells (Wulff H. *et al.,* 2003 (b)). KCa3.1 channel, belonging to the family of the calcium-activated potassium channels, share a six transmembrane topology with Kv1.3 but its activation is strictly depended on Ca^{2+}. The gating occurs after the binding of calmodulin to the cytoplasmatic C-terminal of the channel (Fanger C.M. *et al.,* 1999) triggered by an increase of intracellular Ca^{2+} (Joiner W.J. *et al.,* 1997; Logsdon N.J. *et al.,* 1997) (Figure 88). The channel is found mainly in naïve and T_{CM} cells, but it is also present in activated B cells, macrophages, microglia, vascular endothelium, fibroblast and proliferating smooth muscle cells, whereas its expression is not detected in excitable cells (Wulff H. and Castle N.A., 2010).

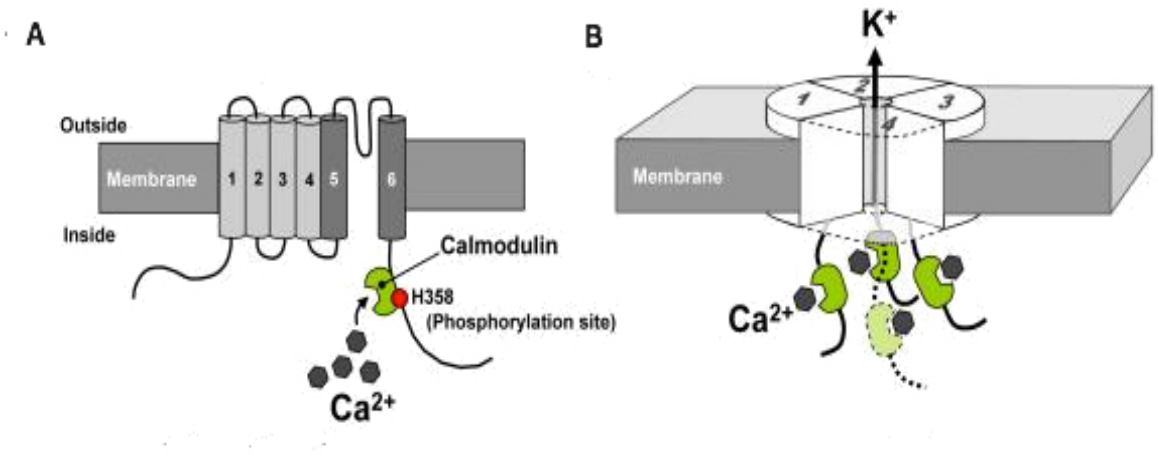

Figure 88. KCa3.1 structure (Adapted and reproduced from Wulff H. and Castle N.A., 2010) A) Kca3.1 transmembrane topology with Calmodulin binding site. **B)** Homo-tetrameric channel with four calmodulin calcium sensors highlighted in green.

Targeting KCa3.1 channel with specific inhibitors, assumes an important role in the suppression of acute immune responses and is attractive for the treatments of a wide array of diseases, as a reflection of the expression of the channel in several cellular compartment. The channel can be blocked by toxins such as maurotoxin, derived from the scorpion venom of *Scorpio maurus* (Castle N.A.*et al.,* 2003) and analogues of charybdotoxin, from the scorpion *Leiurus quinquestriatus*, engineered to enhance selectivity for KCa1 over Kv1.3 channel (Rauer H. *et al.,* 2000). Furthermore, several drugs such as quinine, the vasodilator cetiedil, nifedipine as well as clotrimazole, have been showed to successfully block the channel (Wulff H. and Castle N.A., 2010). The blocker TRAM-34, conceived by *Wulff* and colleagues (Wulff H. *et al.,* 2000), have been evaluated also for the treatment of cardiovascular diseases such as atherosclerosis, (Toyama K. *et al.,* 2008) and post-angioplasty restenosis (Köhler R. *et al.,* 2003; Tharp D.L. et al., 2008). As both channels are involved in the activation of T cells (Rader R.K. *et al.,* 1996), numerous studies have investigated the effect of some potent blockers of the K^+ channels in inhibiting this process and early researches highlighted the beneficial properties of general K^+ channel blockers, such as tetraethylammounium (TEA) and 4-aminopyridine (4-AP), in blocking the activation of phytohemagglutinin (PHA)-stimulated human T cells (Chandy K.G. *et al.,* 1984). *Chandy* and colleagues also described the property of those general K^+ channel blockers to reduce PHA-induced protein synthesis in human T lymphocytes (Chandy K.G. *et al.,* 1984). Interestingly, general calcium channel blockers, such as verapamil and diltiazem, have been found to block both K^+ channel currents (Hagiwara S. and Byerly L., 1981; Lee K. S. and Tsien R.W., 1983) and PHA-induced mitogenesis in T lymphocytes (Chandy K.G. *et al.,* 1984). These evidences, collected at an early stage of K^+ channel currents characterisation in T lymphocytes, indicate that suppressors that inhibits K^+ currents, are also able to suppress T cell proliferation (Deutsch C. *et al.,* 1986; Lee S.C. *et al.,* 1986; Chandy K.G. *et al.,* 1984). Proliferation is triggered by the T cell-synthetised cytokine Interleukin-2 (IL-2), which is considered as a T cell growth factor as, once produced by activated T cells, binds to its specific membrane receptor thus triggering cells to proliferate (Lee S.C. *et al.,* 1986). Therefore, was reported that T cells proliferation is strictly dependent on the free IL-2 concentration, as well as the concentration of IL-2 receptor and its affinity for IL-2 (Smith K.A., 1984). The binding of IL-2 to its receptor, is the event that precedes DNA synthesis (Smith K.A., 1984) and favour differentiation of T cells in T_{EM} cells by the activation of several intracellular pathways (Alberts B. *et al.,* 2002).

Taken together, all those evidences suggest that both Kv1.3 and KCa3.1 channel represent an extremely promising strategy for the treatment of patients with autoimmune and other disorders. The discovery of the differential expression of Kv1.3 and KCa3.1, became an attractive opportunity to reach specific immunosuppression. Selective inhibition of the channel with specific inhibitors, would translate into the inhibition of the immune response. It is dutiful to highlight that the properties that peptides and, more generally, K^+ channels inhibitors showed in suppressing the proliferation of T cells, is a key point for the immunosuppression strategy. In such way, inhibitors can block only the proliferation of autoreactive T cells and leave intact the protective immune response (Varga Z. *et al.,* 2010). At present, encouraging results for Kv1.3 are emerging for *in vitro* and *in vivo* studies with peptides that are able to selectively target the channel. Several *in vivo* studies, aimed also at evaluating important properties of the peptides such as the injections strategy, plasma half-life as well as rapidity in clearance via glomerular filtration, are underlying the importance of finding novel and potent inhibitors of the channel so that the therapeutical strategies can be focused on selectively targeting the channel more than reach general immunosuppressant effects.

6.2 Objectives

In the previous chapters, we presented the characterisation of two novel *ShK*-like peptides in transiently transfected cells expressing hKv1.3, and we have demonstrated their inhibitory activity on the channel. We further showed the selectivity of the two peptides by comparing the inhibitory effect on Kv1.3 to that observed for other members of the voltage-gated K^+ channel family, emphasising the great potential of the peptides as candidates for channel targeted therapies.

In this chapter, we offer further insights into the pharmacological properties of SXCL-1 and SXCL-6, by investigating their effect in a cell type that naturally express the channel, the Jurkat T cells. This human leukemic T cell line is often used for studies aimed at characterising the signalling events during T lymphocytes activation (Fanger C.M. *et al.,* 2001) and represents an excellent tool to evaluate properties of Kv1.3 inhibitors on a wide array of cell functions.
The perforated patch-clamp technique was used to describe the peptide's activity on Kv1.3 in a similar experimental process to that previously shown for tSA201 cells. We then proceeded to investigate the immunological properties of the two novel *ShK-like* peptides by evaluating the effect of these peptides on the release of the effector cytokine, Interleukin-2 (IL-2), which is involved in T cell proliferation, using the ELISA technique.

The results presented in this chapter, can be considered as preliminary data for further studies. In the light of the recent pandemic situation that caused, among everything else, disruptions in our routine and caused a rearrangement to a new lifestyle, we decided to present this set of "*uncomplete*" experiments as preliminary data for further studies that could be performed in the future in combination with other experiments that we propose at the end of the chapter (see discussion, section 6.5). This short piece of work wants to be considered as a basis for all the other routes we wanted to explore but, the current circumstances of the times we are living in, have limited.

6.3. Results

6.3.1 Electrophysiological characterisation of Kv1.3 channel in Jurkat cells

Initial experiments, sort to establish that Kv1.3 channel current is present in Jurkat cells, could be conducted using our protocols and experimental set up. Currents were evoked using the protocol "+50 mV continuously" protocol, as previously used for tsA201 cells (see Materials and Methods). A variant of the whole-cell patch clamp configuration, the perforated patch configuration, was adopted for the Jurkat cells (see Material and Methods, section 2.3.2). This was to allow for stable recordings and for the preservation of the second messenger signalling cascades. The average Kv1.3 perforated whole-cell current (pA) measured at + 50 mV in an extracellular potassium (K^+) control solution of 2.5 mM [K^+] was 1135 pA (95% CI 761.3: 1509 n=18) (Figure 89).

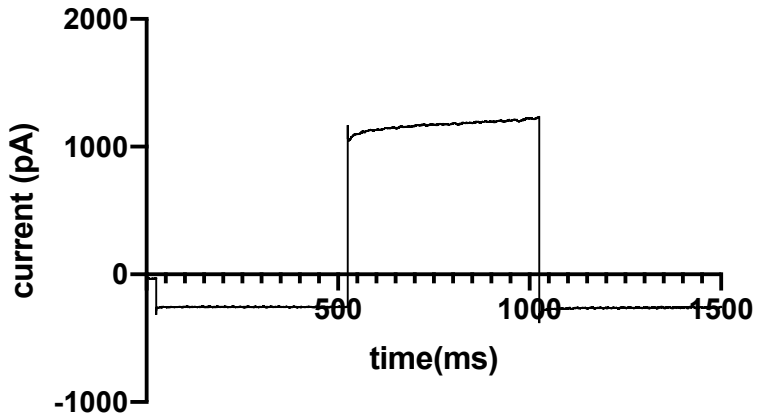

Figure 89. Representative trace of Kv1.3 in Jurkat cells. Kv1.3 average peak current value at +50 mV is 1135 pA (n=18).

6.3.2 Electrophysiological characterisation of the effect of the two novel peptides, SXCL-1 and SXCL-6 on Kv1.3 expressed in Jurkat cells

Having established the presence of recordable Kv1.3 current in Jurkat cells, the next experiments were to measure the effect of the two novel peptides on Kv1.3 current present in these cells to reproduce effects observed in the heterologous cell lines. As for tSA201 cells, Jurkat cells were incubated for 20 minutes in the 5% CO_2 incubator with either SXCL-1 or SXCL-6 peptides and recordings then made from the cells using the perforated-patch clamp technique.

The results of our investigations revealed that that 0.5 nM of SXCL-1 peptide was able to significantly ($P < 0.05$, using one-way ANOVA) inhibits the average Kv1.3 current (pA) from 1135 pA (n=18) to 255 pA (95% CI 142: 368; n=6), with a percentage of inhibition that was equal to 78% (Figure 90, A). At an even lower concentration of SXCL-1, 0.03 nM, current was reduced to 540 pA (95% CI 104: 977; n=5), although this was not found to be significantly ($P > 0.05$, using one-way ANOVA) different from WT levels (Figure 90, B).

A peak current (pA) graphic summarising the results of the investigations are showed in figure 91. Values are representative of peak current (pA) of Kv1.3 in control and in presence of 0.5 nM and 0.03 nM of SXCL-1.

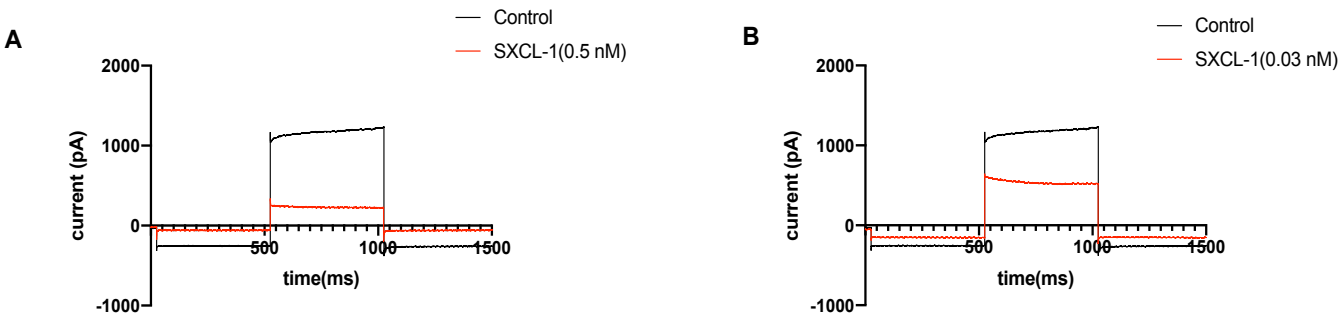

Figure 90. Layout of representative traces of Kv1.3 in control and SXCL-1. A) Kv1.3 in control condition (black trace) and in presence of 0.5 nM of SXCL-1 (red trace). **B)** Kv1.3 in control condition (black trace) and after incubation with 0.03 nM of SXCL-1 (red trace).

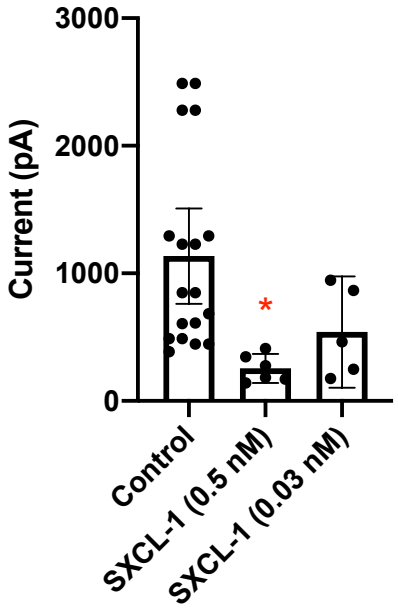

Figure 91. Peak current (pA) graph of Kv1.3 in control conditions expressed in Jurkat cells and in presence of SXCL-1 (0.5 nM and 0.03 nM). Bars are indicative of 95% CI of the mean. SXCL-1 at 0.5 nM (n=6) significantly inhibits the average peak current of Kv1.3 in Jurkat cells (p=0.0120).

We then evaluated the inhibition of the Jurkat cells by SXCL-6 at the same doses, 0.5 nM and 0.03 nM. As was observed for SXCL-1, SXCL-6 was found to potently and significantly ($P < 0.05$) inhibit the current evoked at +50 mV in Jurkat cells (Figure 92). The average peak current measured at +50 mV was reduced to 253 pA (95% CI 147: 358; n=6) in presence of 0.5 nM of SXCL-6 toxin (Figure 92, A), compared to 1135 pA (95% CI 761.3: 1509; n=18) measured in control conditions. This was equivalent to a 78% inhibition of current. Similarly, incubation of Jurkat cells in 0.03 nM of SXCL-6 resulted in an average current measured at + 50 mV of 707 pA (196: 1219; n=4), which was not found to be significantly different ($P > 0.05$) from in control (Figure 92, B). In figure 93, is showed a peak current (pA) graphic that summarize the results of our findings. Graphic is representative of Kv1.3 in control conditions and in presence of 0.5 nM and 0.03 nM of SXCL-6.

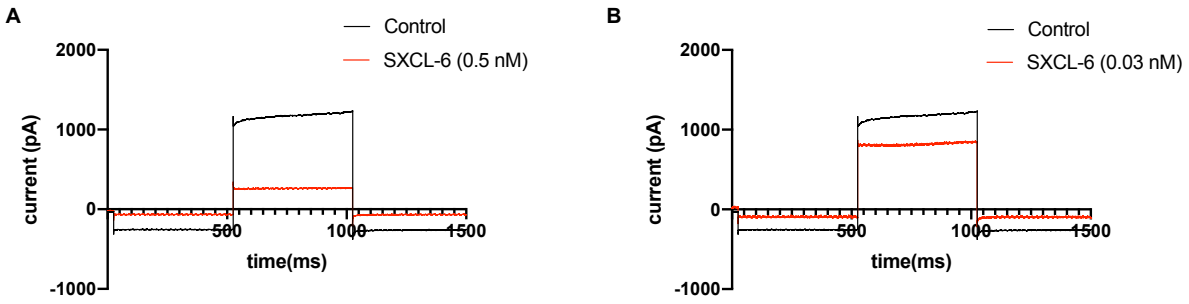

Figure 92. Layout of representative traces of Kv1.3 in control conditions and with SXCL-6. **A)** Kv1.3 in control condition (black trace) and in presence of 0.5 nM of SXCL-6 (red trace). **B)** Kv1.3 in control condition (black trace) and after incubation with 0.03 nM of SXCL-6 (red trace).

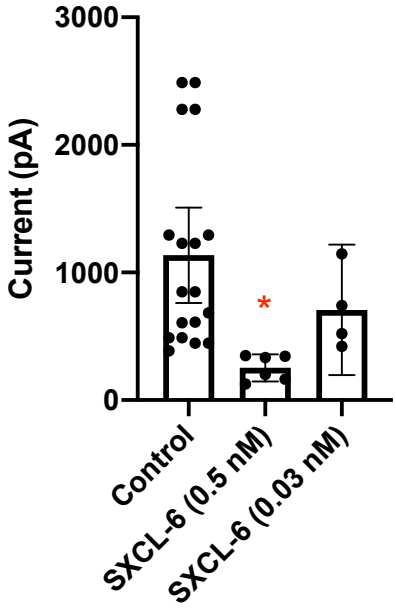

Figure 93. Peak current (pA) graphic of Kv1.3 in control conditions and in presence of SXCL-6 (0.5 nM and 0.03 nM). Bars are representative of 95% CI of the mean. Incubation of the channel with 0.5 nM (n=6) of SXCL-6 determined a significant reduction of the average peak current from 1182 pA in control conditions (n=18) to 253 pA (p=0.0129).

6.4 Investigating the effect of Kv1.3 inhibition by SXCL-1 and SXCL-6 on the release of Interleukin-2 (IL-2)

As it was previously shown, Kv1.3 channel blockade by specific channel inhibitors, influences the release of the cytokine Interleukin-2 (IL-2), as it affects the Ca^{2+}- dependent events that ultimately lead to the production of IL-2 (Zhao N. *et al.,* 2013; Zhao N. *et al.,* 2014). In light of these evidences we went on and investigated whether the two novel peptides, SXCL-1 and SXCL-6, were able to inhibit the release of IL-2, by performing an Indirect ELISA test using the ShK toxin as a positive control. Our preliminary data are the results of investigations conducted using the three peptides at a concentration of 0.5 nM, that we determined in our previous electrophysiological experiments able to significantly inhibit the channel currents present in Jurkat cells. Experimental procedure for ELISA test was described previously in Material and Methods section and data analysis were performed by using one-way ANOVA (Dunnette's multiple comparisons test).

As seen from figure 94, our investigations revealed that there was no significant ($P > 0.05$) reduction of IL-2 release from Jurkat cells, that had been previously treated with 100 nM of PMA and incubated peptide. In control, release of IL-2 in Jurkat stimulated with PMA, was equal to 150 ± 38 (pg/10^6 cells). Following the treatment with 0.5 nM of each peptide, ShK, SXCL-1 and SXCL-6, the IL-2 release was equivalent to 120 ± 16 (pg/10^6 cells); 141 ± 40 (pg/10^6 cells) and 179 ± 28 (pg/10^6 cells), respectively.

This preliminary data suggests that the release of IL-2 is not affected by the peptide inhibition as previously suggested (Figure 94).

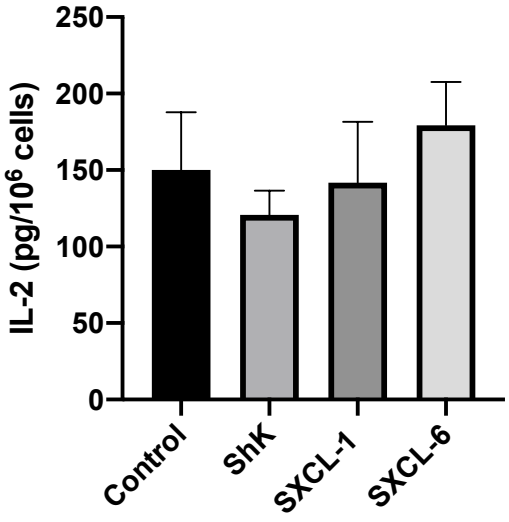

Figure 94. Effect of the three peptides on IL-2 production in activated Jurkat cells. Bars are indicative of SEM**.** IL-2 release in control conditions after 24h stimulation with 100 nM PMA (n=2). For all three Kv1.3 blockers, no effect was detected (adjusted P values, p=0.8558; p=0.9954; p=0.8558, respectively).

6.5 Discussion

The therapeutical benefits of targeting K^+ channel with inhibitors for the treatment of diseases involving T cells, started to be evident since early researches pointed out that, these integral membrane proteins, were involved not only in the regulation of the membrane potential but also influenced key processes such as cell activation, migration, proliferation and homeostasis (Lewis R. S. and Cahalan M. D., 1995). Pioneering work from *DeCoursey* and colleagues revealed, for the first time, that the predominant current in T cells was attributable to a voltage-dependent K^+ channel (DeCoursey T. *et al.,* 1984), confirmed to be Kv1.3, later on. The discovery of the second K^+ current in T lymphocytes, sensitive to high concentrations of internal calcium $[Ca^{2+}]_I$ but insensitive to voltage changes, was confirmed later in 1993 by the work of *Grissmer* and co-workers and addressed as KCa channel (Grissmer S. *et al.,* 1993). Both channels are involved in Ca^{2+} signalling sequence by contributing to the regulation of the membrane potential during the activation of T cells in effector (Cahalan M.D. and Chandy K.G., 2009). The discovery of the differential expression of the channels in the two subset of T cells in response to activation, represented the *momentum* when the two channels were addressed as potent immunomodulators, with the potential of being considered for the treatment of a wide nuance of diseases involving a specific set of memory T cells. Memory cells represent the pool of cells that survive after the first encounter with the antigen and remain for the lifetime, ensuring immediate protection in peripheral tissues and secondary lymphoid organs (Sallusto F. *et al.,* 2004). Memory cells are divided into two types based on the expression of receptors and adhesion molecules, and the presence or absence of effector functions (Sallusto F. *et al.,* 1999). Effector memory T cells, T_{EM} ($CCR7^-CD45RA^{+/-}$), mediates protective memory, migrate rapidly to peripheral sites and perform their effector functions by releasing cytokines (granzyme B and interferon-γ). Central memory T cells, T_{CM} ($CCR7^+$ $CD45RA^-$), account for reactive memory and exhibit more proliferative potency than $T_{EM,}$ so that they can ensure the rising of an efficient response to antigens in secondary lymphoid organs (Sallusto F. *et al.,* 2004). Identification of the subset of T cells mediating a certain autoimmune condition, was pivotal to delineate specific treatments. For example, in MS, autoreactive T_{EM} cells are the main pool of cells involved in the disease, as confirmed from the analysis of the peripheral blood of patients with MS compared to healthy controls (Wulff H. *et al.,* 2003 (b)). As a consequence of the continue exposure to myelin antigen during the progression of the disease, the cells acquire the Kv1.3 ^{high} profile and therefore, are a target for immunosuppression mediated by Kv1.3 blockers (Chandy K.G. *et al.,* 2004). In literature, the

increased expression of Kv1.3 channel following mitogenic stimulation is reported to be linked with either post-transcriptional events that induce the activation of previous "silent" channel, or a surge of the translation's rate (Lewis R.S. and Cahalan M.D., 1995). Alternatively, it is proposed that the higher expression of Kv1.3 channel could have its root in the fact that, after activation, already synthetised channels are then expressed at the cell membrane (Lewis R.S. and Cahalan M.D., 1995). The immunosuppressive effect guaranteed by the inhibition of Kv1.3 channel, is due to membrane depolarization and reduction of the driving force for Ca^{2+} to entry via CRAC channel (Lin C.S. *et al.,* 1993; Chandy K.G. *et al.,* 2004). Therefore, activation of T cells is blocked when channel is selectively targeted with inhibitors (Lewis R. S. and Cahalan M. D., 1995).

In chapter 3, we showed the potent inhibition exhibit by the two novel *ShK-like* peptides, SXCL-1 and SXCL-6, from the nematode *H. polygyrus,* towards Kv1.3 expressed in tSA201 cells. Here, we showed that the two novel peptides, are able to inhibit Kv1.3 expressed in Jurkat cells, with a potency that resembles what we previously reported for tSA201 cells, however with a different pharmacological profile. Therefore, from the *in vitro* results that we obtained on both tSA201 and Jurkat cells, we propose that SXCL-1 and SXCL-6 are potential candidates to add to the increasing list of Kv1.3 inhibitors. Jurkat T cells, a human T leukaemia cell lines, represent an optimal system to study the interaction between endogenously K^+ currents mediated by Kv1.3 and inhibitors. These cells have been widely used in studies aimed at characterising the relationship channel-blockers (Zhao N. *et al*., 2015; Gąsiorowska J. *et al*., 2015) and also for studying the involvement of the channels in events such as cell proliferations, chemokines release (Ding L. *et al.,* 2017; Zhang Y. *et al.,* 2019) and apoptosis (Valencia-Cruz G. *et al.,* 2009). Other than Kv1.3, other two types of K^+ channels are found within the cell membrane of Jurkat cells (Panyi G. *et al.,* 1996; Pottosin I. *et al.,* 2007; Sands, S. B. *et al.,* 1989): the Ca^{2+}-activated small-conductance SKCa2 (Grissman S. *et al.,* 1992; Jäger H. *et al.,* 2000; Hanselmann C. and Grissmer S., 1996), and the two pore domain channel (K2P), TRESK, mediating the so-called *background* current (Pottosin I. *et al.,* 2008).

The aim of our study was to demonstrate that the strong Kv1.3 current inhibition resulting from the application of both *ShK-like* peptides in tSA201 cells, was also perpetuated in cells that naturally express the channel. From our investigations, was clear that the incubation of the cells with 0.5 nM of SXCL-1, determined a significant 78% current inhibition. Similar results were evident for SXCL-6, that was able to reduce Kv1.3 average peak current by 77%, with a

potency profile similar to SXCL-1. Our results suggested that both peptides were able to effectively inhibit the average peak current of Kv1.3 channel expressed in Jurkat cells, however SXCL-6 preserved a slightly more potent inhibition at lower nanomolar concentration of 0.03 nM. The conclusion that both peptides, at a low nanomolar concentration of 0.5 nM, are able to significantly inhibit Kv1.3 average peak currents, is in agreement with previous investigations conducted on tSA201 cells, transiently transfected with hKv1.3. However, the potency of the peptides was found to be lower using the tSA201 cells compared to the Jurkat cells. This may be due to the method we used to record currents from the two types of cells. It is possible that by using perforated whole-cell patch clamp configuration on Jurkat cells, we maintained the integrity of intracellular signalling pathway, which improved the potency of the peptides. Jurkat cells have also been shown to mimic the physiological environment of T cells; indeed, as discussed above, the cells endogenously express other K^+ currents that functionally contribute to maintain the environment of the cells. As such, these underlined differences, might explain why the peptides are more potent in one cell type over another. Overall, the results we obtained show a robust inhibitory profile at low nanomolar concentrations in both cell types and are indicative of a possible application of both peptides for future therapeutical strategies aimed at targeting Kv1.3.

In section 6.4, we showed preliminary data obtained through ELISA test, looking at whether the inhibitory action of the peptides on potassium channels expressed in the Jurkat cells, affected the release of the Interleukin-2. IL-2 production necessitates of an increase of calcium $[Ca^{2+}]_i$ to take place, as requires the translocation of the NFAT transcriptional factors from the cytoplasm to the nucleus, where they start the transcriptions of genes, including IL-2. The IL-2 is essential to ensure the progression of the cells toward effectors and plays a key role in maintaining both the homeostasis and the equilibrium between Treg and Teff cells within the immune system (Xu L. *et al.,* 2019) (Figure 95). Previous studies have shown that an analogue of ShK was able to induce a potent inhibitory effect on the cell proliferation of T_{EM} cells from patients with MS (Wulff H. et al., 2003 (b)). As SXCL-1 and SXCL-6 have a similar inhibitory profile to ShK, then it was hypothesised that they might affect T cell proliferation in a similar manner.

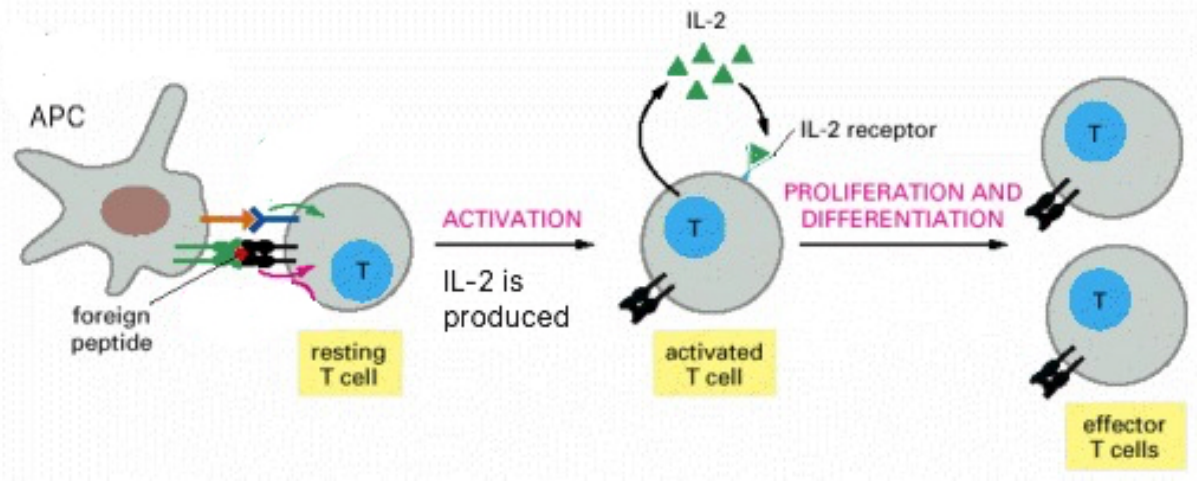

Figure 95. Schematic representation of IL-2 release after T cells activation (figure modified and reproduced from Alberts B. *et al.,* 2002). Activation of T cells requires two main signals: processing of foreign peptide through MHC-II that interacts with TCR receptor (pink arrow) and recognition of B7 proteins on APC by the co-receptor protein CD28 of T cells (green arrow). Once the cell is activated and all the cascades of event take place, IL-2 is released and can bind to IL-2 receptor, ensuring the continuation of the cell proliferation.

Surprisingly, in the preliminary assays, we were unable to observe an inhibition of IL-2 expression levels in pre-stimulated Jurkat cells, either in presence of SXCL-1 and SXCL-6 or indeed for ShK. There may be a number of reasons for this discrepancy which may be overcome by experimental adjustments. For instance, using a higher concentration of the peptides or altering the amount of PMA, or perhaps adding ionomycin to increase calcium production, could represent alternative adjustments to consider. It might be possible that PMA is not working sufficiently on its own and, as we did not measure IL-2 levels in unstimulated cells, we have no reference to baseline levels. Another possibility is that incubation with the peptide might be required first, in order to inhibit the channels and suppress expression of the IL-2, before stimulating them with the addiction of PMA. As we were unable to perfuse the toxins due to the small amount available to us for use, we were unable to determine the speed of action of these peptides on the channels and thus the huge increase in calcium caused by PMA, would overcome any effects exerted by the inhibition of the channels in the cells. Also, in previous studies, an analogue of ShK, ShK-Dap^{22} had been used and as such, might explain the different effects seen here with ShK peptide. As a result of the pandemic restrictions, we were not able to perform any further investigations on this, therefore we conclude that further

investigations in the future are required to clarify the mechanism by which the two peptides might influence the IL-2 production. However, the rationale behind the tests, was that the *ShK-like* peptides might be involved in the IL-2 production by blocking the influx of Ca^{2+}. In the matter of fact, Kv1.3 maintain the resting membrane potential (Vm), thus ensuring the Ca^{2+} entry and all the events that depends on Ca^{2+}; however, when the channel is blocked by inhibitors, all the downstream events linked to Ca^{2+} increase, cease (Lewis R.S. and Cahalan M.D., 1995). A great number of investigations have elucidated the contribution of Kv1.3 in Ca^{2+} signalling in Jurkat cells (Yin S. *et al.,* 2014; Zhao N. *et al.,* 2013). It would be then beneficial, to investigate whether SXCL-1 and SXCL-6 influence Ca^{2+} influx in this type of cells. The measurement of Ca^{2+} influx could be carried out, for example, by using a calcium imaging technique by stimulating the release of Ca^{2+} from the store with specific agents and subsequently by measuring whether the application of the peptides causes a subsequent reduction of the calcium influx. This data would contribute to confirm our initial hypothesis and would certainly contribute to extend the information on the immunological properties of the two novel *ShK-like* peptides, SXCL-1 and SXCL-6, in a cell lines extensively used for studying T cells signalling. Another argumentative point could see as a protagonist the extensively mentioned Ca^{2+}-activated K^{+} channel, Kca3.1 (Kca2.2 in Jurkat cells). Further investigations aimed at confirming the selectivity of the two peptides towards Kv1.3 over the Kca2.2 expressed in Jurkat cells, could be reached by performing electrophysiological investigations with a different setting compared to Kv1.3. Kca2.2 is a calcium-activated channel, thus the channel opening could be induced by application of Ca^{2+} stimulators, such as the Ca^{2+} ionophore ionomycin, directly to the extracellular solution or, alternatively, by using a pipette solution that contain low Ca^{2+} concentration. Furthermore, the two channels-Kca2.2 and Kv1.3-have different kinetics properties and attention must be paid when designing experiments, first of all using a protocol that reflects their biophysical properties. Several Kca (both SK and IK) blockers are available commercially. For example, it is known that Kca2.2 is sensitive to apamin (Benton D.C. *et al.,* 2013) but it is insensitive to Charybdotoxin (CTX) that is known to block Kca3.1 (Wulff H. and Castle N.A., 2010). Ultimately, several studies demonstrated that the inhibition of Kv1.3 determined by channel blockers, can be related to a down-regulation in the channel expression (Zhao N. *et al.,* 2013; Fu X.X. *et al.,* 2013; Zhao N. *et al.,* 2014). Additional experiments aimed at investigating whether or not, the application of the two novel *ShK-like* peptides, SXCL-1 and SXCL-6, are able to reduce the expression of the channel, could represent additional experimental ideas to test in the future.

6.6 Conclusions and Remarks

Our studies are comprehensive and demonstrated the selectivity of SXCL-1 and SXCL-6 towards Kv1.3 but, as a further confirmation for this type of study that include a different cell type, testing the two peptides on Kca2.2 expressed in Jurkat cells would be beneficial.
Nevertheless, the combination of electrophysiological investigations and immunological assays aimed at elucidating the contribution of the two novel Kv1.3 inhibitors, SXCL-1 and SXCL-6, are certainly important to enlarge the data available not only the potency and the selectivity of the peptides towards the voltage-gated Kv1.3 channel, but also how they influence the dynamic in a T cell type.

Taking all together, although we highlighted some limits in our investigations and we proposed additional experiments to conduct in Jurkat cells, our data can give the base for further avenues to undertake for investigating the properties of the two novel *ShK-like* peptides.

Chapter 7: Consolidation

7.1 Introduction

The voltage-activated K^+ channel, Kv1.3, has become an attractive target for the treatment of human disorders, with a particular emphasis on autoimmune diseases. Autoimmune disorders (AD) affect, globally, about 3-5% of the population, with type-1 diabetes mellitus (T1DM) and autoimmune thyroid disorder, estimated to be the most common AD found within the population (Wang L. *et al.,* 2015). The relevance of Kv1.3 in the treatment of these disorders, is related to its expression in the subset of T cells, the effector-memory T cells (T_{EM}), involved diseases including multiple sclerosis (MS), rheumatoid arthritis (RA), type-1 diabetes mellitus (T1DM) and many more (Wullf H. *et al.,* 2003 (b); Beeton C. *et al.,* 2006). These subset of T cells are characterised by an elevated number of Kv1.3 channels after activation, therefore are characteristically indicated as Kv1.3 ^{high} profile cells (Chandy K.G. *et al.,* 2004). The role of Kv1.3 in T cells have been widely described and is linked to the property of the channel to control the membrane potential and to contribute to the regulation of the Ca^{2+} signalling after T cells activation (Cahalan M.D. and Chandy K.G., 2009). Inhibition of Kv1.3 by specific blockers result in a potent immunosuppression (Chandy K.G. *et al.,* 2004). Several researches pointed out the potential use of peptides and toxins, the majority of which are originated from animals, but they can also be found in plants, as potent inhibitors of ion channels. In the specific case of Kv1.3, one of the first ever described toxin that is able to potently inhibits the channel current is the sea anemone toxin ShK, isolated from the sun anemone *Stichodactyla heliantus* (Castañeda O. *et al.,* 1995). Since its discovery, ShK have been widely studied and several chemical modifications have been attempted in order to reach specific effect on Kv1.3, avoiding cross-selectivity with other K^+ channels (Beeton C. *et al.,* 2011). At present, an analogue of the toxin, known as Dalazatide, is on clinical trials for the treatment of several autoimmune disorders (Tarcha E.J. *et al.,* 2017). Of course, ShK is not the only toxin that is able to inhibits Kv1.3 channel and actually, the number of Kv1.3 blockers derived from animal toxins is continuously expanding. More recently, also parasitic worms have been found to secrete peptides that can target Kv1.3 channel (Chhabra S. *et al.,* 2014). Our research project, found its basis in the observation that, the parasitic nematode *Heligmosomoides polygyrus*, otherwise known as *Nematospiroides dubius,* is able to secrete ShK/SXC products that share the characteristic *ShK-like* domain, conserved among toxins that are able to inhibits the voltage-activated K^+ channel, Kv1.3. Therefore, the aim of our investigations was to unravel the pharmacological properties of two of the nine *ShK-like* peptides, found within the HES

(excretory-secretory) products of *H. polygyrus*, SXCL-1 and SXCL-6, on the voltage-activated K^+ channel, Kv1.3.

7.1.2 The pharmacological profile of SXCL-1 and SXCL-6

In Chapter 3, we elucidated the pharmacological profile of both SXCL-1 and SXCL-6 on Kv1.3 transiently expressed in tSA201 cells. Results from our investigations highlighted that both *ShK-like* peptides are able to potently inhibits the channel peak current with a pharmacological profile in the nanomolar (nM) range. SXCL-1 acts more potently at lower nanomolar concentrations (5 nM), with an IC50 of 0.6 nM. SXCL-6 is able to significantly inhibits the peak current of Kv1.3 at a concentration of 10 nM and presents an IC50 of 6 nM. Overall, the results obtained from our investigations revealed that both peptides are potent inhibitors of Kv1.3 channel and represent a novel class of the channel inhibitors, derived from a parasitic worm. The potent inhibitory effect of SXCL-1 and SXCL-6 on Kv1.3 was clear from our investigations, however little was known about the mechanism of action of the two peptides. The initial hypothesis was based on the observation that the two novel peptides, could act as pore blocker peptides and bind to the pore region of the channel, in correspondence of the external vestibule, by using functional residues, in particular a lysine (K), found within the aminoacidic sequence. In fact, both SXCL-1 and SXCL-6, share a characteristic *ShK-like* domain, comprising a 6 cysteines motif and functional Lys that we hypothesised are found at position 21 and 28, respectively. However, determining the exact mechanism of action would require the use of more sophisticated methods including molecular dynamic (MD) simulations. Nevertheless, we were interested in understanding the basis of the interaction between the peptides and the channel. Driven by the observations that both *ShK-like* peptides present a functional domain plus functional Lys within the sequences, we performed computer modelling analysis in combination with computational alanine scanning, to investigate how the peptides and the channel interact between each other, and what residues within the channel pore region are involved in this interaction. Our results conveyed to the identification of three aminoacidic sites that play a pivotal role for the interaction between the peptides and the channel. These aminoacidic residues were found to be D449, H451 and V453. Electrophysiological investigations revealed the importance of those sites in the interaction with the both SXCL-1 and SXCL-6, with a particular emphasis on the histidine at position 451. Indeed, when we created Kv1.3 mutant by substitution of the H residue with a neutral residue such as alanine (A), we did observe that the effect of both peptides was completely abolished. The results

obtained on Kv1.3_H451A conclusively indicate that the H in position 451, covers an important role in determining the affinity of the peptides for the channel. Our observations were based on knowledges of the channel residues located at the pore region that interact with functional lysine 21 and 28 for SXCL-1 and SXCL-6, respectively, yet little is known about other residues within the peptides sequences that might contribute to the binding. As such, in future prospective, we highlight the importance of conducting further investigations aimed first at elucidating the structure of the novel *ShK-like* peptides and then, at evaluating other residues within the peptides sequences that contribute to the binding to the channel. We proposed more detailed experimental routes to consider for this aim in Chapter 3 (discussion, section 3.9). Still, is important to underline the contribution of those experiments to obtain more information about the mechanism of action and the residues involved in the channel-peptides interaction that might be useful when it comes to enhance the selectivity of SXCL-1 and SXCL-6 towards the channel, eliminating the *cross-selectivity* barrier that often arises with other channels belonging to the same family.

7.1.3 The pharmacological profile of SXCL-1 and SXCL-6 on other close-related K^+ channels.

Cross-selectivity is often seen as a major limitation for several animal-derived toxins that, for this reason, fail the clinical trials or, in some cases, even the stage before. As such, is pivotal to test the peptides towards other close-related channels to make sure that no undesired effects on other channels are found. For these reasons in chapter 4, we were interested in investigating the effect of SXCL-1 and SXCL-6 on other voltage-gated K^+ channels and we considered Kv1.1, Kv1.2, Kv1.5 and Kv2.1. The results of our investigations opened up several observations: I) SXCL-1 at 5 nM, is a potent inhibitor of Kv1.3 channel and significantly reduced the average peak current of the channel. At the same concentration, SXCL-1 is able to inhibits the average peak current of Kv1.1 and Kv2.1, however at lower potency compared to the effect observed for Kv1.3. II) SXCL-6 at 5 nM, does not inhibits the average peak current of Kv1.3, but it is able to reduce the average peak current of Kv2.1 (however with no statistical significance). Furthermore, 5 nM of the peptide does not determine any inhibition in the average peak current of Kv1.1, Kv1.2 and Kv1.5. In the lights of these results, we therefore propose that SXCL-1 acts more potently towards Kv1.3 at lower nanomolar concentrations compared to SXCL-6 yet shows some cross-selectivity with Kv1.1 and Kv2.1. In the future, important investigations aimed at underlining more details about the properties of SXCL-1 and

SXCL-6, could be performed by testing higher concentrations of the peptides on the other K^+ channels considered for the investigations. For instance, answering questions like "What would happen if 10 nM of SXCL-1 would be tested on Kv1.1? Would this perhaps lead to a more potent effect of the peptide in inhibiting the channel current?" and "what would happen if 10 nM of SXCL-6 would be tested? Would this perhaps mean that we could see an effect also on the other voltage-gated K^+ channels considered?", is important to draw a complete profile for the two novel *ShK-like* peptides. Driven by those enquires, we proposed further follow up experiments that might be useful to find answers to those and other questions. Of course, one of the major points we wanted to focus the attention on was the importance of presenting peptides that are able to act potently and at lower concentrations. The evidences collected from the results of our investigations on both peptides are exhaustive and emphasise the different properties and pharmacological profile of the two peptides, SXCL-1 and SXCL-6. If we would draw a common feature between the two peptides, this would be the high and significance potency in inhibiting the average peak current of Kv1.3, however at different concentrations. No matter how we turn the prospective and observations, there will still be the cross-selectivity problem to face. The design of analogues, supported by knowledge of residues important for the selectivity of the peptides towards the channel, could represent one possible route to undertake in the future to overcome this problem.

7.2 Future prospective

The final chapter of this work is focused on preliminary data obtained using a naturally expressing Kv1.3 cell line, Jurkat cells. The aim of the whole chapter was to show some of the work that we were planning to conduct before the global pandemic started. Unfortunately, as a consequence of the current situation, we were not able to carry on, leaving the chapter as an "uncomplete" or "short" piece of work. The preliminary data obtained suggest that the two novel *ShK-like* peptides, are able to significantly inhibits the average peak current of Kv1.3 expressed in Jurkat cells. We highlight that further investigations are required in order to define a dose-response profile, IC50, for both peptides in Jurkat cells. Another important aspect that we would have liked to explore, was relevant to the ability of the peptides to inhibits IL-2 release, therefore highlighting the immunological properties that the two peptides might present. Unfortunately, reaching a complete picture from this short piece of work was challenging as such, we would like to consider those results as a basis for future route to explore in the future. However incomplete, our results suggest that the peptides are able to inhibit the

average peak current of Kv1.3 expressed in Jurkat cells and from those results further experiments, could be implemented as discussed in chapter 4-discussion.

7.3 Conclusions

The two novel peptides, SXCL-1 and SXCL-6, are potent inhibitors of the voltage-gated K^+ channel, Kv1.3. The importance of discovery novel and potent inhibitors of the channel is linked to the potential use of those inhibitors for the treatment of diseases that involve the channel. Application of Kv1.3 inhibitors for the treatment of autoimmune disorders is particularly encouraged, as it allows to design T cell-specific therapeutic strategies. This is achievable thanks to the expression of the channel in the subset of T cells involved in autoimmune diseases, the T_{EM} cells. The results obtained from our investigations suggest that both SXCL-1 and SXCL-6 derived from the parasitic nematode *H. polygyrus*, represent a novel class of Kv1.3 blockers that might be used in the future as a therapeutical approach to treat not only autoimmune diseases, but also other disorders.

Chapter 8: Appendix

10 20 30 40 50
MDERLSLLRS PPPPSARHRA HPPQRPASSG GAHTLVNHGY AEPAAGRELP
60 70 80 90 100
PDMTVVPGDH LLEPEVADGG GAPPQGGCGG GGCDRYEPLP PSLPAAGEQD
110 120 130 140 150
CCGERVVINI SGLRFETQLK TLCQFPETLL GDPKRRMRYF DPLRNEYFFD
160 170 180 190 200
RNRPSFDAIL YYYQSGGRIR RPVNVPIDIF SEEIRFYQLG EEAMEKFRED
210 220 230 240 250
EGFLREEERP LPRRDFQRQV WLLFEYPESS GPARGIAIVS VLVILISIVI
260 270 280 290 300
FCLETLPEFR DEKDYPASTS QDSFEAAGNS TSGSRAGASS FSDPFFVVET
310 320 330 340 350
LCIIWFSFEL LVRFFACPSK ATFSRNIMNL IDIVAIIPYF ITLGTELAER
360 370 380 390 400
QGNGQQAMSL AILRVIRLVR VFRIFKLSRH SKGLQILGQT LKASMRELGL
410 420 430 440 450
LIFFLFIGVI LFSSAVYFAE ADDPTSGFSS IPDAFWWAVV TMTTVGYGDM
460 470 480 490 500
HPVTIGGKIV GSLCAIAGVL TIALPVPVIV SNFNYFYHRE TEGEEQSQYM
510 520 530 540 550
HVGSCQHLSS SAEELRKARS NSTLSKSEYM VIEEGGMNHS AFPQTPFKTG
560 570
NSTATCTTNN NPNSCVNIKK IFTDV

Table 5. KCNA3_HUMAN sequence. Uniprot ID: P22001. Length: 575 aminoacidic residues. Mass (Da): 63,842

```
      10        20        30        40        50
MTVMSGENVD EASAAPGHPQ DGSYPRQADH DDHECCERVV INISGLRFET
      60        70        80        90        100
QLKTLAQFPN TLLGNPKKRM RYFDPLRNEY FFDRNRPSFD AILYYYQSGG
      110       120       130       140       150
RLRRPVNVPL DMFSEEIKFY ELGEEAMEKF REDEGFIKEE ERPLPEKEYQ
      160       170       180       190       200
RQVWLLFEYP ESSGPARVIA IVSVMVILIS IVIFCLETLP ELKDDKDFTG
      210       220       230       240       250
TVHRIDNTTV IYNSNIFTDP FFIVETLCII WFSFELVVRF FACPSKTDFF
      260       270       280       290       300
KNIMNFIDIV AIIPYFITLG TEIAEQEGNQ KGEQATSLAI LRVIRLVRVF
      310       320       330       340       350
RIFKLSRHSK GLQILGQTLK ASMRELGLLI FFLFIGVILF SSAVYFAEAE
      360       370       380       390       400
EAESHFSSIP DAFWWAVVSM TTVGYGDMYP VTIGGKIVGS LCAIAGVLTI
      410       420       430       440       450
ALPVPVIVSN FNYFYHRETE GEEQAQLLHV SSPNLASDSD LSRRSSSTMS
      460       470       480       490
KSEYMEIEED MNNSIAHYRQ VNIRTANCTT ANQNCVNKSK LLTDV
```

Table 6. KCNA1_HUMAN sequence. Uniprot ID: Q09470. Length:495 aminoacidic residues. Mass (Da):56,466

```
     10        20        30        40        50
MTVATGDPAD EAAALPGHPQ DTYDPEADHE CCERVVINIS GLRFETQLKT
      60        70        80        90       100
LAQFPETLLG DPKKRMRYFD PLRNEYFFDR NRPSFDAILY YYQSGGRLRR
     110       120       130       140       150
PVNVPLDIFS EEIRFYELGE EAMEMFREDE GYIKEEERPL PENEFQRQVW
     160       170       180       190       200
LLFEYPESSG PARIIAIVSV MVILISIVSF CLETLPIFRD ENEDMHGSGV
     210       220       230       240       250
TFHTYSNSTI GYQQSTSFTD PFFIVETLCI IWFSFEFLVR FFACPSKAGF
     260       270       280       290       300
FTNIMNIIDI VAIIPYFITL GTELAEKPED AQQGQQAMSL AILRVIRLVR
     310       320       330       340       350
VFRIFKLSRH SKGLQILGQT LKASMRELGL LIFFLFIGVI LFSSAVYFAE
     360       370       380       390       400
ADERESQFPS IPDAFWWAVV SMTTVGYGDM VPTTIGGKIV GSLCAIAGVL
     410       420       430       440       450
TIALPVPVIV SNFNYFYHRE TEGEEQAQYL QVTSCPKIPS SPDLKKSRSA
     460       470       480       490
STISKSDYME IQEGVNNSNE DFREENLKTA NCTLANTNYV NITKMLTDV
```

Table 7. KCNA2_HUMAN sequence. Uniprot ID: P16389. Length: 499. Mass (Da): 56,717

```
      10        20        30        40        50
MEIALVPLEN GGAMTVRGGD EARAGCGQAT GGELQCPPTA GLSDGPKEPA
      60        70        80        90       100
PKGRGAQRDA DSGVRPLPPL PDPGVRPLPP LPEELPRPRR PPPEDEEEEG
     110       120       130       140       150
DPGLGTVEDQ ALGTASLHHQ RVHINISGLR FETQLGTLAQ FPNTLLGDPA
     160       170       180       190       200
KRLRYFDPLR NEYFFDRNRP SFDGILYYYQ SGGRLRRPVN VSLDVFADEI
     210       220       230       240       250
RFYQLGDEAM ERFREDEGFI KEEEKPLPRN EFQRQVWLIF EYPESSGSAR
     260       270       280       290       300
AIAIVSVLVI LISIITFCLE TLPEFRDERE LLRHPPAPHQ PPAPAPGANG
     310       320       330       340       350
SGVMAPPSGP TVAPLLPRTL ADPFFIVETT CVIWFTFELL VRFFACPSKA
     360       370       380       390       400
GFSRNIMNII DVVAIFPYFI TLGTELAEQQ PGGGGGGQNG QQAMSLAILR
     410       420       430       440       450
VIRLVRVFRI FKLSRHSKGL QILGKTLQAS MRELGLLIFF LFIGVILFSS
     460       470       480       490       500
AVYFAEADNQ GTHFSSIPDA FWWAVVTMTT VGYGDMRPIT VGGKIVGSLC
     510       520       530       540       550
AIAGVLTIAL PVPVIVSNFN YFYHRETDHE EPAVLKEEQG TQSQGPGLDR
     560       570       580       590       600
GVQRKVSGSR GSFCKAGGTL ENADSARRGS CPLEKCNVKA KSNVDLRRSL
     610
YALCLDTSRE TDL
```

Table 8. KCNA5_HUMAN sequence. Uniprot ID: P22460. Length: 613. Mass (Da): 67,228

10 20 30 40 50
MPAGMTKHGS RSTSSLPPEP MEIVRSKACS RRVRLNVGGL AHEVLWRTLD
60 70 80 90 100
RLPRTRLGKL RDCNTHDSLL EVCDDYSLDD NEYFFDRHPG AFTSILNFYR
110 120 130 140 150
TGRLHMMEEM CALSFSQELD YWGIDEIYLE SCCQARYHQK KEQMNEELKR
160 170 180 190 200
EAETLREREG EEFDNTCCAE KRKKLWDLLE KPNSSVAAKI LAIISIMFIV
210 220 230 240 250
LSTIALSLNT LPELQSLDEF GQSTDNPQLA HVEAVCIAWF TMEYLLRFLS
260 270 280 290 300
SPKKWKFFKG PLNAIDLLAI LPYYVTIFLT ESNKSVLQFQ NVRRVVQIFR
310 320 330 340 350
IMRILRILKL ARHSTGLQSL GFTLRRSYNE LGLLILFLAM GIMIFSSLVF
360 370 380 390 400
FAEKDEDDTK FKSIPASFWW ATITMTTVGY GDIYPKTLLG KIVGGLCCIA
410 420 430 440 450
GVLVIALPIP IIVNNFSEFY KEQKRQEKAI KRREALERAK RNGSIVSMNM
460 470 480 490 500
KDAFARSIEM MDIVVEKNGE NMGKKDKVQD NHLSPNKWKW TKRTLSETSS
510 520 530 540 550
SKSFETKEQG SPEKARSSSS PQHLNVQQLE DMYNKMAKTQ SQPILNTKES
560 570 580 590 600
AAQSKPKEEL EMESIPSPVA PLPTRTEGVI DMRSMSSIDS FISCATDFPE
610 620 630 640 650
ATRFSHSPLT SLPSKTGGST APEVGWRGAL GASGGRFVEA NPSPDASQHS
660 670 680 690 700
SFFIESPKSS MKTNNPLKLR ALKVNFMEGD PSPLLPVLGM YHDPLRNRGS
710 720 730 740 750
AAAAVAGLEC ATLLDKAVLS PESSIYTTAS AKTPPRSPEK HTAIAFNFEA
760 770 780 790 800
GVHQYIDADT DDEGQLLYSV DSSPPKSLPG STSPKFSTGT RSEKNHFESS
810 820 830 840 850
PLPTSPKFLR QNCIYSTEAL TGKGPSGQEK CKLENHISPD VRVLPGGGAH
GSTRDQSI

Table 9. KCNB1_HUMAN sequence. Uniprot ID: Q14721. Length: 858. Mass (Da): 97,878.

Oligo Name	Sequence (5'->3')
Kv1.3_D449A_F	AACAGTGGGTTACGGCGCTATGCACCCAGTGACCAT (36)
Kv1.3_D449A_R	ATGGTCACTGGGTGCATAGCGCCGTAACCCACTGTT (36)
Kv1.3_H451A_F	GTTACGGCGATATGGCCCCAGTGACCATAG (30)
Kv1.3_H451A_R	CTATGGTCACTGGGGCCATATCGCCTAAC (30)
Kv1.3_V453A_F	TACGGCGATATGCACCCAGCGACCATAGGGGGCAAGA (37)
Kv1.3_V452A_R	TCTTGCCCCCTATGGTCGCTGGGTGCATATCGCCGTA (37)
Kv2.1_P17T_F	CGCTCCACCAGCTCGCTGACGCCCGAGCCCATGGAGATC (39)
Kv2.1_P17T_R	GATCTCCATGGGCTCGGGCGTCAGCGAGCTGGTGGAGCG (39)

Table 10. List of primers. Kv1.3_D449A (Forward and Reverse); Kv1.3_H451A (Forward and Reverse); Kv1.3_V453A (Forward and Reverse); Kv2.1_P17T (Forward and Reverse).

Chapter 9: References

Abbott, G.W. (2020) 'KCNQs: Ligand- and Voltage-Gated Potassium Channels' *Front Physiol.*, vol 11:583

Actor, J.K. (2014) 'Introductory immunology basic concepts for interdisciplinary application' 2nd edition Academy Press, pp 42-58

Adams, J. H., East, I. J., Monroy, F. G., Dobson, C. (1988). Sex-specific antigens on the surface and in the secretions of Nematospiroides dubius. *International journal for parasitology*, *18*(7), 999–1001.

Adams, M.E. (2004) 'Agatoxins: ion channel specific toxins from the American funnel web spider, Agelenopsis aperta' *Toxicon,* vol 43(5), pp 509-25

Adams, M.E., Myers, R.A., Imperial, J.S., Olivera, B.M. (1993) 'Toxityping rat brain calcium channels with omega-toxins from spider and cone snail venoms' *Biochemistry,* vol 32(47), pp 12566-70

Agwa, A.J., Henriques, S.T., Schroeder, C.I. (2017) 'Gating modifier toxin interactions with ion channels and lipid bilayers: is the trimolecular complex real?' *Neuropharmacology*, vol 127, pp 32-45 (a)

Agwa, A.J., Huang, Y.H., Craik, D.J., Henriques, S.T., Schroeder, C.I. (2017) 'Lengths of the C-terminus and interconnecting loops impact stability of spider-derived gating modifier toxins' *Toxins*, vol 9(8), 248. (b)

Agwa, A.J., Lawrence, N., Deplazes, E., Cheneval, O., Chen, R.M., Craik, D.J., Schroeder, C.I., Henriques, S.T. (2017) 'Spider peptide toxin HwTx-IV engineered to bind to lipid membranes has an increased inhibitory potency at human voltage-gated sodium channel hNaV1.7' *Biochim Biophys Acta Biomembr*., vol 1859(5), pp 835-844 (c)

Ahmed, R., Bevan, M.J., Reiner, S.L., Fearon, D.T. (2009) 'The precursors of memory: models and controversies' *Nat Rev Immunol*., vol 9(9), pp 662-8

Al-Sabi, A., Kaza, S. K., Dolly, J. O.,Wang, J. (2013). 'Pharmacological characteristics of Kv1.1- and Kv1.2-containing channels are influenced by the stoichiometry and positioning of their α subunits.' *The Biochemical journal*, *454*(1), 101–108.

Alberts B, Johnson A, Lewis J, et al. (2002) 'Molecular Biology of the Cell.' 4th edition. New York: Garland Science. Helper T Cells and Lymphocyte Activation. Available from: https://www.ncbi.nlm.nih.gov/books/NBK26827/

Alessandri-Haber, N., Lecoq, A., Gasparini, S., Grangier-Macmath, G., Jacquet, G., Harvey, A.L., de Medeiros, C., Rowan, E.G., Gola, M., Ménez, A., Crest, M. (1999) 'Mapping the functional anatomy of BgK on Kv1.1, Kv1.2, and Kv1.3. Clues to design analogs with enhanced selectivity' *J Biol Chem.*, vol 274(50), pp 35653-61

Alexandre-Silva, G. M., Brito-Souza, P. A., Oliveira, A., Cerni, F. A., Zottich, U., Pucca, M. B. (2018). 'The hygiene hypothesis at a glance: Early exposures, immune mechanism and novel therapies.' *Acta tropica*, *188*, 16–26.

Allegretta, M., Nicklas, J.A., Sriram, S., Albertini, R.J. (1990) 'T cells responsive to myelin basic protein in patients with multiple sclerosis' *Science,* vol 247(4943), pp 718-21

Allen, N. M., Conroy, J., Shahwan, A., Lynch, B., Correa, R. G., Pena, S. D., McCreary, D., Magalhães, T. R., Ennis, S., Lynch, S. A., King, M. D. (2016). 'Unexplained early onset epileptic encephalopathy: Exome screening and phenotype expansion.' *Epilepsia*, *57*(1), e12–e17.

Almeida, A.J., Souto, E. (2007). 'Solid lipid nanoparticles as a drug delivery system for peptides and proteins.' *Advanced Drug Delivery Reviews,* 59 (6), 478-490.

Alvarez-Baron, C.P., Jonsson, P., Thomas, C., Dryer, S.E., Williams, C. (2011) 'The two-pore domain potassium channel KCNK5: induction by estrogen receptor alpha and role in proliferation of breast cancer cells' *Mol Endocrinol.,* vol 25(8), pp 1326-36

Anderson, C.S., MacKinnon, R., Smith, C., Miller, C. (1988) 'Charybdotoxin block of single Ca^{2+}-activated K^{+} channels. Effects of channel gating, voltage, and ionic strength' *J Gen Physiol.,* vol 91(3), pp 317-33

Andreotti, N., di Luccio, E., Sampieri, F., De Waard, M., Sabatier, J.M. (2005) 'Molecular modeling and docking simulations of scorpion toxins and related analogs on human SKCa2 and SKCa3 channels' *Peptides*, 26:1095–1108.

Anthony, R. M., Rutitzky, L. I., Urban, J. F., Jr, Stadecker, M. J., Gause, W. C. (2007). 'Protective immune mechanisms in helminth infection.' *Nature reviews. Immunology*, *7*(12), 975–987.

Antosova, Z., Mackova, M., Kral, V., Macek, T. (2009). 'Therapeutic application of peptides and proteins: parenteral forever?' *Trends in biotechnology*, *27*(11), 628–635.

Ariotti, S., Haanen, J.B., Schumacher, T.N. (2012) 'Behavior and function of tissue-resident memory T cells' *Adv Immunol.*, vol 114, pp 203-16

Armstong, C.M. (1975) 'Ionic pores, gates and gating currents' *Q. Rev. Biophys.*, vol 7 (2), pp 179-210

B.M. Olivera (1997) 'E.E. Just Lecture, 1996. Conus venom peptides, receptor and ion channel targets, and drug design: 50 million years of neuropharmacology' *Molecular biology of the cell*, *8*(11), 2101–2109.

Baby, J., Jency, G. (2012) 'Scorpion toxins and its applications' *International Journal of Toxicological and Pharmacological research*, vol 4(3), pp 57-61

Bajaj S., Han J. (2019). Venom-Derived Peptide Modulators of Cation-Selective Channels: Friend, Foe or Frenemy. *Frontiers in pharmacology*, *10*, 58.

Barros, F., Domínguez, P., de la Peña, P. (2012). 'Cytoplasmic domains and voltage-dependent potassium channel gating.' *Frontiers in pharmacology*, *3*, 49.

Batard P, Jordan M, Wurm F. (2001). 'Transfer of high copy number plasmid into mammalian cells by calcium phosphate transfection.' *Gene*, 270(1-2), 61-8.

Batista C.V., Gómez-Lagunas, F., Rodríguez de la Vega, R.C., Hajdu, P., Panyi, G., Gáspár, R., Possani, L.D. (2002) 'Two novel toxins from the Amazonian scorpion Tityus cambridgei that block Kv1.3 and Shaker B K(+)-channels with distinctly different affinities' *Biochim Biophys Acta*, vol 1601(2), pp 123-31

Beeler, G.W. Jr, Reuter, H. (1970) 'Voltage clamp experiments on ventricular myocarial fibres' *J Physiol.* vol 207(1), pp 165-90

Beeton, C., Pennington, M. W., Norton, R. S. (2011). 'Analogs of the sea anemone potassium channel blocker ShK for the treatment of autoimmune diseases.' *Inflammation & allergy drug targets*, vol *10*(5), pp 313–321.

Beeton, C., Pennington, M. W., Wulff, H., Singh, S., Nugent, D., Crossley, G., Khaytin, I., Calabresi, P. A., Chen, C. Y., Gutman, G. A., Chandy, K. G. (2005). 'Targeting effector memory T cells with a selective peptide inhibitor of Kv1.3 channels for therapy of autoimmune diseases.' *Molecular pharmacology*, *67*(4), 1369–1381.

Beeton, C., Wulff, H., Singh, S., Botsko, S., Crossley, G., Gutman, G. A., Cahalan, M. D., Pennington, M., Chandy, K. G. (2003). 'A novel fluorescent toxin to detect and investigate Kv1.3 channel up-regulation in chronically activated T lymphocytes.' *The Journal of biological chemistry*, *278*(11), 9928–9937.

Beeton, C., Wulff, H., Standifer, N. E., Azam, P., Mullen, K. M., Pennington, M. W., Kolski-Andreaco, A., Wei, E., Grino, A., Counts, D. R., Wang, P. H., LeeHealey, C. J., S Andrews, B., Sankaranarayanan, A., Homerick, D., Roeck, W. W., Tehranzadeh, J., Stanhope, K. L., Zimin, P., Havel, P. J., … Chandy, K. G. (2006). 'Kv1.3 channels are a therapeutic target for T cell-mediated autoimmune diseases.' *Proceedings of the National Academy of Sciences of the United States of America*, *103*(46), 17414–17419.

Behnke, J. M., Menge, D. M., & Noyes, H. (2009). 'Heligmosomoides bakeri: a model for exploring the biology and genetics of resistance to chronic gastrointestinal nematode infections.' *Parasitology*, *136*(12), 1565–1580.

BenNasr Hmed, Hammami Turky Serria, Zeghal Khaled Mounir (2013) 'Scorpion Peptides: potential use for new drug development" Journal of Toxicology, vol. 2013, 15 pages.

Benoît, R. (2017) 'Ion channel and ion selectivity Essays in Biochemistry' *Essays Biochem.,* vol 61 (2), pp 201-209

Benton, D. C., Garbarg, M., Moss, G. W. (2013). 'The relationship between functional inhibition and binding for K(Ca)2 channel blockers.' *PloS one*, *8*(9), e73328.

Beraud, E., Viola, A., Regaya, I., Confort-Gouny, S., Siaud, P., Ibarrola, D., Le Fur, Y., Barbaria, J., Pellissier, J. F., Sabatier, J. M., Medina, I., Cozzone, P. J. (2006) 'Block of neural Kv1.1 potassium channels for neuroinflammatory disease therapy' *Annals of neurology*, vol 60(5), pp 586–596.

Berndt K.D., Guntert P., Wuthrich K. (1993) 'Nuclear magnetic Resonance solution structure of Dendrotoxin K from the venom of Dendroaspis polylepis polylepis' *J. Mol. Biol*., vol 234 (3) pp 735-750

Bernstein, J. (1902) 'Untersuchungen zur Thermodynamik der bioelektrischen Stro€me' *Pflugers Arch,* vol 92, pp 521–562

Bernstein, J. (1912) 'Elektrobiologie. Die Lehre von den elektrischen Vorgangen im Organismus auf moderner Grundlagen dargestelt' 1st Edition, Braunschweig, Vieweg & Sohn.

Bethony, J., Brooker, S., Albonico, M., Geiger, S. M., Loukas, A., Diemert, D., & Hotez, P. J. (2006). 'Soil-transmitted helminth infections: ascariasis, trichuriasis, and hookworm.' *Lancet (London, England)*, *367*(9521), 1521–1532.

Bezanilla, F. (2008) 'How membrane proteins sense voltage' *Nat Rev Mol Cell Biol*, vol 9 (4), pp 323–332 (b)

Bezanilla, F. (2008) ‘Ion Channels: From Conductance to Structure’ *Neuron*, vol 60(3), pp 456-468 (a)

Bezanilla F. (2000) ‘The voltage sensor in voltage-dependent ion channels’ Physiological reviews, 80 (2), 555-592

Bhargava, P., Calabresi, P.A. (2015) ‘Novel therapies for memory cells in autoimmune diseases’ *Clin Exp Immunol.,* vol 180(3), pp 353-360

Bhattacharjee, P., Bhattacharyya, D. (2014) ‘Therapeutic Use of Snake Venom Components: A Voyage from Ancient to Modern India’ *Mini-Reviews in Organic Chemistry*, vol 11 (1), 45

Bichet, D., Haass, F.A., Jan, L.Y. (2003) ‘Merging functional studies with structures of inward-rectifier K^+channels’ Nat Rev Neurosci vol 4(12), pp 957–967

Bixby, K. A., Nanao, M. H., Shen, N. V., Kreusch, A., Bellamy, H., Pfaffinger, P. J., Choe, S. (1999). ‘Zn2+-binding and molecular determinants of tetramerization in voltage-gated K+ channels.’ *Nature structural biology*, *6*(1), 38–43.

Bloomfield, S. F., Stanwell-Smith, R., Crevel, R. W., & Pickup, J. (2006). ‘Too clean, or not too clean: the hygiene hypothesis and home hygiene.’ *Clinical and experimental allergy : journal of the British Society for Allergy and Clinical Immunology*, *36*(4), 402–425

Bordon, K.C.F., Cologna, C.T., Fornari-Baldo, E.C., Pinheiro-Júnior, E.L., Cerni, F.A., Amorim, F.G., Anjolette, F.A.P., Cordeiro, F.A., Wiezel, G.A., Cardoso, I.A., Ferreira, I.G., de Oliveira, I.S., Boldrini-França, J., Pucca, M.B., Baldo, M.A., Arantes, E.C. (2020) ‘From Animal Poisons and Venoms to Medicines: Achievements, Challenges and Perspectives in Drug Discovery’ *Front Pharmacol*., vol 11, 113

Bortner, C.D., Cidlowski, J.A. (2014) ‘Ion channels and apoptosis in cancer’ *Philos Trans R Soc Lond B Biol Sci*., vol 369(1638): 20130104.

Bosmans, F., Martin-Eauclaire, M. F., Swartz, K. J. (2008). ‘Deconstructing voltage sensor function and pharmacology in sodium channels.’ *Nature*, vol 456(7219), pp 202–208.

Bosmans, F., Rash, L., Zhu, S., Diochot, S., Lazdunski, M., Escoubas, P., Tytgat, J. (2006) 'Four novel tarantula toxins as selective modulators of voltage-gated sodium channel subtypes' *Mol. Pharmacol.*, vol 69 (2), pp 419–429.

Bosmans, F., Swartz, K.J. (2010) 'Targeting voltage sensors in sodium channels with spider toxins' *Trends in Pharmacological Sciences*, vol 31 (4), pp 175-182

Bosmans, F., Tytgat, J. (2007) 'Sea anemone venom as a source of insecticidal peptides acting on voltage-gated Na^+ channels' *Toxicon*, vol 49 (4) pp. 550-560

Braun, A.P. (2012) 'Two-pore domain potassium channels: variation on a structural theme' Channels (Austin) vol 6(3), pp 139-140

Brohawn, S.G., del Mármol, J., MacKinnon, R. (2012) 'Crystal structure of the human K2P TRAAK, a lipid- and mechano-sensitive K+ ion channel' *Science,* vol 335(6067), pp 436-41

Brown, D.A., Gähwiler, B.H., Griffith, W.H., Halliwell, J.W. (1990) 'Chapter 11: Membrane currents in hippocampal neurons' Progress in Brain Research vol 83, pp 141-160, Elsevier

Browne, D. L., Gancher, S. T., Nutt, J. G., Brunt, E. R., Smith, E. A., Kramer, P., Litt, M. (1994) 'Episodic ataxia/myokymia syndrome is associated with point mutations in the human potassium channel gene, KCNA1' *Nature genetics*, vol 8(2), pp 136–140.

Brugada, R., Hong, K., Dumaine, R., Cordeiro, J., Gaita, F., Borggrefe, M., Menendez, T. M., Brugada, J., Pollevick, G. D., Wolpert, C., Burashnikov, E., Matsuo, K., Wu, Y. S., Guerchicoff, A., Bianchi, F., Giustetto, C., Schimpf, R., Brugada, P., & Antzelevitch, C. (2004). 'Sudden death associated with short-QT syndrome linked to mutations in HERG.' *Circulation*, *109*(1), 30–35.

Burkhard, P., Stetefeld, J., Strelkov, S.V. (2001) 'Coiled coils: a highly versatile protein folding motif' *Trends Cell Biol*., vol 11(2), pp 82-8

Burns, J., Bartholomew, B., Lobo, S. (1999) 'Isolation of myelin basic protein-specific T cells predominantly from the memory T-cell compartment in multiple sclerosis' *Ann Neurol*., vol 45(1), pp 33-9

Butler, A., Helliwell, M. V., Zhang, Y., Hancox, J. C., Dempsey, C. E. (2020). 'An Update on the Structure of hERG.' *Frontiers in pharmacology*, *10*, 1572.

Cahalan, M.D., Chandy, K.G. (2009) 'The functional network of ion channels in T lymphocytes' *Immunol Rev.*, vol 231(1), pp 59-87.

Cahalan, M.D., Chandy, K.G., DeCoursey, T.E., Gupta, S.A. (1985) 'Voltage-gated potassium channel in human T lymphocytes' *J Physiol*., vol 358, pp 197–237

Caliskan, F., Quintero-Hernández, V., Restano-Cassulini, R., Coronas-Valderrama, F.I., Corzo, G., Possani, L.D. (2013) 'Molecular cloning and biochemical characterization of the first Na ($^{+}$)-channel α-type toxin peptide (Acra4) from Androctonus crassicauda scorpion venom' *Biochimie.,* vol 95(6), pp 1216-22

Campuzano, O., Fernandez-Falgueras, A., Lemus, X., Sarquella-Brugada, G., Cesar, S., Coll, M., Mates, J., Arbelo, E., Jordà, P., Perez-Serra, A., Del Olmo, B., Ferrer-Costa, C., Iglesias, A., Fiol, V., Puigmulé, M., Lopez, L., Pico, F., Brugada, J., & Brugada, R. (2019). 'Short QT Syndrome: A Comprehensive Genetic Interpretation and Clinical Translation of Rare Variants.' *Journal of clinical medicine*, *8*(7), 1035.

Cao, Z., Di, Z., Wu, Y., Li, W. (2014) 'Overview of scorpion species from China and their toxins' *Toxins* (Basel), vol 6(3), pp 796-815

Carbone, E., Wanke, E., Prestipino, G., Possani, L.D., Maelicke, A. (1982) 'Selective blockage of voltage-dependent K^{+} channels by a novel scorpion toxin' *Nature*, vol 296, 90–91

Cardoso, F.C, Dekan, Z., Rosengren, K.J., Erickson, A., Vetter, I., Deuis, J., Herzig, V., Alewood, P., King, G.F., Lewis, R.J. (2015) 'Identification and characterization of ProTx-III [μ-TRTX-Tp1a], a new voltage-gated sodium channel inhibitor from venom of the tarantula Thrixopelma pruriens' *Mol. Pharmacol.,* vol 88(2), pp 291–303.

Cardoso, F.C., Lewis, R.J. (2019) ‘Structure–Function and therapeutic potential of spider venom-derived cysteine knot peptides targeting sodium channels’ *Front. Pharmacol*., vol 10, 366

Carmeliet, E. (2019) ‘From Bernstein's rheotome to Neher-Sakmann's patch electrode. The action potential’ *Physiol Rep.*, vol 7(1), e13861

Castañeda, O., Sotolongo, V., Amor, A.M., Stöcklin, R., Anderson, A.J., Harvey, A.L., Engström, A., Wernstedt, C., Karlsson, E. (1995) ‘Characterization of a potassium channel toxin from the Caribbean Sea anemone Stichodactyla helianthus’ *Toxicon*, vol 33(5), pp 603-13

Castle, N. A., London, D. O., Creech, C., Fajloun, Z., Stocker, J. W., Sabatier, J. M. (2003). ‘Maurotoxin: a potent inhibitor of intermediate conductance Ca2+-activated potassium channels.’ *Molecular pharmacology*, *63*(2), 409–418.

Catalog,W.S. World Spider Catalog. Available online: https://wsc.nmbe.ch/statistics/ (Accessed online on 22 December 2020)

Catterall, W. A., Cestèle, S., Yarov-Yarovoy, V., Yu, F. H., Konoki, K., Scheuer, T. (2007). ‘Voltage-gated ion channels and gating modifier toxins.’ *Toxicon: official journal of the International Society on Toxinology*, *49*(2), 124–141.

Catterall, W.A. (1986) ‘Voltage-dependent gating of sodium channels: correlating structure and function’ *Trends Neurosci.,* vol 9, pp 7–10 (b)

Catterall, W.A. (2010) ‘Ion channel voltage sensors: structure, function, and pathophysiology’ *Neuron,* vol 67(6), pp 915-928

Catterall, WA. (1986) ‘Molecular properties of voltage-sensitive sodium channels’ *Annu. Rev. Biochem.*, vol 55, pp 953–985 (a)

Cerni, F.A., Pucca, M.B., Peigneur, S., Cremonez, C.M., Bordon, K.C., Tytgat, J., arantes, E.C. (2014) ‘Electrophysiological characterization of Ts6 and Ts7, K+ channel toxins isolated through an improved Tityus serrulatus venom purification procedure’ *Toxins,* vol 6(3), pp 892-913

Chandy, K. G. (1998). 'ShK-Dap22, a potent Kv1.3-specific immunosuppressive polypeptide.' *The Journal of biological chemistry*, *273*(49), 32697–32707.

Chandy, K. G., DeCoursey, T. E., Cahalan, M. D., McLaughlin, C., Gupta, S. (1984). 'Voltage-gated potassium channels are required for human T lymphocyte activation.' *The Journal of experimental medicine*, *160*(2), 369–385.

Chandy, K. G., Norton, R. S. (2017). 'Peptide blockers of $K_v1.3$ channels in T cells as therapeutics for autoimmune disease.' *Current opinion in chemical biology*, *38*, 97–107

Chandy, K. G., Wulff, H., Beeton, C., Pennington, M., Gutman, G. A., Cahalan, M. D. (2004). 'K+ channels as targets for specific immunomodulation.' *Trends in pharmacological sciences*, *25*(5), 280–289.

Chandy, K.G., Cahalan, M., Pennington, M., Norton, R.S., Wulff, H., Gutman, G.A. (2001) 'Potassium channels in T lymphocytes: toxins to therapeutic immunosuppressants' *Toxicon*, vol 39(9), pp 1269-76

Chang, S. C., Huq, R., Chhabra, S., Beeton, C., Pennington, M. W., Smith, B. J., Norton, R. S. (2015). 'N-Terminally extended analogues of the K^+ channel toxin from Stichodactyla helianthus as potent and selective blockers of the voltage-gated potassium channel Kv1.3.' *The FEBS journal*, *282*(12), 2247–2259.

Chang, S.C., Bajaj, S., Chandy, K.G. (2018) 'ShK toxin: history, structure and therapeutic applications for autoimmune diseases' *WikiJourn. of Science*, vol 1(1), 3

Chapman, M. L., Krovetz, H. S., & VanDongen, A. M. (2001). 'GYGD pore motifs in neighbouring potassium channel subunits interact to determine ion selectivity.' *The Journal of physiology*, *530*(Pt 1), 21–33.

Chen C, Okayama H. (1987). 'High-efficiency transformation of mammalian cells by plasmid DNA.' *Mol Cell Biol.,* 7(8):2745-52.

Chen, M., Li, J., Zhang, F., Liu, Z. (2014) 'Isolation and characterization of SsmTx-I, a specific Kv2.1 blocker from the venom of the centipede Scolopendra Subspinipes Mutilans L. Koch' *J. Pept. Sci.*, vol 20 (3), pp 159–164

Chen, N., Xu, S., Zhang, Y., Wang, F. (2018) 'Animal protein toxins: origins and therapeutic applications' *Biophys Rep*., vol 4(5), pp 233-242

Chen, R., Chung, S. H. (2014). 'Binding modes of two scorpion toxins to the voltage-gated potassium channel kv1.3 revealed from molecular dynamics.' *Toxins*, *6*(7), 2149–2161

Chen, R., Chung, S. H. (2018) 'Inhibition of Voltage-Gated K^+ Channel Kv1.5 by Antiarrhythmic Drugs.' *Biochemistry*, vol 57(18), pp 2704–2710.

Chen, R., Chung, S.H. (2012) 'Engineering a potent and specific blocker of voltage-gated potassium channel Kv1.3, a target for autoimmune diseases' *Biochemistry,* vol 51(9), pp 1976-82

Chen, R., Robinson, A., Gordon, D., Chung, S.H. (2011) 'Modeling the binding of three toxins to the voltage-gated potassium channel (Kv1.3)' *Biophys J.*, vol 101(11), pp 2652-60

Cheng, L., Yung, A., Covarrubias, M., Radice, G.L. (2011) 'Cortactin is required for N-cadherin regulation of Kv1.5 channel function' *J Biol Chem*, vol 286(23), pp 20478 –20489

Chhabra, S., Chang, S. C., Nguyen, H. M., Huq, R., Tanner, M. R., Londono, L. M., Estrada, R., Dhawan, V., Chauhan, S., Upadhyay, S. K., Gindin, M., Hotez, P. J., Valenzuela, J. G., Mohanty, B., Swarbrick, J. D., Wulff, H., Iadonato, S. P., Gutman, G. A., Beeton, C., Pennington, M. W., … Chandy, K. G. (2014). 'Kv1.3 channel-blocking immunomodulatory peptides from parasitic worms: implications for autoimmune diseases.' *FASEB journal: official publication of the Federation of American Societies for Experimental Biology*, *28*(9), 3952–3964.

Upadhyay, S. K., Lakey, J. T., Iadonato, S., Wulff, H., Beeton, C., & Chandy, K. G. (2012). 'Development of a sea anemone toxin as an immunomodulator for therapy of autoimmune diseases.' *Toxicon : official journal of the International Society on Toxinology*, *59*(4), 529–546.

Chi, V., Pennington, M.W., Norton, R.S., Tarcha, E.J., Londono, L.M., Sims-Fahey, B., Upadhyay, S.K., Lakey, J.T., Iadonato, S., Wulff, H., Beeton, C., Chandy, K.G. (2012) 'Development of a sea anemone toxin as an immunomodulator for therapy of autoimmune diseases' *Toxicon*, vol 59(4), pp 529-46

Chippaux, J.P., Goyffon, M. (2008) 'Epidemiology of scorpionism: a global appraisal' *Acta Trop.*, vol 107(2), pp 71-9

Choi, K. D., Choi, J. H. (2016) 'Episodic Ataxias: Clinical and Genetic Features' *Journal of movement disorders*, vol 9(3), pp 129–135.

Chu, Y., Qiu, P., Yu, R. (2020) 'Centipede Venom Peptides Acting on Ion Channels' *Toxins,* vol 12(4), 230.

Clark, G.C., Casewell, N.R., Elliott, C.T., Harvey, A.L., Jamieson, A.G., Strong, P.N., Turner, A. D. (2019) 'Friends or Foes? Emerging Impacts of Biological Toxins' *Trends in Biochemical Sciences,* vol 44 (4), pp 365-379

Coetzee, W. A., Amarillo, Y., Chiu, J., Chow, A., Lau, D., McCormack, T., Moreno, H., Nadal, M. S., Ozaita, A., Pountney, D., Saganich, M., Vega-Saenz de Miera, E., Rudy, B. (1999). 'Molecular diversity of K+ channels.' *Annals of the New York Academy of Sciences*, *868*, 233–285.

Cole, K.S., Curtis, H.J. (1939) 'Electric impedance of the squid giant axon during activity' *J Gen Physiol.,* vol 22(5), pp 649-70

Coleman, S. K., Newcombe, J., Pryke, J., Dolly, J. O. (1999). 'Subunit composition of Kv1 channels in human CNS.' *Journal of neurochemistry*, *73*(2), 849–858.

Collingridge, G.L., Olsen, R.W., Peters, J., Spedding, M. (2009) 'A nomenclature for ligand-gated ion channels' *Neuropharmacology*, vol 56 (1), pp 2-5

Columbus-Shenkar, Y.Y., Sachkova, M.Y., Macrander, J., Fridrich, A., Modepalli, V., Reitzel, A.M., Sunagar, K., Moran, Y. (2018) 'Dynamics of venom composition across a complex life cycle' *Elife*, vol 7, e35014

Cooper P. J. (2009). 'Interactions between helminth parasites and allergy.' *Current opinion in allergy and clinical immunology*, *9*(1), 29–37.

Corona, M., Gurrola, G. B., Merino, E., Cassulini, R. R., Valdez-Cruz, N. A., García, B., Ramírez-Domínguez, M. E., Coronas, F. I., Zamudio, F. Z., Wanke, E., Possani, L. D. (2002). 'A large number of novel Ergtoxin-like genes and ERG K+-channels blocking peptides from scorpions of the genus Centruroides.' *FEBS letters*, *532*(1-2), 121–126.

Correale, J., Farez, M. F. (2007) "Association between parasite infection and immune responses in multiple sclerosis "*Annals of neurology* vol 61(2), pp 97–108

Correale, J., Farez, M. F. (2011) "The impact of parasite infections on the course of multiple sclerosis" *Journal of Neuroimmun,* vol 233 (1-2), pp 6-11

Corzo, G., Escoubas, P. (2003) 'Pharmacologically active spider peptide toxins' CMLS, *Cell. Mol. Life Sci,.* vol 60, 2409–2426

Cotton, J., Crest, M., Bouet, F., Alessandri, N., Gola, M., Forest, E., Karlsson, E., Castañeda, O., Harvey, A. L., Vita, C., Ménez, A. (1997) "A potassium-channel toxin from the sea anemone *Bunodosoma granulifera*, an inhibitor for Kv1 channels. Revision of the amino acid sequence, disulfide-bridge assignment, chemical synthesis, and biological activity" *European journal of biochemistry,* vol *244*(1), pp 192–202

Coutinho, A. E., Chapman, K. E. (2011). 'The anti-inflammatory and immunosuppressive effects of glucocorticoids, recent developments and mechanistic insights.' *Molecular and cellular endocrinology*, vol *335*(1), pp 2–13.

Cremonez, C. M., Maiti, M., Peigneur, S., Cassoli, J. S., Dutra, A. A., Waelkens, E., Lescrinier, E., Herdewijn, P., de Lima, M. E., Pimenta, A. M., Arantes, E. C., Tytgat, J. (2016) 'Structural

and Functional Elucidation of Peptide Ts11 Shows Evidence of a Novel Subfamily of Scorpion Venom Toxins' *Toxins*, vol *8*(10), pp 288.

Crest, M., Jacquet, G., Gola, M., Zerrouk, H., Benslimane, A., Rochat, H., Mansuelle, P., Martin-Eauclaire, M.F.(1992) 'Kaliotoxin, a novel peptidyl inhibitor of neuronal BK-type $Ca(^{2+})$-activated K^+ channels characterized from Androctonus mauretanicus mauretanicus venom' *J Biol Chem*., vol 267(3), pp 1640-7

Cunningham, K.P., Holden, R.G., Escribano-Subias, P.M., Cogolludo, A., Veale, E.L., Mathie, A. (2019) 'Characterization and regulation of wild-type and mutant TASK-1 two pore domain potassium channels indicated in pulmonary arterial hypertension' *The Journal of physiology*, *597*(4), 1087–1101.

Curran, M. E., Splawski, I., Timothy, K. W., Vincent, G. M., Green, E. D., Keating, M. T. (1995). 'A molecular basis for cardiac arrhythmia: HERG mutations cause long QT syndrome.' *Cell*, *80*(5), 795–803.

Cushman, D. W., Cheung, H. S., Sabo, E. F., Ondetti, M. A. (1977) 'Design of potent competitive inhibitors of angiotensin-converting enzyme. Carboxyalkanoyl and mercaptoalkanoyl amino acids' *Biochemistry*, vol 16 (25), pp 5484–5491

Cushman, D. W., Ondetti, M. A. (1999) 'Design of angiotensin converting enzyme inhibitors' *Nat. Med*., vol 5(10), pp 1110–1113

Cushman, S. J., Nanao, M. H., Jahng, A. W., DeRubeis, D., Choe, S., Pfaffinger, P. J. (2000). 'Voltage dependent activation of potassium channels is coupled to T1 domain structure.' *Nature structural biology*, *7*(5), 403–407.

D'Adamo, M. C., Liantonio, A., Rolland, J. F., Pessia, M., Imbrici, P. (2020) 'Kv1.1 Channelopathies: Pathophysiological Mechanisms and Therapeutic Approaches' *International journal of molecular sciences*, vol 21(8), pp 2935.

Damak, M., Riant, F., Boukobza, M., Tournier-Lasserve, E., Bousser, M. G., Vahedi, K. (2009) 'Late onset hereditary episodic ataxia' *Journal of neurology, neurosurgery, and psychiatry*, vol 80(5), pp 566–568.

Das Gupta, S., Debnath, A., Saha, A., Giri, B., Tripathi, G., Vedasiromoni, J.R., Gomes, A., Gomes, A. (2006) 'Indian black scorpion (Heterometrus bengalensis Koch) venom induced antiproliferative and apoptogenic activity against human leukemic cell lines U937 and K562' Leuk Res. vol 31(6), pp 817-25

Dauplais, M., Lecoq, A., Song, J., Cotton, J., Jamin, N., Gilquin, B., Roumestand, C., Vita, C., de Medeiros, C.L., Rowan, E.G., Harvey, A.L., Ménez, A. (1997) 'On the convergent evolution of animal toxins. Conservation of a diad of functional residues in potassium channel-blocking toxins with unrelated structures' J Biol Chem. vol 272(7), pp 4302-9

Davis M.M., Bjorkmant, P.J. (1998) 'T-cell antigen receptor genes and T-cell recognition' Nature vol 334 (6181), pp 395-402

de Freitas, J.C., Sawaya, M.I. (1989) 'Anomalies in sea-urchin egg development induced by a novel purine isolated from the sea-anemone Bunodosoma caissarum' Toxicon. vol 24(8), pp 751-5

de Kovel, C., Syrbe, S., Brilstra, E. H., Verbeek, N., Kerr, B., Dubbs, H., Bayat, A., Desai, S., Naidu, S., Srivastava, S., Cagaylan, H., Yis, U., Saunders, C., Rook, M., Plugge, S., Muhle, H., Afawi, Z., Klein, K. M., Jayaraman, V., Rajagopalan, R., … Koeleman, B. (2017). Neurodevelopmental Disorders Caused by De Novo Variants in KCNB1 Genotypes and Phenotypes. *JAMA neurology*, *74*(10), 1228–1236.

de Silva, N. R., Brooker, S., Hotez, P. J., Montresor, A., Engels, D., Savioli, L. (2003). Soil-transmitted helminth infections: updating the global picture. *Trends in parasitology*, *19*(12), 547–551.

DeBin, J.A., Strichartz, G.R. (1991) 'Chloride channel inhibition by the venom of the scorpion Leiurus quinquestriatus' Toxicon vol 29(11), pp 1403-8

DeCoursey, T. E., Chandy, K. G., Gupta, S., Cahalan, M. D. (1984). Voltage-gated K^+ channels in human T lymphocytes: a role in mitogenesis? *Nature*, *307*(5950), 465–468.

del Camino, D., Yellen, G. (2001) ‘Tight steric closure at the intracellular activation gate of a voltage-gated K^+ channel’. Neuron vol 20; 32(4), pp 649-56

Delepierre, M., Prochnicka-Chalufour, A., Possani, L.D. (1997) ‘A novel potassium channel blocking toxin from the scorpion Pandinus imperator: A 1H NMR analysis using a nano-NMR probe’ Biochemistry vol 36(9), pp 2649-58

Deutsch, C., Krause, D., Lee, S. C. (1986). Voltage-gated potassium conductance in human T lymphocytes stimulated with phorbol ester. *The Journal of physiology*, *372*, 405–423.

Devarajan, P., Chen, Z. (2013) ‘Autoimmune effector memory T cells: the bad and the good’ Immunol Res. vol 57(1-3), pp 12-22

Dias, G. S., Kitano, E. S., Pagotto, A. H., Sant'anna, S. S., Rocha, M. M., Zelanis, A., Serrano, S. M.T. (2013) ’Individual variability in the venom proteome of juvenile Bothrops jararaca specimens’ J. Proteome Res. 12(10), 4585–4598

Diego-García, E., Abdel-Mottaleb, Y., Schwartz, E.F., Rodríguez de la Vega, R.C., Tytgat, T., Possani, L.D. (2008) ‘Cytolytic and K^+ channel blocking activities of β-KTx and scorpine-like peptides purified from scorpion venoms’ Cell. Mol. Life Sci. vol 65, 187

Ding, L., Chen, J., Hao, J., Zhang, J., Huang, X., Hu, F., Wu, Z., Liu, Y., Li, W., Cao, Z., Wu, Y., Li, J., Li, S., Liu, H., Wu, W., Chen, Z. (2017). Discovery of three toxin peptides with Kv1.3 channel and IL-2 cytokine-inhibiting activities from Non-Buthidae scorpions, Chaerilus tricostatus and Chaerilus tryznai. *Peptides*, *91*, 13–19.

Diochot, S., Drici, M.D., Moinier, D., Fink, M., Lazdunski, M. (1999) ‘Effects of phrixotoxins on the Kv4 family of potassium channels and implications for the role of Ito1 in cardiac electrogenesis’ Br J Pharmacol. vol 126(1), pp 251-63

Diochot, S., Loret, E., Bruhn, T., Béress, L., Lazdunski, M. (2003). APETx1, a new toxin from the sea anemone Anthopleura elegantissima, blocks voltage-gated human ether-a-go-go-related gene potassium channels. *Molecular pharmacology*, *64*(1), 59–69.

Dodson, P. D., Forsythe, I. D. (2004) 'Presynaptic K+ channels: electrifying regulators of synaptic terminal excitability' *Trends in neurosciences*, vol *27*(4), pp 210–217.

Doley, R., Kini, R.M. (2009) 'Protein complexes in snake venom' Cell Mol Life Sci. vol 66(17), pp 2851-71

Domingos Possani, L., Martin, B.M., Svendsen, I. (1982) 'The primary structure of noxiustoxin: A K^+ channel blocking peptide, purified from the venom of the scorpion Centruroides noxius Hoffmann' Carlsberg Res. Commun. vol 47, 285–289

Dongol Y., Cardoso, F.C., Lewis, R.J. (2019) 'Spider knottin pharmacology at voltage-gated sodium channels and their potential to modulate pain pathways' Toxins vol 11(11), 626

Dorian P. (2003) 'Antiarrhythmic drug therapy of atrial fibrillation: focus on new agents' *Journal of cardiovascular pharmacology and therapeutics*, vol 8 (1), pp S27–S31.

Döring, F., Scholz, H., Kühnlein, R.P., Karschin, A., Wischmeyer, E. (2006) 'Novel Drosophila two-pore domain K channels: rescue of channel function by heteromeric assembly' Eur J Neurosci. vol 24(8), pp 2264-74

Dorn, A., Hermann, F., Ebneth, A., Bothmann, H., Trube, G., Christensen, K., Apfel, C. (2005). Evaluation of a high-throughput fluorescence assay method for HERG potassium channel inhibition. *Journal of biomolecular screening*, *10*(4), 339–347.

Doyle, D.A., Morais, C.J., Pfuetzner, R.A., Kuo, A., Gulbis, J.M., Cohen, S.L., Chait, B.T., MacKinnon, R. (1998) 'The structure of the potassium channel: molecular basis of K^+ conduction and selectivity' *Science*, vol 280(5360), pp 69-77

Drolet, B., Simard, C., Mizoue, L., Roden, D. M. (2005) 'Human cardiac potassium channel DNA polymorphism modulates access to drug-binding site and causes drug resistance' *The Journal of clinical investigation*, vol 115(8), 2209–2213.

Drucker D. J. (2020). Advances in oral peptide therapeutics. *Nature reviews. Drug discovery*, *19*(4), 277–289.

Du, C., Li, J., Shao, Z., Mwangi, J., Xu, R., Tian, H., Mo, G., Lai, R., Yang, S. (2019) 'Centipede KCNQ inhibitor SsTx also targets Kv1.3' Toxins (Basel) vol 11(2), 76

Du, J., Haak, L. L., Phillips-Tansey, E., Russell, J. T., McBain, C. J. (2000). Frequency-dependent regulation of rat hippocampal somato-dendritic excitability by the K+ channel subunit Kv2.1. *The Journal of physiology*, vol 522 (Pt 1), 19–31.

Du, X., Li, Y., Xia, Y. L., Ai, S. M., Liang, J., Sang, P., Ji, X. L., Liu, S. Q. (2016). Insights into Protein-Ligand Interactions: Mechanisms, Models, and Methods. *International journal of molecular sciences*, *17*(2), 144.

Duprat, F., Lesage, F., Fink, M., Reyes, R., Heurteaux, C., Lazdunski, M. (1997) 'TASK, a human background K^+ channel to sense external pH variations near physiological pH' EMBO J vol 16, 5464–5471.

Durban, J., Juarez, P., Angulo, Y., Lomonte, B., Flores-Diaz, M., Alape-Giron, A., Sasa, M., sanz, L., Gutiérrez, J.M., Dopazo, J., Conesa, A., Calvete, J.J. (2011) 'Profiling the venom gland transcriptomes of Costa Rican snakes by 454 pyrosequencin' BMC Genom. 12:259.

Duskey, J.T., Belletti, D., Pederzoli, F., Vandelli, M.A., Forni, F., Ruozi, B., Tosi, G. (2017) 'Current Strategies for the Delivery of Therapeutic Proteins and Enzymes to Treat Brain Disorders' Int Rev Neurobiol. Vol 137, 1-28

Dutertre, S., Lewis, R.J. (2010) 'Use of venom peptides to probe ion channel structure and function' J Biol Chem. vol 285(18), pp 13315-13320

Ebbinghaus, J., Legros, C., Nolting, A., Guette, C., Celerier, M.L., Pongs, O., Bähring, R. (2004) 'Modulation of K_V4.2 channels by a peptide isolated from the venom of the giant bird-eating tarantula Theraphosa leblondi' Toxicon vol 43(8), pp 923–932.

Elliott, D. E., Li, J., Blum, A., Metwali, A., Qadir, K., Urban, J. F., Jr, Weinstock, J. V. (2003). Exposure to schistosome eggs protects mice from TNBS-induced colitis. *American journal of physiology. Gastrointestinal and liver physiology*, *284*(3), G385–G391.

Elliott, D. E., Setiawan, T., Metwali, A., Blum, A., Urban, J. F., Jr, Weinstock, J. V. (2004). Heligmosomoides polygyrus inhibits established colitis in IL-10-deficient mice. *European journal of immunology*, *34*(10), 2690–2698.

Elliott, D. E., Weinstock, J. V. (2012). Helminth-host immunological interactions: prevention and control of immune-mediated diseases. *Annals of the New York Academy of Sciences*, *1247*, 83–96.

Enyedi, P., Braun, G., Czirják, G. (2012) 'TRESK: the lone ranger of two-pore domain potassium channels' Mol Cell Endocrinol. vol 353(1-2), pp 75-81

Enyedi, P., Czirják, G. (2010) 'Molecular background of leak K+ currents: two-pore domain potassium channels' Physiol Rev. vol 90(2), pp 559-605 Erratum in: Front Neurosci.14:163.

Escoubas, P., Diochot, S., Célérier, M.L., Nakajima, T., Lazdunski, M. (2002) 'Novel tarantula toxins for subtypes of voltage-dependent potassium channels in the Kv2 and Kv4 subfamilies' Mol Pharmacol. vol 62(1), pp 48-57

Escoubas, P., Quinton, L., Nicholson, G.M. (2008) 'Venomics: Unravelling the complexity of animal venoms with mass spectrometry' J. Mass Spectrom. vol 43 (3), pp 279–295.

Fan, L., Guan, X., Wang, W., Zhao, J. Y., Zhang, H., Tiwari, V., Hoffman, P. N., Li, M., Tao, Y. X. (2014). Impaired neuropathic pain and preserved acute pain in rats overexpressing voltage-gated potassium channel subunit Kv1.2 in primary afferent neurons. *Molecular pain*, *10*, 8.

Fanger, C. M., Ghanshani, S., Logsdon, N. J., Rauer, H., Kalman, K., Zhou, J., Beckingham, K., Chandy, K. G., Cahalan, M. D., Aiyar, J. (1999). Calmodulin mediates calcium-dependent activation of the intermediate conductance KCa channel, IKCa1. *The Journal of biological chemistry*, *274*(9), 5746–5754.

Fanger, C. M., Rauer, H., Neben, A. L., Miller, M. J., Rauer, H., Wulff, H., Rosa, J. C., Ganellin, C. R., Chandy, K. G., Cahalan, M. D. (2001). Calcium-activated potassium channels sustain calcium signaling in T lymphocytes. Selective blockers and manipulated channel expression levels. *The Journal of biological chemistry*, *276*(15), 12249–12256

Fautin, D.G. (2009) 'Structural diversity, systematics, and evolution of cnidae' *Toxicon : official journal of the International Society on Toxinology*, *54*(8), 1054–1064.

Fedida, D., Wible, B., Wang, Z., Fermini, B., Faust, F., Nattel, S., Brown, A. M. (1993) 'Identity of a novel delayed rectifier current from human heart with a cloned K+ channel current' *Circulation research*, 73(1), 210–216.

Feliciangeli, S., Chatelain, F.C., Bichet, D., Lesage, F. (2015) 'The family of K2P channels: salient structural and functional properties' J Physiol. vol 593(12), pp 2587-2603.

Feng, J., Wible, B., Li, G. R., Wang, Z., Nattel, S. (1997). 'Antisense oligodeoxynucleotides directed against Kv1.5 mRNA specifically inhibit ultrarapid delayed rectifier K+ current in cultured adult human atrial myocytes' *Circulation research*, vol 80(4), pp 572–579.

Feske, S. (2007) 'Calcium signalling in lymphocyte activation and disease' Nat Rev Immunol vol 7(9), pp 690–702

Feske, S., Skolnik, E.Y., Prakriya, M. (2012) 'Ion channels and transporters in lymphocyte function and immunity' Nat Rev Immunol. vol 12(7), pp 532-47

Ficker, E., Taglialatela, M., Wible, B.A., Henley, C.M., Brown, A.M. (1994) 'Spermine and spermidine as gating molecules for inward rectifier K^+ channels' Science 1994 vol 266(5187), pp 1068-72

Fink, M., Duprat, F., Lesage, F., Reyes, R., Romey, G., Heurteaux, C., Lazdunski, M. (1996) 'Cloning, functional expression and brain localization of a novel unconventional outward rectifier K+ channel' EMBO J. vol 15(24), pp 6854-62

Finlayson, K, Turnbull, L, January, C.T., Sharkey, J. Kelly, J.S. (2001). [3H] Dofetilide binding to HERG transfected membranes: a potential high throughput preclinical screen. European Journal of Pharmacology, 430 (1), 147-148

Fornera, S., Walde, P. (2010). Spectrophotometric quantification of horseradish peroxidase with o-phenylenediamine. *Analytical biochemistry*, *407*(2), 293–295.

Fox, P. D., Loftus, R. J., & Tamkun, M. M. (2013). Regulation of Kv2.1 K(+) conductance by cell surface channel density. *The Journal of neuroscience : the official journal of the Society for Neuroscience*, *33*(3), 1259–1270.

Fracchia, K. M., Pai, C. Y., Walsh, C. M. (2013). Modulation of T Cell Metabolism and Function through Calcium Signaling. *Frontiers in immunology*, *4*, 324.

Freedman, B.D., Fleischmann, B.K., Punt, J.A., Gaulton, G., Hashimoto, Y., Kotlikoff, M.I. (1995) 'Identification of Kv1.1 expression by murine CD4-CD8- thymocytes. A role for voltage-dependent K^+ channels in murine thymocyte development' J Biol Chem. vol 270(38), pp 22406-11

Fry, B.G., Roelants, K., Champagne, D.E., Scheib, H., Tyndall, J.D., King, G.F., Nevalainen, T.J., Norman, J.A., Lewis, R.J., Norton, R.S., Renjifo, C., de la Vega, R.C. (2009) 'The toxicogenomic multiverse: convergent recruitment of proteins into animal venoms' Annu Rev Genomics Hum Genet. vol 10, pp 483-511

Fry, B.G., Scheib, H., van der Weerd, L., Young, B., McNaughtan, J., Ramjan, S.F., Vidal, N., Poelmann, R.E., Norman, J.A.(2008) 'Evolution of an arsenal: structural and functional diversification of the venom system in the advanced snakes (Caenophidia)' Mol Cell Proteomics. vol 7(2), pp 215-46

Fu, X. X., Du, L. L., Zhao, N., Dong, Q., Liao, Y. H., Du, Y. M. (2013). 18β-Glycyrrhetinic acid potently inhibits Kv1.3 potassium channels and T cell activation in human Jurkat T cells. *Journal of ethnopharmacology*, *148*(2), 647–654.

Gähwiler, B.H., Brown, D.A. (1985) 'GABAB-receptor-activated K+ current in voltage-clamped CA3 pyramidal cells in hippocampal cultures' Proc Natl Acad Sci USA. vol 82(5), pp 1558-62

Galvez, A., Gimenez-Gallego, G., Reuben, J.P., Roy-Contancin, L., Feigenbaum, P., Kaczorowski, G.J., Garcia, M.L. (1990) 'Purification and characterization of a unique, potent, peptidyl probe for the high conductance calcium-activated potassium channel from venom of the scorpion Buthus tamulus' J Biol Chem. vol 265(19), pp 11083-90

Gao, B., Harvey, P.J., Craik, D.J., Ronjat, M., De Waard, M., Zhu, S. (2013) 'Functional evolution of scorpion venom peptides with an inhibitor cystine knot fold' Biosci Rep. vol 33(3), e00047

Garcia-Calvo, M., Leonard, R.J., Novick, J., Stevens, S.P., Schmalhofer, W., Kaczorowski, G.J., Garcia, M.L. (1993) 'Purification, characterization, and biosynthesis of margatoxin, a component of Centruroides margaritatus venom that selectively inhibits voltage-dependent potassium channels' J Biol Chem. vol 268(25), pp18866-74

Gąsiorowska, J., Teisseyre, A., Uryga, A., Michalak, K. (2015). Inhibition of Kv1.3 Channels in Human Jurkat T Cells by Xanthohumol and Isoxanthohumol. *The Journal of membrane biology*, *248*(4), 705–711.

Gasparini, S., Danse, J.M., Lecoq, A., Pinkasfeld, S., Zinn-Justin, S., Young, L.C., de Medeiros, C.C., Rowan, E.G., Harvey, A.L., Ménez, A. (1998) 'Delineation of the functional site of alpha-dendrotoxin. The functional topographies of dendrotoxins are different but share a conserved core with those of other Kv1 potassium channel-blocking toxins' J Biol Chem. vol 273(39), pp 25393-403

Geller, J.B., Fitzgerald, L.J., King, C.E. (2005) 'Fission in sea anemones: integrative studies of life cycle evolution' Integr Comp Biol. vol 45(4), pp 615-22

George, A.L. (2005) ‘Inherited disorders of voltage-gated sodium channels” J Clin Invest vol 115(8), pp 1990-1999

Gerdol, M., Cervelli, M., Mariottini, P., Oliverio, M., Dutertre, S., Modica, M. V. (2019). “A Recurrent Motif: Diversity and Evolution of ShKT Domain Containing Proteins in the Vampire Snail *Cumia reticulata*” *Toxins* vol *11*(2), pp 106.

Giangiacomo, K.M., Ceralde, Y., Mullmann, T.J. (2004) ‘Molecular basis of alpha-KTx specificity’ Toxicon vol 43(8), pp 877-86

Giangiacomo, K.M., Garcia, M.L., McManus, O.B. (1992) ‘Mechanism of iberiotoxin block of the large-conductance calcium-activated potassium channel from bovine aortic smooth muscle’ Biochemistry vol 31(29), pp 6719-27

Gilchrist, J., Olivera, B. M., Bosmans, F. (2014). Animal toxins influence voltage-gated sodium channel function. *Handbook of experimental pharmacology*, *221*, 203–229.

Gilquin, B., Braud, S., Eriksson, M.A., Roux, B., Bailey, T.D., Priest, B.T., Garcia, M.L., Ménez, A., Gasparini, S. (2005) ‘A variable residue in the pore of Kv1 channels is critical for the high affinity of blockers from sea anemones and scorpions’ J Biol Chem. vol 280(29), pp 27093-102

Glasscock, E., Voigt, N., McCauley, M. D., Sun, Q., Li, N., Chiang, D. Y., Zhou, X. B., Molina, C. E., Thomas, D., Schmidt, C., Skapura, D. G., Noebels, J. L., Dobrev, D., Wehrens, X. H. (2015) ‘Expression and function of Kv1.1 potassium channels in human atria from patients with atrial fibrillation’ *Basic research in cardiology*, vol 110(5), pp 505.

Glaudemans, B., van der Wijst, J., Scola, R. H., Lorenzoni, P. J., Heister, A., van der Kemp, A. W., Knoers, N. V., Hoenderop, J. G., Bindels, R. J. (2009). ‘A missense mutation in the Kv1.1 voltage-gated potassium channel-encoding gene KCNA1 is linked to human autosomal dominant hypomagnesemia’ *The Journal of clinical investigation*, *119*(4), 936–942.

Glowatzki, E., Fakler, G., Brandle, U., Rexhausen, U., Zenner, H.P., Ruppersberg, J.P., Fakler, B. (1995) 'Subunit-dependent assembly of in- ward-rectifier K^+ channels' Proc Biol Sci vol 261, pp 251–261

Goldstein, M., Rinné, S., Kiper, A.K, Ramírez, D., Netter, M.F., Bustos, D., Ortiz-Bonnin, B., González, W., Decher, N. (2016) ' Functional mutagenesis screens reveal the 'cap structure' formation in disulfide-bridge free TASK channels' Sci Rep. vol 6:19492

Goldstein, S. A., Bockenhauer, D., O'Kelly, I., Zilberberg N. (2001) 'Potassium leak channels and the KCNK family of two-P-domain subunits' Nat. Rev. Neurosci. vol 2(3), pp 175–184

Goldstein, S.A, Bayliss, D.A., Kim, D., Lesage, F., Plant, L.D., Rajan, S. (2005) 'International Union of Pharmacology. LV. Nomenclature and molecular relationships of two-P potassium channels' Pharmacol Rev. vol 57(4), pp 527-40

Goldstein, S.A., Bockenhauer, D., O'Kelly, I., Zilberberg, N. (2001) 'Potassium leak channels and the KCNK family of two-P-domain subunits' Nat Rev Neurosci vol 2(3), pp 175-84

Goldstein, S.A., Miller, C. (1993) 'Mechanism of charybdotoxin block of a voltage-gated K^+ channel'. Biophys J. vol 65(4), pp 1613-9

Gómez-Varela, D., Zwick-Wallasch, E., Knötgen, H., Sánchez, A., Hettmann, T., Ossipov, D., Weseloh, R., Contreras-Jurado, C., Rothe, M., Stühmer, W., Pardo, L.A. (2007) 'Monoclonal antibody blockade of the human Eag1 potassium channel function exerts antitumor activity' Cancer Res. vol 67(15), pp 7343-9

Gonçalves-Machado, L., Pla, D., Sanz, L., Jorge, R.J.B., Leitão-De-Araújo, M., Alves, M.L.M., Alvares, D.J., De Miranda, J., Nowatzki, J., de Morais-Zani, K., Fernandes, W., Tanaka-Azevedo, A.M., Fernández, J., Zingali, R.B., Gutiérrez, J.M., Corrêa-Netto, C., Calvete, J.J. (2016) 'Combined venomics, venom gland transcriptomics, bioactivities, and antivenomics of two Bothrops jararaca populations from geographic isolated regions within the Brazilian Atlantic rainforest' J Proteomics vol 135, pp 73-89

Graham, F. L., van der Eb, A. J. (1973). ‘A new technique for the assay of infectivity of human adenovirus 5 DNA.’ *Virology*, *52*(2), 456–467.

Graham, F. L., Smiley, J., Russell, W. C., & Nairn, R. (1977). ‘Characteristics of a human cell line transformed by DNA from human adenovirus type 5.’ *The Journal of general virology*, *36*(1), 59–74.

Greger, R., Bleich, M., Schlatter, E. (1990) ‘Ion channels in the thick ascending limb of Henle's loop’ Ren Physiol Biochem. vol 13(1-2), pp 37-50

Grimaldi, A., D'Alessandro, G., Di Castro, M.A., Lauro, C., Singh, V., Pagani, F., Sforna, L., Grassi, F., Di Angelantonio, S., Catacuzzeno, L., Wulff, H., Limatola, C., Catalano, M. (2018) ‘Kv1.3 activity perturbs the homeostatic properties of astrocytes in glioma’ Sci Rep. vol 8(1), pp 7654.

Grissmer, S., Cahalan, M. (1989) ‘TEA prevents inactivation while blocking open K^+ channels in human T lymphocytes’ Biophys J. vol 55(1), pp 203–206.

Grissmer, S., Lewis, R. S., & Cahalan, M. D. (1992). Ca (2+)-activated K+ channels in human leukemic T cells. *The Journal of general physiology*, *99*(1), 63–84.

Grissmer, S., Nguyen, A. N., Cahalan, M. D. (1993). Calcium-activated potassium channels in resting and activated human T lymphocytes. Expression levels, calcium dependence, ion selectivity, and pharmacology. *The Journal of general physiology*, *102*(4), 601–630.

Guan, D., Armstrong, W. E., Foehring, R. C. (2013). Kv2 channels regulate firing rate in pyramidal neurons from rat sensorimotor cortex. *The Journal of physiology*, vol 591(19), pp 4807–4825.

Guan, D., Tkatch, T., Surmeier, D. J., Armstrong, W. E., Foehring, R. C. (2007). Kv2 subunits underlie slowly inactivating potassium current in rat neocortical pyramidal neurons. *The Journal of physiology*, vol 581(Pt 3), pp 941–960.

Gubensek, F., Sket, D., Turk, V., Lebez, D. (1974) 'Fractionation of Vipera ammodytes venom and seasonal variation of its composition' Toxicon vol 12(2), 167–171

Gumbiner B. (1987). Structure, biochemistry, and assembly of epithelial tight junctions. *The American journal of physiology*, *253*(6 Pt 1), C749–C758.

Gurrola, G. B., Rosati, B., Rocchetti, M., Pimienta, G., Zaza, A., Arcangeli, A., Olivotto, M., Possani, L. D., Wanke, E. (1999). A toxin to nervous, cardiac, and endocrine ERG K+ channels isolated from Centruroides noxius scorpion venom. *FASEB journal : official publication of the Federation of American Societies for Experimental Biology*, *13*(8), 953–962.

Gutman, G.A., Chandy, K.G., Grissmer, S., Lazdunski, M., Mckinnon, D., Pardo, L.A., Robertson, G.A., Rudy, B., Sanguinetti, M.C., Stühmer, W., Wang, X. (2005) 'International Union of Pharmacology. LIII. Nomenclature and molecular relationships of voltage-gated potassium channels' Pharmacol Rev. vol 57(4), pp 473-508

Guy, H.R., Seetharamulu, P. (1986) 'Molecular model of the action potential sodium channel' Proc Natl AcadSci USA vol 83 (2), pp 508–512

Hagiwara, S., Byerly, L. (1981). Calcium channel. *Annual review of neuroscience*, vol *4*, 69–125.

Hamill, O.P., Marty, A., Neher, E., Sakmann, B., Sigworth, F.J. (1981) 'Improved patch-clamp techniques for high-resolution current recording from cells and cell-free membrane patches' Pflugers Arch. vol 391(2), pp 85–100

Hamman, J.H., Enslin, G.M. Kotzé, A.F. (2005) Oral Delivery of Peptide Drugs. *BioDrugs* 19**,** 165–177

Hancox, J. C., McPate, M. J., El Harchi, A., Zhang, Y. H. (2008). The hERG potassium channel and hERG screening for drug-induced torsades de pointes. *Pharmacology & therapeutics*, *119*(2), 118–132.

Hancox, J. C., McPate, M. J., El Harchi, A., Zhang, Y. H. (2008). The hERG potassium channel and hERG screening for drug-induced torsades de pointes. *Pharmacology & therapeutics*, *119*(2), 118–132.

Hancox, J.C., Whittaker, D.G., Zhang, H. *et al.* (2019). Learning from studying very rare cardiac conditions: the example of short QT syndrome. *J Congenit Heart Dis* 3 **(**3)

Hanselmann, C., Grissmer, S. (1996). Characterization of apamin-sensitive Ca(2+)-activated potassium channels in human leukaemic T lymphocytes. *The Journal of physiology*, *496 (Pt 3)*(Pt 3), 627–637.

Harris N. L., Pleass R., Behnke, J. M. (2014). Understanding the role of antibodies in murine infections with Heligmosomoides (polygyrus) bakeri: 35 years ago, now and 35 years ahead. *Parasite immunology*, *36*(3), 115–124.

Harvey, A. L. (2014) 'Toxins and drug discovery' *Toxicon* vol 92, 193–200

Harvey, A.L. (2001) 'Twenty years of dendrotoxins' *Toxicon* vol 39(1), pp 15-26

Harvey, A.L. (2002) 'Toxins 'R' Us: more pharmacological tools from nature's superstore' *Trends Pharmacol.* Sci., 23 (5), pp 201-203

Harvey, A.L., Anderson, A.J. (1985) 'Dendrotoxins: snake toxins that block potassium channels and facilitate neurotransmitter release' *Pharmac. Ther.* vol 31 (1-2), pp 33-55

He, F. Z., McLeod, H. L., Zhang, W. (2013). Current pharmacogenomic studies on hERG potassium channels. *Trends in molecular medicine*, *19*(4), 227–238.

Hebert, S.C., Desir, G., Giebisch, G., Wang,W. (2005) 'Molecular diversity and regulation of renal potassium channels' *Physiol Rev*. vol 85(1), pp 319-371

Heginbotham, L., Lu, Z., Abramson, T., MacKinnon, R. (1994). Mutations in the K+ channel signature sequence. *Biophysical journal*, *66*(4), 1061–1067.

Henriques, S.T., Deplazes, E., Lawrence, N., Cheneval, O., Chaousis, S., Inserra, M., Thongyoo, P., King, G.F., Mark, A.E., Vetter, I., Craik, D.J., Schroeder, C.I. (2016) 'Interaction of tarantula venom peptide ProTx-II with lipid membranes is a prerequisite for its inhibition of human voltage-gated sodium channel $Na_V1.7$. *J. Biol. Chem*. 291 (33), pp 17049–17065.

Herrington, J., Zhou, Y.P., Bugianesi, R.M., Dulski, P.M., Feng, Y., Warren, V.A., Smith, M.M., Kohler, M.G., Garsky, V.M., Sanchez, M., Wagner, M., Raphaelli, K., Banerjee, P., Ahaghotu, C., Wunderler, D., Priest, B.T., Mehl, J.T., Garcia, M.L., McManus, O.B., Kaczorowski, G.J., Slaughter, R.S. (2006) 'Blockers of the delayed-rectifier potassium current in pancreatic beta-cells enhance glucose-dependent insulin secretion' *Diabetes*, vol 55(4), pp 1034-42

Hewitson, J. P., Ivens, A. C., Harcus, Y., Filbey, K. J., McSorley, H. J., Murray, J., Bridgett, S., Ashford, D., Dowle, A. A., Maizels, R. M. (2013). Secretion of protective antigens by tissue-stage nematode larvae revealed by proteomic analysis and vaccination-induced sterile immunity. *PLoS pathogens*, *9*(8), e1003492.

Hewitson, J.P., Harcus, Y., Murray, J., van Agtmaal, M., Filbey, K.J., Grainger, J.R., Bridgett, S., Blaxter, M.L., Ashton, P.D., Ashford, D.A., Curwen, R.S., Wilson, R.A., Dowle, A.A., Maizels, R.M. (2011) "Proteomic analysis of secretory products from the model gastrointestinal nematode *Heligmosomoides polygyrus* reveals dominance of venom allergen-like (VAL) proteins" *J Proteomics* vol 74(9), pp 1573-94.

Hibino, H., Inanobe, A., Furutani, K., Murakami, S., Findlay, I., Kurachi, Y. (2010) 'Inwardly rectifying potassium channels: their structure, function, and physiological roles' *Physiol Rev.* vol 90(1), pp 291-366

Hidalgo, P., MacKinnon, R. (1995). Revealing the architecture of a K+ channel pore through mutant cycles with a peptide inhibitor. *Science (New York, N.Y.)*, *268*(5208), 307–310.

Hille, B. (1978) 'Ionic channels in excitable membranes. Current problems and biophysics approaches' *Biophysic. J.* vol 22(2), pp 283-294

Hille, B. (1992) ‘Ionic channels of excitable membranes’ 2nd edition, Sunderland, MA, Sinauer Associates

Hille, B. (2001) ‘Ion channels of excitable membrane’. 3rd edition. Sunderland, MA: Sinauer Associates

Hinterberger, V., Wang, W., Damm, C., Wawra, S., Thoma, M., Peukert, W. (2018). Microwave-assisted one-step synthesis of white light-emitting carbon dot suspensions. *Optical Materials*, 80, 110-119.

Hmed, B., Serria, H.T., Mounir, Z.K. (2013) ‘Scorpion peptides: potential use for new drug development’ *Journal of Toxicology,* vol 2013, 958797

Hochman, J., Artursson, P. (1994). Mechanisms of absorption enhancement and tight junction regulation. *Journal of Controlled Release*, 29 (3), 253-267.

HOFF, H. E., GEDDES, L. A. (1957). *Bulletin of the history of medicine*, *31*(3)

Hodgkin, A.L., Huxley A. (1939) ‘Action Potentials Recorded from Inside a Nerve Fibre’ *Nature*, vol 144, pp 710–711

Hodgkin, A.L., Katz, B. (1949) ‘The effect of sodium ions on the electrical activity of giant axon of the squid’ *J Physiol,* vol 108(1), pp 37-77

Honma, T., Shiomi, K. (2006) ‘Peptide toxins in sea anemones: structural and functional aspects’ *Mar Biotechnol* (NY), vol 8(1), pp 1-10

Horn, R., Marty, A. (1988). Muscarinic activation of ionic currents measured by a new whole-cell recording method. *The Journal of general physiology*, *92*(2), 145–159.

Horovitz A. (1996). Double-mutant cycles: a powerful tool for analyzing protein structure and function. *Folding & design*, *1*(6), R121–R126.

Hoshi, T., Zagotta, W. N., Aldrich, R. W. (1990). Biophysical and molecular mechanisms of Shaker potassium channel inactivation. *Science (New York, N.Y.)*, *250*(4980), 533–538.

Hoshi, T., Zagotta, W. N., Aldrich, R. W. (1991). Two types of inactivation in Shaker K+ channels: effects of alterations in the carboxy-terminal region. *Neuron*, *7*(4), 547–556.

Hu, W., Pasare, C. (2013) 'Location, location, location: tissue-specific regulation of immune responses' *J Leukoc Biol.*, vol 94(3), pp 409-421

Hughes, S., Foster, R., Peirson, S. et al. (2017) 'Expression and localisation of two-pore domain (K2P) background leak potassium ion channels in the mouse retina' *Sci Rep*, vol 7, 46085

Huppa, J.B., Davis, M.M. (2003) 'T-cell-antigen recognition and the immunological synapse' *Nat Rev Immunol,.* vol 3(12), pp 973-83

Ibraheem, D., Elaissari, A., Fessi, H. (2014) 'Administration strategies for proteins and peptide' *Int. J. Pharm*., vol 477(1-2), pp 578–589

Imperial, J. S., Chen, P., Sporning, A., Terlau, H., Daly, N. L., Craik, D. J., Alewood, P. F., Olivera, B. M. (2008) 'Tyrosine-rich conopeptides affect voltage-gated K^+ channels' *The Journal of biological chemistry*, vol *283*(34), pp 23026–23032.

Jacobsson, E., Andersson, H.S., Strand, M., Peigneur, S., Eriksson, C., Lodén, H., Shariatgorji, M., Andrén, P.E., Lebbe, E. K. M., Rosengrean, J., Tytgat, Goransson, U. (2018) 'Peptide ion channel toxins from the bootlace worm, the longest animal on Earth' *Sci Rep*, vol 8, 4596

Jäger, H., Adelman, J. P., Grissmer, S. (2000). SK2 encodes the apamin-sensitive Ca (2+)-activated K(+) channels in the human leukemic T cell line, Jurkat. *FEBS letters*, *469*(2-3), 196–202.

Jain, P., Sharma, S., Tripathi, M. (2013). Diagnosis and management of epileptic encephalopathies in children. *Epilepsy research and treatment*, 501981.

Jan, L. Y. and Jan, Y. N. (2012). Voltage-gated potassium channels and the diversity of electrical signalling. *The Journal of physiology*, *590*(11), 2591–2599.

Jan, L.Y., Jan, Y.N. (1990) 'A superfamily of ion channels' *Nature*, vol 345(6277), pp 672

Jang, S. H., Ryu, P. D., Lee, S. Y. (2011) 'Dendrotoxin-κ suppresses tumor growth induced by human lung adenocarcinoma A549 cells in nude mice' *Journal of veterinary science*, 12(1), 35–40.

Janin J. (1995). Protein-protein recognition. *Progress in biophysics and molecular biology*, *64*(2-3), 145–166.

Jeon, W. I., Ryu, P. D., Lee, S. Y. (2012) 'Effects of voltage-gated K+ channel blockers in gefitinib-resistant H460 non-small cell lung cancer cells' *Anticancer research*, 32(12), 5279–5284.

Jiang, Y., Lee, A., Chen, J., Ruta, V., Cadene, M., Chait, B.T., MacKinnon, R. (2003) 'X-ray structure of a voltage-dependent K^+ channel' *Nature,* vol 423(6935), pp 33-41

Jin, L., Boyd, B. J., White, P. J., Pennington, M. W., Norton, R. S., Nicolazzo, J. A. (2015). Buccal mucosal delivery of a potent peptide leads to therapeutically-relevant plasma concentrations for the treatment of autoimmune diseases. *Journal of controlled release : official journal of the Controlled Release Society*, *199*, 37–44.

Jin, L., Zhou, Q. T., Chan, H. K., Larson, I. C., Pennington, M. W., Morales, R., Boyd, B. J., Norton, R. S., Nicolazzo, J. A. (2016). Pulmonary Delivery of the Kv1.3-Blocking Peptide HsTX1[R14A] for the Treatment of Autoimmune Diseases. *Journal of pharmaceutical sciences*, *105*(2), 650–656.

Johnston, C. J., Robertson, E., Harcus, Y., Grainger, J. R., Coakley, G., Smyth, D. J., McSorley, H. J., Maizels, R. (2015). "Cultivation of *Heligmosomoides polygyrus*: an immunomodulatory nematode parasite and its secreted products" *Journal of visualized experiments: JoVE* vol 98, e52412.

Joiner, W. J., Wang, L. Y., Tang, M. D., Kaczmarek, L. K. (1997). hSK4, a member of a novel subfamily of calcium-activated potassium channels. *Proceedings of the National Academy of Sciences of the United States of America*, *94*(20), 11013–11018.

Jones, R. G., Thompson, C. B. (2007). Revving the engine: signal transduction fuels T cell activation. *Immunity*, *27*(2), 173–178.

Jou, I., Pyo, H., Chung, S., Jung, S. Y., Gwag, B. J., Joe, E. H. (1998) 'Expression of Kv1.5 K+ channels in activated microglia in vivo' *Glia*, 24(4), 408–414.

Jungo, F., Bairoch, A. (2005) 'Tox-Prot, the toxin protein annotation program of the Swiss-Prot protein knowledgebase' *Toxicon*, vol 45(3), pp 293-301

Kahan B. D. (1993). Cyclosporine: the base for immunosuppressive therapy--present and future. *Transplantation proceedings*, *25*(1 Pt 1), 508–510.

Kalia, J., Milescu, M., Salvatierra, J., Wagner, J., Klint, J. K., King, G. F., Olivera, B. M., Bosmans, F. (2015). From foe to friend: using animal toxins to investigate ion channel function. *Journal of molecular biology*, *427*(1), 158–175.

Kalman, K., Pennington, M.W., Lanigan, M.D., Nguyen, A., Rauer, H., Mahnir, V., Paschetto, K., Kem, W.R., Grissmer, S., Gutman, G.A., Christian, E.P., Cahalan, M.D., Norton, R.S., Chandy, K.G. (1998) 'ShK-Dap22, a Potent Kv1.3-specific Immunosuppressive Polypeptide' *Journ. Biolog. Chemistr.*, vol 273 (49), pp 32697-32707

Kalyaanamoorthy, S., Barakat, K. H. (2018). Development of Safe Drugs: The hERG Challenge. *Medicinal research reviews*, *38*(2), 525–555.

Kamb, A., Tseng-Crank, J., Tanouye M.A. 'Multiple products of the Drosophila Shaker gene may contribute to potassium channel diversity' Neuron vol 1, pp 421-430

Katz, B. (1949) 'Les constantes électriques de la membrane du muscle' *Arch. Sci. Physiol*,. vol 2, pp 285-99

Khan, W. I., Blennerhasset, P. A., Varghese, A. K., Chowdhury, S. K., Omsted, P., Deng, Y., Collins, S. M. (2002). Intestinal nematode infection ameliorates experimental colitis in mice. *Infection and immunity*, *70*(11), 5931–5937.

Khan, W. I., Collins, S. M. (2004). Immune-mediated alteration in gut physiology and its role in host defence in nematode infection. *Parasite immunology*, *26*(8-9), 319–326.

Killian, J.A., von Heijne G. (2000) 'How proteins adapt to a membrane–water interface' *Trends in Biochemical Sciences*, vol 25 (9), pp 429-434

Kim J. B. (2014). Channelopathies. *Korean journal of pediatrics*, *57*(1), 1–18.

Kim, DM and Nimigean, CM. (2016) 'Voltage-Gated Potassium Channels: A Structural Examination of Selectivity and Gating' Cold Spring Harb Perspect Biol. vol 8(5), a029231

King, G.F. (2007) 'Modulation of insect Ca_V channels by peptidic spider toxins' *Toxicon,* vol 49 (4), pp 513-530

King, G.F. (2011) 'Venoms as a platform for human drugs: translating toxins into therapeutics' *Expert Opin Biol Ther.,* vol11(11), pp 1469-84

King, G.F., Gentz, M.C., Escoubas, P., Nicholson, G.M. (2008) 'A rational nomenclature for naming peptide toxins from spiders and other venomous animals' *Toxicon*, vol 52(2), pp 264-276 (a)

King, G.F., Hardy, M.C. (2013) 'Spider-venom peptides: Structure, pharmacology, and potential for control of insect pests' *Annu. Rev. Entomol.*, vol 58, 475–496.

King, G.F., P. Escoubas, P., G.M. Nicholson, G.M. (2008) 'Peptide toxins that selectively target insect Na_V and Ca_V channels' *Channels* (Austin), vol 2 (2), pp 100-116 (b)

Klemic, K. G., Kirsch, G. E., Jones, S. W. (2001). U-type inactivation of Kv3.1 and Shaker potassium channels. *Biophysical journal*, *81*(2), 814–826.

Klemic, K. G., Shieh, C. C., Kirsch, G. E., Jones, S. W. (1998). Inactivation of Kv2.1 potassium channels. *Biophysical journal*, *74*(4), 1779–1789.

Klint, J.K., Chin, Y.K., Mobli, M. (2015) 'Rational engineering defines a molecular switch that is essential for activity of spider-venom peptides against the analgesics target Na$_V$1.7' *Mol. Pharmacol*., vol 88 (6), pp 1002–1010.

Kofuji, P., Biedermann, B., Siddharthan, V., Raap, M., Iandiev, I., Milenkovic, I., Thomzig, A., Veh, R.W., Bringmann, A., Reichenbach, A. (2002) 'Kir potassium channel subunit expression in retinal glial cells: implications for spatial potassium buffering' *Glia*, vol 39(3), pp 292-303

Koh, D.C., Armugam, A., Jeyaseelan, K. (2006) 'Snake venom components and their applications in biomedicine' *Cell Mol Life Sci.*, vol 63(24), pp 3030-41

Köhler, R., Wulff, H., Eichler, I., Kneifel, M., Neumann, D., Knorr, A., Grgic, I., Kämpfe, D., Si, H., Wibawa, J., Real, R., Borner, K., Brakemeier, S., Orzechowski, H. D., Reusch, H. P., Paul, M., Chandy, K. G., Hoyer, J. (2003). Blockade of the intermediate-conductance calcium-activated potassium channel as a new therapeutic strategy for restenosis. *Circulation*, *108*(9), 1119–1125.

Koshy, S., Wu, D., Hu, X., Tajhya, R.B., Huq, R., Khan, F.S., Pennington, M.W., Wulff, H., Yotnda, P., Beeton, C. (2013) 'Blocking KCa3.1 channels increases tumor cell killing by a subpopulation of human natural killer lymphocytes' *PLoS One,* vol 8(10), pp e76740

Koulouridis, E., Koulouridis, I. (2015) 'Molecular pathophysiology of Bartter's and Gitelman's syndromes' *World J Pediatr*, vol 11 (2), pp 113–125

Koval, O.M., Fan, Y., Rothberg, B.S. (2007) 'A role for the S0 transmembrane segment in voltage-dependent gating of BK channels' *J Gen Physiol*., vol 129(3), pp 209-20.

Kradin, R. L., Badizadegan, K., Auluck, P., Korzenik, J., Lauwers, G. Y. (2006). Iatrogenic Trichuris suis infection in a patient with Crohn disease. *Archives of pathology & laboratory medicine*, *130*(5), 718–720.

Kramer, J. W., Post, M. A., Brown, A. M., Kirsch, G. E. (1998). Modulation of potassium channel gating by coexpression of Kv2.1 with regulatory Kv5.1 or Kv6.1 alpha-subunits. *The American journal of physiology*, *274*(6), C1501–C1510.

Kreusch, A., Pfaffinger, P. J., Stevens, C. F., Choe, S. (1998). Crystal structure of the tetramerization domain of the Shaker potassium channel. *Nature*, *392*(6679), 945–948.

Krishnarjuna, B., Villegas-Moreno, J., Mitchell, M. L., Csoti, A., Peigneur, S., Amero, C., Pennington, M. W., Tytgat, J., Panyi, G., Norton, R. S. (2018) "Synthesis, folding, structure and activity of a predicted peptide from the sea anemone *Oulactis sp.* with an ShKT fold" *Toxicon : official journal of the International Society on Toxinology 150*, 50–59

Kuang, Q., Purhonen, P., Hebert, H. (2015) 'Structure of potassium channels' *Cell Mol Life Sci.*, vol 72(19), pp 3677-3693

Kuffler, S.W., Nicholls, J.G. (1966) 'The physiology of neuroglial cells' *Ergeb Physiol*., vol 57, pp 1-90

Kuhn-Nentwig, L., Stöcklin, R., Nentwig, W. (2011) 'Venom Composition and Strategies in Spiders: Is Everything Possible?' *Adv. Insect Physiol.*, vol 40, pp 1–86.

Kunzelmann, K. (2005) 'Ion channels and cancer' *J Membr Biol.,* vol 205(3), pp 159-73.

Kuo, M.M., Haynes, W.J., Loukin, S.H., Kung, C., Saimi, Y. (2005) 'Prokaryotic K(+) channels: from crystal structures to diversity' *FEMS Microbiol Rev.*, vol 29(5), pp 961-85

Kurachi, Y. (1985) 'Voltage-dependent activation of the inward-rectifier potassium channel in the ventricular cell membrane of guinea-pig heart' *J Physiol.,* vol 366(1), pp 365-85

Kurata, H. T., Soon, G. S., Eldstrom, J. R., Lu, G. W., Steele, D. F., Fedida, D. (2002). Amino-terminal determinants of U-type inactivation of voltage-gated K+ channels. *The Journal of biological chemistry*, *277*(32), 29045–29053.

Kuzmenkov, A.I., Grishin, E.V., Vassilevski, A.A. (2015) 'Diversity of Potassium Channel Ligands: Focus on Scorpion Toxins' *Biochemistry* (Mosc), vol 80(13), pp 1764-99

Kuzmenkov, A.I., Krylov, N.A., Chugunov, A.O., Grishin, E.V., Vassilevski, A.A. (2016) 'Kalium: a database of potassium channel toxins from scorpion venom' Database (Oxford) baw056

Lacey, M.G., Mercuri, N.B., North, R.A. (1988) 'On the potassium conductance increase activated by GABAB and dopamine D2 receptors in rat substantia nigra neurones' *J Physiol.*, vol 401, pp 437-53

Laitinen, P., Fodstad, H., Piippo, K., Swan, H., Toivonen, L., Viitasalo, M., Kaprio, J., Kontula, K. (2000). Survey of the coding region of the HERG gene in long QT syndrome reveals six novel mutations and an amino acid polymorphism with possible phenotypic effects. *Human mutation*, *15*(6), 580–581.

Lam, J., Wulff, H. (2011). The Lymphocyte Potassium Channels Kv1.3 and KCa3.1 as Targets for Immunosuppression. *Drug development research*, *72*(7), 573–584.

Lang, F., Föller, M., Lang, K., Lang, P., Ritter, M., Vereninov, A., Szabo, I., Huber, S.M., Gulbins, E. (2007) 'Cell volume regulatory ion channels in cell proliferation and cell death' *Methods Enzymol,* vol 428, pp 209-225

Langenegger, N., Nentwig, W., Kuhn-Nentwig, L. (2019) 'Spider Venom: Components, Modes of Action, and Novel Strategies in Transcriptomic and Proteomic Analyses' *Toxins* (Basel), vol 11(10), 611

Lanigan, M. D., Kalman, K., Lefievre, Y., Pennington, M. W., Chandy, K. G., Norton, R. S. (2002). Mutating a critical lysine in ShK toxin alters its binding configuration in the pore-vestibule region of the voltage-gated potassium channel, Kv1.3. *Biochemistry*, *41*(40), 11963–11971.

Lastraioli, E., Iorio, J., Arcangeli, A. (2015) 'Ion channel expression as promising cancer biomarker' *Biochim Biophys Acta,* vol 1848(10 Pt B), pp 2685-702

Lawrence, N., Wu, B., Ligutti, J., Cheneval, O., Agwa, A.J., Benfield, A.H., Biswas, K., Craik, D.J., Miranda, L.P., Henriques, S.T. (2018) 'Peptide-membrane interactions affect the inhibitory potency and selectivity of spider toxins ProTx-II and GpTx-1' *ACS Chem. Biol*., vol 14 (1), pp 118–130

Lebrun, B., Romi-Lebrun, R., Martin-Eauclaire, M. F., Yasuda, A., Ishiguro, M., Oyama, Y., Pongs, O., Nakajima, T. (1997). A four-disulphide-bridged toxin, with high affinity towards voltage-gated K+ channels, isolated from Heterometrus spinnifer (Scorpionidae) venom. *The Biochemical journal*, 328(Pt 1), 321–327.

Lee, C.W., Kim, S., Roh, S.H., Endoh, H., Kodera, Y., Maeda, T., Wang, J.M., Swartz, K.J., Kim, J.I. (2004) 'Solution structure and functional characterization of SGTx1, a modifier of Kv2.1 channel gating' *Biochemistry,* vol 43(4), pp 890-897

Lee, H., Lin, M. C., Kornblum, H. I., Papazian, D. M., Nelson, S. F. (2014). Exome sequencing identifies de novo gain of function missense mutation in KCND2 in identical twins with autism and seizures that slows potassium channel inactivation. *Human molecular genetics*, vol 23(13), pp 3481–3489.

Lee, K. S., Tsien, R. W. (1983). Mechanism of calcium channel blockade by verapamil, D600, diltiazem and nitrendipine in single dialysed heart cells. *Nature*, *302*(5911), 790–794.

Lee, S. C., Sabath, D. E., Deutsch, C., Prystowsky, M. B. (1986). Increased voltage-gated potassium conductance during interleukin 2-stimulated proliferation of a mouse helper T lymphocyte clone. *The Journal of cell biology*, *102*(4), 1200–1208.

Lee, S.Y., Lee, A., Chen, J., MacKinnon, R. (2005) 'Structure of the KvAP voltage-dependent K^+ channel and its dependence on the lipid membrane' *Proc Natl Acad Sci USA,* vol 102 (43), pp 15441–15446.

Lesage, F., Guillemare, E., Fink, M., Duprat, F., Lazdunski, M., Romey, G., Barhanin, J. (1996) 'TWIK-1, a ubiquitous human weakly inward rectifying K+ channel with a novel structure' *EMBO J*., vol 15(5), pp 1004-11 (b)

Lesage, F., Lazdunski, M. (2000) 'Molecular and functional properties of two-pore-domain potassium channels' *Am J Physiol Renal Physiol.,* vol 279(5), pp F793-801

Lesage, F., Reyes, R., Fink, M., Duprat, F., Guillemare, E., Lazdunski, M. (1996) 'Dimerization of TWIK-1 K^+ channel subunits via a disulfide bridge' *EMBO J.*, vol 15(23), pp 6400-6407 (a)

Letunic, I., Khedkar, S.,Bork, P. (2020) 'SMART: recent updates, new developments and status in 2020' *Nucleic Acids Research*, vol 49 (D1), pp D458-D460

Lev, B., Murail, S., Poitevin F., Cromer, B.A., Baaden, M., Delarue, M., Allen, T.W. (2017) 'String method solution of the gating pathways for a pentameric ligand-gated ion channel' *Pnas*, vol 114 (21), pp E4158-E4167

Levite, M., Cahalon, L., Peretz, A., Hershkoviz, R., Sobko, A., Ariel, A., Desai, R., Attali, B., Lider, O. (2000) 'Extracellular K^+ and opening of voltage- gated potassium channels activate T cell integrin function: physical and functional association between Kv1.3 channels and beta1 integrins' *J Exp Med*, vol 191(7), pp 1167–1176

Lewis, D.L., Ikeda, S.R., Aryee, D., Joho, R.H. (1991) 'Expression of an inwardly rectifying K+ channel from rat basophilic leukemia cell mRNA in Xenopus oocytes' *FEBS Lett.,* vol 290(1-2), pp 17-21

Lewis, R. J. (2015) 'Case study 1: development of the analgesic drugs Prialt® and Xen2174 from cone snail venoms' in Venoms to drugs: venom as a source for the development of human therapeutics. Ed. King, G. F. (London: Royal Society of Chemistry), Chapter 9, pp 245–254.

Lewis, R. S., Cahalan, M. D. (1995). Potassium and calcium channels in lymphocytes. *Annual review of immunology*, *13*, 623–653.

Lewis, R., Garcia, M. (2003) 'Therapeutic potential of venom peptides' *Nat Rev Drug Discov,* vol 2(10), pp 790–802

Li, H., Guo, W., Mellor, R. L., Nerbonne, J. M. (2005) 'KChIP2 modulates the cell surface expression of Kv 1.5-encoded K(+) channels' *Journal of molecular and cellular cardiology*, 39(1), 121–132.

Li, M., Jan, Y. N., Jan, L. Y. (1992) 'Specification of subunit assembly by the hydrophilic amino-terminal domain of the Shaker potassium channel' *Science (New York, N.Y.)*, *257*(5074), 1225–1230.

Lin, C. S., Boltz, R. C., Blake, J. T., Nguyen, M., Talento, A., Fischer, P. A., Springer, M. S., Sigal, N. H., Slaughter, R. S., Garcia, M. L. (1993). Voltage-gated potassium channels regulate calcium-dependent pathways involved in human T lymphocyte activation. *The Journal of experimental medicine*, *177*(3), 637–645.

Lin, J., Miller, M. J., Shaw, A.S. (2005) 'The c-SMAC: sorting it all out (or in)' *The Journal of Cell Biology*, vol.170 (2), pp 177-182

Linley J. E. (2013). Perforated whole-cell patch-clamp recording. *Methods in molecular biology (Clifton, N.J.)*, *998*, 149–157.

Lippiat J. D. (2008). Whole-cell recording using the perforated patch clamp technique. *Methods in molecular biology (Clifton, N.J.)*, *491*, 141–149.

Liu, P. W., Bean, B. P. (2014). Kv2 channel regulation of action potential repolarization and firing patterns in superior cervical ganglion neurons and hippocampal CA1 pyramidal neurons. *The Journal of neuroscience: the official journal of the Society for Neuroscience*, 34(14), 4991–5002.

Liu, Q.H., Fleischmann, B.K., Hondowicz, B., Maier, C.C., Turka, L.A., Yui, K., Kotlikoff, M.I., Wells, A.D., Freedman, B.D. (2002) 'Modulation of Kv channel expression and function by TCR and costimulatory signals during peripheral CD4(+) lymphocyte differentiation' *J Exp Med,.* vol 196(7), pp 897-909

Liu, Y., Holmgren, M., Jurman, M.E., Yellen, G. (1997) 'Gated access to the pore of a voltage-dependent K^+ channel' *Neuron,* vol 19(1), pp 175-84

Liu, Y., Li, D., Wu, Z., Li, J., Nie, D., Xiang, Y., Liu, Z. (2012) 'A positively charged surface patch is important for hainantoxin-IV binding to voltage-gated sodium channels' *J. Pept. Sci*., vol 18 (10), 643–649.

Liu, Z.C., Zhang, R., Zhao, F., Chen, Z.M., Liu, H.W., Wang, Y.J., Jiang, P., Zhang, Y., Wu, Y., Ding, J.P., Lee, W.H., Zhang, Y. (2012) 'Venomic and transcriptomic analysis of centipede Scolopendra subspinipes dehaani' *J Proteome Res.,* vol 11(12), pp 6197-212

Logsdon, N. J., Kang, J., Togo, J. A., Christian, E. P., Aiyar, J. (1997). A novel gene, hKCa4, encodes the calcium-activated potassium channel in human T lymphocytes. *The Journal of biological chemistry*, *272*(52), 32723–32726.

Long, S.B., Campbell, E.B., MacKinnon, R (2005) 'Crystal structure of a mammalian voltage-dependent Shaker family K^+ channel' *Science*, vol 309 (5736), pp 897–903 (a)

Long, S.B., Campbell, E.B., MacKinnon, R. (2005) 'Voltage sensor of Kv1.2: structural basis of electromechanical coupling' *Science,* vol 309(5736), pp 903–908 (b)

Lopatin, A.N., Makhina, E.N., Nichols, C.G. (1994) 'Potassium channel block by cytoplasmic polyamines as the mechanism of intrinsic rectification' Nature vol 372(6504), pp 366 –369

Lorenz, J.N., Baird, N.R., Judd, L.M., Noonan, W.T., Andringa, A., Doetschman, T., Manning, P.A., Liu, L.H., Miller, M.L., Shull, G.E. (2002) 'Impaired renal NaCl absorption in mice lacking the ROMK potassium channel, a model for type II Bartter's syndrome' *J Biol Chem.*, vol 277(40), pp 37871-80

Lotshaw, D.P. (2007) 'Biophysical, pharmacological, and functional characteristics of cloned and native mammalian two-pore domain K+ channels' *Cell Biochem Biophys*., vol 47(2), pp 209-56

Loyd, J.E., Kass, R.S., Chung, W.K. (2013) 'A novel channelopathy in pulmonary arterial hypertension' *N Engl J Med.*, vol 369(4), pp 351-361

Lu, M., Wang, T., Yan, Q., Yang, X., Dong, K., Knepper, M.A., Wang, W., Giebisch, G., Shull, G.E., Hebert, S.C. (2002) 'Absence of small conductance K+ channel (SK) activity in

apical membranes of thick ascending limb and cortical collecting duct in ROMK (Bartter's) knockout mice' *J Biol Chem.,* vol 277(40), pp 37881-7

Luna-Ramírez, K., Bartok, A., Restano-Cassulini, R., Quintero-Hernández, V., Coronas, F. I., Christensen, J., Wright, C. E., Panyi, G., Possani, L. D. (2014). Structure, molecular modeling, and function of the novel potassium channel blocker urotoxin isolated from the venom of the Australian scorpion Urodacus yaschenkoi. *Molecular pharmacology*, vol 86(1), pp 28–41.

Lund, M. E., Greer, J., Dixit, A., Alvarado, R., McCauley-Winter, P., To, J., Tanaka, A., Hutchinson, A. T., Robinson, M. W., Simpson, A. M., O'Brien, B. A., Dalton, J. P., Donnelly, S. (2016). A parasite-derived 68-mer peptide ameliorates autoimmune disease in murine models of Type 1 diabetes and multiple sclerosis. *Scientific reports*, *6*, 37789.

Luo, J., Zhang, Y., Gong, M., Lu, S., Ma, Y., Zeng, X., Liang, S. (2014) 'Molecular surface of JZTX-V (β-Theraphotoxin-Cj2a) interacting with voltage-gated sodium channel subtype $Na_V1.4$' *Toxins*, vol 6(7) pp 2177–2193

Luo, L., Li, B., Wang, S., Wu, F., Wang, X., Liang, P., Ombati, R., Chen, J., Lu, X., Cui, J., Lu, Q., Zhang, L., Zhou, M., Tian, C., Yang, S., Lai, R. (2018) 'Centipedes subdue giant prey by blocking KCNQ channels' *Proc Natl Acad Sci U S A*, vol 115(7), pp 1646-1651

Lyons, S.A., O'Neal, J., Sontheimer, H. (2002) 'Chlorotoxin, a scorpion-derived peptide, specifically binds to gliomas and tumors of neuroectodermal origin' *Glia*, vol 39(2), pp 162-73

Ma, L., Roman-Campos, D., Austin, E.D., Eyries, M., Sampson, K.S., Soubrier, F., Germain, M., Trégouët, D.A., Borczuk, A., Rosenzweig, E.B., Girerd, B., Montani, D., Humbert, M., Loyd, J.E., Kass, R.S., Chung, W.K. (2013). 'A novel channelopathy in pulmonary arterial hypertension.' *NEJM,* 369(4), pp 351-361

Ma, R.S.Y., Kayani, K., Whyte-Oshodi, D., Whyte-Oshodi, A., Nachiappan, N., Gnanarajah, S., Mohammed, R. (2019) 'Voltage gated sodium channels as therapeutic targets for chronic pain' *J Pain Res.,* vol 12, pp 2709-2722

Ma, Z., Lavebratt, C., Almgren, M., Portwood, N., Forsberg, L. E., Bränström, R., Berglund, E., Falkmer, S., Sundler, F., Wierup, N., Björklund, A. (2011) 'Evidence for presence and functional effects of Kv1.1 channels in β-cells: general survey and results from mceph/mceph mice' *PloS one*, vol 6(4), e18213.

Macian, F. (2005) 'NFAT proteins: key regulators of T-cell development and function' *Nat Rev Immunol*, vol 5(6), pp 472–484

Mackinnon, R. (2003) 'Potassium channels' *FEBS Letters*, vol 555, pp 62-65

MacKinnon, R., Heginbotham, L., Abramson, T. (1990) 'Mapping the receptor site for charybdotoxin, a pore-blocking potassium channel inhibitor' *Neuron*, vol 5(6), pp 767-71

MacKinnon, R., Miller, C. (1988) 'Mechanism of charybdotoxin block of the high-conductance, Ca^{2+}-activated K^{+} channel' *J Gen Physiol.*, vol 91(3), pp 335-49

MacKinnon, R., Miller, C. (1989) 'Mutant potassium channels with altered binding of charybdotoxin, a pore-blocking peptide inhibitor' *Science*, vol 245(4924), pp1382-5.

Madara J. L. (1989). Loosening tight junctions. Lessons from the intestine. *The Journal of clinical investigation*, *83*(4), 1089–1094.

Madio, B., King, G.F., Undheim, E.A.B. (2019) 'Sea Anemone Toxins: A Structural Overview' *Mar Drugs*, vol 17(6), pp 325

Mahida, S., Lubitz, S. A., Rienstra, M., Milan, D. J., Ellinor, P. T. (2011). 'Monogenic atrial fibrillation as pathophysiological paradigms' *Cardiovascular research*, vol 89(4), pp 692–700.

Maizels, R. M., Balic, A., Gomez-Escobar, N., Nair, M., Taylor, M. D., Allen, J. E. (2004) "Helminth parasites--masters of regulation" *Immunological reviews* vol 201, pp 89–116

Maizels, R. M., Hewitson, J. P., Murray, J., Harcus, Y. M., Dayer, B., Filbey, K. J., Grainger, J. R., McSorley, H. J., Reynolds, L. A., Smith, K. A. (2012). Immune modulation and

modulators in Heligmosomoides polygyrus infection. *Experimental parasitology*, *132*(1), 76–89.

Mannuzzu, L.M., Moronne, M.M., Isacoff, E.Y. (1996) 'Direct physical measure of conformational rearrangement underlying potassium channel gating' *Science*, vol 271(5246), pp 213–216.

Marks, D.R., Fadool, D.A. (2007) 'Post-synaptic density perturbs insulin-induced Kv1.3 channel modulation via a clustering mechanism involving the SH3 domain' *J Neurochem.*, vol 103(4), pp 1608-1627

Martens, J. R., Kwak, Y. G., Tamkun, M. M. (1999) 'Modulation of Kv channel alpha/beta subunit interactions' *Trends in cardiovascular medicine*, vol 9(8), pp 253–258

Marvin, L., De E, Cosette P., Gagnon, J., Molle, G., Lange, C. (1999) 'Isolation, amino acid sequence and functional assays of SGTx1. The first toxin purified from the venom of the spider scodra griseipes' *Eur J Biochem*., vol 265(2), pp 572-9

Massacand, J. C., Stettler, R. C., Meier, R., Humphreys, N. E., Grencis, R. K., Marsland, B. J., Harris, N. L. (2009). Helminth products bypass the need for TSLP in Th2 immune responses by directly modulating dendritic cell function. *Proceedings of the National Academy of Sciences of the United States of America*, *106*(33), 13968–13973.

Mathie, A. (2010) 'Ion channels as novel therapeutic targets in the treatment of pain' *J Pharm Pharmacol.*, vol 62(9), pp 1089-95

Mathie, A., Veale, E.L. (2015) 'Two-pore domain potassium channels: potential therapeutic targets for the treatment of pain' *Pflugers Arch - Eur J Physiol*, vol 467(5), pp 931–943

Mathie, A., Veale, E.L., Cunningham, K.P., Holden, R.G., Wright, P.D. (2020) 'Two-Pore domain potassium channels as dug targets: anesthesia and beyond' *Annual review of pharmacology and toxicology,* vol 61, pp 401-420

Mathie, A., Veale, E. L., Holden, R. G. (2021). Heterologous Expression of Ion Channels in Mammalian Cell Lines. *Methods in molecular biology (Clifton, N.J.)*, *2188*, 51–65.

Mathie, A., Veale, EL., (2007) 'Therapeutic potential of neuronal two-pore domain potassium-channel modulators' *Curr Opin Investig Drugs*, vol 8(7), pp 555-62.

Matsuda, H., Saigusa, A., Irisawa, H. (1987) 'Ohmic conductance through the inwardly rectifying K channel and blocking by internal Mg^{2+}' *Nature*, vol 325, pp 156–159

Matteson, D.R., Deutsch, C. (1984) 'K channels in T lymphocytes: a patch clamp study using monoclonal antibody adhesion' *Nature*, vol 307(5950), pp 468-471.

Mayor, A. (2008) 'Greek Fire, Poison Arrows & Scorpion Bombs: Biological and Chemical Warfare in the Ancient World' New York, New York Overlook Books

Major, A (2010) 'The poison king: the life and legend of Mithradates, Rome's deadliest enemy' Princeton University Press

McAllister, R.E, Noble, D. (1966) 'The time and voltage dependence of the slow outward current in cardiac Purkinje fibres' *J Physiol.*, vol 186(3), pp 632-62

McDonough S. I. (2007). Gating modifier toxins of voltage-gated calcium channels. *Toxicon: official journal of the International Society on Toxinology*, *49*(2), 202–212.

McIntosh, J.M., Olivera, B.M., Cruz, L.J. (1999) 'Conus peptides as probes for ion channels' *Methods Enzymol.*, vol 294, pp. 605-624

McKinney, L.C., Gallin, E.K. (1988) 'Inwardly rectifying whole-cell and single-channel K currents in the murine macrophage cell line J774.1' *J. Membrain Biol*., vol 103, pp 41–53

Meera, P., Wallner, M., Song, M., Toro, L. (1997) 'Large conductance voltage- and calcium-dependent K+ channel, a distinct member of voltage-dependent ion channels with seven N-terminal transmembrane segments (S0-S6), an extracellular N terminus, and an intracellular (S9-S10) C terminus' *Proc Natl Acad Sci U S A.*, vol 94(25), pp14066-71

Mekler, V.M. and Bystryak, S.M. (1992). Application of o-phenylenediamine as a fluorogenic substrate in peroxidase-mediated enzyme-linked immunosorbent assay. *Analytica Chimica Acta,* 264 (2), 359-363

Menezes, M. C., Furtado, M. F., Travaglia-Cardoso, S. R., Camargo, A. C., and Serrano, S. M. (2006) 'Sex-based individual variation of snake venom proteome among eighteen Bothrops jararaca siblings' *Toxicon,* 47(3), 304–312.

Meuth, S.G., Bittner, S., Meuth, P., Simon, O.J., Budde, T., Wiendl, H. (2008)'TWIK-related acid-sensitive K^+ channel 1 (TASK1) and TASK3 critically influence T lymphocyte effector functions' *J Biol Chem.*, vol 283(21), pp 14559-70

Meyer, H. (1899) 'Zur Teorie der Alkoholnarkose. Naunyn Schmiedeberg' *Arch. Exp. Path. Pharmak.*, vol 42, pp 109–118

Middleton, R.E., Sanchez, M., Linde, A.R., Bugianesi, R.M., Dai, G., Felix, J.P., Koprak, S.L., Staruch, M.J., Bruguera, M., Cox, R., Ghosh, A., Hwang, J., Jones, S., Kohler, M., Slaughter, R.S., McManus, O.B., Kaczorowski, G.J., Garcia, M.L. (2003) 'Substitution of a single residue in Stichodactyla helianthus peptide, ShK-Dap22, reveals a novel pharmacological profile' *Biochemistry*, vol 42(46), pp 13698-707

Middleton, R.E., Warren, V.A., Kraus, R.L., Hwang, J.C., Liu, J.C., Dai, G., Brochu, R.M., Kohler, M.G., Gao, Y.-D., Garsky, V.M., Bogusky, M.J., Mehl, J.T., Cohen, C.J., Smith, M.M. (2002)'Two tarantula peptides inhibit activation of multiple sodium channels' *Biochemistry*, vol 41(50), pp 14734-14747

Milescu, M., Lee, H. C., Bae, C. H., Kim, J. I., Swartz, K. J. (2013). Opening the shaker K+ channel with hanatoxin. *The Journal of general physiology*, *141*(2), 203–216.

Milescu, M., Lee, H.C., Bae, C.H., Kim, J.I., Swartz, K.J. (2013) 'Opening the shaker K^+ channel with hanatoxin' *J. Gen. Physiol.*, vol 141(2), pp 203–216

Miller C. (1995). The charybdotoxin family of K+ channel-blocking peptides. *Neuron*, *15*(1), 5–10.

Miller, A.N., Long, S.B. (2012) 'Crystal structure of the human two-pore domain potassium channel K2P1' *Science*, vol 335(6067), pp 432-6

Miller, C. (1988) 'Competition for block of a Ca^{2+}-activated K^+ channel by charybdotoxin and tetraethylammonium' *Neuron*, vol 1(10), pp 1003-6

Miller, C. (1995) 'The charybdotoxin family of K^+ channel-blocking peptides' *Neuron*, vol 15(1), pp 5-10

Minassian, N.A., Gibbs, A., Shih, A.Y., Liu, Y., Neff, R.A., Sutton, S.W., Mirzadegan, T., Connor, J., Fellows, R., Husovsky, M., Nelson, S., Hunter, M.J.,Flinspach, M., Wickenden, A. (2013) 'Analysis of the structural and molecular basis of voltage-sensitive sodium channel inhibition by the spider toxin huwentoxin-IV (mu-TRTX-Hh2a)' *J. Biol. Chem.*, 288 (31), pp 22707–22720

Minor, D. L., Lin, Y. F., Mobley, B. C., Avelar, A., Jan, Y. N., Jan, L. Y., Berger, J. M. (2000). The polar T1 interface is linked to conformational changes that open the voltage-gated potassium channel. *Cell*, *102*(5), 657–670.

Minor, D.L. Jr, Masseling, S.J., Jan, Y.N., Jan, L.Y. (1999) 'Transmembrane structure of an inwardly rectifying potassium channel' *Cell,* vol 96(6), pp 879 – 891

Mishra, P.K., Patel, N., Wu, W., Bleich, D., Gause, W.C. (2013) "Prevention of type 1 diabetes through infection with an intestinal nematode parasite requires IL-10 in the absence of a Th2-type response" *Mucosal Immunol.,* vol 6(2), pp 297-308

Miyasaka, Y., Barnes, M. E., Gersh, B. J., Cha, S. S., Bailey, K. R., Abhayaratna, W. P., Seward, J. B., Tsang, T. S. (2006) 'Secular trends in incidence of atrial fibrillation in Olmsted County, Minnesota, 1980 to 2000, and implications on the projections for future prevalence' *Circulation*, vol 114(2), pp 119–125.

Mizuno, M., Nishikawa, K., Yuzawa, Y., Kanie, T., Mori, H., Araki, Y., Hotta, N., Matsuo, S. (2000) 'Acute renal failure after a sea anemone sting' *Am J Kidney Dis*., vol 36(2), pp E10

Mizuno, M., Nozaki, M., Morine, N., Suzuki, N., Nishikawa, K., Morgan, B.P., Matsuo, S. (2007) 'A protein toxin from the sea anemone Phyllodiscus semoni targets the kidney and causes a severe renal injury with predominant glomerular endothelial damage' *Am J Pathol.,* vol 171(2), pp 402-14

Mohamed Abd El-Aziz, T., Soares, A.G., Stockand, J.D. (2019) 'Snake Venoms in Drug Discovery: Valuable Therapeutic Tools for Life Saving' *Toxins*, vol 11 (10), 564.
Mol. Biol. Cell vol 8 (11), pp. 2101-9

Monks, C.R., Freiberg, B.A., Kupfer, H., Sciaky, N., Kupfer, A. (1998) 'Three-dimensional segregation of supramolecular activation clusters in T cells' *Nature*, vol 395(6697), pp 82-6

Moran, Y., Genikhovich, G., Gordon, D., Wienkoop, S., Zenkert, C., Ozbek, S., Technau, U., Gurevitz, M. (2012) 'Neurotoxin localization to ectodermal gland cells uncovers an alternative mechanism of venom delivery in sea anemones' *Proc Biol Sci.,* vol 279(1732), pp 1351-8.

Morelli, M. B., Liberati, S., Amantini, C., Nabiss, M., Santoni, M., Farfariello, V., Santoni, G. (2013). Expression and function of the transient receptor potential ion channel family in the hematologic malignancies. *Current molecular pharmacology*, *6*(3), 137–148.

Moreno, Y., Gros, P. P., Tam, M., Segura, M., Valanparambil, R., Geary, T. G., Stevenson, M. M. (2011). Proteomic analysis of excretory-secretory products of Heligmosomoides polygyrus assessed with next-generation sequencing transcriptomic information. *PLoS neglected tropical diseases*, *5*(10), e1370.

Morton, M.J., Abohamed, A., Sivaprasadaro, M.H. (2005) 'pH sensing in the two-pore domain K^+ channel, TASK2' *Proceedings of the National Academy of Sciences*, vol 102 (44), pp 16102-16106

Morton, M.J., O'Connell, A.D., Sivaprasadarao, A., Hunter, M. (2003) 'Determinants of pH sensing in the two-pore domain K (+) channels TASK-1 and -2' *Pflugers Arch*.,vol 445(5), pp 577-83

Mouhat, S., Andreotti, N., Jouirou, B., Sabatier, J.M. (2008) 'Animal toxins acting on voltage-gated potassium channels' *Curr Pharm Des*., vol 14(24), pp 2503-18

Mouhat, S., Jouirou, B., Mosbah, A., De Waard, M., Sabatier, J.M. (2004) 'Diversity of folds in animal toxins acting on ion channels' *Biochem J*., vol 378(Pt 3), pp 717-26

Mu, D., Chen, L., Zhang, X., See, L.H., Koch, C.M., Yen, C., Tong, J.J., Spiegel, L., Nguyen, K.C., Servoss, A., Peng, Y., Pei, L., Marks, J.R., Lowe, S., Hoey, T., Jan, L.Y., McCombie, W.R., Wigler, M.H., Powers, S. (2003) 'Genomic amplification and oncogenic properties of the KCNK9 potassium channel gene' *Cancer Cell*, vol 3(3), pp 297-302

Murray, J.K., Ligutti, J., Liu, D., Zou, A., Poppe, L., Li, H., Andrews, K.L., Moyer, B.D., McDonough, S.I., Favreau, P. (2015) 'Engineering potent and selective analogues of GpTx-1, a tarantula venom peptide antagonist of the $Na_V1.7$ sodium channel' *J. Med. Chem*., vol 58 (5), pp 2299–2314

Navarro, M. A., Milescu, L. S., Milescu, M. (2019). Unlocking the gating mechanism of Kv2.1 using guangxitoxin. *The Journal of general physiology*, *151*(3), 275–278.

Neher, E., Sakmann, B. (1976) 'Noise analysis of drug induced voltage clamp currents in denervated frog muscle fibres' *J Physiol.*, vol 258(3), pp 705-29 (a)

Neher, E., Sakmann, B. (1976) 'Single-channel currents recorded from membrane of denervated frog muscle fibres' *Nature,* vol 260(5554), pp 799-802 (b)

Nelson M, McClelland M. (1992). Use of DNA methyltransferase/endonuclease enzyme combinations for megabase mapping of chromosomes. *Methods Enzymol,* 216:279-303.

Nentwig, W., Kuhn-Nentwig, L. (2013) 'Spider Venoms Potentially Lethal to Humans' In Spider Ecophysiology; Nentwig, W., Ed.; Springer: Berlin/Heidelberg, Germany, 2013; pp. 253–264

Neusch, C., Weishaupt, J.H., Bähr, M. (2003) 'Kir channels in the CNS: emerging new roles and implications for neurological diseases' *Cell Tissue Res*., vol 311(2), pp 131-8.

Newman, E.A. (1984) ‘Regional specialization of retinal glial cell membrane’ *Nature*, vol 309(5964), pp 155-7

Nguyen, A., Kath, J.C., Hanson, D.C., Biggers, M.S., Canniff, P.C., Donovan, C.B., Mather, R.J., Bruns, M.J., Rauer, H., Aiyar, J., Lepple-Wienhues, A., Gutman, G.A., Grissmer, S., Cahalan, M.D., Chandy, K.G. (1996) ‘Novel nonpeptide agents potently block the C-type inactivated conformation of Kv1.3 and suppress T cell activation’ *Mol Pharmacol*., vol 50(6), pp 1672–1679

Nguyen, H.L., Pieper, G.H., Wilders, R. (2013) ‘Andersen-Tawil syndrome: clinical and molecular aspects’ *Int J Cardiol.* ,vol 170(1), pp 1-16

Nicholson, C.G., Lopatin, A.N. (1997) ‘Inward rectifier potassium channel’ *Ann. Rev. Physiology*, vol 59, pp 171-191

Nicolaou, S.A., Neumeier, L., Peng, Y., Devor, D.C., Conforti, L. (2007) ‘The Ca ($^{2+}$)-activated K($^{+}$) channel KCa3.1 compartmentalizes in the immunological synapse of human T lymphocytes’ *Am J Physiol Cell Physiol*,. vol 292(4), pp C1431-9 (b)

Nicolaou, S.A., Neumeier, L., Steckly, A., Kucher, V., Takimoto, K., Conforti, L. (2009) ‘Localization of Kv1.3 channels in the immunological synapse modulates the calcium response to antigen stimulation in T lymphocytes’ *J Immunol.*, vol 183(10), pp 6296-6302.

Nicolaou, S.A., Szigligeti, P., Neumeier, L., Lee, S.M., Duncan, H.J., Kant, S.K., Mongey, A.B., Filipovich, A.H., Conforti, L. (2007) ‘Altered dynamics of Kv1.3 channel compartmentalization in the immunological synapse in systemic lupus erythematosus’ *J Immunol.*, vol 179(1), pp 346-56 (a)

Niday, Z., Tzingounis, A. V. (2018). Potassium Channel Gain of Function in Epilepsy: An Unresolved Paradox. *The Neuroscientist : a review journal bringing neurobiology, neurology and psychiatry*, *24*(4), 368–380. https://doi.org/10.1177/1073858418763752

Nielsen, B.R., Ratzer, R., Börnsen, L., von Essen, M.R., Christensen, J.R., Sellebjerg, F. (2017) 'Characterization of naïve, memory and effector T cells in progressive multiple sclerosis' *J Neuroimmunol.*, vol 310, pp 17-25

Niemeyer, M.I., Cid, L.P., González, W., Sepúlveda, F.V. (2016) 'Gating, Regulation, and Structure in K2P K^+ Channels: In Varietate Concordia?' *Mol Pharmacol.*, vol 90(3), pp 309-17

Noble, D. (1965) 'Electrical properties of cardiac muscle attributable to inward going (anomalous) rectification' *J Cells Comp. Physiol*,. vol 66, pp 127-136

Noda, M., Shimizu, S., Tanabe, T., Takai, T., Kayano, T., Ikeda, T., Takahashi, H., Nakayama, H., Kanaoka, Y., Minamino, N., et al. (1984) 'Primary structure of Electrophorus electricus sodium channel deduced from cDNA sequence' *Nature,* vol 312(5990), pp 121-127

Noda, M., Takahashi, H., Tanabe, T., Toyosato, M., Kikyotani, S., Hirose, T., Asai, M., Takashima, H., Inayama, S., Miyata, T., Numa, S. (1983) ' Primary structures of beta- and delta-subunit precursors of Torpedo californica acetylcholine receptor deduced from cDNA sequences' *Nature*, vol 20- 301(5897), pp 251-5 (a)

Noda, M., Takahashi, H., Tanabe, T., Toyosato, M., Kikyotani, S., Furutani, Y., Hirose, T., Takashima, H., Inayama, S., Miyata, T., Numa, S. (1983) 'Structural homology of Torpedo californica acetylcholine receptor subunits' *Nature*, vol 302(5908), pp 528-32 (b)

North, R., Williams, J.T., Surprenant, A., Christie, M.J. (1987) 'Mu and delta receptors belong to a family of receptors that are coupled to potassium channels' *Proc Natl Acad Sci USA*,. vol 84(15), pp 5487-91

O'Connell, K. M., Loftus, R., Tamkun, M. M. (2010). Localization-dependent activity of the Kv2.1 delayed-rectifier K+ channel. *Proceedings of the National Academy of Sciences of the United States of America*, *107*(27), 12351–12356.

Ogden, D., Stanfield, P. (1999) 'Chapter 4 Patch clamp techniques for single channel and whole-cell recordings' Material Science

Olamendi-Portugal, T., Gómez-Lagunas, F., Gurrola, G.B., Possani, L.D. (1996) 'A novel structural class of K^+channel blocking toxin from the scorpion Pandinus imperator' *Biochem J.*, vol 315 (Pt 3), pp 977-81

Oliveira, I.S., Ferreira, I.G., Alexandre-Silva, G.M., Cerni, F.A., Cremonez, C.M., Arantes, E.C., Zottich, U., Pucca, M.B. (2019) 'Scorpion toxins targeting Kv1.3 channels: insights into immunosuppression' *J Venom Anim Toxins Incl Trop Dis*., vol 25, e148118

Oliver, D., Hahn, H., Antz, C., Ruppersberg, J.P., Fakler, B. (1998) 'Interaction of permeant and blocking ions in cloned inward-rectifier K^+ channels' *Biophys J*., vol 74(5), pp 2318-2326.

Olson, T. M., Alekseev, A. E., Liu, X. K., Park, S., Zingman, L. V., Bienengraeber, M., Sattiraju, S., Ballew, J. D., Jahangir, A., Terzic, A. (2006) 'Kv1.5 channelopathy due to KCNA5 loss-of-function mutation causes human atrial fibrillation' *Human molecular genetics*, vol 15(14), pp 2185–2191.

Ouadid-Ahidouch, H., Ahidouch, A (2013) 'K^+ channels and cell cycle progression in tumor cells' *Front Physiol*., vol 4, pp 220

Ouadid-Ahidouch, H., Chaussade, F., Roudbaraki, M., Slomianny, C., Dewailly, E., Delcourt, P., Prevarskaya, N. (2000) 'KV1.1 K(+) channels identification in human breast carcinoma cells: involvement in cell proliferation' *Biochemical and biophysical research communications*, vol *278*(2), pp 272–277.

Overton, E. (1901) 'Studien uber die Narkose zugleich ein Beitrag zur allgemeinen Pharmakologie' Jena.

Panyi, G. (2005) 'Biophysical and pharmacological aspects of K^+channels in T lymphocytes' *Eur Biophys J.*, vol 34(6), pp 515-29

Panyi, G., Deutsch, C. (1996). Assembly and suppression of endogenous Kv1.3 channels in human T cells. *The Journal of general physiology*, *107*(3), 409–420.

Panyi, G., Sheng, Z., Deutsch, C. (1995) 'C-type inactivation of a voltage-gated K^+ channel occurs by a cooperative mechanism' *Biophys J.*, vol 69 (3), pp 896–903.

Pardo-Lopez, L., Zhang, M., Liu, J., Jiang, M., Possani, L. D., Tseng, G. N. (2002). Mapping the binding site of a human ether-a-go-go-related gene-specific peptide toxin (ErgTx) to the channel's outer vestibule. *The Journal of biological chemistry*, *277*(19), 16403–16411.

Pardo, L.A. (2004) 'Voltage-gated potassium channels in cell proliferation' *Physiology* (Bethesda) vol 19, pp 285-292

Park, C.S., Miller, C. (1992) 'Interaction of charybdotoxin with permeant ions inside the pore of a K^+ channel' *Neuron*, vol 9(2), pp 307-13

Pau, V., Zhou, Y., Ramu, Y., Xu, Y., Lu, Z. (2017) 'Crystal structure of an inactivated mutant mammalian voltage-gated K^+ channel.' *Nature structural & molecular biology*, vol 24(10), pp 857–865.

Pauletti, G.M., Gangwar, S., Knipp, G.T., Nerurkar, M.M., Okumu, F.W., Tamura, K., Siahaan, T.J., Borchardt, R.T. (1996) Structural requirements for intestinal absorption of peptide drugs. *Journal of Controlled Release,* 41 (1–2), 3-17.

Paulhus, K., Ammerman, L., Glasscock, E. (2020) 'Clinical Spectrum of *KCNA1* Mutations: New Insights into Episodic Ataxia and Epilepsy Comorbidity' *International journal of molecular sciences*, vol *21*(8), pp 2802.

Paulussen, A., Yang, P., Pangalos, M., Verhasselt, P., Marrannes, R., Verfaille, C., Vandenberk, I., Crabbe, R., Konings, F., Luyten, W., Armstrong, M. (2000). Analysis of the human KCNH2(HERG) gene: identification and characterization of a novel mutation Y667X associated with long QT syndrome and a non-pathological 9 bp insertion. *Human mutation*, *15*(5), 483.

Pedersen, S. F., Stock, C. (2013). Ion channels and transporters in cancer: pathophysiology, regulation, and clinical potential. *Cancer research*, *73*(6), 1658–1661.

Pelly, V. S., Kannan, Y., Coomes, S. M., Entwistle, L. J., Rückerl, D., Seddon, B., MacDonald, A. S., McKenzie, A., Wilson, M. S. (2016). "IL-4-producing ILC2s are required for the differentiation of T_H2 cells following *Heligmosomoides polygyrus* infection" *Mucosal immunology 9*(6), 1407–1417

Pennington, M.W., Beeton, C., Galea, C.A., Smith, B.J., Chi, V., Monaghan, K.P., Garcia, A., Rangaraju, S., Giuffrida, A., Plank, D., Crossley, G., Nugent, D., Khaytin, I., Lefievre, Y., Peshenko, I., Dixon, C., Chauhan, S., Orzel, A., Inoue, T., Hu, X., Moore, R.V., Norton, R.S., Chandy, K.G. (2009) 'Engineering a stable and selective peptide blocker of the Kv1.3 channel in T lymphocytes' *Mol Pharmacol.*, 2009 vol 75(4), pp 762-73

Pennington, M.W., Czerwinski, A., Norton, R.S. (2018) 'Peptide therapeutics from venom: Current status and potential' *Bioorg Med Chem.*, vol 26(10), pp 2738-2758

Pennington, M.W., Mahnir, V.M., Khaytin, I., Zaydenberg, I., Byrnes, M.E., Kem, W.R. (1996) 'An essential binding surface for ShK toxin interaction with rat brain potassium channels' *Biochemistry,* vol 35(51), pp 16407-11

Pennington, M. W., Harunur Rashid, M., Tajhya, R. B., Beeton, C., Kuyucak, S., & Norton, R. S. (2012). A C-terminally amidated analogue of ShK is a potent and selective blocker of the voltage-gated potassium channel Kv1.3. *FEBS letters*, *586*(22), 3996–4001.

Pérez-García, M.T., Cidad, P., López-López, J.R. (2018) 'The secret life of ion channels: Kv1.3 potassium channels and proliferation' *Am J Physiol Cell Physiol.*, vol 314(1), pp C27-C42

Piccolino, M. (2008) 'Visual images in Luigi Galvani's path to animal electricity' *J Hist Neurosci.,* vol 17(3), pp 335-48

Pierce BG, Wiehe K, Hwang H, Kim BH, Vreven T, Weng Z (2014) ZDOCK server: interactive docking prediction of protein-protein complexes and symmetric multimers. *Bioinformatics.* 30(12), 1771-3.

Pohl, J., Hubalek, F., Byrnes, M.E., Nielsen, K.R., Woods, A., Pennington, M.W. (1995) 'Assignment of the three disulfide bonds in ShK toxin: A potent potassium channel inhibitor from the sea anemone Stichodactyla helianthus' *Lett Pept Sci*, vol 1, pp 291–297

Pongs, O., Kecskemethy, N., Müller, R., Krah-Jentgens, I., Baumann, A., Kiltz, H.H., Canal, I., Llamazares, S., Ferrus, A. (1988) ' Shaker encodes a family of putative potassium channel proteins in the nervous system of Drosophila' *EMBO J.*, vol 7(4), pp 1087-96

Pongs, O., Schwarz, J.R. (2010) 'Ancillary subunits associated with voltage-dependent K+ channels' *Physiol Rev.*, vol 90(2), pp 755-96

Possani, L.D., Merino, E., Corona, M., Bolivar, F., Becerril, B. (2000) 'Peptides and genes coding for scorpion toxins that affect ion-channels' *Biochimie.,* vol 82(9-10), pp 861-8

Possani, L.D., Selisko, B., Gurrola, G.B. (1999) 'Structure and function of scorpion toxins affecting K^+ channels' *Perspectives in Drug Discovery and Design*, vol 15, pp15–40

Post, M. A., Kirsch, G. E., Brown, A. M. (1996). Kv2.1 and electrically silent Kv6.1 potassium channel subunits combine and express a novel current. *FEBS letters*, *399*(1-2), 177–182.

Pottosin, I. I., Bonales-Alatorre, E., Valencia-Cruz, G., Mendoza-Magaña, M. L., Dobrovinskaya, O. R. (2008). TRESK-like potassium channels in leukemic T cells. *Pflugers Archiv : European journal of physiology*, *456*(6), 1037–1048.

Pottosin, I. I., Valencia-Cruz, G., Bonales-Alatorre, E., Shabala, S. N., Dobrovinskaya, O. R. (2007). Methyl-beta-cyclodextrin reversibly alters the gating of lipid rafts-associated Kv1.3 channels in Jurkat T lymphocytes. *Pflugers Archiv : European journal of physiology*, *454*(2), 235–244.

Prendini, L., Wheeler, W.C. (2005) 'Scorpion higher phylogeny and classification, taxonomic anarchy, and standards for peer review in online publishing' Cladistics vol 21 (5), pp 446-494
Prentis, P. J., Pavasovic, A., Norton, R. S. (2018) "Sea Anemones: Quiet Achievers in the Field of Peptide Toxins" *Toxins* vol 10 (1), pp 36.

Prentis, P.J., Pavasovic, A., Norton, R.S. (2018) 'Sea Anemones: Quiet Achievers in the Field of Peptide Toxins' *Toxins* (Basel), vol 10(1), pp 36

Pyo, H., Chung, S., Jou, I., Gwag, B., Joe, E. H. (1997) 'Expression and function of outward K+ channels induced by lipopolysaccharide in microglia' *Molecules and cells*, vol 7(5), pp 610–614.

Quintero-Hernández, V., Jiménez-Vargas, J.M., Gurrola, G.B., Valdivia, H.H., Possani, L.D. (2013) 'Scorpion venom components that affect ion-channels function' *Toxicon*, vol 76, pp 328-42

Rader, R. K., Kahn, L. E., Anderson, G. D., Martin, C. L., Chinn, K. S., Gregory, S. A. (1996). T cell activation is regulated by voltage-dependent and calcium-activated potassium channels. *Journal of immunology (Baltimore, Md. : 1950)*, *156*(4), 1425–1430.

Rae, J., Cooper, K., Gates, P., Watsky, M. (1991). Low access resistance perforated patch recordings using amphotericin B. *Journal of neuroscience methods*, *37*(1), 15–26.

Ranganathan, R., Lewis, J. H., MacKinnon, R. (1996). Spatial localization of the K+ channel selectivity filter by mutant cycle-based structure analysis. *Neuron*, *16*(1), 131–139.

Rao, A., Luo, C., Hogan, P. G. (1997). Transcription factors of the NFAT family: regulation and function. *Annual review of immunology*, *15*, 707–747.

Raphael, I., Joern, R.R., Forsthuber, T.G. (2020) 'Memory $CD4^+$ T Cells in Immunity and Autoimmune Diseases' *Cells,* vol 9(3), pp 531.

Rashid, M. H., Huq, R., Tanner, M. R., Chhabra, S., Khoo, K. K., Estrada, R., Dhawan, V., Chauhan, S., Pennington, M. W., Beeton, C., Kuyucak, S., Norton, R. S. (2014). A potent and Kv1.3-selective analogue of the scorpion toxin HsTX1 as a potential therapeutic for autoimmune diseases. *Scientific reports*, *4*, 4509.

Rashid, M.H., Heinzelmann, G., Huq, R., Tajhya, R.B., Chang, S.C., Chhabra, S., Pennington, M.W., Beeton, C., Norton, R.S., Kuyucak, S. (2013) 'A potent and selective peptide blocker

of the Kv1.3 channel: prediction from free-energy simulations and experimental confirmation' *PLoS One,* vol 8(11), pp e78712

Rauer, H., Lanigan, M. D., Pennington, M. W., Aiyar, J., Ghanshani, S., Cahalan, M. D., Norton, R. S., Chandy, K. G. (2000). Structure-guided transformation of charybdotoxin yields an analog that selectively targets Ca(2+)-activated over voltage-gated K(+) channels. *The Journal of biological chemistry*, *275*(2), 1201–1208.

Rauer, H., Pennington, M., Cahalan, M., Chandy, K.G. (1999) 'Structural conservation of the pores of calcium-activated and voltage-gated potassium channels determined by a sea anemone toxin' *J Biol Chem.*, vol 274(31), pp 21885-92

Reardon, C., Sanchez, A., Hogaboam, C. M., McKay, D. M. (2001). Tapeworm infection reduces epithelial ion transport abnormalities in murine dextran sulfate sodium-induced colitis. *Infection and immunity*, *69*(7), 4417–4423.

Redi F. 'Osservazioni Intorno alle Vipere' Florence: All'Insegna della Stella. Availiable from: URL:https://books.google.ru/books/reader?id=h3FVAAAAcAAJ&hl=ru&printsec=frontcover&output= reader&pg=GBS.PP1

Reichold, M., Zdebik, A.A., Lieberer, E., Rapedius, M., Schmidt, K., Bandulik, S., Sterner, C., Tegtmeier, I., Penton, D., Baukrowitz, T., Hulton, S.A., Witzgall, R., Ben-Zeev, B., Howie, A.J., Kleta, R., Bockenhauer, D., Warth, R. (2010) 'KCNJ10 gene mutations causing EAST syndrome (epilepsy, ataxia, sensorineural deafness, and tubulopathy) disrupt channel function' *Proc Natl Acad Sci U S A.*, 107(32), pp 14490-5

Reynolds, L. A., Filbey, K. J., Maizels, R. M. (2012). Immunity to the model intestinal helminth parasite Heligmosomoides polygyrus. *Seminars in immunopathology*, *34*(6), 829–846.

Rhee, J. S., Ebihara, S., Akaike, N. (1994). Gramicidin perforated patch-clamp technique reveals glycine-gated outward chloride current in dissociated nucleus solitarii neurons of the rat. *Journal of neurophysiology*, *72*(3), 1103–1108.

Ringer S. (1882) ‘Regarding the Action of Hydrate of Soda, Hydrate of Ammonia, and Hydrate of Potash on the Ventricle of the Frog's Heart’ *J Physiol.*, vol 3(3-4), pp 195-202.6 (b)

Ringer, S. (1882) ‘Concerning the influence exerted by each of the constituents of the blood on the contraction of the ventricle’ *J. Physiol.*, vol 3 (5-6), pp 380-393 (a)

Ringer, S. (1883) ‘A further Contribution regarding the influence of the different Constituents of the Blood on the Contraction of the Heart’ *J Physiol.,* vol 4(1), pp 29-42 (a)

Ringer, S. (1883) ‘A third contribution regarding the Influence of the Inorganic Constituents of the Blood on the Ventricular Contraction’ *J. Physiol.,* vol 4 (2-3), pp 222-225 (b)

Ringer, S. (1884) ‘An Investigation regarding the Action of Rubidium and Caesium Salts compared with the Action of Potassium Salts on the Ventricle of the Frog's Heart’ *J Physiol*., vol 4(6), pp 370-386

Ringer, S. (1885) ‘Regarding the influence of the Organic Constituents of the blood on the Contractility of the Ventricle’ *J Physiol.*, vol 6(6), pp 361-463.7

Ringer, S., Buxton, D.W. (1887) ‘Upon the Similarity and Dissimilarity of the behaviour of Cardiac and Skeletal Muscle when brought into relation with Solutions containing Sodium, Calcium and Potassium Salts’ *J Physiol.*, vol 8(5), pp 288-295

Robbins, C. A., Tempel, B. L. (2012). Kv1.1 and Kv1.2: similar channels, different seizure models. *Epilepsia*, *53 Suppl 1*, 134–141.

Robey, E., Fowlkes, B.J (1994) ‘Selective events in T cells development’ *Annu. Rev. Immunol.,* vol 12, pp 675-705

Robinson, M., Wahid, F., Behnke, J. M., Gilbert, F. S. (1989). Immunological relationships during primary infection with Heligmosomoides polygyrus (Nematospiroides dubius): dose-dependent expulsion of adult worms. *Parasitology*, *98 (Pt 1)*, 115–124.

Roden D. M. (2003) ‘Antiarrhythmic drugs: past, present and future’ *Journal of cardiovascular electrophysiology*, 14(12), 1389–1396.

Rodríguez de la Vega, R.C., Possani, L.D. (2004) ‘Current views on scorpion toxins specific for K^+ channels’ *Toxicon*, vol 43(8), pp 865-75

Roepke, T. K., Kontogeorgis, A., Ovanez, C., Xu, X., Young, J. B., Purtell, K., Goldstein, P. A., Christini, D. J., Peters, N. S., Akar, F. G., Gutstein, D. E., Lerner, D. J., Abbott, G. W. (2008) ‘Targeted deletion of kcne2 impairs ventricular repolarization via disruption of I(K,slow1) and I(to,f)’ *FASEB journal : official publication of the Federation of American Societies for Experimental Biology*, 22(10), 3648–3660.

Rougier, O., Vassort, G., Stämpfli, R. (1968) ‘Voltage clamp experiments on frog atrial heart muscle fibres with the sucrose gap technique’ *Pflugers Arch Gesamte Physiol Menschen Tiere*, vol 301(2), pp 91-108

Rouzaire-Dubois, B., Milandri, J., Bostel, S., Dubois, J.M. (2000) ‘Control of cell proliferation by cell volume alterations in rat C6 glioma cells’ *Pflügers Arch - Eur J Physiol*., vol 440 (6), pp 881–888

Ruppersberg, J.P. (2000) ‘Intracellular regulation of inward rectifier K^+ channels’ *Pflugers Arch.,* vol 441(1), pp 1-11

Ruta V., Jiang Y., Lee A., Chen J., Mackinnon R. (2003) ‘Functional analysis of an archaebacterial voltage-dependent K^+ channel’ *Nature*, vol 422 (6928), pp 180-185

Ruta, V., MacKinnon, R. (2004) ‘Localization of the voltage-sensor toxin receptor on KvAP’ *Biochemistry*, vol 43(31), pp 10071-9

Ruyssers, N. E., De Winter, B. Y., De Man, J. G., Loukas, A., Herman, A. G., Pelckmans, P. A., Moreels, T. G. (2008). ‘Worms and the treatment of inflammatory bowel disease: are molecules the answer?’ *Clinical & developmental immunology*, *2008*, 567314.

Sachdev, M., Gaínza-Lein, M., Tchapyjnikov, D., Jiang, Y. H., Loddenkemper, T., Mikati, M. A. (2017). 'Novel clinical manifestations in patients with KCNA2 mutations' *Seizure*, *51*, 74–76.

Saito, Y. A., Strege, P. R., Tester, D. J., Locke, G. R., 3rd, Talley, N. J., Bernard, C. E., Rae, J. L., Makielski, J. C., Ackerman, M. J., Farrugia, G. (2009). 'Sodium channel mutation in irritable bowel syndrome: evidence for an ion channelopathy'. *American journal of physiology. Gastrointestinal and liver physiology*, *296*(2), G211–G218.

Saitsu, H., Akita, T., Tohyama, J., Goldberg-Stern, H., Kobayashi, Y., Cohen, R., Kato, M., Ohba, C., Miyatake, S., Tsurusaki, Y., Nakashima, M., Miyake, N., Fukuda, A., Matsumoto, N. (2015). 'De novo KCNB1 mutations in infantile epilepsy inhibit repetitive neuronal firing'. *Scientific reports*, *5*, 15199.

Sala-Rabanal, M., Kucheryavykh, L.Y., Skatchkov, S.N., Eaton, M.J., Nichols, C.G. (2010) 'Molecular mechanisms of EAST/SeSAME syndrome mutations in Kir4.1' J Biol Chem. vol 285(46), pp 36040-36048

Sallusto, F., Geginat, J., Lanzavecchia, A. (2004). 'Central memory and effector memory T cell subsets: function, generation, and maintenance' *Annual review of immunology*, *22*, 745–763.

Sallusto, F., Lenig, D., Förster, R., Lipp, M., Lanzavecchia, A. (1999). 'Two subsets of memory T lymphocytes with distinct homing potentials and effector functions.' *Nature*, *401*(6754), 708–712.

Sandhiya, S., Dkhar, S.A. (2009) 'Potassium channels in health, disease & development of channel modulators' *Indian J Med Res.*, vol 129(3), pp 223-32

Sands, S. B., Lewis, R. S., Cahalan, M. D. (1989). 'Charybdotoxin blocks voltage-gated K+ channels in human and murine T lymphocytes.' *The Journal of general physiology*, *93*(6), 1061–1074.

Sanguinetti, M. C., Jiang, C., Curran, M. E., Keating, M. T. (1995). 'A mechanistic link between an inherited and an acquired cardiac arrhythmia: HERG encodes the IKr potassium channel' *Cell*, *81*(2), 299–307.

Sanguinetti, M. C., Tristani-Firouzi, M. (2006). 'hERG potassium channels and cardiac arrhythmia.' *Nature*, *440*(7083), 463–469

Sanguinetti, M.C., Johnson, J.H., Hammerland, L.G., Kelbaugh, P.R., Volkmann, R.A., Saccomano, N.A., Mueller, A.L. (1997) 'Heteropodatoxins: peptides isolated from spider venom that block Kv4.2 potassium channels' *Mol Pharmacol.*, vol 51(3), pp 491-8

Sarciaux, J.M., Acar, L., Sado, P.A. (1995) 'Using microemulsion formulations for oral drug delivery of therapeutic peptides.' *International Journal of Pharmaceutics,* 120 (2), 127-136

Scaldaferri, F., Fiocchi, C. (2007). 'Inflammatory bowel disease: progress and current concepts of etiopathogenesis.' *Journal of digestive diseases*, *8*(4), 171–178.

Scaloni, A., Bottiglieri, C., Ferrara, L., Corona, M., Gurrola, G. B., Batista, C., Wanke, E., Possani, L. D. (2000). 'Disulfide bridges of ergtoxin, a member of a new sub-family of peptide blockers of the ether-a-go-go-related K+ channel.' *FEBS letters*, *479*(3), 156–157.

Schewe, M., Nematian-Ardestani, E., Sun H., Musinszki, M., Cordeiro, S., Bucci, G., de Groot, B. L., Tucker, S. J., Rapedius, M., Baukrowitz, T. (2016) 'A Non-canonical Voltage-Sensing Mechanism Controls Gating in K2P K+ Channels' *Cell*, vol 164(5), pp 937-949

Schmidt, C., Wiedmann, F., Kallenberger, S.M., Ratte, A., Schulte, J.S., Scholz, B., Müller, F.U., Voigt, N., Zafeiriou, M.P., Ehrlich, J.R., Tochtermann, U., Veres, G., Ruhparwar, A., Karck, M., Katus, H.A., Thomas, D. (2017) 'Stretch-activated two-pore-domain (K2P) potassium channels in the heart: Focus on atrial fibrillation and heart failure' *Progress in Biophysics and Molecular Biology*, vol 130 (Part B), pp 233-243

Schweitz, H., Bruhn, T., Guillemare, E., Moinier, D., Lancelin, J.M., Béress, L., M Lazdunski, M. (1995) 'Kalicludines and kaliseptine: two different classes of sea anemone toxins for voltage-sensitive K^+ channels' J. *Biol. Chem*., vol 270 (42), pp. 25121-25126

Segura, M., Su, Z., Piccirillo, C., Stevenson, M. M. (2007). Impairment of dendritic cell function by excretory-secretory products: a potential mechanism for nematode-induced immunosuppression. *European journal of immunology*, *37*(7), 1887–1904.

Seoh, S.A., Sigg, D., Papazian, D.M., Bezanilla, F. (1996) 'Voltage-sensing residues in the S2 and S4 segments of the Shaker K^+ channel' *Neuron.*, vol 16(6), pp 1159-67

Seyfarth, E.A. (2006) 'Julius Bernstein (1839-1917): pioneer neurobiologist and biophysicist' *Biol Cybern.*, vol 94(1), pp 2-8

Shen, K.Z., Lagrutta, A., Davies, N.W., Standen, N.B., Adelman, J.P., North, R.A. (1994) 'Tetraethylammonium block of Slowpoke calcium-activated potassium channels expressed in Xenopus oocytes: evidence for tetrameric channel formation' *Pflugers Arch.*, vol 426(5), pp 440-5

Si, M., Trosclair, K., Hamilton, K. A., Glasscock, E. (2019) 'Genetic ablation or pharmacological inhibition of Kv1.1 potassium channel subunits impairs atrial repolarization in mice' *American journal of physiology. Cell physiology*, 316(2), C154–C161.

Sigg, D. (2014) 'Modelling ion channels: past, present and future' *J. Gen. Physiol.*, vol 144(1), pp.7-26

Sigworth, F.J. (1994) 'Voltage gating of ion channels' *Q Rev Biophys.,* vol 27(1), pp 1-40.

Silver, M.R., DeCoursey, T.E. (1990) 'Intrinsic gating of inward rectifier in bovine pulmonary artery endothelial cells in the presence or absence of internal Mg^{2+} ' *The Journal of general physiology*, *96*(1), 109–133

Simard, C., Drolet, B., Yang, P., Kim, R. B., Roden, D. M. (2005) 'Polymorphism screening in the cardiac K+ channel gene KCNA5. *Clinical pharmacology and therapeutics*, *77*(3), 138–144.

Sims, S.M., Dixon, S.J. (1989) 'Inwardly rectifying K+ current in osteoclasts' *Am J Physiol.*, vol 256(6 Pt 1), pp C1277-82

Singer, S.J., Nicolson, G.L. (1972) 'The fluid mosaic model of the structure of cell membranes' *Science*, vol 175(4023), pp 720-31

Smith KA (1984) Interleukin 2. *Annu Rev Immunol*. 2:3 pp 19-33

Smith, J.J., Cummins, T.R., Alphy, S., Blumenthal, K.M. (2007) 'Molecular interactions of the gating modifier toxin, ProTx-II, with Na$_V$1.5: Implied existence of a novel toxin binding site coupled to activation' *J. Biol. Chem.* vol 282(17), pp 12687-97

Snyders, D. J., Tamkun, M. M., Bennett, P. B. (1993) 'A rapidly activating and slowly inactivating potassium channel cloned from human heart. Functional analysis after stable mammalian cell culture expression' *The Journal of general physiology*, 101(4), 513–543.

Soden, S. E., Saunders, C. J., Willig, L. K., Farrow, E. G., Smith, L. D., Petrikin, J. E., LePichon, J. B., Miller, N. A., Thiffault, I., Dinwiddie, D. L., Twist, G., Noll, A., Heese, B. A., Zellmer, L., Atherton, A. M., Abdelmoity, A. T., Safina, N., Nyp, S. S., Zuccarelli, B., Larson, I. A., … Kingsmore, S. F. (2014). Effectiveness of exome and genome sequencing guided by acuity of illness for diagnosis of neurodevelopmental disorders. *Science translational medicine*, 6(265), 265ra168.

Sorum, B., Rietmeijer, R. A., Gopakumar, K., Adesnik, H., Brohawn, S. G. (2021) 'Ultrasound activates mechanosensitive TRAAK K^+ channels through the lipid membrane' *Proceedings of the National Academy of Sciences of the United States of America*, 118(6), e2006980118

Spector, P. S., Curran, M. E., Keating, M. T., Sanguinetti, M. C. (1996). 'Class III antiarrhythmic drugs block HERG, a human cardiac delayed rectifier K+ channel.' Open-channel block by methanesulfonanilides. *Circulation research*, *78*(3), 499–503.

Splawski, I., Shen, J., Timothy, K. W., Lehmann, M. H., Priori, S., Robinson, J. L., Moss, A. J., Schwartz, P. J., Towbin, J. A., Vincent, G. M., Keating, M. T. (2000). 'Spectrum of

mutations in long-QT syndrome genes. KVLQT1, HERG, SCN5A, KCNE1, and KCNE2'. *Circulation*, *102*(10), 1178–1185.

Sprunger, L. K., Stewig, N. J., O'Grady, S. M. (1996). 'Effects of charybdotoxin on K+ channel (KV1.2) deactivation and inactivation kinetics.' *European journal of pharmacology*, *314*(3), 357–364.

Srivastava, S., Cohen, J. S., Vernon, H., Barañano, K., McClellan, R., Jamal, L., Naidu, S., & Fatemi, A. (2014). Clinical whole exome sequencing in child neurology practice. *Annals of neurology*, *76*(4), 473–483.

Stanbury, R. M., Graham, E. M. (1998). 'Systemic corticosteroid therapy--side effects and their management.' *The British journal of ophthalmology*, v*82*(6), 704–708.

Stocker, M., Hellwig, M., Kerschensteiner, D. (1999). 'Subunit assembly and domain analysis of electrically silent K+ channel alpha-subunits of the rat Kv9 subfamily.' *Journal of neurochemistry*, *72*(4), 1725–1734.

Stocker, M., Miller, C. (1994). 'Electrostatic distance geometry in a K+ channel vestibule.' *Proceedings of the National Academy of Sciences of the United States of America*, *91*(20), 9509–9513.

Strachan D. P. (1989). 'Hay fever, hygiene, and household size.' *BMJ (Clinical research ed.)*, *299*(6710), 1259–1260.

Sugg, E.E., Garcia, M.L., Reuben, J.P., Patchett, A.A., Kaczorowski, G.J. (1990) 'Synthesis and structural characterization of charybdotoxin, a potent peptidyl inhibitor of the high conductance Ca2($^{+}$)-activated K^{+} channel' *J Biol Chem*., vol 265(31), pp18745-8.

Sukhwal, A.; Sowdhamini, R. (2013). 'Oligomerisation status and evolutionary conservation of interfaces of protein structural domain superfamilies.' *Mol. Biosyst.*, 9 (7), 1652-1661.

Sun, P., Wu, F., Wen, M., Yang, X., Wang, C., Li, Y., He, S., Zhang, L., Zhang, Y., Tian, C. (2015) 'A distinct three-helix centipede toxin SSD609 inhibits I(ks) channels by interacting with the KCNE1 auxiliary subunit' *Sci Rep*., vol 5, 13399

Sunanda, P, Krishnarjuna, B, Peigneur, S., Mitchell, M.L., Estrada, R., Villegas-Moreno, J., Pennington, M.W., Tytgat, J., Norton, R.S. (2018) 'Identification, chemical synthesis, structure, and function of a new K_V1 channel blocking peptide from *Oulactis* sp.' *Peptide Science*, vol 110 (4), e24073.

Swartz K. J. (2007). 'Tarantula toxins interacting with voltage sensors in potassium channels.' *Toxicon: official journal of the International Society on Toxinology*, *49*(2), 213–230.

Swartz, K. J., MacKinnon, R. (1995). 'An inhibitor of the Kv2.1 potassium channel isolated from the venom of a Chilean tarantula.' *Neuron*, vol *15*(4), pp 941–949.

Swartz, K. J., MacKinnon, R. (1997). 'Mapping the receptor site for hanatoxin, a gating modifier of voltage-dependent K+ channels.' *Neuron*, vol *18*(4), pp 675–682 (b)

Swartz, K.J., MacKinnon, R. (1997) 'Hanatoxin Modifies the Gating of a Voltage-Dependent K+ Channel through Multiple Binding Sites' *Neuron*, vol 18 (4), pp 665-673 (a)

Syrbe, S., Hedrich, U., Riesch, E., Djémié, T., Müller, S., Møller, R. S., Maher, B., Hernandez-Hernandez, L., Synofzik, M., Caglayan, H. S., Arslan, M., Serratosa, J. M., Nothnagel, M., May, P., Krause, R., Löffler, H., Detert, K., Dorn, T., Vogt, H., Krämer, G., … Lemke, J. R. (2015). 'De novo loss- or gain-of-function mutations in KCNA2 cause epileptic encephalopathy' *Nature genetics*, *47*(4), 393–399.

Szabó, I., Bock, J., Grassmé, H., Soddemann, M., Wilker, B., Lang, F., Zoratti, M., Gulbins, E. (2008) 'Mitochondrial potassium channel Kv1.3 mediates Bax-induced apoptosis in lymphocytes. *Proc Natl Acad Sci USA*., vol 105(39):14861-6

Szabò, I., Bock, J., Jekle, A., Soddemann, M., Adams, C., Lang, F., Zoratti, M., Gulbins, E. (2005) 'A novel potassium channel in lymphocyte mitochondria' *J Biol Chem.,* 2005 vol 280(13), pp 12790-8

Szabò, I., Zoratti, M., Gulbins, E. (2010) 'Contribution of voltage-gated potassium channels to the regulation of apoptosis' *FEBS Lett.,* vol 584(10), pp 2049-56

Szilágyi, O., Boratkó, A., Panyi, G., Hajdu, P. (2013) 'The role of PSD-95 in the rearrangement of Kv1.3 channels to the immunological synapse' *Pflugers Arch*., vol 465(9), pp 1341-53

Taglialatela, M., Ficker, E., Wible, B.A., Brown, A.M. (1995) 'C-terminus determinants for Mg^{2+} and polyamine block of the inward rectifier K^{+} channel IRK1' *EMBO J.*, vol 14(22), pp 5532-41

Takahashi, T. (1990) 'Inward rectification in neonatal rat spinal motoneurones.' *The Journal of physiology*, *423*, 47–62.

Tamargo J. (2000) 'Drug-induced torsade de pointes: from molecular biology to bedside.' *Japanese journal of pharmacology*, *83*(1), 1–19.

Tamargo, J., Caballero, R., Gómez, R., Valenzuela, C., Delpón, E. (2004) 'Pharmacology of cardiac potassium channels' *Cardiovascular research*, vol 62(1), pp 9–33.

Tamargo, J., Caballero, R., Gómez, R., Delpón, E. (2009) 'I(Kur)/Kv1.5 channel blockers for the treatment of atrial fibrillation' *Expert opinion on investigational drugs*, 18(4), 399–416.

Tarcha, E. J., Olsen, C. M., Probst, P., Peckham, D., Muñoz-Elías, E. J., Kruger, J. G., Iadonato, S. P. (2017). 'Safety and pharmacodynamics of dalazatide, a Kv1.3 channel inhibitor, in the treatment of plaque psoriasis: A randomized phase 1b trial.' *PloS one*, *12*(7), e0180762.

Tasoulis, T., and Isbister, G. K. (2017). 'A review and database of snake venom proteomes.' *Toxins*, 9(9), pp 290

Tedford, H.W., Sollod, B.L., Maggio, F., King, G.F. (2004) 'Australian funnel-web spiders: master insecticide chemists' *Toxicon*, 43 (5), pp. 601-618

Tempel, B.L., Papazian, D.M., Schwarz, T.L., Jan, Y.N., Jan, L.Y. (1987) 'Sequence of a probable potassium channel component encoded at Shaker locus of Drosophila' *Science*, vol 237(4816), pp. 770-775

Terstappen, G.C. (1999). 'Functional Analysis of Native and Recombinant Ion Channels Using a High-Capacity Nonradioactive Rubidium Efflux Assay.' *Analytical Biochemistry*, 272 (2), 149-155

Tharp, D. L., Wamhoff, B. R., Wulff, H., Raman, G., Cheong, A., Bowles, D. K. (2008).' Local delivery of the KCa3.1 blocker, TRAM-34, prevents acute angioplasty-induced coronary smooth muscle phenotypic modulation and limits stenosis.' *Arteriosclerosis, thrombosis, and vascular biology*, *28*(6), 1084–1089.

Thomas P, Smart TG (2005) 'HEK293 cell line: a vehicle for the expression of recombinant proteins.' *J Pharmacol Toxicol Methods,* 51(3), 187-200.

Thiffault, I., Speca, D. J., Austin, D. C., Cobb, M. M., Eum, K. S., Safina, N. P., Grote, L., Farrow, E. G., Miller, N., Soden, S., Kingsmore, S. F., Trimmer, J. S., Saunders, C. J., Sack, J. T. (2015). 'A novel epileptic encephalopathy mutation in KCNB1 disrupts Kv2.1 ion selectivity, expression, and localization.' *The Journal of general physiology*, *146*(5), 399–410.

Tian, C., Zhu, R., Zhu, L., Qiu, T., Cao, Z., Kang, T. (2014) 'Potassium channels: structures, diseases, and modulators' *Chem Biol Drug Des.*, vol 83(1), pp 1-26

Tikhonov, D. B., Zhorov, B. S. (2014) 'Homology modeling of Kv1.5 channel block by cationic and electroneutral ligands' *Biochimica et biophysica acta*, vol 1838(3), pp 978–987.

Tilley, D. C., Angueyra, J. M., Eum, K. S., Kim, H., Chao, L. H., Peng, A. W., Sack, J. T. (2019). 'The tarantula toxin GxTx detains K^+ channel gating charges in their resting conformation.' *The Journal of general physiology*, *151*(3), 292–315.

Torkamani, A., Bersell, K., Jorge, B. S., Bjork, R. L., Jr, Friedman, J. R., Bloss, C. S., Cohen, J., Gupta, S., Naidu, S., Vanoye, C. G., George, A. L., Jr, Kearney, J. A. (2014). 'De novo KCNB1 mutations in epileptic encephalopathy.' *Annals of neurology*, *76*(4), 529–540.

Toyama, K., Wulff, H., Chandy, K. G., Azam, P., Raman, G., Saito, T., Fujiwara, Y., Mattson, D. L., Das, S., Melvin, J. E., Pratt, P. F., Hatoum, O. A., Gutterman, D. D., Harder, D. R., Miura, H. (2008). 'The intermediate-conductance calcium-activated potassium channel KCa3.1 contributes to atherogenesis in mice and humans.' *The Journal of clinical investigation*, *118*(9), 3025–3037.

Trebak, M., Kinet, J. P. (2019). 'Calcium signalling in T cells.' *Nature reviews. Immunology*, *19*(3), 154–169.

Trimmer J. S. (2015) 'Subcellular localization of K+ channels in mammalian brain neurons: remarkable precision in the midst of extraordinary complexity' *Neuron*, *85*(2), 238–256.

Triplett, D. A., Stocker, K. F., Unger, G. A., Barna, L. K. (1993) 'The Textarin/Ecarin ratio: a confirmatory test for lupus anticoagulants' *Thromb. Haemost.*, vol 70 (6), pp 925–931

Trosclair, K., Si, M., Watts, M., Gautier, N. M., Voigt, N., Traylor, J., Bitay, M., Baczko, I., Dobrev, D., Hamilton, K. A., Bhuiyan, M. S., Dominic, P., Glasscock, E. (2021) 'Kv1.1 potassium channel subunit deficiency alters ventricular arrhythmia susceptibility, contractility, and repolarization' *Physiological reports*, vol 9(1), e14702

Tytgat, J., Chandy, K.G., Garcia, M.L., Gutman, G.A., Martin-Eauclaire, M.F., van der Walt, J.J., Possani, L.D. (1999) 'A unified nomenclature for short-chain peptides isolated from scorpion venoms: alpha-KTx molecular subfamilies' *Trends Pharmacol Sci*., vol 20(11), pp 444-7

Scholl, U., Choi, M., Liu, T., Ramaekers, V., Häusler, M., Grimmer, J., Tobe, S., Farhi, A., Nelson-Williams, C., Lifton, R. (2009) 'Seizures, sensorineural deafness, ataxia, mental retardation, and electrolyte imbalance (SeSAME syndrome) caused by mutations in KCNJ10' *Proc. Natl. Acad. Sci. U.S.A*., vol 106 (14), pp 5842–5847.

Utkin, Y.N. (2015) 'Animal venom studies: Current benefits and future developments' *World J Biol Chem*., vol 6(2), pp 28-33

Vaeth, M., Feske, S. (2018). ‘Ion channelopathies of the immune system.’ *Current opinion in immunology*, *52*, 39–50.

Valencia-Cruz, G., Shabala, L., Delgado-Enciso, I., Shabala, S., Bonales-Alatorre, E., Pottosin, I. I., Dobrovinskaya, O. R. (2009). ‘K(bg) and Kv1.3 channels mediate potassium efflux in the early phase of apoptosis in Jurkat T lymphocytes’. *American journal of physiology. Cell physiology*, *297*(6), C1544–C1553.

van Riet, E., Hartgers, F. C., Yazdanbakhsh, M. (2007). ‘Chronic helminth infections induce immunomodulation: consequences and mechanisms.’ *Immunobiology*, *212*(6), 475–490.

Vandenberg, J. I., Perry, M. D., Perrin, M. J., Mann, S. A., Ke, Y., Hill, A. P. (2012). ‘hERG K(+) channels: structure, function, and clinical significance.’ *Physiological reviews*, *92*(3), 1393–1478.

Vandenberg, J. I., Walker, B. D., Campbell, T. J. (2001). ‘HERG K+ channels: friend and foe.’ *Trends in pharmacological sciences*, *22*(5), 240–246.

VanDyke, D. H., Griggs, R. C., Murphy, M. J., Goldstein, M. N. (1975) ‘Hereditary myokymia and periodic ataxia’ *Journal of the neurological sciences*, 25(1), 109–118.

Varga, Z., Hajdu, P., Panyi, G. (2010). ‘Ion channels in T lymphocytes: an update on facts, mechanisms and therapeutic targeting in autoimmune diseases.’ *Immunology letters*, *130*(1-2), 19–25.

Vetter, S. W., Leclerc, E. (2003). ‘Novel aspects of calmodulin target recognition and activation.’ *European journal of biochemistry*, *270*(3), 404–414.

Vicente, R., Escalada, A., Villalonga, N., Texidó, L., Roura-Ferrer, M., Martín-Satué, M., López-Iglesias, C., Soler, C., Solsona, C., Tamkun, M. M., Felipe, A. (2006) ‘Association of Kv1.5 and Kv1.3 contributes to the major voltage-dependent K+ channel in macrophages’ *The Journal of biological chemistry*, 281(49), 37675–37685.

Villalonga, N., David, M., Bielanska, J., Vicente, R., Comes, N., Valenzuela, C., Felipe, A. (2010). 'Immunomodulation of voltage-dependent K+ channels in macrophages: molecular and biophysical consequences' *The Journal of general physiology*, 135(2), 135–147.

Villalonga, N., Escalada, A., Vicente, R., Sánchez-Tilló, E., Celada, A., Solsona, C., Felipe, A. (2007) 'Kv1.3/Kv1.5 heteromeric channels compromise pharmacological responses in macrophages' *Biochemical and biophysical research communications*, 352(4), 913–918.
vol 54(8), pp1054-64

Wakili, R., Voigt, N., Kääb, S., Dobrev, D., Nattel, S. (2011) 'Recent advances in the molecular pathophysiology of atrial fibrillation' *The Journal of clinical investigation*, 121(8), 2955–brohawn2968.

Wallner, M., Meera, P., Toro, L. (1996) 'Determinant for beta-subunit regulation in high-conductance voltage-activated and Ca(2+)-sensitive K^+ channels: an additional transmembrane region at the N terminus' *Proc Natl Acad Sci U S A.*, vol 93(25), pp 14922-14927.

Wang, F. C., Bell, N., Reid, P., Smith, L. A., McIntosh, P., Robertson, B., & Dolly, J. O. (1999). 'Identification of residues in dendrotoxin K responsible for its discrimination between neuronal K+ channels containing Kv1.1 and 1.2 alpha subunits.' *European journal of biochemistry*, *263*(1), 222–229.

Wang, F., Li, H., Liu, M.N., Song, H., Han, H.M., Wang, Q.L., Yin, C.C., Zhou, Y.C., Qi, Z., Shu, Y.Y., Lin, Z.J., Jiang, T. (2006) 'Structural and functional analysis of natrin, a venom protein that targets various ion channels' *Biochem Biophys Res Commun.*, vol 351(2), pp 443-8

Wang, H., Kunkel, D. D., Martin, T. M., Schwartzkroin, P. A., Tempel, B. L. (1993). 'Heteromultimeric K+ channels in terminal and juxtaparanodal regions of neurons.' *Nature*, *365*(6441), 75–79.

Wang, H., Kunkel, D. D., Schwartzkroin, P. A., Tempel, B. L. (1994). 'Localization of Kv1.1 and Kv1.2, two K channel proteins, to synaptic terminals, somata, and dendrites in the mouse

brain.' *The Journal of neuroscience: the official journal of the Society for Neuroscience*, *14*(8), 4588–4599.

Wang, L., Wang, F. S., Gershwin, M. E. (2015). 'Human autoimmune diseases: a comprehensive update.' *Journal of internal medicine*, *278*(4), 369–395.

Wang, J.M., Roh, S.H., Kim, S., Lee, C.W., Kim, J.I., Swartz, K.J. (2004) 'Molecular surface of tarantula toxins interacting with voltage sensors in K_V channels' *J. Gen. Physiol*., vol 123(4), pp 455–467

Wang, X., Li, G., Guo, J., Zhang, Z., Zhang, S., Zhu, Y., Cheng, J., Yu, L., Ji, Y., Tao, J. (2020) 'Kv1.3 Channel as a Key Therapeutic Target for Neuroinflammatory Diseases: State of the Art and Beyond' *Front Neurosci*., vol 13, pp 1393

Wang, Y., Li, X., Yang, M., Wu, C., Zou, Z., Tang, J., Yang, X. (2017) 'Centipede venom peptide SsmTX-I with two intramolecular disulfide bonds shows analgesic activities in animal models' *J. Pept. Sci*., vol 23 (5), pp 384–391

Wang, Z. (2004) 'Roles of K^+ channels in regulating tumour cell proliferation and apoptosis' *Pflugers Arch - Eur J Physiol*, vol 448(3), pp 274–286

Wang, Z., Fermini, B., Nattel, S. (1993) 'Sustained depolarization-induced outward current in human atrial myocytes. Evidence for a novel delayed rectifier K^+ current similar to Kv1.5 cloned channel currents' *Circulation research*, 73(6), 1061–1076.

Waterhouse A, Bertoni M, Bienert S, Studer G, Tauriello G, Gumienny R, Heer FT, de Beer TAP, Rempfer C, Bordoli L, Lepore R, Schwede T (2018). 'SWISS-MODEL: homology modelling of protein structures and complexes.' *Nucleic Acids Res.*, 46(W1): W296-W303.

Wettwer, E., Terlau, H. (2014) 'Pharmacology of voltage-gated potassium channel Kv1.5--impact on cardiac excitability' *Current opinion in pharmacology*, vol 15, pp 115–121.

White, M., Johnston, C., Grainger, J. R., Konkel, J. E., O'Connor, R. A., Anderton, S. M., Maizels, R. M. (2020) 'The Helminth Parasite *Heligmosomoides polygyrus* Attenuates EAE in an IL-4Rα-Dependent Manner'. *Frontiers in immunology* 11, 1830

Wible, B. A., Hawryluk, P., Ficker, E., Kuryshev, Y. A., Kirsch, G., Brown, A. M. (2005). HERG-Lite: a novel comprehensive high-throughput screen for drug-induced hERG risk. *Journal of pharmacological and toxicological methods*, *52*(1), 136–145.

Wickman, K., Clapham, DE. (1995) 'Ion channel regulation by G proteins' *Physiol Rev*., vol 75(4), pp 865-885

Williams, J.T., Colmers, W.F., Pan, Z.Z. (1988) 'Voltage- and ligand-activated inwardly rectifying currents in dorsal raphe neurons in vitro' *J Neurosci.*, vol 8(9), pp 3499-3506.

Winterfield, J. R., Swartz, K. J. (2000). 'A hot spot for the interaction of gating modifier toxins with voltage-dependent ion channels.' *The Journal of general physiology*, vol 116(5), pp 637–644.

Wonderlin, W., Strobl, J. (1996) 'Potassium Channels, Proliferation and G1 Progression' *J. Membrane Biol.*, vol 154(2), pp 91–107

Wu, B., Wu, B. F., Feng, Y. J., Tao, J., Ji, Y. H. (2016). 'Mapping the Interaction Anatomy of BmP02 on Kv1.3 Channel.' *Scientific reports*, *6*, 29431.

Wu, J., Ding, W. G., Matsuura, H., Tsuji, K., Zang, W. J., Horie, M. (2009) 'Inhibitory actions of the phosphatidylinositol 3-kinase inhibitor LY294002 on the human Kv1.5 channel' *British journal of pharmacology*, 156(2), 377–387.

Wu, J., Yan, Z., Li., Z, Qian, X., Lu, S., Dong, M., Zhou, Q., Yan, N. (2016) 'Structure of the voltage-gated calcium channel Ca(v)1.1 at 3.6 Å resolution' Nature vol 537(7619), pp 191-196
Wu, W. K., Li, G. R., Wong, H. P., Hui, M. K., Tai, E. K., Lam, E. K., Shin, V. Y., Ye, Y. N., Li, P., Yang, Y. H., Luo, J. C., Cho, C. H. (2006) 'Involvement of Kv1.1 and Nav1.5 in proliferation of gastric epithelial cells' *Journal of cellular physiology*, 207(2), 437–444.

Wulff, H., Beeton, C., Chandy, K. G. (2003). 'Potassium channels as therapeutic targets for autoimmune disorders.' *Current opinion in drug discovery & development*, *6*(5), 640–647 (a)

Wulff, H., Calabresi, P. A., Allie, R., Yun, S., Pennington, M., Beeton, C., Chandy, K. G. (2003). 'The voltage-gated Kv1.3 K (+) channel in effector memory T cells as new target for MS.' *The Journal of clinical investigation*, *111*(11), 1703–1713 (b)

Wulff, H., Castle, N. A. (2010). 'Therapeutic potential of KCa3.1 blockers: recent advances and promising trends.' *Expert review of clinical pharmacology*, *3*(3), 385–396.

Wulff, H., Castle, N. A., Pardo, L. A. (2009). 'Voltage-gated potassium channels as therapeutic targets.' *Nature reviews. Drug discovery*, *8*(12), 982–1001.

Wulff, H., Knaus, H.G., Pennington, M., Chandy, K.G. (2004) 'K^+ channel expression during B cell differentiation: implications for immunomodulation and autoimmunity' *J Immunol*., vol 173(2), pp 776-86

Wulff, H., Miller, M. J., Hansel, W., Grissmer, S., Cahalan, M. D., Chandy, K. G. (2000). 'Design of a potent and selective inhibitor of the intermediate-conductance Ca2+-activated K+ channel, IKCa1: a potential immunosuppressant.' *Proceedings of the National Academy of Sciences of the United States of America*, *97*(14), 8151–8156.

Wulff, H., Zhorov, B.S. (2008) 'K+ channel modulators for the treatment of neurological disorders and autoimmune diseases' *Chem Rev.*, vol 108(5), pp 1744-1773

Xu, C.Q., Zhu, S.Y., Chi, C.W., Tytgat, J. (2003) 'Turret and pore block of K^+ channels: what is the difference?' *Trends Pharmacol Sci.*, vol 24(9), pp 446-8

Xu, L., Song, X., Su, L., Zheng, Y., Li, R., Sun, J. (2019). 'New therapeutic strategies based on IL-2 to modulate Treg cells for autoimmune diseases.' *International immunopharmacology*, *72*, 322–329.

Y. Li-Smerin, Y., Swartz, K.J. (1998) 'Gating modifier toxins reveal a conserved structural motif in voltage-gated Ca^{2+} and K^+ channels' *Proc. Natl. Acad. Sci. U. S. A*., vol 95 (15), pp. 8585-8589

Yan, L., Herrington, J., Goldberg, E., Dulski, P. M., Bugianesi, R. M., Slaughter, R. S., Banerjee, P., Brochu, R. M., Priest, B. T., Kaczorowski, G. J., Rudy, B., Garcia, M. L. (2005). 'Stichodactyla helianthus peptide, a pharmacological tool for studying Kv3.2 channels.' *Molecular pharmacology*, vol *67*(5), pp 1513–1521.

Yang, J. F., Cheng, N., Ren, S., Liu, X. M., Li, X. T. (2018). 'Characterization and molecular basis for the block of Kv1.3 channels induced by carvedilol in HEK293 cells.' *European journal of pharmacology*, *834*, 206–212.

Yang, J., Jan, Y.N., Jan, L.Y. (1995) 'Control of rectification and permeation by residues in two distinct domains in an inward rectifier K^+ channel' *Neuron.,* vol 14(5), pp 1047-54 (a)

Yang, J., Jan, Y.N., Jan, L.Y. (1995) 'Determination of the subunit stoichiometry of an inwardly rectifying potassium channel' *Neuron*, vol 15(6), pp 1441– 1447 (b)

Yang, J., Zhao, J., Yang, Y., Zhang, L., Yang, X., Zhu, X., Ji, M., Sun, N., Su, C. (2007). 'Schistosoma japonicum egg antigens stimulate CD4 CD25 T cells and modulate airway inflammation in a murine model of asthma.' *Immunology*, *120*(1), 8–18.

Yang, S., Liu, Z., Xiao, Y., Li, Y., Rong, M., Liang, S., Zhang, Z., Yu, H., King, G.F., Lai, R., (2012) 'Chemical punch packed in venoms makes centipedes excellent predators' *Mol Cell Proteomics*, vol 11(9), pp 640-50.

Yau, K.W., Baylor, D.A. (1989) 'Cyclic GMP-activated conductance of retinal photorecepor cells' *Annual Review Neuroscience*, vol 12, pp 289-327

Yellen, G. (1998) 'The moving parts of voltage-gated ion channels' *Q. Rev. Biophys*., vol 31, pp 239–295.

Yellen, G. (2002) 'The voltage-gated potassium channels and their relatives' *Nature,* vol 5; 419 (6902), pp 35-42

Yellen, G., Jurman, M.E., Abramson, T., MacKinnon, R. (1991) 'Mutations affecting internal TEA blockade identify the probable pore-forming region of a K^+ channel' *Science vol*, 251(4996), 939–942

Yin, S., Hu, Q., Luo, J., Li, Y., Lu, C., Chen, X., Hu, H. (2014). 'Loureirin B, an essential component of Sanguis Draxonis, inhibits Kv1.3 channel and suppresses cytokine release from Jurkat T cells.' *Cell & bioscience*, *4*, 78.

Yoon K. H. (2010). 'Efficacy and cytokine modulating effects of tacrolimus in systemic lupus erythematosus: a review.' *Journal of biomedicine & biotechnology*, *2010*, 686480.

Zaccone, P., Cooke, A. (2013). 'Vaccine against autoimmune disease: can helminths or their products provide a therapy?' *Current opinion in immunology*, *25*(3), 418–423.

Zaccone, P., Fehérvári, Z., Jones, F. M., Sidobre, S., Kronenberg, M., Dunne, D. W., Cooke, A. (2003). 'Schistosoma mansoni antigens modulate the activity of the innate immune response and prevent onset of type 1 diabetes.' *European journal of immunology*, *33*(5), 1439–1449.

Zagotta, W.N., Siegelbaum, S.A. (1996) 'Structure and function of cyclic nucleotide-gated channels' *Annu.Rev.Neurosci.*, vol 19, pp 235-63

Zakeri, A., Hansen, E. P., Andersen, S. D., Williams, A. R., Nejsum, P. (2018). 'Immunomodulation by Helminths: Intracellular Pathways and Extracellular Vesicles.' *Frontiers in immunology*, *9*, 2349.

Zangerl-Plessl, E.M., Qile, M., Bloothooft, M., Stary-Weinzinger, A., van der Heyden, M.A.G. (2019) 'Disease Associated Mutations in K_{IR} Proteins Linked to Aberrant Inward Rectifier Channel Trafficking' *Biomolecules*, vol 9(11), pp 650

Zarayskiy, V.V., Balasubramanian, G., Bondarenko, V.E., Morales, M.J. (2005) 'Heteropoda toxin 2 is a gating modifier toxin specific for voltage-gated K^+ channels of the K_V4 family' *Toxicon,* vol 45 (4), pp 431–442

Zelanis, A., Menezes, M. C., Kitano, E. S., Liberato, T., Tashima, A. K., Pinto, A. F., et al. (2016). 'Proteomic identification of gender molecular markers in Bothrops jararaca venom.' *J. Proteomics*, vol 139, pp 26–37.

Zhang Y. (2015). ‘Why do we study animal toxins?’ *Dong wu xue yan jiu = Zoological research*, 36(4), 183–222.

Zhang, M., Korolkova, Y.V., Liu, J., Jiang, M., Grishin, E.V., Tseng, G. (2003) ‘BeKm-1 is a HERG-specific toxin that shares the structure with ChTx but the mechanism of action with ErgTx1’ *Biophysical Journal*., vol 84(5), pp 3022-3036

Zhang, M., Liu, X. S., Diochot, S., Lazdunski, M., Tseng, G. N. (2007). ‘APETx1 from sea anemone Anthopleura elegantissima is a gating modifier peptide toxin of the human ether-a-go-go- related potassium channel.’ *Molecular pharmacology*, *72*(2), 259–268.

Zhang, Y. Z., Li, Y. Y. (2014). ‘Inflammatory bowel disease: pathogenesis.’ *World journal of gastroenterology*, 20(1), 91–99.

Zhang, Y., Zhang, F., Shi, S., Liu, X., Cai, W., Han, G., Ke, C., Long, S., Di, Z., Yin, S., & Li, H. (2019). ‘Immunosuppressive effects of a novel potassium channel toxin Ktx-Sp2 from Scorpiops Pocoki.’ *Cell & bioscience*, *9*, 99.

Zhao, N., Dong, Q., Du, L. L., Fu, X. X., Du, Y. M., Liao, Y. H. (2013). ‘Potent suppression of Kv1.3 potassium channel and IL-2 secretion by diphenyl phosphine oxide-1 in human T cells.’ *PloS one*, *8*(5), e64629.

Zhao, N., Dong, Q., Fu, X. X., Du, L. L., Cheng, X., Du, Y. M., Liao, Y. H. (2014). ‘Acacetin blocks kv1.3 channels and inhibits human T cell activation.’ *Cellular physiology and biochemistry: international journal of experimental cellular physiology, biochemistry, and pharmacology*, 34(4), 1359–1372.

Zhao, N., Dong, Q., Qian, C., Li, S., Wu, Q. F., Ding, D., Li, J., Wang, B. B., Guo, K. F., Xie, J. J., Cheng, X., Liao, Y. H., Du, Y. M. (2015). ‘Lovastatin blocks Kv1.3 channel in human T cells: a new mechanism to explain its immunomodulatory properties.’ *Scientific reports*, *5*, 17381.

Zhao, Y., Huang, J., Yuan, A., Peng, B., Liu, W., Han, S., He, X. (2015) 'Toxins targeting Kv1.3 channel: potential immunomodulators for autoimmune diseases' *Toxins*, vol 7(5), pp 1749-1764

Zhao, Z., Ruan, S., Ma, X., Feng, Q., Xie, Z., Nie, Z., Fan, P., Qian, M., He, X., Wu, S., Zhang, Y., Zheng, X. (2019) 'Challenges Faced with Small Molecular Modulators of Potassium Current Channel Isoform Kv1.5' *Biomolecules*, 10(1), 10.

Zhu, S., Darbon, H., Dyason, K., Verdonck, F., Tytgat, J. (2003) 'Evolutionary origin of inhibitor cystine knot peptides' *FASEB J.*, vol 17(12), pp 1765-7

Zobel-Thropp, P.A., Bulger, E.A.,Cordes, M.H.J., Binford, G.J., Gillespie, R.G., Brewer, M.S. (2018) 'Sexually dimorphic venom proteins in long-jawed orb-weaving spiders (Tetragnatha) comprise novel gene families' *PeerJ* , vol 6, e4691.

Zufall, F., Firestein, S., Shepherd, G.M. (1994) 'Cyclic nucleotide-gated ion channels and sensory transduction in olfactory receptor neurons' *Annu. Rev. Biophys. Biomol. Struct*., vol 23, pp 577-607

Zúñiga, L., Zúñiga, R. (2016) 'Understanding the Cap Structure in K2P Channels' *Front Physiol.*, vol 7:228.